A Smart-Charging Algorithm Development Considering Uncertainties in the System

1

Damianakis Nikolaos

TU Delft

1 Adapted from [107]

A Smart-Charging Algorithm Development Considering Uncertainties in the System

by

Damianakis Nikolaos

to obtain the degree of Master of Science in
Electrical Power Engineering
at the Delft University of Technology
to be defended publicly on Wednesday August 25, 2021 at 02:00 PM.

Supervisors:
Dr.ing.ir P. Bauer
Dr.ir. G. R. Chandra Mouli
MSc. Y. Yu

Thesis Committee:
Dr.ing.ir P. Bauer
Dr.ir. G. R. Chandra Mouli
Dr. S.H. Tindemans

Student Number: 5018366
Project Duration: December 1, 2020 – August 25, 2021

Abstract

With the current urge around the globe for switching to "green energy" and Renewable Energy Sources (RES) utilization, the electrification of the transportation sector has become a necessity. While the emerging Electric Vehicles (EVs) can provide several benefits to the power grid, such as voltage and frequency regulation and power quality improvement, the large and immense EV fleets penetration can have the exact opposite results, if no suitable charging method is utilized. Therefore, the uncontrollable EV charging, that is being utilized today, will not be capable of offering sustainable energy to the future EVs with respect to the power grid limits and hence, today's research field has turned to optimized smart-charging techniques. However, most of these algorithms treat the problem of smart-charging deterministically, assuming 100% accurate prediction of the input data, while it has been shown that the optimality of results can be seriously deteriorated even under small prediction error.

This thesis purpose is to address the impact and potential management of several uncertainties related with EV smart charging: PV Generation, Load Demand, arrival SOC, Arrival and Departure time of the EVs & (Frequency Containment Regulation) FCR Reserves provision uncertainties. The main handling technique, utilized in this thesis, is the Robust Optimization (RO) approach, taking advantage of its very lower computational expense and protection against the worst-case scenario of the uncertainty, with the combination of the Receding Horizon Optimization (RHO), that is already implemented in the Benchmark algorithm. After improving the Benchmark algorithm by providing it with prediction feature, this thesis proves the capability of improved robustly EV charging with the combination of RO-RHO approach with prediction, which reduces the economical (in terms of charging costs/income) and "customer satisfaction" (in terms of unfinished charging gap impacts) of all the uncertainties considered. A more robust and "realistic" FCR reserves provision model has been developed, as well. Last but not least, the well-known RO drawback of potential over-conservativeness, in other words high deterioration of optimality at expense of robustness, is address for every uncertainty.

The results of the investigation provide valuable results about which uncertainty has the greater impact, is more robustly manageable or inflicts the highest "Price of Robustness", regarding overconservativeness. For example, it has been found that the FCR reserves uncertainty inflicts the highest economical and charging gap impacts, however it is the most robustly manageable uncertainty as well, if RO and prediction feature are utilized. Moreover, while arrival SOC and Parking Time uncertainties affect highly the unfinished charging gap, the PV Generation and Load Demand have practically only economic impact, which is also lower than the other uncertainties, hence they are defined as the "uncertainties with the least impact". Finally, there are 3 types of nodes studied: the "Home" Node, the "Semi-Public" Node & the "Public" Nodes. Observing their behavior during the different uncertainties' study cases, interesting results have been found about their robust management and affection by the various uncertainties. Finally, comparing the Benchmark and the Prediction – Capable (P-C) algorithms for the management of the uncertainties, the value of the prediction feature insertion has been proved, as well.

Acknowledgements

Having completed my MSc. studies on Electrical Power Engineering and acquired the ingenieur (ir.) degree, I would like to express my sincere gratitude to all the people, who have contributed to the fulfillment of my goal.

Firstly, I would like to acknowledge the "DC Systems, Energy Conversion & Storage (DCE&S) research group and my supervisor Prof. dr. Pavol Bauer for granting me with the opportunity to work on a so interesting and challenge project. This project has enhanced my knowledge and experience in the field of Electric Vehicles and Smart-Charging, which is the field to which, I am willing to dedicate my future career. Secondly, I would also like to express my appreciation to my 3rd committee member Dr. S.H. Tindemans for the time he has devoted to read my thesis and discuss the project.

Furthermore, I feel the need to express my profound gratitude to my supervisor and 2nd committee member Dr.ir. G. R. Chandra Muli and Y. Yunhe for their dedicated valuable guidelines and time, which have been indispensable for the completion of this thesis. They both have shared and provided me with essential information and background, such in the field of EV smart-charging, as in the Optimization field, as well. Finally, I wish also to additionally thank all my committee members and people, who saved a little time from their summer, to watch and participate in my thesis defense.

Last but not least, my miles-away priceless family and friends back in Greece. Without the economic support from my family, I would never have the opportunity to study at a university of the scientific level of "TU Delft". Moreover, there are no words to thank my beloved friends, who stand there, besides my family, to provide me with psychological support and love, such during my stay in the Netherlands, as in all other parts of my life.

Damianakis Nikolaos
Delft, August 2021

List of Figures

List of Tables

List of Abbreviations

RES	Renewable Energy Sources
EV	Electric Vehicle
SOC	State of Charge
FCR	Frequency Containment Regulation
SO	Stochastic Optimization
RO	Robust Optimization
DRO	Distributional Robust Optimization
SRO	Static Robust Optimization
ARO	Adaptive Robust Optimization
RHO	Receding Horizon Optimization
RO – RHO	Robust Optimization and Receding Horizon Optimization (combined approach)
P-C	Prediction-Capable
PEVs	Plug-in Electric Vehicles
EPA	Environmental Protection Agency
UC	Uncontrolled Charging
DC	Delayed Charging
AC	Average Charging
DSO	Distributional System Operator
TSO	Transmission System Operator
V2G	Vehicle to Grid
G2V	Grid to Vehicle
IGDT	Information Gap Decision Theory
MILP	Mixed-Integer Linear Programming
DSM	Demand Side Management
UC	Unit Commitment
ED	Economic Dispatch
PDF	Probability Density Function
CDF	Cumulative Density Function
ML	Method of Maximum Likelihood
ME	Method of Moments
GOF	Goodness of Fitness (Statistics)
EDF	Empirical Distribution Function
MCS	Monte-Carlo Simulation
LHS	Latin Hybercube Sampling
SBA	Scenario-based Approach

UAV	Unmanned Aerial Vehicle
PEM	Point Estimate Method
FMP	Fuzzy Mathematical Programming
DG	Distributed Generator
DS	Distributed System
MG	Micro-Grid
DER	Distributed Energy Resources
SDN	Smart Distributional Network
RC	Robust Counterpart
HEMS	Home Energy Management System
MPC	Model Predictive Control
SH	Scheduling Horizon
PH	Prediction Horizon
CH	Control Horizon
CC	Constant Current (EV charging region)
CV	Constant Voltage (EV charging region)
DAM	Day-Ahead Market
IDM	Intra-Day Market
BRP	Balance Responsible Party
MIP	Marginal Incremental Price
MDP	Marginal Decremental Price
AGC	Automatic Generation Control
ACE	Area Control Error
SMP	System Marginal Price (auction market)
PAB	Pay-as-Bid (auction market)
GA	Generic Algorithm
S.C	Smart-Charging

Contents

Chapter 1 Introduction

1.1 Electrification of Transportation Sector & Futuristic Power Grids

The environmental impact of the conventional energy sources utilization and the forthcoming depletion of fossil fuels are some of the most critical issues of the energy sector that need to be addressed. Moreover, according to the United States Environmental Protection Agency (EPA), the 28% of the total U.S. greenhouse gas emissions origins from the transportation sector [1]. Furthermore, the Canadian transportation sector is responsible for the 2nd largest amount of greenhouse emissions. For example, it can be clearly seen in Fig. 1.1, that transportation emissions integrated in 2013 the 23% of the total amount, after the emissions of the oil & gas sector [2]. Therefore, the need for electrification of the majority of the transportation system with the emerging EVs, becomes more and more evident and many countries around the Globe have already put relative targets in the future years [1]. Many countries have already made important steps towards the electrification of the transportation sector. As depicted in Table 1.1, in 2013, USA was the first country regarding the size of the Plug-In Electric Vehicles (PEVs) fleet, while Norway was the pioneer, regarding the integration of the PEVs in the market share.

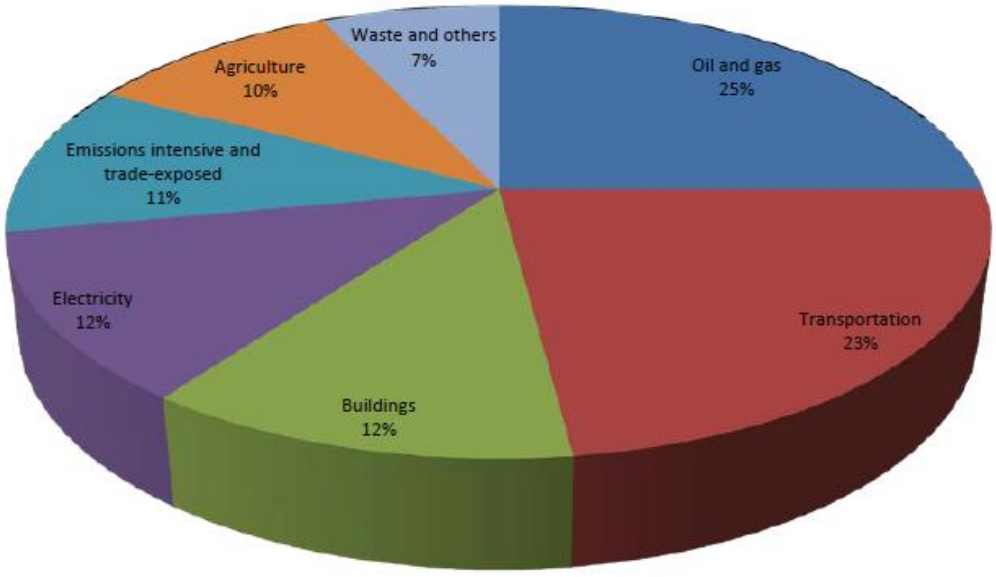

Fig. 1. 1: Distribution of Greenhouse Emissions in Canada (2013) [2]

Table 1. 1: Top 6 Countries on PEV Fleet, Population & Sales Market Share (2013)

Country	PEV Fleet	Population	PEV market share (%)
United States	172.000	320.050.716	0,62
Japan	74.124	127.143.577	0,85
China	38.592	1.385.566.537	0,08
Netherlands	28.673	16.759.229	5,37
France	28.560	64.291.280	0,67
Norway	20.486	5.042.671	5,60

1.2 EVs benefits & Challenges

On the same direction, the emerging increasing use of Renewable Energy Sources (RES) instead of the use of fossil fuels, generate new challenges in the future power grids, such as generation fluctuations due to their intermittent generation character [3]. On the one hand, EVs can cope with the generation deviations of RES, acting as "smart-loads" and providing ancillary services, such as storage and spinning reserves capabilities. They are capable of improving stability actively with Demand-Side Management (DSM) programs, offering reserve services and Vehicle-to-Grid (V2G) technology. Therefore, frequency and voltage regulation, reactive power compensation, power quality improvement and congestion management are only some of the major contributions that EVs can offer to the future power grids [4]. However, all of the above can be accomplished, only if their integration is accomplished on a "smart" and coordinated manner. On the other hand, increased and un-coordinated employment of EVs can provoke several negative impacts on the future power grids. Some of them can be power and voltage quality reduction (voltage instability, phase unbalance, harmonics distortion), distribution network components overloading and defects (transformers and lines saturation), power losses increase as well as congestions and reliability issues, due to the significant rise of new power demand [5], [6], [4]. In Fig. 1.2, the positive and negative impacts of the future EVs integration into the power grid are summarized [4].

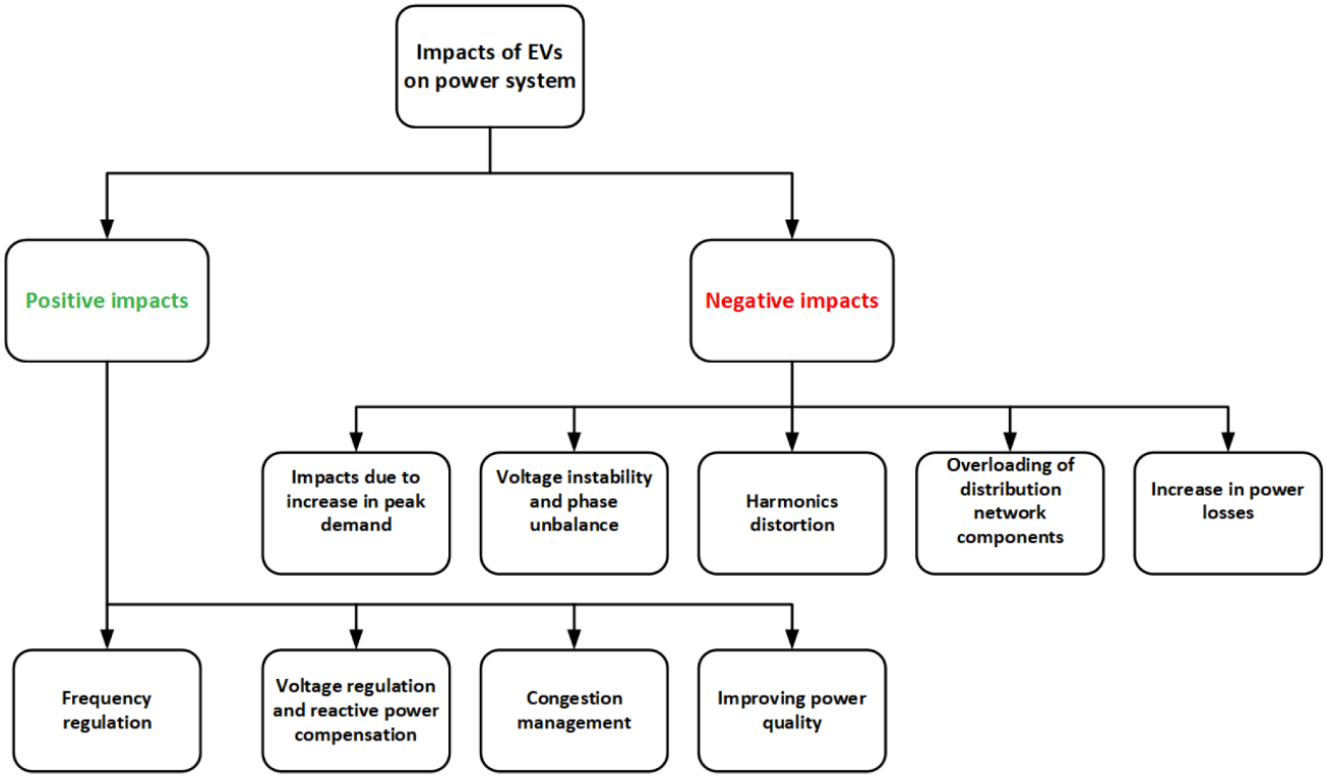

Fig. 1. 2: Positive and Negative Impacts of EVs to the future Distribution Networks [4]

1.3 EV charging & Thesis Motivation

One major part of the "smart" and coordinated integration of the future EV large fleets into the power grid is related with the charging method. The conventional charging techniques can be categorized as:

- Uncontrolled-Immediate Charging: Represents the simplest and most commonly used charging technique that is applied today. The moment that the EV is plugged in, it is free to receive the full rated

power of the EV charger without any control from the operator, until the State-of-Charge (SOC) reaches the 100% or the minimum specified value from the EV user. While, at present, it is still a viable option, it is considered that Uncontrolled Charging (UC) will enhance greatly the aforementioned potential negative impacts of the forthcoming large EV penetration, if no strategy is applied to avoid the high peak loads. Therefore, especially during the high power-demand periods (6-8a.m when people park their cars before work or 6-8p.m when they return home), this method is going to create severe issues, regarding grid stability in the future [4], [7], [8].

- Delayed Charging: Represents a charging method that is in position to reduce the negative impacts of the Uncontrolled Charging, shifting the load to off-peak periods of the day. This is accomplished generally by increasing the energy price during peak periods and reducing it during off-peak, incentivizing the customers to use the EV charger during low price periods. While Delayed Charging (DC) is considered to be a "safer" charging method than UC, it controls the charging time but not the charging power. As a consequence, incentivizing the EV users to charge during off-peak periods, it is very likely to induce another peak-load during off-peak periods, especially at the end of the peak periods [4],
- Average Charging: Regarding the particular charging method, the charging period is initiated when the EV is plugged in the EV charger, such as in UC. However, instead of receiving the rated power of the charger, the EV receives a constant charging power during the whole parking time interval. The constant charging power is determined by the total energy and the total parking time, which have been set by the EV user at the start of the charging period. The main goal of Average Charging (AC) is to fully utilize the parking time of the EV. Equation (5) defines the charging time and is presented below [8]:

$$P_{avg} = \frac{E_{asked}}{T_{dep} - T_{arr}} \quad (1)$$

Where:

E_{asked}: the required charging enery
T_{arr}: time of arrival
T_{dep}: time of departure
P_{avg}: average charging power

Controlled-Charging

Due to the increasing number of EV penetration, the conventional charging techniques, especially the commonly used uncontrolled charging schedules will no longer be able to cope with the induced negative impact on the system stability. Multiple smart-charging algorithms have been developed in order to firstly satisfy the customer needs and requirements and secondly facilitate the power flow in the power distribution system, taking advantage of the fact that most of the EVs are parked at their parking slots for considerable time intervals, while working or during the night. Either Centralized Smart-Charging (with the use of a central entity) or Decentralized Smart-Charging are applied, controlled charging is capable of controlling charging time and power, depending on several constraints such as total power demand, system components' stress, voltage stability and losses. The objective of the majority of the Smart-Charging optimizations is the minimization of the charging cost [4]. The potential benefits of Smart-Charging are summarized below [9]:

- Reduction of potential need of grid reinforcement costs due to reduction of demand peaks
- Increase of energy cost savings with the use of Time-of-Use tariffs by the EV users
- Self-Consumption increase, incentivizing "prosumers" (consumers who are capable of producing their own energy e.g PV panels) to use effectively both the grid and their own power depending on the market energy prices and the grid physical limits

- EV Ancillary Services provision to the Distribution System Operators / Transmission System Operators (DSOs/TSOs) (e.g real-time energy balancing) with the utilization of the EV fleets as "flexible loads" and of emerging technologies such as the Vehicle-to-Grid Technology (V2G)

In Fig. 1.3, the Smart-Charging method is presented, compared with the conventional charging methods, regarding a normal daily EV power profile [10]:

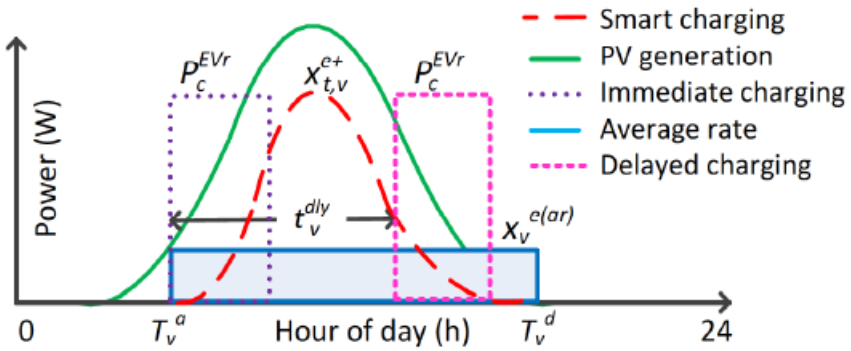

Fig. 1. 3: Daily EV power profile with the application of different charging methods [10]

Motivation

Most of the investigated smart charging algorithms treat EV charging as a static offline scheduling problem. Moreover, other researches investigate Smart-Charging as a dynamic scheduling problem, considering perfect prediction of the various data inputs for the extraction of their optimal charging results such as in [11]. However, there are certain variables of the charging optimization model, which cannot be perfectly predicted, such as the EV user driving patters, e.g the arrival and departure time of the EV users [13], [12]. Moreover, it is well-known that RES (PV) generation, that is usually an inherent part of every EV charging station, is intermittent and prone to forecasting errors. Furthermore, load variations and energy prices constitute two more non-trivial uncertainties, since neither the exact timely load nor the exact bids of the market parties can be predicted with 100% accuracy [2].

Considering the stochastic nature of the aforementioned and many other variables, integrated into the power systems: the results of Smart-Charging investigations, with no uncertainties considered, can be reasonably questioned. The validity of the results, especially of the uncontrolled common charging techniques, but of the emerging smart-charging techniques as well, can be essentially undermined and deteriorated. The importance of the impact of the potential prediction errors on the robustness of the "optimality" of existing deterministic schedulers has been shown in [11]. The authors in [11], inserted an increasing error from zero to 5% on the optimal scheduler of [14] and proved the magnitude of optimality deterioration even under small prediction errors. In Fig. 1.4, the optimal load results computed by the scheduling algorithm of [14] with 5% and without prediction error. Therefore, various uncertainty handling techniques have been proposed in order to tackle with the system uncertainties, which will be explained in Chapter 2, such as stochastic optimization (probabilistic, possibilistic), robust optimization, Information Gap Decision Theory (IGDT) etc.

1.4 Research Goal Statement, Thesis Objectives & Research Questions

Several researches have investigated the uncertainties modelling with stochastic-based approaches or robust-based approaches comparing them with the deterministic smart-charging techniques. Regarding the thesis objectives, this thesis aims to address the importance of uncertainties consideration, associated

with the EV charging methods, regarding their impact on the pioneering smart-charging algorithms and their potential management. The uncertainties considered are: PV Generation, Load Demand, EV user driving patterns (arrival time, arrival SOC, departure time) and power capacity reserves offered to the grid, with the use of Robust Optimization. On that manner, much fewer investigations have addressed the presence of so many uncertainties and combination of them, where this thesis aims to contribute to. Moreover, this thesis aims to enhance the knowledge on combining Robust Optimization with an uncertainty handling technique of another nature, called Receding Horizon Approach, which is already integrated in the benchmark Smart-Charging Algorithm. Furthermore, this thesis contributes to a development of a more robust and evolved smart-charging model, which integrates "prediction – expectation" capabilities in terms of EV user driving patterns (future – predicted EV arrivals are integrated in the optimization horizon) and "called – activated" FCR by the TSO. On the same manner, the thesis has developed a more "realistic" and robust PV Generation and Load demand forecasting curves utilization, with the use of "real" data and the RHO advantage of considering new updated real data at every re-optimization.

Finally, this thesis aims to reveal the performance and effectiveness of RO, combined with Receding Horizon Optimization (RHO), regarding the nominal algorithm objective: the minimization of the charging cost. Finally, one more aspect that the particular thesis aims to enlighten is the trade-off between uncertainty tolerance and deterioration of the algorithm optimal results, called "protection-overconservativeness trade-off", regarding Robust Optimization.

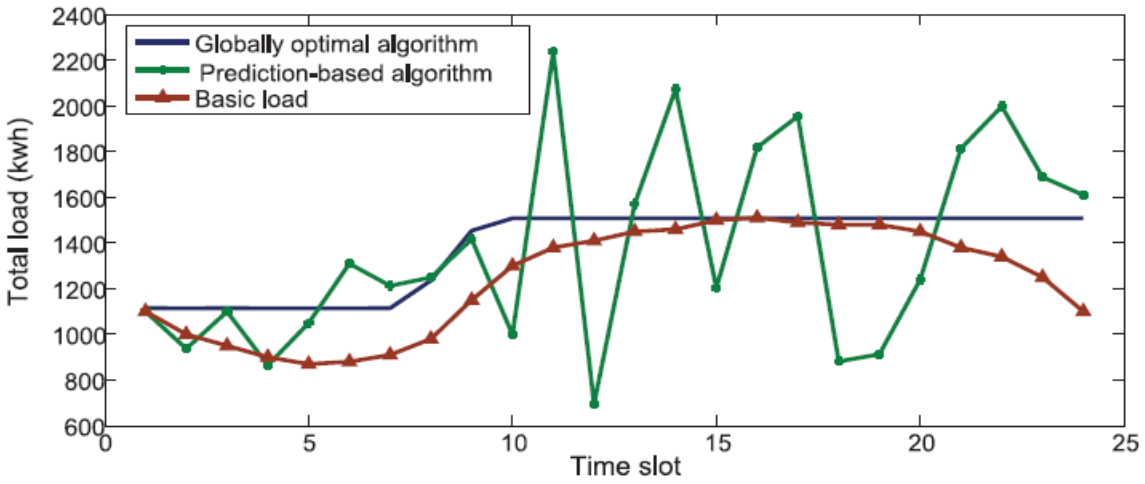

Fig. 1. 4: Optimal Load Profiles by the Globally Optimal Algorithm [14] under 100% accuracy of prediction and by the Prediction Algorithm [14] under 5% prediction error

Considering all of the above, the Research Goal Statement can be formulated as follows:

"How to address the impact and management of system uncertainties on the optimality of Smart – Charging with the use of Robust Optimization"

More specifically, the thesis will focus on the smart-charging algorithm of the "Orchestrating Smart Charging in mass Deployment" (OSCD) project, developed by the particular thesis PhD Supervisor Mrs. Yunhe Yu, under the supervision of Prof. dr. Pavol Bauer and Dr.ir. G. R. Chandra Muli [15]. The "OSCD" algorithm will serve as the benchmark smart-charging algorithm, on which Robust Optimization will be employed for the management of the various uncertainties. The

benchmark algorithm has already been evaluated in various investigations, considering however 100% prediction accuracy (no uncertainties considered). The severity of the uncertainties impact will be addressed by observing the deterioration of the benchmark algorithm optimal cost and customer charging satisfaction (EVs unfinished charging gaps) for each and every aforementioned uncertainty considered.

The Research questions, that can be derived by the aforementioned thesis objectives, can be formulated as follows:

Main Research Questions (regarding system uncertainties):

- Which system uncertainty is more crucial in terms of impact on the optimality of the smart-charging results and which system uncertainty is more robustly manageable in a Smart-Charging Algorithm, that utilizes Robust Optimization Approach and prediction capabilities?
- How to develop a Smart-Charging Mixed-Integer Linear Programming (MILP) algorithm, that can manage uncertainties robustly?
- How much can the optimality of results be deteriorated at expense of robustness, regarding each system uncertainty?

Secondary Research Questions (Regarding Robust Optimization):

- What is the performance of the RHO-RO approach (combination of RHO and RO approaches) in terms of management of uncertainties in the system?
- What is the importance of prediction capabilities in a Robust Smart-Charging Algorithm?

1.5 Thesis Outline

Finally, the outline of the particular thesis is presented below, while the flow-chart of this thesis milestones and objectives is presented in Fig. 1.5.

- **Chapter 1 Introduction:** Explanation of the research background and motivation and statement of the research objectives & questions
- **Chapter 2 Handling Uncertainty:** Summarization of the various uncertainty handling techniques from the existing literature on EV charging optimization under uncertainties.
- **Chapter 3 Robust Optimization Methodology:** The optimization model of the "Robust Smart-Charging Algorithm" is formulated mathematically. On that manner, explanation of the benchmark smart-charging algorithm with the related objectives and constraints is integrated in the particular chapter. All the considered uncertainties, apart from the regulation reserves provision which are addressed individually in Chapter 6, are taken into account in the formulation. Finally, the utilized software and optimization solver are discussed, as well.
- **Chapter 4 Management of Smart-Charging Uncertainties:** In Chapter 4, the evolution of the RHO approach of the benchmark smart-charging algorithm with the integration of RO is explained. This chapter divides this thesis investigation into two separate studies. The first study integrates analysis of the management concepts of the uncertainties: PV generation, Load demand, Arrival & Departure Times and Arrival SOC, as well as, the decision of the corresponding "uncertainty sets". The second study investigates the ancillary services (FCR reserves) that the algorithm provides to the power grid and the related uncertainty integrated. A separate study is devoted to the issue of FCR reserves provision due to its stand-alone character and distinction from the other uncertainties and the computational expense of its management.
- **Chapter 5 Study Cases & Results of the PV Generation, Load Demand & EV user patterns uncertainties' management:** Chapter 5 contains the study cases and gathered results of the

performed simulation runs for every uncertainty considered in Study 1 (PV Generation, Load Demand, arrival SOC and Arrival & Departure Time). Considering the particular uncertainties, their impact as well as the performance of RO and prediction for their management are evaluated.

- **Chapter 6 Study Cases & Results of the FCR reserves uncertainty management:** Chapter 6 contains the study cases and gathered results of the performed simulation runs for FCR reserves uncertainty, investigated in Study 2. Such as in Chapter 5, the impact of FCR uncertainty and its potential robust management are addressed.
- **Chapter 7 Summary & Discussion of Results from Smart-Charging Uncertainties management:** Chapter 7 summarizes all the results from Chapter 5 & Chapter 6. The goal of Chapter 7 is to answer the above-stated research questions, stated at Chapter 1, regarding firstly the impact and management of the various uncertainties existing in Smart-Charging and secondly Robust Optimization price & performance.
- **Chapter 8 Conclusions & Future Work Motivation:** The conclusions, related firstly with the simulation results & discussion of the 1st study and secondly with the research on FCR reserves provision of the 2nd study, are presented in Chapter 8. Furthermore, proposals for future researches are also added in the particular chapter.
- **References:** The references and bibliography of the thesis

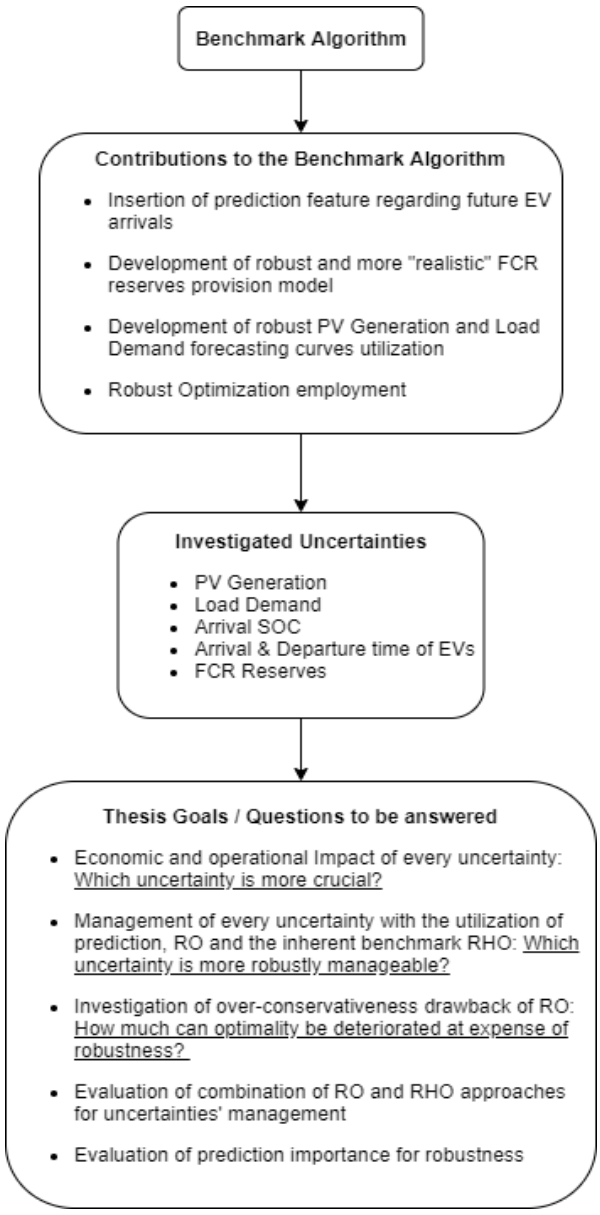

Fig. 1. 5: Flowchart of Thesis Milestones & Objectives

Chapter 2 Handling Uncertainty

2.1 Uncertainties in the Power Systems

Uncertainty is defined as the probability of deviation of the observed real value of variable from the corresponding forecasted one [16].

In the new electric power systems and in the coming years, new electric aspects and components are being constantly added up, which introduce new uncertainties in the system that should be taken into consideration. Such aspects could be the integration of Renewable Energy Sources (RES) generation, whose intermittent character aggravates the power balance between generation and supply. Considering also the uncertain behavior of the EV users, dealing with the aforementioned problems becomes even more challenging. Furthermore, the emerging bi-directional electric system with the introduction of new factors and concepts in the energy market, such as aggregators, "prosumers" and smart-loads influence the forecasting energy price value in Day-Ahead Markets (DAM) but in Intra-Day Markets, as well [13]. Moreover, if we consider the massive expected integration of EV fleets in the nearest future, the economic impact on the energy economy fluctuations will become even more important [5]. Finally, neither the various non-smart loads can be perfectly predicted, nor the potential system failures and power outages. Generally, the uncertain variables in power system studies can be divided into the 2 following main categories (see Fig. 2.1) [17].

- Technical Parameters: Consisted of the Topological Parameters (failures or outages of lines-generators-metering devices) & Operational Parameters (generation, demand)
- Economical Parameters: Consisted of the Microeconomic Parameters (unemployment rates or economic growth) & Macroeconomics Parameters (Price levels or Government Regulations)

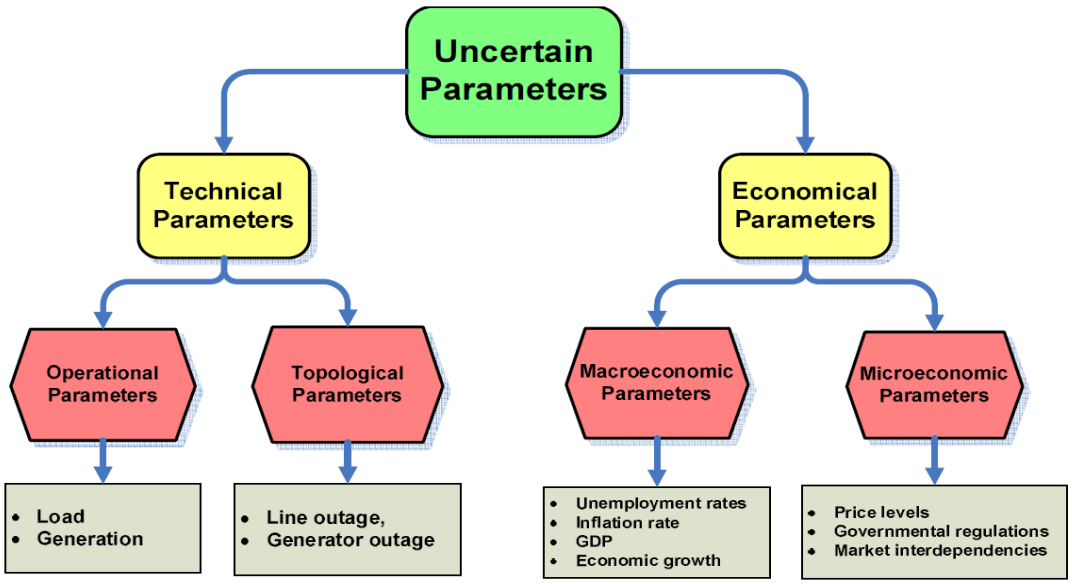

Fig. 2. 1: General Classification of Uncertain Parameters in energy system studies [17]

Most of these uncertainties become significantly evident in micro-grids such as EV charging stations. Charging stations integrate PV production with the well-known stochasticity in order to provide "green" charging energy to the customers [18], [19]. Moreover, multiple uncertainties such as the EV user's habits, e.g the EV arrival and departure times, the timely not easily predicted no-EV loads, the energy price

deviations and the inevitable system failures also characterize the charging networks. While conventional energy scheduling is arranged a day in advance with Day-Ahead Market, because forecasting errors provoke a minor impact regarding conventional grids (therefore a perfect forecast is reasonable), in EV charging stations that cannot be assumed. Hence, traditional energy generation scheduling techniques, such as Unit Commitment (UC) or Economic Dispatch (ED) are substituted in generation energy scheduling applications, that consider uncertainties. As we can see in Fig. 2.2 and it will be thoroughly explained later in the chapter, the main two approaches that can be utilized are Stochastic Optimization (S.O) & Robust Optimization (R.O) [5].

Moreover, Fig. 2.3 depicts the flowchart of a typical optimization problem, which considers uncertainties in the system [18]. As it can be seen, firstly system modelling (with optimizer) and uncertainties modelling are performed. Subsequently, the stochastic-based or robust-based optimization is initialized. Depending on the selected technique, the deterministic optimizer is called and statistical data of each evaluation results are stored, until the termination criterion is met. Finally, the reliable (or global) optimal result is computed from the stored iterations data.

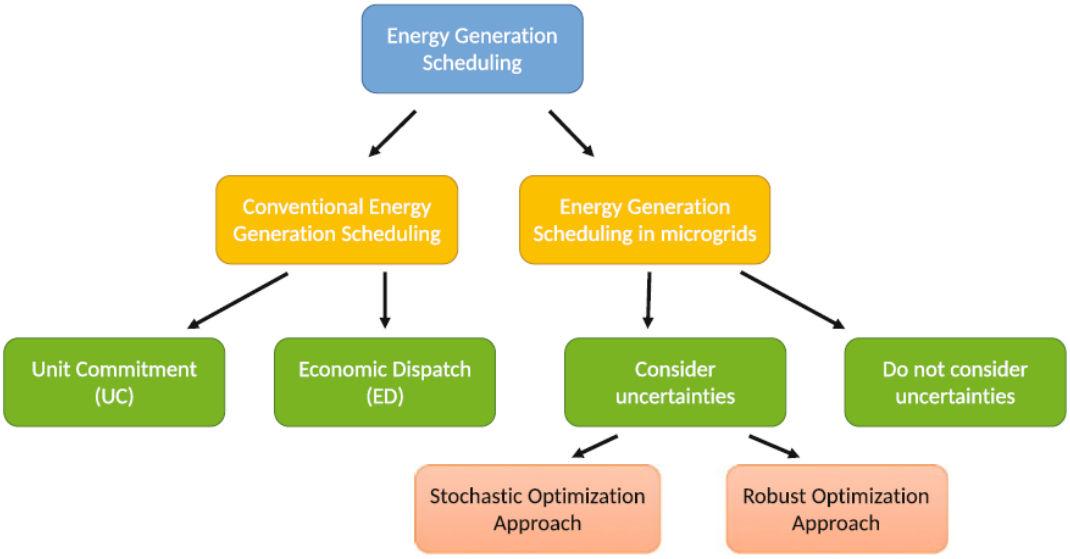

Fig. 2. 2: Overview of Energy Generation Scheduling Approaches [5]

Multiple different handling approaches have been proposed on the base of Stochastic or Robust Optimization, for dealing with uncertainties. The main existing uncertainty handling techniques, which are going to be furtherly explained in the next paragraphs, are presented in Fig. 2.4.

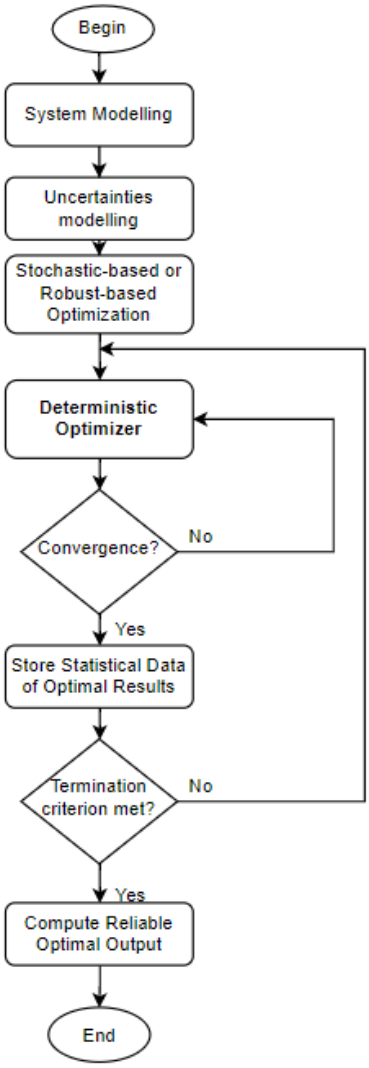

Fig. 2. 3: Flow-chart of an optimization problem considering uncertainties [18]

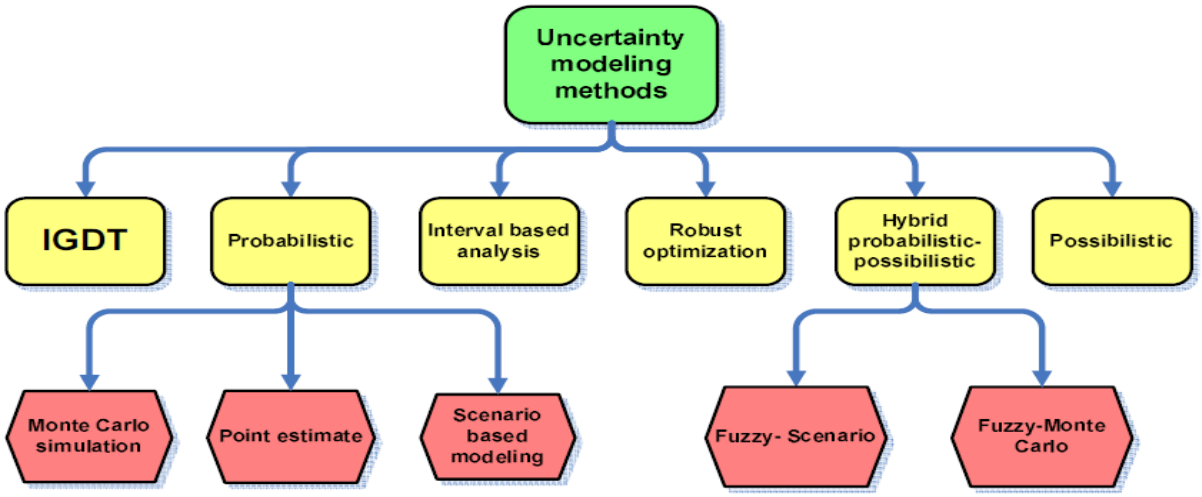

Fig. 2. 4: Uncertainty Handling Techniques [17]

Regarding Stochastic Optimization, the approaches can be mainly divided into three main categories: the probabilistic, possibilistic and hybrid probabilistic-possibilistic approaches [18].

2.2 Probabilistic Approaches

2.2.1 Introduction in Probability

Probability Density Functions (PDFs) & Cumulative Density Functions (CDFs)

The first uncertainty handling technique, which is the most commonly used, takes advantage of the probability density functions (PDFs) and cumulative density functions (CDFs), which model the uncertain discrete or continuous input random variables, respectively [18]. More particularly, the probability (or statistical) distributions of the stochastic input variables describe the results of varying a variable and the related probability of these results. They represent the distributions, which govern the stochastic variables, and are derived by a number of available historical data [20] Therefore, a pdf or a cdf provides the different probabilities, regarding the different possible outcomes of an experiment. The most commonly used distribution functions for continuous variables are Uniform, Normal, Gamma, Exponential, Beta, Weibull and Pareto distributions, while the most common for discrete functions are Bernoulli, Binomial, Discrete uniform, Geometric & Poisson distributions [20].

Identification of PDFs from available historical data sets: Fitting Routines

Firstly, a small introduction is presented about the various ways, that can be implemented, in order to identify the distribution of an input variable utilizing the related historical data set (distribution fitting). Various different numerical methods have been proposed for the extraction of the corresponding probability distributions when historical data is available, which are called "fitting routines". Their purpose is mainly to identify the most appropriate distribution for every stochastic variable [20]. The most important distribution fitting routines are summarized below:

→ Method of Maximum Likelihood (ML)

The particular method aims to identify the distribution parameters, from which the data are more likely to arise, considering that the derived data from the PDF are independent and identically distributed. ML method is asymptotically unbiased, meaning that the method bias is close to zero as the sampling data approach infinity. Moreover, it is considered to be asymptotically efficient, meaning that no unbiased estimator has lower mean squared error than ML.

→ Method of Moments (ME)

This method combines observed sample moments with unobserved moments, derived by theoretical equations, in order to perform estimation for various distribution parameters such as mean, variance and median. The most important advantage of ME is that the ME can be easily calculated by hand, whereas the relative ML estimators may be intractable even with the use of computers. However, ML estimating parameters are more likely closer to the real quantities and ME may provide estimates outside the parameter and cannot be utilized.

→ Nonlinear Optimization

Utilizing as decision variables the unknown parameters of a distribution and as objective functions the minimization of Goodness-Of-Fit Statistics or the sum-squared difference of the sample moments (mean, variance, skewness, kurtosis), Nonlinear Optimization can be used for the estimation. However, it needs more time and it is considered as less efficient.

Goodness-Of-Fitness Statistics (GOF): evaluation of distribution fitting

After having fitted the data from the historical sets in distribution functions, creating the relative PDFs of uncertainty variables, GOF Statistic measures can be used for the evaluation of the performance of the fitting routines for the probability distributions. GOF Statistics perform as evaluation tests of the validity of the formerly created PDFs in order to provide acceptance criteria, before the corresponding PDF is used in the optimization problem. They can be used in various software and the most well-known are the following:

- Chi-Square Test
- Empirical Distribution Function (EDF) Statistics
  - Kolmogorov-Smirnov Statistics (KS)
  - Quadratic Statistics
  - Cramer-von Mises Statistic
  - Anderson-Darling Statistic (AD)

Most Common PDFs of various power system uncertain parameters

Regarding electric power systems such as the EV charging stations the most common distribution functions used for the usual uncertain parameters are: [18]

- Load (power system planning and operation studies): Gaussian PDF with mean the forecasted value
- Wind Power Generation: Weighbull PDF
- Photovoltaic Generation: Beta distribution function which mainly characterize the solar irradiation
- Electricity Price: Gaussian PDF with mean the forecasted price value

2.2.2 Monte-Carlo Simulation (MCS)

The most common method for handling uncertainties in power system is called Monte Carlo Simulation and utilizes repeated sampling in order to extract the results via statistical analysis [20]. It is related with random experiments, elaborating on the "what-if analysis" and it can be expressed as follows: [18]

$y = f(X, Z)$, where:

X: set of uncertain input variables
Z: set of decision variables
y: system output

Therefore, extracting random values from each probability distribution of each stochastic variable, a set of output variables is derived from a set of input variables using the corresponding input-output relationship, while the termination criterion is not met. This set of output variables represents a specific resulting scenario from each simulation run. Summing up all the outcome scenarios from the total of the simulation runs and performing statistical analysis on the output values (e.g std: standard deviation calculation), the method proceeds to the final decision-making and characterization of the objective output variation. Hence, the mean of objective values is finally considered as the merit of the individual outcome. The pseudocode of the MCS method can be seen below:

MCS pseudocode

Generate sample $X_{e,i}$ using PDF of uncertain decision variables
Calculate $Y_{e,i} = f(X_{e,i}, Z)$

$$me = \sum_{i=1}^{n} Ye, i \tag{2}$$

$$std = \sqrt{\sum_{i=1}^{n} \frac{(Ye, i - me)^2}{n}} \tag{3}$$

It is evident that as the used samples of the stochastic variables and the simulation runs increase, the accuracy of the method is increased. However, the computational burden of the MCS increases as well. While MCS represents the most simply-structured method for handling uncertainties, it is considered to be computationally expensive, since it needs to consider k^n different scenarios for all the possible different outcomes of the input random variables for validity of the results, where: n the number of the uncertain variables & k the samples used for each uncertain variable. Hence, the MCS computation burden is defined as $O(k^n)$. However, several methods have been introduced for the reduction of the computational burden of MCS. Some of the most commonly known are [17]:

- Latin Hybercube Sampling (LHS)
- Sample-Splitting Approach
- Fission & Roulette Method

In [22] MCS has been performed in order to generate different scenarios for various uncertainties such as the feeder load profiles, the time of EV charging and the battery initial SOC. In [23], the EV user charging habit has been modeled by Binomial distribution and the EV uncertainty charging demand has been addressed by MCS. Various advances in sampling techniques regarding Monte Carlo Simulation has been introduced in [24], as well.

2.2.3 Scenario-based Approach (SBA)

The SBA method represents another probabilistic approach, which deals with uncertain parameters. The SBA concept basically relies on the division of the stochastic variable PDF in a number of regions. Each i region represents a particular scenario i with a corresponding probability P_i, while each region is denoted with the value X_i. X_i is the average value of the lower and upper bound of each region and the sum of all scenarios' probabilities P_i is unity. Finally, the value of the expected output variable is derived by equation (4): [18]

$$y = \sum(Pi * Xi), where: \mathrm{i} = 1, 2, \ldots, \mathrm{K}\ (\text{PDF regions} - \text{scenarios}) \tag{4}$$

In [25], a 2-stage scenario-based approach has been proposed in order to control the multi-objective dynamic systems motion where the relative position of the objects plays the most important role. More specifically, the SBA changes the formation of an Unmanned Aerial Vehicles (UAV) group from an arbitrary initial state to a specific required minimizing the sum of all UAV paths. In [26], the airport apron capacity is robustly estimated by a scenario-based optimization approach taking uncertainties into consideration, such as weather or taxing time. Furthermore, the SBA has been used for a network reconfiguration-framework after a complete black-out, maximizing the total number of nodes

to be restored and minimizing the total charging capacitor of the restoration paths. The SBA has been proposed in order to deal with the uncertainties of the transmission lines (Tls) [27]. More specifically, the two objective functions are the following equations (18) & (20):

$$\max(f1) = \sum_{s=1}^{\Omega} P(s) * \sum_{i=1}^{\Psi} Vi \tag{5}$$

$$\min(f2) = \sum_{s=1}^{\Omega} P(s) * \sum_{Cij=1}^{\Phi} Cij \tag{6}$$

where V_i: the total restored number of nodes to maximized

C_{ij}: the total charging capacitor of restoration paths to be minimized

s: the total number of possible scenarios

$P(s)$: the probability-weight of each scenario considered

As it can obviously be seen the accuracy increases with the increase of the number of scenarios considered and the SBA method has the same computational burden as MCS (k^n). However, a very large number of scenarios can be reduced by selecting a smaller number of scenarios which can represent the original one ($\Omega_s \subset \Omega_i$). Nevertheless, the trade-off between loss of data and computational burden reduction must be thoroughly investigated. Below, the scenario reduction technique is presented:

Scenario Reduction Technique

Construct Probability Distance Matrix (consists of the distance between each pair $c(s, s')$ of probability π_s)

Select the first scenario s_1:

$$s_1 = \arg\{min_{s' \in \Omega_j} \sum_{s \in \Omega_j} \pi_s c(s, s')\} \tag{7}$$

$$\Omega_{s=\{s_1\},}\ \Omega_j = \Omega_j - \Omega_s \tag{8}$$

Select the next scenario for Ω_s:

$$s_n = \arg\{min_{s' \in \Omega_j} \sum_{s'' \in \Omega_S \cup \{s\}} \pi_s c(s, s'')\} \tag{9}$$

$$\Omega_j = \Omega_j - \Omega_s, where: \Omega_s = \Omega_S \cup \{s_n\} \tag{10}$$

If cardinality of Ω_s is sufficient, select next scenario. Else continue.

Add the probability of each non-selected scenario to its closest scenario in the selected set & End. [17]

2.2.4 Point Estimate Method (PEM)

Despite the simple structure and satisfying accuracy of the two previous handling uncertainty methods, the disadvantage of the computational expense cannot be ignored, especially in the multi-objective smart-charging optimization field. The PEM method has been frequently used in order to

handle uncertainties in power systems, elaborating on the "moments" of the uncertain input variables and producing the corresponding PDFs of the output variables of the problem [18].

Therefore, avoiding the computational expense of the MCS/SBA and the simplifications/assumptions of the analytical-deterministic solutions, PEM provides deterministic routines for solving optimization problems computationally inexpensively without the need of perfect knowledge of the corresponding PDFs. On the contrary, only the mean, variance, skewness & kurtosis of the distributions of the stochastic variables are needed. Multiple PEM schemes can be used for the realization of the PEM method, most of them summarized in Table 2.1 [28].

Table 2. 1: Qualitative Description of Different PEM Schemes

Method's author	Number of Simulations	Efficiency in Large Scale	Ability To Handle	
			Correlated variables	Asymmetric variables
Rosenblueth	2^m	Very Low	Yes	Yes
Li	$O(m^3)$	Low	Yes	Yes
Harr	$2m$	High	Yes	No
Hong	$Km\ or\ Km+1$	High	No	Yes

From the aforementioned methods, the first PEM scheme requires great computational expense, very often even greater than the corresponding computational burden of MCS. Li's method reduces the required number of simulation iterations, however the efficiency of the method still remains significantly lower than the MCS efficiency. Harr method accomplishes to minimize the computational expense, however only symmetric stochastic variables can be used for the realization of the method. Finally, Hong's PEM scheme of $K * m$ or $K * m + 1$ simulation iterations achieve the required efficiency, accuracy and low computational expense, where K: the evaluation "moments - concentrations" and m: the number of the stochastic input variables of the optimization problem. The Hog's different usable schemes are the following:

- 2m Scheme ($K = 2$)
- 3m Scheme ($K = 3$)
- 2m + 1 Scheme ($K = 2$)
- 4m + 1 Scheme ($K = 4$)

The first method uses only 2 concentrations for each stochastic variable and while providing simplicity, the most important drawback of the particular scheme is the probability of the variable "moments" relying on regions of the PDF that are unknown, or even out of it. This drawback accompanies all $K * m$ schemes, while the $K * m + 1$ schemes avoid it keeping the computational expense low (especially the $2m + 1$ Scheme needs only 1 more iteration!). The $4m + 1$ is similarly accurate and efficient, however the number of simulation iterations is increased considerably. Therefore, only the $2m + 1$ scheme will be explained below. [28], [29]

PEM $2m + 1$ Scheme

- The statistical information of each random input variable is concentrated in K points for each variable, named "concentrations"
- The kth concentration of each variable is the pair $(p_{l,k}, w_{l,k})$, where $p_{l,k}$ is the location (value) of the random variable and $w_{l,k}$ the weight (relative importance) in the kth point
- The optimization function has to be evaluated only $K = 2$ times using the $p_{l,k}$ value of the l

variable at the k point and the $m-1$ mean values of all the rest input random variables $(\mu_{p_1}, \dots, p_{l,k}, \dots . \mu_{p_m})$

- Until the previous step, the procedure is the same as in the $2m$ Scheme. The $2m\ +\ 1$ scheme takes into account one more iteration considering the mean values of all the random variables $(\mu_{p_1}, \dots \dots \dots, \mu_{p_m})$
- Determination of $p_{l,k}\ =\ \mu_{p,l}\ +\ \xi_{l,k}\ *\ \sigma_{p,l}$, where $\mu_{p,l}$ & $\sigma_{p,l}$: the mean and standard deviation of the p_l variable and $\xi_{l,k}$: the standard location of the variable at the particular point
- Standard location $\xi_{l,k}$ and weight $w_{l,k}$ computation is derived by equations (11) & (12) respectively:

$$\sum_{k=1}^{K} W_{l,k} = \frac{1}{m} \tag{11}$$

$$\sum_{k=1}^{K} \left(W_{l,k} * \left(\xi_{l,k}\right)^j \right) = \lambda(l,j), \qquad j\ =\ 1, \dots, 2K\ -1 \tag{12}$$

where:

$$\lambda(l,j) = \frac{Mj(pl)}{\sigma(pl)^j}\text{: the jth standard central moment of the random variable } p_l \tag{13}$$

$$Mj(pl) = \int_{-\infty}^{\infty} \left(p_l - \mu(p_l)\right)^j f(p_l) d(p_l) \tag{14}$$

f(pl): the probability density function of p_l

- For the $2m\ +\ 1$ PEM Scheme and with the aforementioned NL problem solved by the Miller & Rice procedure, which integrates equations (15), (16) & (17).

$$\xi_{l,k}\ =\ \frac{\lambda(l,3)}{2} +\ (-1)^{3-k} \sqrt{\lambda(l,4) - \frac{3}{4} * \lambda(l,3)^2}\ for\ k = 1,2\ \&\ \xi_{l,3}\ =\ 0 \tag{15}$$

$$w_{l,k}\ = \frac{(-1)^{3-k}}{\xi(l,k) * [\xi(l,1) - \xi(l,2)]}\ for\ k\ =\ 1,2 \tag{16}$$

$$w_{l,3} = \frac{1}{m} - \frac{1}{\lambda(l,4)\ -\ \lambda(l,3)^2} \tag{17}$$

- For the final simulation iteration at the point $(\mu_{p_1}, \dots \mu_{p_m})$, the following weight is used derived by equation (18):

$$W_0\ =\ \sum_{l=1}^{m} w(l,3) = 1 - \sum_{l=1}^{m} \frac{1}{\lambda(l,\ 4)\ -\lambda(l,3)^2} \tag{18}$$

The flow diagram of the PEM algorithm is presented in Fig. 2.5 [28]. As it can be seen, the

deterministic power flow $Z(l,k)$ is solved only $K*m$ $(or\ K*m\ +\ 1)$ times depending on the number of the stochastic variables and the points-concentrations considered.

- The final step is the computation of the statistical output information which is described by the equation (19):

$$\mu_j = E\left[Z^j\right] = \sum_{l=1}^{m} \sum_{k=1}^{K} w_k * \left(Z(l,k)\right)^j \tag{19}$$

PEM method has been proven a remarkable tool for handling uncertainties in various researches so far. In [28], different PEM schemes have been proposed in order to cope with the uncertainties, related with the generation units (binomial distribution) and load demand active and reactive powers (normal distributions). In [29], PEM has been used for the same reason for Smart Distribution Systems considering Demand Response Programs, while in [30] we can see PEM handling wind speed and load demand uncertainties in a multi-objective problem, regarding Distribution System Planning. PEM can be utilized in combination with other stochastic methods, such as in [31], where PEM is applied for modelling wind power and solar power uncertainties whereas Robust Optimization is used for the load demand uncertainties.

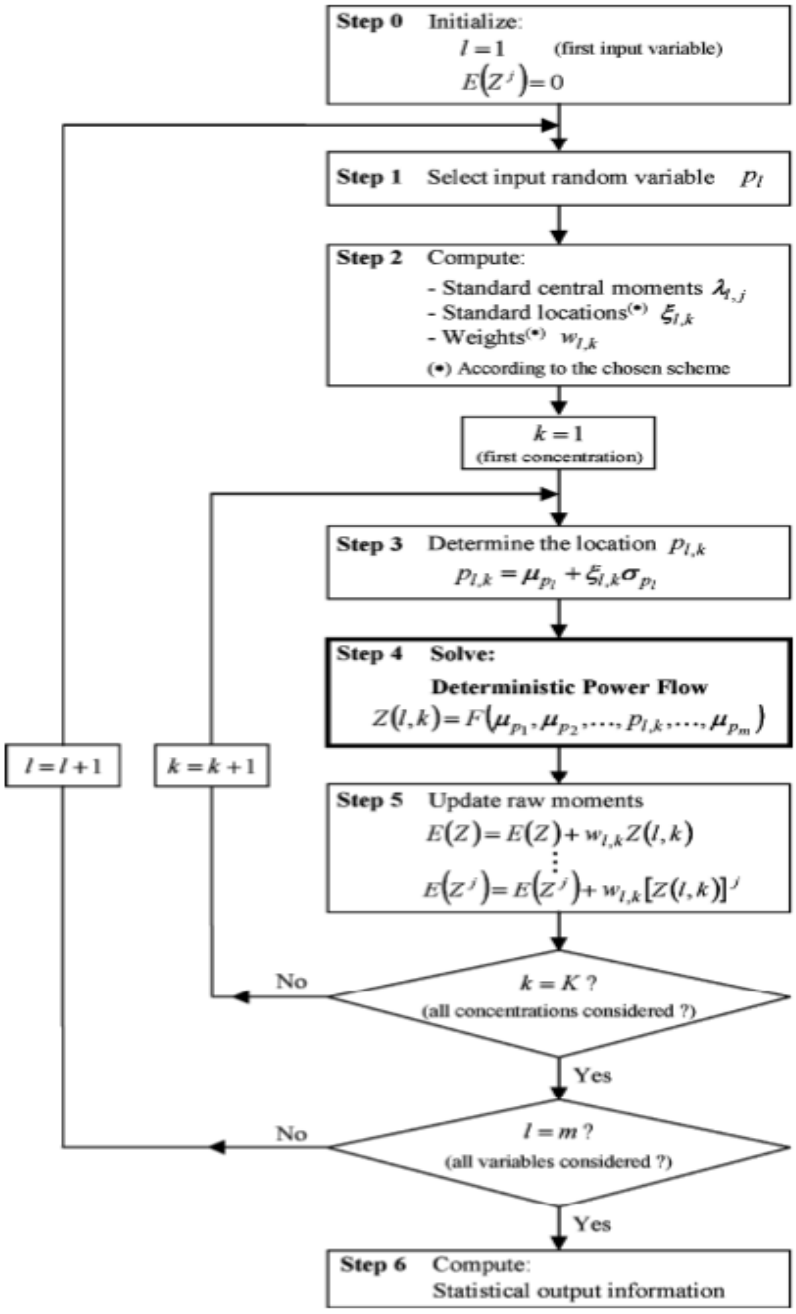

Fig. 2. 5: Flow Diagram of PEM algorithm [28]

2.3 Possibilistic Approaches

Apart from probabilistic uncertainty modelling, the possibilistic approaches represent another modelling method of uncertainty in power systems. More specifically, it is more commonly used when no or little data is available about the random input variables, which are modelled by appropriate "fuzzy membership functions". These functions combined with "a-cut method" provide the fuzzy membership function of the output variable. Hence, "a-cut method" is defined as the method used in order to transform a fuzzy membership function to the main concept of the application, acting as a bridge between the fuzzy optimization theory and the practical application which needs to be modelled [32]. Finally, a

defuzzification strategy is needed for the extraction of the final output value [33]. The first formulation of fuzzy optimization has been realized in "Decision-Making in a Fuzzy Environment: [33] by Bellman & Zadeh in 1970s. Moreover, the subsequent works of Zimmermann set the fundamental basis of fuzzy optimization theory and applications [34].

Brief Explanation of Fuzzy Optimization

Solving an optimization problem in a fuzzy environment consists of the fuzzy modelling and fuzzy optimization. While the former is responsible for building a fuzzy model with the use of the fuzzy information, the latter applies the fuzzy optimization techniques to solve the problem, based on the fuzzy memberships or possibility distribution functions of the fuzzy info [35].

While a classical crisp-deterministic set of values can be defined listing all the possible values that belong to the set or defining membership conditions, various levels of membership are defined for every element of a given "fuzzy set". More specifically, a fuzzy set can be defined as follows:

If X a set of objects denoted by x, then a fuzzy set $\tilde{A}$ in X is a set of ordered pairs:

$$\tilde{A} = \{(x, \mu_A(x)) | \, x \in X\}, \text{ where:}$$

$\mu_A(x)$: membership function (or degree of truth) of x in $\tilde{A}$, which locates x at membership space inside $\tilde{A}$. The membership function is a subset with non-negative real numbers with a finite supremum [36]

The whole fuzzy optimization procedure can be summarized in the following 7 stages [35].

1) Problem Understanding: States, goals and constraints of the system with the corresponding relationships between them, are defined and expressed by sets
2) Fuzziness analysis: Represents the stage in which the analysis and summary of the possible fuzzy information-elements, that are involved in the problem, takes place
3) Fuzzy Model development: Mathematical tools and relationships are utilized in order to construct the appropriate fuzzy optimization model. The model can be formed as fuzzy (N)LP programming, fuzzy dynamic programming, fuzzy multi-objective programming etc.
4) Fuzzy information description and formulation: Represents the stage of transition from fuzzy modelling to fuzzy optimization. Applying fuzzy mathematics, the quantification of the fuzzy information (identified in stage 2) is performed with the use of appropriate tools and theory and fuzzy membership functions are developed for every fuzzy variable
5) Transformation of the fuzzy optimization model to an equivalent crisp optimization model, which mainly integrates the stages of optimal solution determination, interpretation and transformation. It must be noted that for a specific fuzzy model, various deterministic models can be generated according to the selected optimal solution and interpretation. This step is called "Defuzzification"
6) Solution of the deterministic model: By applying appropriate optimization techniques and algorithms (e.g common heuristic algorithm or smart optimization techniques), the approximate deterministic model, derived by the fuzzy model, is solved
7) Validity examination: The optimal solution of stage 6 must be evaluated. If it is unreasonable, the fuzzy modelling process or the optimization technique (or both) can be improved by iterations.

Classification of fuzzy mathematical programming problems

The Fuzzy Mathematical Programming FMP (or Fuzzy Optimization Problem) can be generally expressed with equation (20):

$$f(x,r) \rightarrow max$$
$$s.t.\, x \in C = \{x \in X = |\mathrm{gi(x,s)} \leq 0, \mathrm{i} = 1,.2,\ldots \mathrm{m}\} \quad (20)$$

where C: the system of fuzzy constraints

The fuzziness may appear in various forms, such as a fuzzy goal (a goal expressed vaguely), fuzzy constraints (constraints expressed with tolerances) or fuzzy coefficients in the objective function and constraints. On that manner, various different fuzzy problems' formulations can be derived which introduce fuzziness either in the goal and/or in the objective function coefficients and/or in the optimization constraints. The various fuzzy optimization problems can be solved with various approaches (depending on the fuzzy type) such as symmetric or asymmetric approaches, possibility and necessity measure-based approaches, the interactive satisfying solution approach, the Angelov's generalized approach, the fuzzy genetic algorithm, the penalty-function based approach etc [35].

The most important benefit of fuzzy optimization is that it can generate deterministic (crisp) solutions from uncertainties maintaining balance between efficiency and effectiveness, without the need of known historic PDFs of the random input variables in advance [37]. While the probabilistic approaches can indeed deal with specific uncertainties, there is a variety of imprecisions that cannot be covered probabilistically. Such imprecisions can be related with inexactness, ill-definedness or vagueness and refer to uncertainties about the exactness of concepts, correctness of judgements and degree of credibility. These uncertainties are not strongly related to the occurrence of events and distribution functions of the random variables (if available) can be meaningless or misleading regarding the extraction of valid conclusions [38].

However, the main challenges, that are accompanied with the fuzzy techniques, are the well-stated formulation and interpretation of the fuzzy optimization model, in order to apply the fuzzy optimization in the specific practical problem. Moreover, a very important question that arises is:

"How can the Membership Function (MF) of the output y be determined when only the MFs of the uncertain input X are known?"

The solution can be provided by the α-cut method [39]. For a given fuzzy set $\tilde{\tilde{A}}$ in U, the crisp set A^a (from which the a-cut of each uncertain variable x_i^α is identified) is defined as:

$$A^a = \{x \in U \,|\mu_A(x) \geq a\} = (A^a, \overline{A^a}) \quad (21)$$

The α-cut of output y (y^α) is calculated as:

$$y^\alpha = (y^a, \overline{y^a})$$
$$y^\alpha = \left(\min_{X^a} f(X^a), \max_{X^a} f(X^a)\right) \quad (22)$$

In each α-cut, the upper and lower bounds of y^α are maximized & minimized respectively until the defuzzification process [17].

2.4 Hybrid Probabilistic-Possibilistic Approaches

When there is availability of some of the random input variables, these variables can be modelled probabilistically, whereas the others with unknown historical data can be modelled possibilistically with fuzzy membership functions. These approaches are named as "Hybrid Probabilistic-Possibilistic" [18]. For example, a hybrid approach has been used in [40], combining the SBA method with the fuzzy arithmetic technique, in order to address the effect of operation of Distributed Generators (DGs) in Distribution Systems (DS) under uncertainties. While wind power generation has been modelled probabilistically due to known distribution, the decisions of the DG owners and the loads have been modelled with fuzzy trapezoidal membership functions. In this regard, the load demand modelling has been expressed by the following fuzzy trapezoidal equation (41):

$$\widetilde{S_{i,t}^{D}} = \left(1 - D_u, 1 - \frac{D_u}{2}, 1 + \frac{D_u}{2}, 1 + D_u\right) S_{i,t}{}^{D}(1 + \varepsilon_D)^2 \tag{23}$$

Where $S_{i,t}^{D}$: the forecasted load apparent power at bus i and year t

ε_D : the annual demand growth rate &

D_u: the uncertainty factor of load

Two common Hybrid Probabilistic-Possibilistic Approaches are presented below: the Possibilistic-MCS approach & the Possibilistic-SBA approach [17].

2.4.1 Possibilistic-MCS Approach

For each $z_i \in Z$, generate a value from the corresponding PDF: z_i^e

Calculate the upper and lower bounds of the α-cut output y as (24):

$$\begin{aligned} \underline{(y^\alpha)^e} &= (\min f(Z^e, X^\alpha) \\ \overline{(y^\alpha)^e} &= \max f(Z^e, X^\alpha) \end{aligned} \tag{24}$$

Repeat until statistical data, such as PDF of the output value, is obtained

2.4.2 Possibilistic-SBA Approach

Generate the original scenario set describing the uncertain variables vector Z: Ω_J

Apply scenario reduction technique to obtain Ω_s

Calculate the upper and lower bounds of the α-cut output y as (25):

$$\begin{aligned} \underline{(y^\alpha)^e} &= \min \sum_{s \in \Omega_s} \pi_s * f(Z_s, X^\alpha) \\ \overline{(y^\alpha)^e} &= \max \sum_{s \in \Omega_s} \pi_s * f(Z_s, X^\alpha) \end{aligned} \tag{25}$$

De-fuzzify the output y

2.5 Robust Optimization

As already stated, various uncertainties shall be considered, when dealing with a real-world design or optimization problem. Most of them can be categorized as follows [42]

- Changing Environmental & operating conditions
- Production tolerances and actuator imprecision (the real-optimal parameters of the integrated components of a system are never absolutely certain)
- Uncertainties in the system output & performance
- Feasibility uncertainties (related to the fulfillment of constraints that the system must provide)

Moreover, uncertainties can be mainly divided to random (or aleatory) and epistemic uncertainties. Regarding the former category, the stochasticity is intrinsically irreducible, meaning that they are of physical nature and cannot be avoided. On the contrary, epistemic uncertainties are risen by the lack of knowledge of the designer about the problem confronted. Therefore, these uncertainties can be minimized as far as possible.

When a deterministic optimization problem needs to take uncertainties under consideration, either stochastic or robust optimization shall be applied. Apart from stochastic approaches (Probabilistic, Possibilistic, Hybrid (reader referred to [43], [44]), another way of dealing with the various uncertainties integrated in an optimization problem, is Robust Optimization (RO). Stochastic Optimization provides effective results if a well-known PDF of the uncertain variable is available [45]. However, even with the use of possibilistic solutions which rely less on the variables' PDFs, a vast number of different scenarios should be performed for the extraction of valid and accurate results, apart from the already discussed PEM. Already having mentioned multiple uncertainties integrated in an electric power system, such as an EV charging station, the complexity and computational burden of the optimization problem rapidly escalates with the increase of the input random variables considered [41], [45]. Moreover, due to the various complex operation details and practical constraints in practice, the perfect distribution function of a variable can never be acquired, compromising the optimal solution of the stochastic-based energy scheduling [45]. All of the above may deteriorate the reliability of the problem optimality.

Robust Optimization intends to overcome the aforementioned limitation of the stochastic approaches. It originates from the novel highly influential work of G. Taguchi on robust design optimization [46]. However, due to the emerging high-speed computers, Robust Optimization has gained attention in the past few decades [42]. More specifically in RO, instead of the use of deterministic values or PDFs. the stochastic variables are represented by uncertainty sets, in which the variables can receive values. Therefore, only the lower and upper limit of the set of possible random values are needed for every variable [47]. Some of the RO advantages are summarized below [45]:

- Elimination of the need of the variable PDF, offering a distribution-free problem formulation to deal with the uncertainties, using only some limited historical data that can easily be obtained
- Consideration of the worst-case operation scenario during the modelling process, providing immunity of optimality under realization of all possible scenarios in practice.

Robust Optimization Formulation

A typical robust formulation of a problem with a linear-form objective function is presented below (26) [45]:

$$\{min\{c^T * x : Ax \leq b\}, \qquad (c, A, b) \in U\} \tag{26}$$

where:

$x \in R^k$: vector of decision variables

$c \in R^k$: vector of coefficients

A_{mxk} & $b \in R^m$: coefficients for the constraints

When Robust Optimization is worst-case oriented, the robust optimal solution should be feasible and meaningful for every (c, A, b) from the uncertainty set U. Therefore, the final robust solution optimizes the worst-case value of the aforementioned equation and is formulated as the following minmax problem (48):

$$min\{sup\ c^T * x: Ax\ \leq\ b, \qquad \forall\ (c, A, b) \in U\} \tag{27}$$

which is equivalent to the following optimization LP (28):

$$min\{\varepsilon: c^T * x \leq \varepsilon, Ax\ \leq\ b,\ \ \forall\ (c, A, b) \in U\} \tag{28}$$

which is called the "robust counterpart of the original LP optimization problem and the minimum value of ε represents the worst-case scenario. The inner max problem is transformed to its related dual min problem, based on the "duality theory", whose main characteristics are presented in Table 2.2 [36].

In several investigations, such as in [49], a parameter Γ has been introduced which represents the maximum total forecasted error that can be tolerated. As Γ increases, the conservativeness-robustness of the decision-making problem increases as well. This is justified by the fact that a higher selected value of Γ broadens the uncertainty set U. Consequently, the value of the random variable is more likely to belong to the corresponding uncertainty set and the optimization problem becomes more robust. However, this usually comes at expense of a higher optimal minimum cost of the objective function [47], [49]. All of the above will be explained extensively in Chapter 3.

Table 2. 2: Relationship Between Primal & Dual Problem

Primal Problem			Dual Problem
Objective Function	To maximize	Objective Function	To minimize
Variable Bound	≥ 0 free ≤ 0	Constraint Type	≥ 0 = 0 ≤ 0
Constraint Type	≤ 0 = 0 ≥ 0	Variable Bound	≥ 0 free ≤ 0

Despite the aforementioned advantages, Robust Optimization is characterized by two main challenges [48]:

1) The reformulation (or the approximation) of the robust counterpart of the original optimization problem is not always "computationally" tractable
2) The specification of appropriate and reasonable uncertainty sets U for the specific application constitutes often a significant challenge

It must be noted that the predecessor of RO is called "interval analysis" approach. In this method, every random input variable receives values within a specified interval. The output of the objective function y is a multivariate function, while the lower and upper bounds of every input x_i random variable are known. The goal is the identification of the lower and upper bound of the method's output [17].

2.6 Information Gap Decision Theory (IGDT)

IGDT represents another handling uncertainty technique and is the most commonly used approach for uncertainties, for which no historical data is available (PDFs, Membership Functions, Interval of

uncertainties e.g lower & upper bounds) [18]. While it also belongs to the robust-based optimization approaches, it usually results in more conservative solutions than RO, therefore it is utilized mostly for severe uncertainties' cases. Below, a typical optimization problem formulation is presented (28): (X: random input variables & Z: degrees of freedom)

$$\begin{gathered} y = f(X,Z) \\ \text{s.t. } G(X,\ Z) \le 0 \\ H(X,Z) = 0 \end{gathered} \tag{28}$$

During the first step, no forecasting error is considered assuming 100% accuracy of the uncertain variables $\ddot{X}$, while the optimal output y is represented by $\dot{y}$ (optimal objective value under no prediction error). Regarding the next steps of the solving procedure, the IGDT models are divided to "Risk-Averse IGDT models" & "Risk-Seeking IGDT models"

Risk-Averse IGDT Modelling

In Risk-Averse IGDT models, the goal is the identification of a solution, which is robust-immune under prediction errors of the stochastic variables. Therefore, the IGDT model intends to maintain the value of the objective function below a predefined threshold I_c and independent from the distance of the occurring values of the uncertain variables from the nominal ones. The above-stated optimization problem is transformed to (29):

$$\begin{gathered} y = f(X,Z) \le Ic \\ Ic = \delta * \dot{y} \\ \delta = 1 + \varepsilon \\ \text{s.t. } G(X,\ Z) \le 0 \\ H(X,Z) = 0 \end{gathered} \tag{29}$$

Moreover, equation (30) dictates the uncertain variables X:

$$\begin{gathered} X\ \in U(a,\ddot{X}) \\ U(a,\ddot{X}) = \left\{ X \left| \frac{X - \ddot{X}}{\ddot{X}} \right| \le a \right\} \end{gathered} \tag{30}$$

Where ε: the level tolerance of the objective deviation from the forecasted value & α: the uncertainty horizon of X.

Therefore, decisions of the variables Z depend on the minimum value of the threshold I_C and the maximum value α, for which the decision maker is sure that none of the constraints is violated. The final optimization problem formulation of the Risk-Averse IGDT Model is transformed to (31) and is presented below:

$$\begin{gathered} Maxa(Ic,Z) \\ \forall\ X \in U(a,\ddot{X}) \\ f(X,Z) \le Ic \\ Ic = \delta * \dot{y} \\ G(X,Z) \le 0 \\ H(X,Z) = 0 \end{gathered} \tag{31}$$

Risk-Seeking IGDT Modelling (Opportunistic)

On the contrary, a risk-seeking IGDT model seeks to provide the decision-maker with the lower required deviation from the forecasted value of the random input variable, which achieves at least the I_w value as optimization objective. The Risk-Seeking IGDT formulation is presented below in (32):

$$\begin{gathered} target\ performance: Iw = \gamma * \dot{y}, where\ \gamma\ > 1 \\ Mina(I_w, Z) \\ \forall\ X \in U(a, \ddot{X}) \\ f(X, Z) > I_w \\ G(X, Z) \leq 0 \\ H(X, Z) = 0 \end{gathered} \tag{32}$$

The mechanism description of the IGDT uncertainty handling method is presented in Fig. 2.6. The two different IGDT agents can be seen, the risk-averse and the risk seeker. While the risk-averse agent's goal is to find the optimal degrees of freedom which lead to maximization of the tolerance of uncertainty, the risk-seeker agent to find the optimal degrees of freedom to increase the chance of reduction of the objective function output (optimization objective to be minimized) [50].

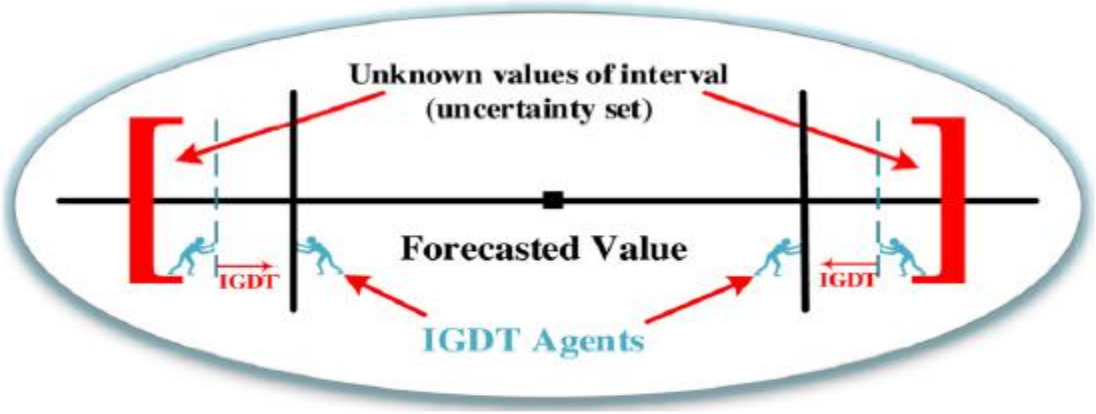

Fig. 2. 6: Description of IGDT method for handling severe uncertainty [50]

Multiple researches have investigated the use of IGDT method, taking advantage of its efficiency and capability of handling severe uncertainty. In [51], IGDT has been used to model the price uncertainty in a project of intelligent EV charging with the use of an EV aggregator considering both (V2G) and (G2V) capabilities. In [52], the uncertain RES generation has been modelled by the IGDT approach for the optimal operational scheduling of a Microgrid (MG) with Distributed Energy Resources (DERs), participating in energy and reserve markets.

2.7 "Z-Numbers" Uncertainty Technique

The most recent and promising handling technique was introduced by Zadeh in 2011. The Z-numbers are expressed as pairs $Z = (A, B)$, where A is usually a fuzzy set and B represents the certainty degree, expressed by a PDF or a fuzzy set. Both A & B oppose restriction to the behavior of Z. The main difference from the classic fuzzy decision-making is that in Fuzzy techniques only A is known and Z is likely to belong to A. On the contrary, in Z-numbers, the random number Z is presented by the set A, but with a degree of certainty/reliability B. Therefore, on that manner:

$$Z = \{x | x \in A \; with \; certainty \; degree \; equal \; to \; B\}$$

For example, let's assume that a normal PDF is appropriate for modelling load demand. Moreover, it is almost certain (set B_2) that in a particular node, the load demand is low (set A_1). $Prob$ and $G(Prob)$ represent that the probability that the load demand is low and $G(Prob)$ the certainty degree that $Prob$ belongs to A_1. Finally, Prob & G(Prob) are formulated in the following equations (33) & (34):

$$Prob = \int_a^d A_1 \frac{1}{\sigma\sqrt{2\pi}} e^{-\frac{(x-\mu)^2}{2\sigma^2}} = \frac{1}{\sigma\sqrt{2\pi}} \left[\int_a^b \frac{x-\alpha}{b-a} e^{-\frac{(x-\mu)^2}{2\sigma^2}} + \int_b^c e^{-\frac{(x-\mu)^2}{2\sigma^2}} + \int_c^d \frac{x-d}{c-d} e^{-\frac{(x-\mu)^2}{2\sigma^2}} \right] \quad (33)$$

$$G(Prob) = \mu_{B_2}(Prob) \quad (34)$$

Therefore, the load demand that is represented by a Z-number $L = (A_1, B_2)$ is actually a possibility distribution $G(Prob)$ over an interval of various probability distributions (μ_i, σ_i), where μ_i: the mean value & σ_i: the standard deviation of every probability distribution. In Fig. 2.7, the above concept of Z-numbers in the load demand modelling is presented [17].

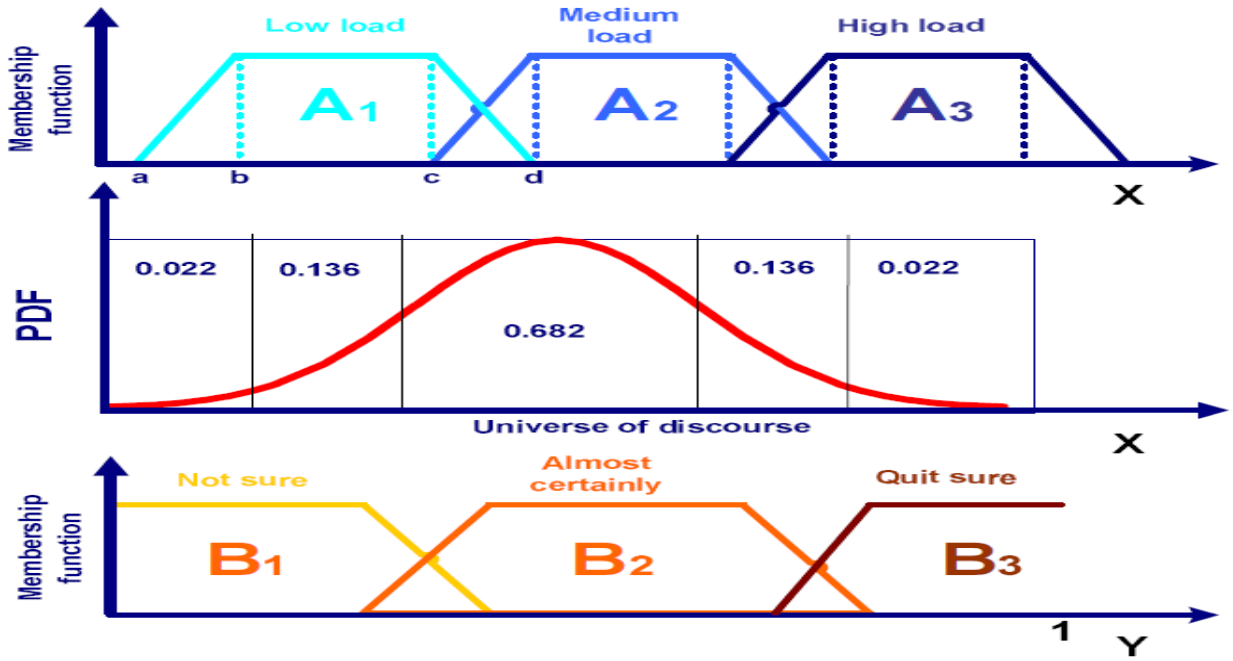

Fig. 2. 7: Load Demand Modelling with the concept of "Z numbers" [17]

2.9 Uncertainty Handling Methods Summary

Table 2.3 summarizes their input-output characteristics, advantages & disadvantages [17]. Summarizing Chapter 2, the uncertainties in optimization problems related with power systems, can be handled either applying Stochastic-based Optimization (Probabilistic, Possibilistic, Hybrid) or Robust-based Optimization (Robust Optimization, IGDT).

Regarding Stochastic Optimization, probabilistic approaches have the advantage of easy implementation. However, they strongly depend on the availability of PDFs (or at least some PDF

parameters), which is not always feasible, and moreover they usually need large number of simulated scenarios for accurate results, with the exemption of PEM method. On the other hand, Fuzzy Stochastic Optimization provides the benefit of transforming linguistic knowledge to mathematical expressions without the need of available historical data of probability. However, the complexity of implementation is very high, compared with the probabilistic approaches. Hybrid combinations of Probabilistic and Possibilistic Approaches are capable of combining several advantages from different methods, however the computational expense still remains high.

On the contrary, Robust Optimization eliminates the need of historical data availability, apart from the lower & upper bounds of uncertainty sets. Furthermore, it avoids the need of consideration of multiple different scenarios, since it already considers the worst-case scenario. It can produce various different objective outputs depending on the selected "conservativeness", but over-conservativeness can lead to highly deteriorated objective value. Moreover, applying R.O in Non-linear Optimization models is a highly difficult task. IGDT represents another robust-based uncertainty handling technique, whose main advantage is the capability of addressing severe uncertainties. Nevertheless, this usually comes at expense of extreme problem conservativeness. Interval analysis represents an older way of uncertainty handling, which is similar to R.O, without however considering the correlations of the different uncertainty sets. Finally, the emerging Z-numbers technique, which intends to combine characteristics from both probabilistic and possibilistic approaches, is a very promising technique, regarding efficiency and accuracy of results.

Table 2. 3: Summarization of Characteristics, Advantages & Disadvantages of the Uncertainty Handling Techniques

Method	Input Representation	Output Attributes	Advantages	Disadvantages
Probabilistic	PDF	Statistics (Expectation, Variance)	Easy Implementation	Computationally expensive, need for large amount of historic data
Possibilistic	MF	MF	Conversion of linguistic knowledge to numerical values	Complex Implementation
Hybrid	MF or PDF	MF with probabilistic parameters	Dealing with both uncertainty types simultaneously	Computationally expensive
IGDT	Forecasted Values	Decision Variables satisfying Requirements	Useful for severe Uncertainties	Too conservative
Robust Optimization	Intervals	Controlled conservativeness	Useful when just an interval is available	Difficult use in non-linear models
Interval Analysis	Intervals	Bounds of outputs	Useful when just an interval is available	Correlation between intervals neglected: too conservative

All of the uncertainty handling techniques, discussed so far, have found extended use in EV smart-charging and several related researches. For example, probabilistic methods have been utilized in [53] & [54]. In [53], authors focused on formulating probabilistically the aggregated representation of the EV fleet, determining the optimal bidding strategy of an EV aggregator in the Day-Ahead Market using Stochastic Optimization. Moreover, [54] elaborates on the development of an EV aggregator, utilizing Monte Carlo Simulation for the generation of different EV user driving parameters to deal with the driving pattern uncertainty. The impact of EVs on the power grid has been addressed probabilistically, compared with deterministic approaches in [55], while in [56] the availability of EVs for ancillary services provision to the grid has been estimated using MCS and stochastic model for profiles generation. Furthermore, Robust Optimization techniques have been thoroughly investigated for EV charging related researches, as well. In [45], authors have utilized Robust Optimization for robust energy scheduling

design in V2G networks, formulating robust solution methodologies for each category of applications, while authors in [57] have developed a robust model for bi-directional dispatch control of large-scale EV fleets, that utilize V2G technology. Furthermore, the uncertainties of active and re-active loads, charging rates of batteries and charging capacities of EVs are formulated with uncertainty sets in [41], for a robust active and re-active management in Smart Distribution Networks (SDNs) with the use of EVs as "smart-loads", while Robust Optimization has been utilized to deal with the energy price uncertainty in EV Smart-Charging in [49]. Finally, a risk-averse IGDT model has been also utilized in [50] to manage the revenue risk of EV managers in an energy-scheduling topic, related with heterogeneous EV aggregations with V2G and G2V capabilities.

Chapter 3: Robust Optimization Methodology

3.1 Evolution of Robust Optimization

Soyster's Method

Robust Optimization has gained high attention in the last 20 years, however it is not considered a new idea. On the contrary, it was introduced by Soyster in 1973. Soyster considers column-wise uncertainty formulating linear models, protected by data uncertainty [58]. Soyster's model (35) is presented below [59]:

$$\begin{aligned} & maximize\ c'x \\ subject\ to \sum_j a_{ij}x_j + \sum_j \hat{a}_{ij}y_j \ \le\ b_i, \quad & \forall i \\ -y_j \le x_j \le y_j, \quad & \forall j \\ l \ \le x \le u & \\ y \ge 0 & \end{aligned} \tag{35}$$

Where: a_{ij}: the elements of the constraint matrix A (forecasted values)

$\hat{a}_{ij}$: the corresponding maximum deviations from the forecasted values a_{ij}

x_j: the decision variables of the optimization problem

If x^* the optimal solution of the above formulation, it is clear that at optimality, (36) is derived:

$$\begin{aligned} & y_j = |x_j{}^*| \\ \sum_j a_{ij}x^*{}_j + \sum_{j\in J_i} \hat{a}_{ij}|x_j{}^*| \ \le\ b_i, \quad & \forall i \end{aligned} \tag{36}$$

Therefore, for every possible real value $\widetilde{a_{ij}}$ of the uncertain variable, the solution remains "robust" and (36) is transformed to (37), where $\sum_{j\in J_i}\widetilde{a_{ij}}|x_j{}^*|$ represents the protection needed for the particular constraint [60].

$$\sum_j \widetilde{a_{ij}}x^*{}_j = \sum_j a_{ij}x^*{}_j + \sum_{j\in J_i}\eta_{ij}\hat{a}_{ij}x_j{}^* \ \le \sum_j a_{ij}x^*{}_j + \sum_{j\in J_i}\hat{a}_{ij}|x_j{}^*| \ \le\ b_i, \quad \forall i \tag{37}$$

Where: $\widetilde{a_{ij}}$: the robust elements of the robust constraint matrix $\tilde{A}$

η_{ij}: the random variables $\frac{\widetilde{a_{ij}}-a_{ij}}{\hat{a}_{ij}}$

Soyster's method provides the maximum protection to the nominal linear problem, however it is simultaneously the most conservative solution, deteriorating highly the output value of the objective function.

Ben-Tal & Nemirovski Method

Ben-Tal & Nemirovski reintroduced Robust Optimization for linear programming problems (LP) with the use of ellipsoid uncertainty set in 1998 in order to cope with the over-conservativeness of Soyster's formulation. More specifically, they proved that the Robust Counterpart (RC) of an LP

formulation is computationally tractable if an ellipsoid uncertainty set is utilized, transforming the RC to an equivalent second-order cone problem [58], [59]. The Ben-Tal & Nemirovski's formulation (38) is presented below:

$$\begin{gathered} maximize\ c'x \\ subject\ to \sum_j a_{ij}x_j + \sum_j \hat{a}_{ij}y_j + \Omega_i \sqrt{\sum_{j\in J_i} {\hat{a}_{ij}}^2 {z_{ij}}^2} \leq b_i, \quad \forall i \\ -y_{ij} \leq x_j - z_{ij} \leq y_{ij}, \quad \forall i,j \in J_i \\ l \leq x \leq u \\ y \geq 0 \end{gathered} \tag{38}$$

The authors have proved that the given i^{th} constraint is violated with probability at most $e^{(-\Omega_i{}^2)}$. If k the uncertain coefficients, n the number of variables and m the number of the constraints: Soyster's method is an LP with $2n$ variables and $m + 2n$ constraints and Ben-Tal & Nemirovski's method is a 2nd order cone problem with $n + 2k$ variables and $m + 2k$ constraints. Regarding conservativeness, every feasible solution of the latter formulation is a feasible solution of the former formulation, hence Ben-Tal & Nemirovski method indeed decreases conservativeness of the RO formulation. However, the Robust Counterpart is transformed to a nonlinear one and it is less applicable to robust discrete optimization models [58], [60].

Polyhedral Uncertainty

A polyhedral uncertainty set U can be considered as a special occasion of the ellipsoid uncertainty set, formerly introduced by Ben -Tal & Nemirovski, and transforms the Robust Counterpart to the LP problem of (39) [61].

$$\begin{gathered} \min c^T x \\ s.t. \max_{D_i a_i \leq d_i} {a_i}^T x \leq b_i, \quad i = 1, \dots, m \end{gathered} \tag{39}$$

Performing duality to the inner max problem, the robust counterpart is transformed to the following linear optimization problem (40). The computational burden increases polynomially in size according to the nominal problem size and uncertainty set dimensions. Finally, in Fig. 3.1, the feasible LP set with polyhedral uncertainty is depicted, compared with the feasible set of a deterministic LP problem [62].

$$\begin{gathered} \min c^T x \\ s.t. \quad {p_i}^T d_i \leq b_i, \quad i = 1, \dots, m \\ {p_i}^T D_i \leq x, \quad i = 1, \dots, m \\ p_i \geq 0, \quad i = 1, \dots, m \end{gathered} \tag{40}$$

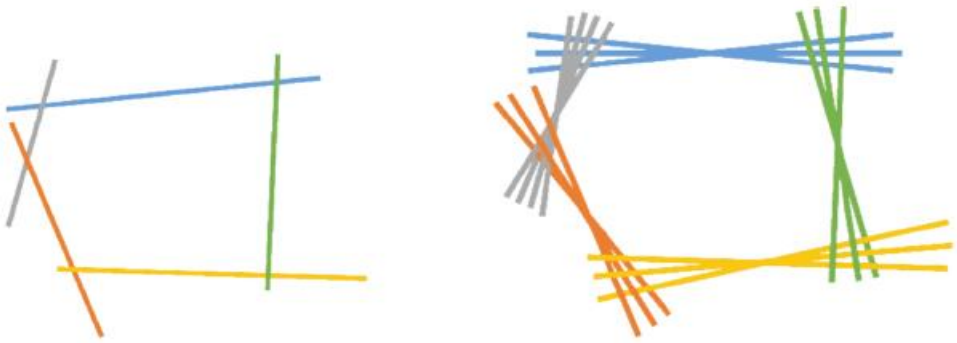

Fig. 3. 1: Feasible set of a LP problem with no uncertainty (on the left) and of a LP with polyhedral uncertainty considered (on the right) [62]

Bertsimas & Sim Method (Cardinality Constrained Uncertainty)

Bertsimas & Sim addressed the non-linearity issue of Tal & Nemirovski's method adopting the polyhedron uncertainty and introducing the so-called concept of "budget of uncertainty" in 2004. They proposed a linear Robust Optimization formulation, which can adjust the level of uncertainty that can be tolerated under the data uncertainty model U, therefore controlling the level of deterioration of the optimal objective value at expense of robustness. Moreover, it can directly be extended to discrete optimization problems. According to this RO formulation, every real entry of matrix A that is subjected to uncertainty $\tilde{a}_{ij}$, takes values in a symmetric interval with mean the forecasted value a_{ij} and bounds depended on a maximum deviation $\hat{a}_{ij}$. Therefore, for the i^{th} constraint (41): [63]

$$\tilde{a}_{ij} \in \left[a_{ij} - \hat{a}_{ij}, a_{ij} + \hat{a}_{ij}\right], \forall i, j \in J_i \tag{41}$$

For every i^{th} constraint of the nominal problem $a_i{}' x \leq b_i$, where J_i are the number of the uncertain coefficients, a parameter $\Gamma_i \in$ N is introduced, which lies within the interval $[0, |J_i|]$. Γ_i controls the trade-off between the levels of robustness and conservatism, which are chosen for the problem. Since, the simultaneous realization of the worst-case scenario of every coefficient is unlikely to occur, Bertsimas & Sim's formulation protects against the deviation of up to $[\Gamma_i]$ coefficients and the deviation of one coefficient $a_{i\tau}$ to $(\Gamma_i - [\Gamma_i])\hat{a}_{i\tau}$. Bertsimas & Sim showed that if a subset of coefficients is allowed to deviate, the LP problem can be solved deterministically and even if more coefficients are changed, the solution remains feasible under high probability [63]. Bertsimas & Sim formulation (42) is presented below. The initial non-linear formulation is as follows:

$$\begin{gathered} \max c'x \\ s.t. \sum_j a_{ij}x_j + \max_{\{S_i \cup \{t_i\} | S_i \subseteq J_i, |S_i| = [\Gamma_i], t_i \in J_i \setminus S_i\}} \{\sum_{j \in S_i} \hat{a}_{ij}\, y_j + (\Gamma_i - [\Gamma_i])\hat{a}_{it_i} y_t\} \leq b_i, \quad \forall i \\ -y_j \leq x_j \leq y_j, \quad \forall j \\ l \leq x \leq u \\ y \geq 0 \end{gathered} \tag{42}$$

If $\Gamma_i = 0$, then Bertsimas & Sim's model is transformed to the nominal problem (no robustness), whereas if $\Gamma_i = |J_i|$, it is transformed to the Soyster's method (100% conservatism). By varying $\Gamma_i \in [0, |J_i|]$, the optimal trade-off between robustness and conservatism can be adjusted. By applying strong

duality, Bertsimas & Sim finally transforms the aforementioned formulation to an equivalent linear formulation (43), which is presented below. It integrates $n + k + 1$ variables & $m + k + n$ constraints, where $k = \sum_i |J_i|$: the uncertain coefficients considered. For more information, the reader is referred to [59], [61], [63]. Finally, the lineage of the contribution of some of the most important robust optimization formulation to the research community is depicted in Fig. 3.2 [64].

$$
\begin{aligned}
& max c'x \\
subject\ to \quad & \sum_j a_{ij}x_j + z_i\Gamma_i + \sum_{j \in J_i} p_{ij} \leq b_i, \quad \forall i \\
& z_i + p_{ij} \geq \hat{a}_{ij} y_j \quad \forall i, j \in J_i \\
& -y_j \leq x_j \leq y_j, \quad \forall j \\
& l_j \leq x_j \leq u_j, \quad \forall j \\
& p_{ij} \geq 0, \quad \forall i, j \in J_i \\
& y_j \geq 0, \quad \forall j \\
& z_i \geq 0, \quad \forall i.
\end{aligned} \tag{43}
$$

On that manner, the uncertainty set (A matrix) is formulated as follows in (44) [65]:

$$A = \{(\tilde{a}_{ij}) \mid \tilde{a}_{ij} = a_{ij} + \hat{a}_{ij} z_{ij}, \forall i, j, z \in Z\} \tag{44}$$

$$where: \quad Z = \{z \mid |z_{ij}| \leq 1, \forall i, j, \sum_j |z_{ij}| \leq \Gamma_i, \forall i\} \tag{45}$$

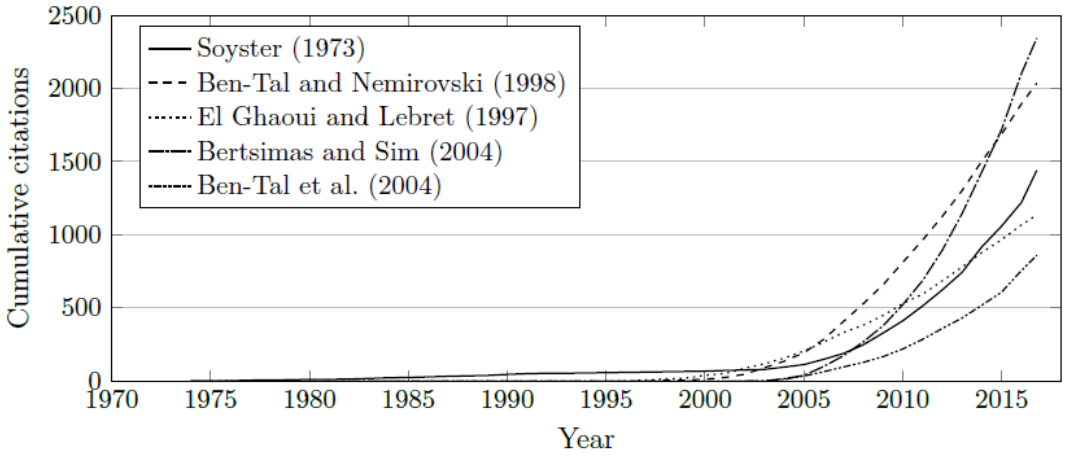

Fig. 3. 2: Cumulative citations of the most influential papers on Robust Optimization [64]

3.2 Robust & Stochastic Optimization: Distributional Robust Optimization (DRO)

Distributional Robust Optimization (DRO) can be considered as a "bridge" between Stochastic Optimization (SO) and Robust Optimization (RO). While Robust Optimization addresses the issue of computational burden and necessity for knowledge on probability distributions of the nominal problem's uncertainties in SO, the optimal objective value can be highly jeopardized at expense of robustness. DRO combines the advantages of SO and RO, utilizing the uncertainty set of the probability distribution, and can be formulated using moment information or directly on the probability distributions [66], [67].

Let's consider $u(x, \xi)$ a function, where ξ: a random parameter that takes values within a known interval and u: a concave, non-decreasing payoff function. While, the assumption of the knowledge of

the whole distribution of ξ may be unrealistic, the distribution of ξ within specified subsets of the entire uncertainty set can still be known with high probability [61]. It has been shown in [66], that for any subset Q, there exists a convex, non-increasing, translation-invariant, positive homogeneous function μ on the uncertainty space, described by equation (46):

$$inf_{i\in Q} E_i[u(x,\xi] \geq 0 \ \leftrightarrow \mu\big(u(x,\xi)\big) \leq 0 \tag{46}$$

The aforementioned function μ is defined as a "coherent risk measure". According to risk management setting, if X is a random variable, $\mu(X)$ represents the amount that needs to be added to X in order to make it "acceptable" [68]. In that perspective, Bertsimas & Brown in [61] used the risk management tools in order to develop uncertainty sets' structures in Robust LP problems. More specifically, utilizing duality theory, they proved that a risk constraint $\mu(\tilde{a}'x - b) \leq 0$ on a linear constraint can be transformed to the following equivalent form (47):

$$\mu(\tilde{a}'x - b) \leq 0 \ \leftrightarrow \ a'x \ \geq b, \quad \forall a \in U \tag{47}$$

where: $U = conv(E_i[a]: i \in Q), Q$: generating family of μ

One of the most famous coherent risk measures that has been used in Electrical Engineering Optimization studies and DRO approaches, is the "conditional value-at-risk" (CVaR), which is expressed below in (48):

$$\mu(X) \triangleq \ inf_{v\in R}\{v + \frac{1}{\alpha}E[(-v - X)^+\}, \quad \alpha \in (0,1] \tag{48}$$

Distributional Robust Optimization represents a new field of research, which aims to apply the Stochastic Optimization benefits in Robust Optimization. In [67], DRO has been used for the development of a scheduling strategy for load distribution in Home Energy Management System (HEMS) under uncertain environment. Moreover, a DRO approach has been applied in [69] in order to cope with uncertainties derived by active and reactive load variations & electricity and reactive power price deviations for the flexible bidirectional power management of Electric Vehicles (EVs) in smart Distribution Networks (SDNs). Finally, authors in [70] formulate multiple uncertainty models with known probability distributions, based on DRO, addressing various well-known PDFs.

3.3 Static Robust Optimization (SRO) & Adaptive Robust Optimization (ARO)

Robust Optimization falls into the category of decision-making problems under uncertainty, which can furtherly be divided to the categories of static and dynamic. In static decision-making problems, the decision-maker takes all the decisions in the beginning, before any realization of uncertainty occurs. These decisions are called "here and now" decisions, because no recourse action is made consequently, when the various uncertainties are realized [58]. Therefore, in Static Robust Optimization (SRO), all the uncertainties are addressed in the beginning of the optimization and all protection decisions of the nominal problem are realized simultaneously in "one-shot" case, formulating a single-stage optimization problem [61]. SRO can integrate focus on uncertainty on feasibility and focus on uncertainty on objective value. Regarding the first category, RO searches for a feasible solution under any possible uncertain parameter realization, while the second one searches for a solution that extracts nearly optimal results for any uncertain scenario. Moreover, when uncertainty has an impact on optimality such as in the second

category, SRO can be a "single-objective" or a "multiple-objective" optimization approach [71].

However, the majority of optimization problems in reality requires decision-making in several stages, or else the so-called "sequential decision making". In sequential decision making, the decisions can be divided to "here and now" and "wait and see" decisions. While the former ones are realized before any provided information on occurrence of the uncertain parameters, the latter forms recourse actions, which are made at the instants of uncertainties realization [72]. For example, in an inventory management problem that considers uncertain demand, every quantity ordered or saved is addressed after the observation of the demand realization of the previous period. Therefore, all decisions in the beginning of the planning horizon can be called as "here and now", while all decisions made in the next steps can be called "wait and see", since they depend on the realization values of the uncertain parameters [73]. Authors in certain papers, such as Dean, Goemans and Vondrak in [74] & Bertsimas and Goyal in [75], have proved that the value of the optimal adaptive solution in their formulations is up to a certain constant factor times the optimal static solution and therefore the computational expense of the adaptive approach is not attractive. However, considering also the inherent tendency to over-conservativeness of Robust Optimization, the SRO usually results in highly deteriorated optimal results and the use of ARO is unavoidable.

The use of multiple stages in Robust Optimization is highly computationally difficult, therefore most researches have focused on two-stage ARO. However, even the use of two stages of Robust Optimization in linear cases can result in intractable problem. Various approaches have been introduced for the convergence of both optimization stages, such as "cutting-plane" algorithms or affine decision rules, such as the "Bender's decomposition" algorithm [76]. If the recourse is fixed, ARO usually results in a tractable LP problem, but that is not always the case for problem with unfixed recourses [76]. In [72], ARO has been used for the optimal operation of Microgrids considering EV user uncertain patterns and RES generation. The first-stage decisions are the determination of the day-ahead unit commitment of the Distributed Generators (DGs), whereas computation of all other continuous variables, such as power flows, are made in the next stage. In the security constrained unit commitment problem with nodal injection uncertainty of [77], again the first-stage unit-commitment decisions are robust against all possible uncertainty realizations, while the second-stage decisions are all the consequent adaptive dispatch actions. Finally, a bilevel ARO is used for the decision-making of an EV charging station which aims to incorporate an active role of the EV owners in the charging decisions. While the first stage represents the initial static decisions about the optimal configuration of the station and pricing schemes, the charging decisions of the EV owners form the "wait and see" decisions of the problem computed in the 2nd stage [78]. The first generic formulation of a two-stage ARO formulation is presented below in (49) [79]. While the feasible set is convex, the two-stage LP with deterministic uncertainty is not always computationally tractable [61].

$$\min c^T x_1$$
$$s.t: A_1(u)x_1 + A_2(u)x_2(u) \leq b, \quad \forall u \in U. \tag{49}$$

Since $x_2(.)$ Is an arbitrary function of u, the above formulation can be explicitly written in the first-stage decision feasible set (50) [79]:

$$\min c^T x_1$$
$$s.t: x_1 \in \{x_1: \forall u \in U, \exists x_2 \; s.t. A_1(u)x_1 + A_2(u)x_2(u) \leq b\}. \tag{50}$$

3.4 Receding Horizon Optimization (RHO) & Robust Optimization (RO)

Receding Horizon is another approach that deals with optimization uncertainties and falls under the category of Model Predictive Control (MPC). MPC mainly performs online replanning, utilizing numerical optimization and a system model in order to predict the future (the subsequent optimization stages). More particularly the state x at time t is computed online by a specific control signal $\hat{u}$ which solves a finite horizon optimization problem over the interval $[t, t+T]$. In the following steps, the process is repeated [80]. Its main advantage is that it can work closely to the boundaries and still provide highly optimal results [81].

On that manner, RHO is based on updating information and performing optimization with the updated data in a rolling fashion, depending on certain predefined events that trigger the new optimization horizon [67]. The first-stage decisions are the computation of the static solutions of all stages (that do not depend on the uncertainties). The second-stage decisions are the results of all the subsequent optimizations in the next stage, since they depend on the new updated data [61], [82]. The main advantages considered are firstly the tractability of the particular approach and secondly the fact that the use of updated information, during the process, eliminates the interdependency of the uncertainties of subsequent optimization stages, minimizing the effect of uncertainties of previous steps. However, the first-stage decisions can still result over-conservative, since they are made without adaptability [61], [67].

Combining the Receding Horizon approach and Robust Optimization in a LP Optimization problem provides the capability of forming an Adaptive Robust Optimization problem, avoiding the high computational expense of the typical two-stage ARO, which can lead to a computationally intractable problem. All the "here and now" decisions are made up front, in the start of the scheduling horizon. Then a prediction horizon is determined, depended on a pre-decided uncertainty realization event that triggers re-optimization. Every decision made after the first prediction horizon can be considered as "wait and see" and is adapted to the realizations of the considered uncertainties of the previous stages. Re-optimization is performed for every prediction horizon, which is divided in pre-defined timesteps (control horizons of the prediction horizon). In every re-optimization stage, the worst-case scenarios of the integrated uncertainties are computed and taken into consideration for the computation of the decision variables. If a new trigger event occurs, the next prediction horizon is scheduled and updated input information and worst-case scenarios for the uncertain parameters are considered. On that manner, an Adaptive Robust Optimization model is developed, which is always tractable and takes advantage of the benefits of the receding horizon approach.

Fig 3.3 depicts all the aforementioned associated concepts of the receding horizon approach for clarity [83]. The Scheduling horizon (SH) constitutes the total duration of the optimization problem, which needs to be scheduled. At every iteration, a Prediction Horizon (PH) is scheduled, which is always a part of the SH. Hence, at the first time instant, the first PH is set (PH – 1). Every PH integrates a Control Horizon (CH), which is responsible to trigger new re-optimizations and set a new PH, if the pre-decided triggering event occurs. On that manner, the CH constitutes always a part of the corresponding PH and the end of the previous CH provokes the start of the next PH. Therefore, when the Control Horizon (CH – 1) of the Prediction Horizon (PH – 1) finished, the new Prediction Horizon (PH – 2) is set.

Finally, Sequential decision-making can be integrated into a Robust Optimization framework by also using Stochastic Optimization or Dynamic Robust Optimization (e.g Markov decision process settings), however these approaches are not reviewed in the thesis [61].

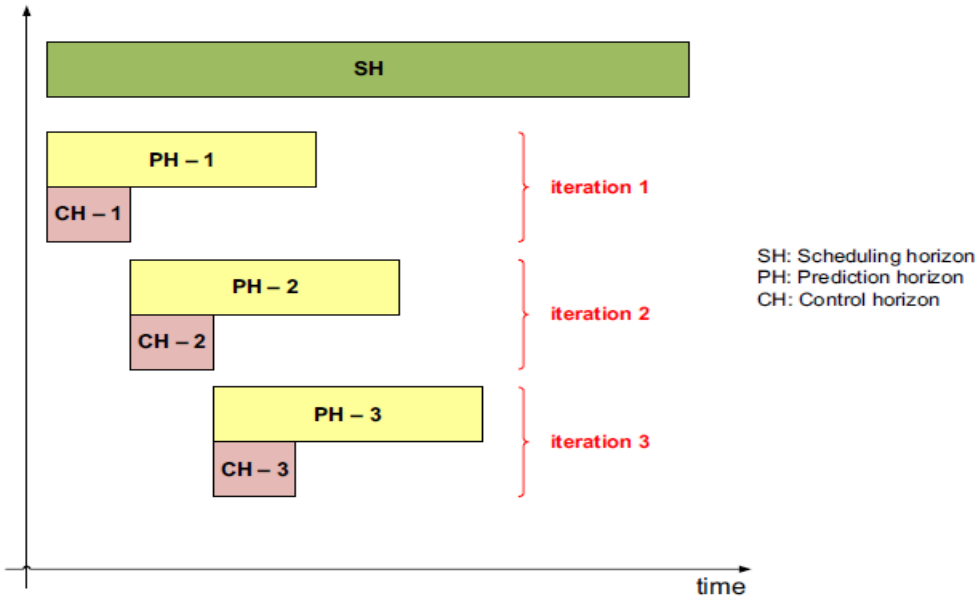

Fig. 3. 3: Concepts associated with Receding Horizon Approach [83]

3.5 The Benchmark Smart-Charging Algorithm

Benchmark Smart-Charging Algorithm Introduction-Description

This thesis investigates the use of Robust Optimization on the deterministic smart-charging algorithms. The objective of the benchmark algorithm is the minimization of the EV charging costs considering RES (PV) Generation forecast, EV user preferences and patterns (arrival, departure and requested energy), local load demand, regulation reserves provision and energy market prices. The benchmark algorithm is formulated as a mixed-integer linear programming problem (MILP) and is capable of controlling the EV charging, providing simultaneously up & down regulation services as well as exporting (selling) power to the grid, depending on the aforementioned considerations. On that manner, an Energy Services Company (ECSo) acts as a bridge between the wholesale market and the EV users and aims to perform energy scheduling, in such a way that the charging cost is minimized, regulation services are provided to the Independent System Operator (ISO) and income from PV generation is increased. All the knowledge provided below in this section is derived by [15], where the reader is referred to for further information.

Receding Horizon Approach

The benchmark algorithm already formulates an Energy Management System (EMS), which uses a receding horizon model predictive control of timestep ΔT to deal with uncertainties and minimize prediction errors. The MIP optimization is triggered and a new optimization horizon is set whenever a new EV arrival is realized at any timestep ΔT. In Fig. 3.4 an example of the implementation of flexible receding horizon approach on smart-charging is depicted. Let's consider that 4 chargers exist at node n. At time instant t_i , a new EV arrival is realized at Charger 1, while Chargers 2 & 4 have already a car connected and Charger 3 is empty. The new optimization horizon is set until the latest EV departure of the 3 cars ${T_2}^d$ (e.g the EV connected to Charger 2): ${T^d}_{max} = \max\{{T^d}_j \mid j \in J\}$ and can be calculated as: $T_i = {T^d}_{max} - t_i$. The reason why horizon is set until ${T_2}^d$, is because the benchmark algorithm cannot predict ("see") the EVs, which are going to come in the future. Therefore, taking into account only the EVs, that are currently connected to the chargers, the horizon is set until the latest departure.

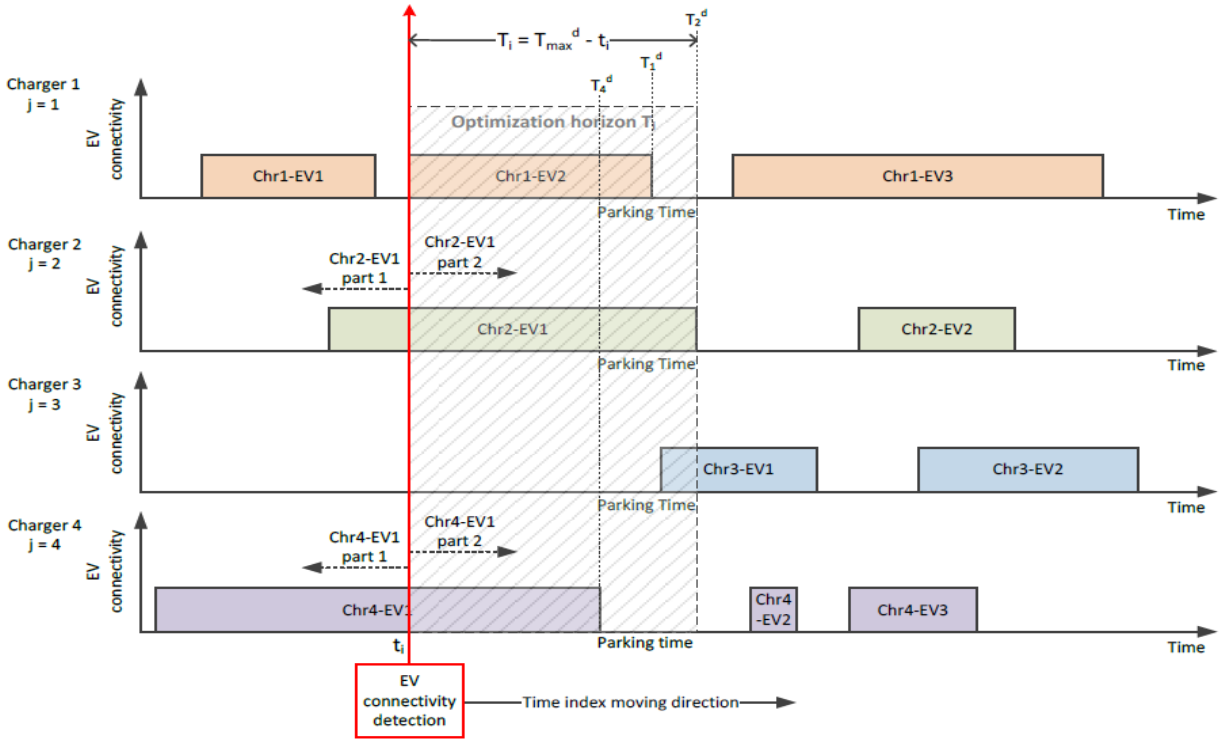

Fig. 3. 4: Receding Horizon Approach Implementation in Smart-Charging [15]

As it can be clearly observed in Fig. 3.4, in order to avoid influence of the previous horizon to the optimization of the next one, at the start of every new optimization horizon, the already connected cars are divided into two parts: part 1 & part 2, which represent the past & the future respectively. Hence, the related optimization parameters, such as the remaining parking time and energy demand, are updated and utilized in the next optimization round [15].

Objective Function & Robust Counterpart

The objective function of the benchmark algorithm is presented below in (51). As it can be seen, the cost minimization depends on several terms. The first term represents the penalty cost paid to the unsatisfied customer, if the requested energy is not met by the departure time. The second term represents the cost of the PV utilization, paid to the PV owners, if PV Generation is not owned by the EMS, but rather is installed by third parties. Moreover, the third term integrates the cost of buying energy as well as the income of selling energy to the grid, while the last term integrates the income from the regulation services provision of the EMS to the ISO.

$$min\ {C_n}^{opt} = \sum_{j=1}^{J} ({B_{n,j}}^{a} + d_{n,j} - {B_{n,j,\tilde{T}^d}}_{n,j}){C^p}_{n,j}$$
$$+ \Delta T \sum_{t=1}^{T} {p^{PV}}_{n,t} C^{PV} + \Delta T \sum_{t=1}^{T} ({p^{g(imp)}}_{n,t} {C^{e(buy)}}_t - {p^{g(ex)}}_{n,t}\ {C^{e(sell)}}_t)$$
$$- \Delta T \sum_{t=1}^{T} \sum_{j=1}^{J} ({p^{r(up)}}_{n,j,t} {C^{r(up)}}_t + {p^{r(dn)}}_{n,j,t}\ {C^{r(dn)}}_t) \quad (51)$$

The Decision Variables of the MILP OSCD optimization are the following:

- ${p^{e+}}_{n,j,t}$: Charging Power of EV: j connected to node: n at time: t (kW)
- ${i^{e+}}_{n,j,t}$: Charging Current of EV: j connected to node: n at time: t (kW)
- $B_{n,j,t}$: Battery Energy of EV: j connected to node: n at time: t (kWh)
- ${p^{PV}}_{n,t}$: Generated PV Power by RES installation at node: n at time: t (kW)
- ${p^{r(up)}}_{n,j,t}$, ${p^{r(dn)}}_{n,j,t}$: Up & Down Regulation Reserves by EV: j at node: n at time: t (kW)
- (${p^{g(imp)}}_{n,t}$, ${p^{g(ex)}}_{n,t}$: Imported & Exported Power to the grid at node: n at time: t (kW)

Moreover: ${C_n}^{opt}$: Optimal charging cost of node n (€)

${B_{n,j}}^{a}$: Battery capacity upon arrival at charger j of node n (kWh)

$d_{n,j}$: Requested energy at charger j of node n (kWh)

$B_{n,j,\tilde{T}^d{}_{n,j}}$: Battery capacity upon departure at charger j of node n (kWh)

${C^p}_{n,j}$: Penalty Cost $[\frac{10€}{1\%\ SOC}]$ paid to the customer for unsatisfying (unfinished) EV charging.

It must be noted here that due to an inherent drawback of Discrete Optimization, which will be explained more thoroughly in Chapter 5, the penalty cost is neglected if the ratio of charging gap divided by requested energy is lower than 1% or the departure SOC is greater than 98%.

C^{PV}: Cost of PV Generation (in this thesis, assumed zero, hence the charging station owns the PV park) (€)

$C^{e(buy)}$: Cost of importing power from the grid (€)

$C^{e(sell)}$: Income from exporting power to the grid (€)

Considering that the imported & exported powers (${p^{g(imp)}}_{n,t}$ & ${p^{g(ex)}}_{n,t}$ respectively) traded by the EMS, are relatively much lower than the power traded in the market, it is assumed that the EMS does not influence the energy prices that circulate in the market. Moreover, the investigation will be divided into two studies. For the scope of Study 1, up and down regulation reserves will be ignored. This is because Study 2 is entirely devoted to the FCR reserves provision and the uncertainty integrated in them. The robust formulation of FCR reserves provision is separately described in Study 2 of Chapter 4, due to its stand-alone character and distinction from the other uncertainties. This distinction has been decided due to the fact that a whole new and improved FCR provision model has been developed for a more "real" and robust FCR provision. The combination of FCR with the other uncertainties would increase extremely the computational expense and simulation time and therefore a separate study (Study 2) has been devoted to FCR reserves in Chapters 4 & 5. Paragraph 3.6 describes the mathematical formulation

of the MILP Robust Optimization Problem without consideration of FCR uncertainty variables.

Hence, uncertainty is integrated only into the first term of the objective function and the Robust Counterpart of the benchmark objective function is identified as in (52). Fig. 3.5 depicts the schematic of the EV parking lot with the integrated components (PV Generation, Local Load, EV chargers etc.) and the power flow among them.

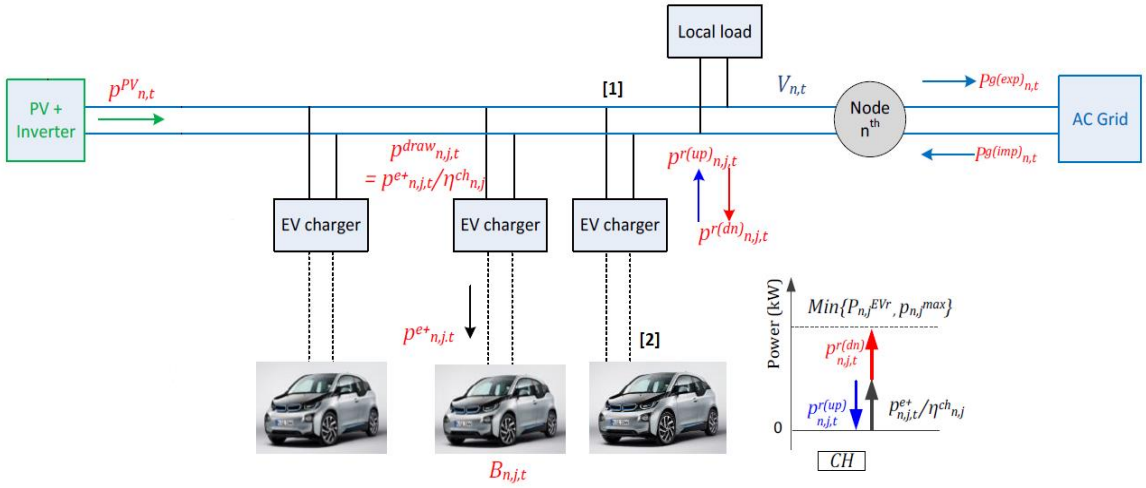

Fig. 3. 5: Schematic of the Power Flow and Components of the solar powered EV parking lot with EV chargers [15]

$$min\ C_n{}^{opt} = \min\left\{ \Delta T \sum_{t=1}^{T} p^{PV}{}_{n,t} C^{PV} + \Delta T \sum_{t=1}^{T} (p^{g(imp)}{}_{n,t} C^{e(buy)}{}_{t} - p^{g(ex)}{}_{n,t}\, C^{e(sell)}{}_{t}) + \max_{U} \{ \sum_{j=1}^{J} (B_{n,j}{}^{a} + d_{n,j} - B_{n,j,\tilde{T}^{d}{}_{n,j}}) C^{p}{}_{n,j} \} \right\} \quad (52)$$

3.6 Robust Formulation of the MIP Benchmark Deterministic Algorithm

3.6.1 Considered Uncertainties & Construction of the Uncertainty Sets

The benchmark algorithm is formulated until now considering 100% prediction accuracy of the input data in every stage of the receding horizon. However, as already stated above, there are certain input information that can never be predicted with total accuracy. The considered uncertainties are the following:

- PV generation: Due to the intermittent character of PV production which arises from the uncertain solar irradiation, the real produced PV power in the optimization problem is always subjected to uncertainty.
- Load Demand: The Load Demand is also highly uncertain, since it depends on human behavior, which can never be precisely predicted.
- EV user driving patterns: Every EV owner has informed the EV charging station about the preferred arrival and departure time (T_a & T_d respectively). However, since both these parameters depend on the drivers' behavior, they should also be considered uncertain for the extraction of optimal results.

- Requested Charging Energy – Arrival SOC: Every EV owner has informed the EV charging station about the SOC of the EV upon arrival and the requested energy (S_{T^a} & d respectively). As it is furtherly explained below, the EV owner can ask for a certain SOC the EV should have upon departure, but the arrival SOC of the EV at the station can never be certain, which consequently has an impact on the requested energy. Therefore, the arrival SOC and the dependent requested charging energy is another one uncertainty considered in this thesis.
- FCR Regulation Reserves: The benchmark algorithm, apart from charging "smartly" and sustainably the EV fleets, is capable of providing ancillary services (FCR reserves) to the power grid, hence to the TSO. However, there is a high level of uncertainty regarding the offered reserves to the bidding market and the exact amount of offered reserves that will be actually "called" in real-time, which has not been considered in the benchmark algorithm.

Uncertainty Sets Formulation

This thesis adopts the uncertainty set structure, as formulated by Bertsimas & Sim [63], which has already been used effectively in various researches, such as in [84], where uncertainties in surgery duration and length-of-stay in intensive care unit have been addressed for elective surgeries scheduling. However, due to limited available historical knowledge on PV generation and Load demand and incentive of management of all potential worst-case scenarios of EV user arrivals and departures, no "budget of uncertainty" has been introduced in the system uncertainties, apart from the FCR provision uncertainty.

On that manner, the uncertainty set formulation is the following (53):

$$U_i{}^t = \left\{\tilde{u}_i{}^t \in R^n : \tilde{u}_i{}^t \in \left[\bar{u}_i{}^t - \hat{u}_i{}^t, \bar{u}_i{}^t + \hat{u}_i{}^t\right], \forall t \in T\right\} = \left\{\tilde{u}_i{}^t \in R^n : \tilde{u}_i{}^t = \bar{u}_i{}^t + z_i{}^t * \hat{u}_i{}^t, -1 \le z_i{}^t \le 1, \forall t \in T\right\} \quad (53)$$

Where $\tilde{u}_i{}^t$: the real value, $\bar{u}_i{}^t$: the forecasted value & $\hat{u}_i{}^t$: the maximum considered deviation at time instant t, T: the optimization horizon and z_i: "the prediction error" factor

Therefore, the following uncertainty sets for PV generation, Load demand, Arrival & Departure times and arrival SOC are formulated as in (54), (55), (56), (57) & (58) respectively. As explained, the departure SOC has been assumed certain in this thesis, considering the fact that most EV drivers do not know the exact arrival SOC, with which they are going to arrive, but they are certain for the SOC, that they want to have upon leaving the station.

1. PV Generation

$$U_p = \left\{\tilde{P}_{t,n}{}^{PV} \in R^n : \tilde{P}_{t,n}{}^{PV} = P_{t,n}{}^{PV(fc)} + z_{p_{t,n}} \hat{P}_{t,n}{}^{PV}, \left|z_{p_{t,n}}\right| \le 1\right\}, \forall t, n \quad (54)$$

Where: $P_{t,n}{}^{PV(fc)}$: the forecasted PV generation at node at time t (kW)

2. Load Demand

$$U_L = \left\{\tilde{P}_{t,n}{}^{loc} \in R^n : \tilde{P}_{t,n}{}^{loc} = P_{t,n}{}^{loc} + z_{L_{t,n}} \hat{P}_{t,n}{}^{loc}, \left|z_{L_{t,n}}\right| \le 1\right\}, \forall t, n \quad (55)$$

Where: $P_{t,n}{}^{loc}$: the forecasted Load demand at node at time t (kW)

3. Arrival Time

$$U_{T^a{}_{n,j}} = \left\{\tilde{T}^a{}_{n,j} \in R^{n*j} : \tilde{T}^a{}_{n,j} = T^a{}_{n,j} + z_{T^a{}_{n,j}} \hat{T}^a{}_{n,j}, \left|z_{T^a{}_{n,j}}\right| \leq 1\right\}, \forall t, n \quad (56)$$

Where $T^a{}_{n,j}$: the arrival time of j^{th} EV of node n (h)

4. Departure Time

$$U_{T^d{}_{n,j}} = \left\{\tilde{T}^d{}_{n,j} \in R^{n*j} : \tilde{T}^d{}_{n,j} = T^d{}_{n,j} + z_{T^d{}_{n,j}} \hat{T}^d{}_{n,j}, \left|z_{T^d{}_{n,j}}\right| \leq 1\right\}, \forall t, n \quad (57)$$

Where $T^d{}_{n,j}$: the departure time of j^{th} EV of node n (h)

5. Arrival SOC

$$U_{S^a{}_{n,j}} = \left\{\tilde{S}^a{}_{n,j} \in R^{n*j} : \tilde{S}^a{}_{n,j} = S^a{}_{n,j} + z_{S^a{}_{n,j}} \hat{S}^a{}_{n,j}, \left|z_{S^a{}_{n,j}}\right| \leq 1\right\}, \forall t, n \quad (58)$$

Where $S^a{}_{n,j}$: the arrival SOC of j^{th} EV of node n

3.6.2 Robust Formulation of PV generation uncertainty constraint

Regarding PV Generation, assuming that the PV converter is connected to the PV array via MPPT tracker and extracts maximum power, the power from PV generation depends on the forecasted value, the efficiency of the inverter η_{inv} and a scaling factor $K^{PV}{}_{n,t}$ with respect to the rated PV power $p_n{}^{PVr}$ which scales the optimality of installation characteristics (e.g. azimuth, tilt, module parameters), hence it is dictated by equation (59). For this thesis the scaling factor and the inverter have been assumed ideal (unity).

$$p^{PV}{}_{n,t} \leq K^{PV}{}_{n,t} * p_n{}^{PVr} * p^{PV(fc)}{}_{n,t} * \eta_{inv} \quad (59)$$

Substituting (54) in (59):

$$p^{PV}{}_{n,t} \leq K^{PV}{}_{n,t} * p_n{}^{PVr} * \eta_{inv} * \left(P_{t,n}{}^{PV(fc)} + z_{p_{t,n}} \hat{P}_{t,n}{}^{PV}\right) \quad (60)$$

As the authors propose in [85], the inequality constraint with uncertainty in the right-hand side should be investigated at the lower bound, where the worst-case scenario of the constraint feasibility occurs. For that reason, it is obvious that PV generation decrease should be investigated, which forces the inequality to function in the limits. Therefore equation (60) is transformed to model (61):

$$p^{PV}{}_{n,t} \leq K^{PV}{}_{n,t} * p_n{}^{PVr} * \eta_{inv} * \left(P_{t,n}{}^{PV(fc)} - z_{p_{t,n}{}_{max}} \hat{P}_{t,n}{}^{PV}\right)$$

$$0 \leq z_{p_{t,n}{}_{max}} \leq 1, \quad \forall t, n \quad (61)$$

Addressing again the robust counterpart of the objective function, decreased PV generation leads to a lower (more optimal) objective output value. However, PV generation power is contradictory to the imported power from the grid. Hence, assuming that $C^{e(buy)}{}_t \gg C^{PV}$, (the cost of importing power from the grid is higher that the pay-off cost for PV generation, if PV park is installed by third party) increased

imported power will increase (deteriorate) the total charging cost. In this thesis, C^{PV} is assumed zero.

PV Generation uncertainty sets & maximum deviations

The worst-case scenario for decreased PV generation represents zero production. For that reason, the maximum accepted deviation is equal to the forecasted value: $\hat{P}_{t,n}{}^{PV} = P_{t,n}{}^{PV(fc)}, \forall t, n$. When $z_{p_{t,n}max} = 1$, PV generation is zero. Hence, (61) is transformed to (62):

$$p^{PV}{}_{n,t} \leq K^{PV}{}_{n,t} * p_n{}^{PVr} * \eta_{inv} * P_{t,n}{}^{PV(fc)} \left(1 - z_{p_{t,n}max}\right), \quad \forall t, n$$

$$0 \leq z_{p_{t,n}max} \leq 1, \quad \forall t, n \tag{62}$$

3.6.3 Robust Formulation of Load Demand uncertainty constraint

The uncertain parameter of the load demand appears in the EV charger & car park constraints and more specifically in the power balance equation. The AC grid is utilized for power exchanges between the EV chargers, PV arrays, local load demands and the grid. Hence, the intra-park power exchanges between the chargers and the PV park are directly related to the imported/exported power to the grid. The formulation of the power balance equation is presented in (63), where $\eta^{ch}{}_{n,j}$: the efficiency of the charger j of node n.

Moreover, the imported and exported powers do not have simultaneously non-zero values, as expressed in (64). Finally, the cost of the imported power is equal or slightly higher than the cost of the exported power, hence $C^{e(sell)}{}_t = 0.95 * C^{e(buy)}{}_t$.

$$\sum_{j=1}^{J} \left(p^{e+}{}_{n,j,t} \Big/ \eta^{ch}{}_{n,j} \right) + p^{local}{}_{n,t} - p^{PV}{}_{n,t} = p^{diff}{}_{n,t} = p^{g(imp)}{}_{n,t} - p^{g(ex)}{}_{n,t}, \quad \forall n, j, t \tag{63}$$

$$p^{g(imp)}{}_{n,t} = \left\{ p^{diff}{}_{n,t} \middle| p^{diff}{}_{n,t} > 0 \right\}, \quad \forall n, j, t$$
$$p^{g(ex)}{}_{n,t} = -1 * \left\{ p^{diff}{}_{n,t} \middle| p^{diff}{}_{n,t} < 0 \right\}, \quad \forall n, j, t \tag{64}$$

Substituting the uncertain load demand (55) in the power balance equation (63):

$$\sum_{j=1}^{J} \left(p^{e+}{}_{n,j,t} \Big/ \eta^{ch}{}_{n,j} \right) + \tilde{p}^{local}{}_{n,t} - p^{PV}{}_{n,t} = p^{g(imp)}{}_{n,t} - p^{g(ex)}{}_{n,t} \leftrightarrow$$

$$\sum_{j=1}^{J} \left(p^{e+}{}_{n,j,t} \Big/ \eta^{ch}{}_{n,j} \right) + p^{local}{}_{n,t} + z_{L_{t,n}} \hat{p}^{local}{}_{n,t} = p^{g(imp)}{}_{n,t} + p^{PV}{}_{n,t} - p^{g(ex)}{}_{n,t}, \quad \forall n, j, t \tag{65}$$

Due the lowest uncertain PV power considered in the previous step, the EV charging stations has to increase the imported power from the grid or to export less in order to cope with the load demand and charging energy. Therefore, assuming certain charging energy, a maximum increase in load demand represents the worst-case scenario for the particular equation, having the most severe impact on the objective value. Therefore, the power balance is transformed to the following robust balance equation (66):

$$\sum_{j=1}^{J}\left({p^{e+}}_{n,j,t}/{\eta^{ch}}_{n,j}\right)+{p^{local}}_{n,t}+z_{L_{t,n}max}\hat{p}^{local}{}_{n,t}-{p^{PV}}_{n,t}={p^{diff}}_{n,t}\ =$$
$${p^{g(imp)}}_{n,t}-{p^{g(ex)}}_{n,t},\ \ \forall n,j,t$$

$$0\le z_{L_{t,n}max}\le 1,\ \ \forall t,n \tag{66}$$

Load Demand uncertainty sets & maximum deviations

The load demand uncertainty is formulated in a similar way such as PV generation. The expected maximum deviation is considered to be a double load, hence $\hat{p}^{local}{}_{n,t}=p^{local}{}_{n,t},\forall t,n.$ When $z_{L_{t,n}max}=1$, the load demand is 2 times the forecasted value, whereas when $z_{L_{t,n}max}=0$, the real load demand value is equal to the forecasted. The balance power equation is transformed to (67):

$$\sum_{j=1}^{J}\left({p^{e+}}_{n,j,t}/{\eta^{ch}}_{n,j}\right)+{p^{local}}_{n,t}(1+z_{L_{t,n}max})-{p^{PV}}_{n,t}={p^{diff}}_{n,t}\ =$$
$${p^{g(imp)}}_{n,t}-{p^{g(ex)}}_{n,t},\ \ \forall n,j,t$$

$$0\le z_{L_{t,n}max}\le 1,\ \ \forall t,n \tag{67}$$

3.6.4 Robust Formulation of Arrival & Departure time uncertainties

The uncertain arrival and departure times mainly appear in the time duration constraint (68), which is one of the two charger-EV acceptance criteria. More particularly, upon EV arrival at EV part of node n, the user is informed regarding the charger to which the EV should be connected. The first criteria states that the requested energy during the parking time interval must be within the power limits of the charger. On that manner:

$$\frac{d_{n,j}}{{T^d}_{n,j}-{T^a}_{n,j}}\le\min\left\{{p^{EVr}}_{n,j},{p^{max}}_{n,j}\right\}\ \leftrightarrow$$
$${T^d}_{n,j}-{T^a}_{n,j}\ge {d_{n,j}}/{\min\left\{{p^{EVr}}_{n,j},{p^{max}}_{n,j}\right\}},\ \ \forall n,j \tag{68}$$

Where: ${p^{EVr}}_{n,j}$: the rated power of the EV charger connected to the j^{th} EV (kW)

${p^{max}}_{n,j}$: maximum charging power of j^{th} EV when its SOC is ${S_{n,j}}^{CV}$ (SOC value when the battery process shifts from Constant Current (CC) to Constant Volta (CV) stage of the j^{th} EV, here 80%)

Again, as authors propose in [80], the constraint should be investigated at the limit, therefore keeping steady the requested energy at charger j of node n: $d_{n,j}$, equation (68) is transformed to equation (69):

$$({\tilde{T}^d}_{n,j}-{\tilde{T}^a}_{n,j})_{min}\ge {d_{n,j}}/{\min\left\{{p^{EVr}}_{n,j},{p^{max}}_{n,j}\right\}}\ \leftrightarrow$$
$$({T^d}_{n,j}+z_{{T^d}_{n,j}}{\hat{T}^d}_{n,j}-({T^a}_{n,j}+z_{{T^a}_{n,j}}{\hat{T}^a}_{n,j}))_{min}\ge {d_{n,j}}/{\min\left\{{p^{EVr}}_{n,j},{p^{max}}_{n,j}\right\}} \tag{69}$$

Parking Time uncertainty sets & maximum deviations

Uncertainty on the EV arrival & departure time can be considered as the most severe, since apart from affecting the outcome of the objective function and the feasibility of constraints, it also has an impact on the triggering of the re-optimizations.

Furthermore, from the time duration constraint, it becomes obvious that the minimum parking time (latest arrival time and earliest departure time) should be considered for the worst-case scenario of the objective and the feasibility of the constraint. It must be noted that a potential issue of uncertainty on the drivers' patterns, that is not addressed considering minimum parking time, is time overlap between consequent vehicles at the same charger. Therefore, the maximum parking time (earliest EV arrival – latest EV departure), while it can be considered the most optimal scenario for the optimization objective function and constraints, it represents the worst-case scenario for potential time overlaps. Therefore:

- Minimum Parking time: Worst-case scenario for objective output and feasibility of constraints
- Maximum Parking time: Worst-case scenario for potential time overlaps [72]

However, for the scope and the time management of this thesis, the potential time-overlap issue of increased parking time uncertainty is ignored and only the minimum parking time is investigated. The two cases A & B of the deterministic and minimum parking time respectively are presented below in models (67) & (68).

- Case A: Deterministic (forecasted) Arrival & Departure times

$$\tilde{T}^{d}{}_{n,j} = T^{d}{}_{n,j}, \quad \forall n,j$$

$$\tilde{T}^{a}{}_{n,j} = T^{a}{}_{n,j}, \quad \forall n,j$$

$$\hat{T}^{d}{}_{n,j}, \hat{T}^{a}{}_{n,j} = 0, \quad \forall n,j \tag{67}$$

- Case B: Minimum Parking time (focus on objective & feasibility)

$$\tilde{T}^{d}{}_{n,j} = T^{d}{}_{n,j} - z_{T^{d}{}_{n,j}{}_{max}} \hat{T}^{d}{}_{n,j}, \quad \forall n,j$$

$$\tilde{T}^{a}{}_{n,j} = T^{a}{}_{n,j} + z_{T^{a}{}_{n,j}{}_{max}} \hat{T}^{a}{}_{n,j}, \quad \forall n,j$$

$$0 \leq z_{T^{d}{}_{n,j}{}_{max}}, z_{T^{a}{}_{n,j}{}_{max}} \leq 1, \quad \forall n,j \tag{68}$$

3.6.5 Robust Nominal objective function, arrival SOC uncertainty & rest of constraint

Rest of Acceptance Criteria

The second charger – EV acceptance criteria (69) states that the arrival EV capacity must be above the minimum limit as set by the EV user. Moreover, the smart-charging availability constraint (70) decides if smart-charging algorithm can be initiated by the EMS on the EV, which is possible if the EV capacity $B_{n,j,t}$ is no less than the emergency capacity value $B_{n,j}{}^{SC}$, which is 20% in this thesis. Moreover, the arrival capacity $B_{n,j}{}^{a}$ of j^{th} EV must always be equal or greater than the j^{th} EV specific minimum

capacity: ${B_{n,j}}^{min}$

$$ {B_{n,j}}^{min} \leq {B_{n,j}}^{a}, \ \forall n,j \tag{69} $$

$$ B_{n,j,t} \geq {B_{n,j}}^{SC}, \ \forall n,j \tag{70} $$

Subfunctions

The subfunctions of the optimization problem define the relation between the variables & parameters of the smart-charging algorithm. While the former two equations (71) & (72) set the battery capacity in every time instant of the optimization according to the charging power ${p^{e+}}_{n,j,t}$ & the efficiency ${\eta^{ev}}_{n,j}$, the latter (73) & (74) define how the charging current ${i^{e+}}_{n,j,t}$ & EV SOC $S_{n,j,t}$ are calculated. $S_{n,j,t}$ represents the SOC of the j^{th} EV of node n at the time instant t while ${\eta^{ev}}_{n,j}$ the efficiency of battery charging of j^{th} EV including the losses of the battery. The bounds of the time intervals have been substituted by the real arrival and departure times.

$$ B_{n,j,t} = {B_{n,j}}^{a} + \Delta T \sum_{{\tilde{T}_{n,j}}^{a}}^{t} ({p^{e+}}_{n,j,t} {\eta^{ev}}_{n,j}), \quad \forall \, t \in n,j,\left[{\tilde{T}^{a}}_{n,j}, {\tilde{T}^{d}}_{n,j}\right] \tag{71} $$

$$ B_{n,j,{\tilde{T}^{d}}_{n,j}} = {B_{n,j}}^{a} + \Delta T \sum_{t}^{{\tilde{T}^{d}}_{n,j}} ({p^{e+}}_{n,j,t} {\eta^{ev}}_{n,j}), \quad \forall \, t \in n,j,\left[{\tilde{T}^{a}}_{n,j}, {\tilde{T}^{d}}_{n,j}\right] \tag{72} $$

$$ {i^{e+}}_{n,j,t} = {{p^{e+}}_{n,j,t}}\Big/{V_{n,t}}, \qquad \forall \, t \in n,j,\left[{\tilde{T}^{a}}_{n,j}, {\tilde{T}^{d}}_{n,j}\right] \tag{73} $$

Where: $V_{n,t}$: the voltage of node n at time instant t, which is in this thesis has been assumed 0,23 kV and that everything connected to it has the same voltage

$$ S_{n,j,t} = \frac{B_{n,j,t} - {B_{n,j}}^{min}}{\left({B_{n,j}}^{max} - {B_{n,j}}^{min}\right)}, \ \forall \, t \in n,j,\left[{\tilde{T}^{a}}_{n,j}, {\tilde{T}^{d}}_{n,j}\right] \tag{74} $$

"EV and user input" constraints

Equation (75) states that the charging power must be within the power limits of the EV charger ${P^{EVr}}_{n,j}$. Moreover, charging power depends on the EV battery SOC. The CC-CV charging model has been adopted, which states that the charging power linearly increases along with the battery SOC from the EV specific minimum to maximum charging power: ${p^{CCO}}_{n,j}$ & ${p^{max}}_{n,j}$ until 80% SOC: ${S^{CV}}_{n,j}$ (Constant Current charging region), as dictated by equation (76). This is because, during this stage, the voltage or the battery linearly increases with the rising value of the SOC. From 80% to 100% SOC, which is the Constant Voltage charging region (CV region), it is assumed that the charging power linearly decreases from ${p^{max}}_{n,j}$ to zero, as dictated by equation (77) (${S^{CV}}_{n,j} = 0.8$). It must be noted that in reality the dependence of the battery power on the SOC value is non-linear. However, this feature has been ignored for the scope of this thesis in order to formulate the EV charging as a MILP optimization problem. The CC-CV EV charging model is depicted in Fig. 3.6. More information can be found on [15]. The related equations are the following:

$$p^{e+}{}_{n,j,t} \leq P^{EVr}{}_{n,j}, \qquad \forall\, t \in n,j,\left[\tilde{T}^{a}{}_{n,j},\tilde{T}^{d}{}_{n,j}\right] \tag{75}$$

$$p^{e+}{}_{n,j,t} \leq \frac{p^{max}{}_{n,j} - p^{CCO}{}_{n,j}}{S^{CV}{}_{n,j}} * S_{n,j,t} + p^{CCO}{}_{n,j}, \quad \forall\, t \in n,j,\left[\tilde{T}^{a}{}_{n,j},\tilde{T}^{d}{}_{n,j}\right] \,\&\, S_{n,j,t} \leq S^{CV}{}_{n,j} \tag{76}$$

$$p^{e+}{}_{n,j,t} \leq \frac{p^{max}{}_{n,j}}{\left(1-S^{CV}{}_{n,j}\right)} * \left(1 - S_{n,j,t}\right), \quad \forall\, t \in n,j,\left[\tilde{T}^{a}{}_{n,j},\tilde{T}^{d}{}_{n,j}\right] \,\&\, S_{n,j,t} > S^{CV}{}_{n,j} \tag{77}$$

Moreover, equations (79) & (80) express that the battery capacity must be within the EV specific capacity limits $B_{n,j}{}^{min}$ & $B_{n,j}{}^{max}$ and the EV must not receive more energy than the requested, when the EV is connected to the charger j. On the contrary, when the EV is not connected, all charging related variables are set to zero, as shown in equation (81).

$$B_{n,j,t} \geq B_{n,j}{}^{a}, \quad \forall\, t \in n,j,\left[\tilde{T}^{a}{}_{n,j},\tilde{T}^{d}{}_{n,j}\right] \tag{78}$$

$$B_{n,j,t} \leq \min\left\{d_{n,j} + B_{n,j}{}^{a}, B_{n,j}{}^{max}\right\}, \quad \forall\, t \in n,j,\left[\tilde{T}^{a}{}_{n,j},\tilde{T}^{d}{}_{n,j}\right] \tag{79}$$

$$B_{n,j,t} \geq B_{n,j}{}^{min}, \quad \forall\, t \in n,j,\left[\tilde{T}^{a}{}_{n,j},\tilde{T}^{d}{}_{n,j}\right] \tag{80}$$

$$i^{e+}{}_{n,j,t}, p^{e+}{}_{n,j,t}, B_{n,j,t} = 0, \qquad \forall\, t < \tilde{T}^{a}{}_{n,j} \,\&\, t \geq \tilde{T}^{d}{}_{n,j} \tag{81}$$

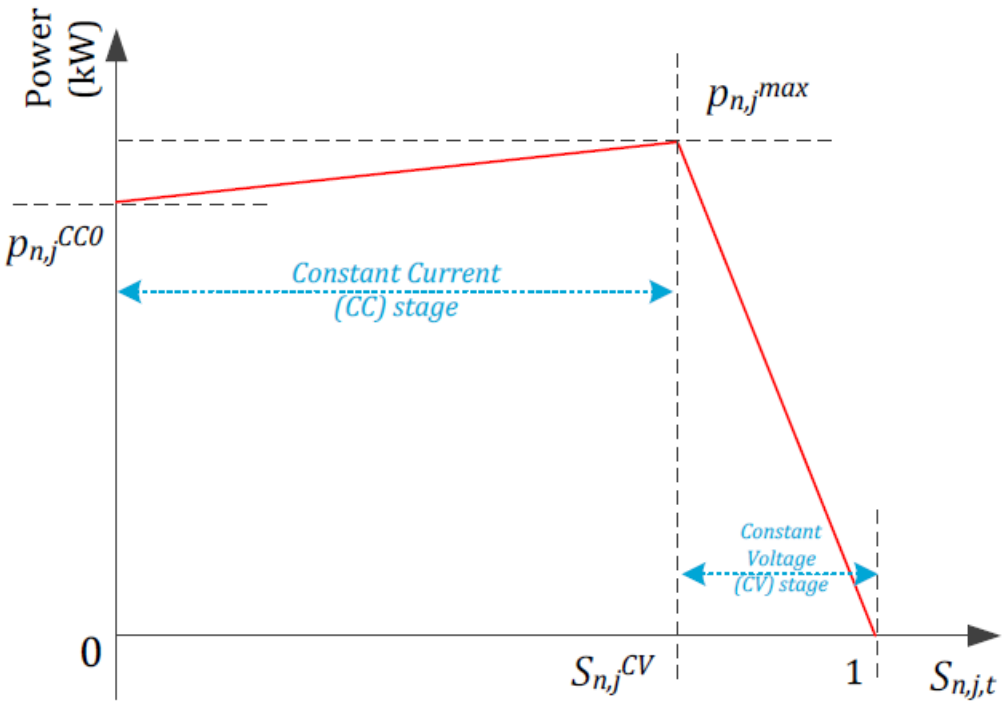

Fig. 3. 6: The CC-CV EV charging model [15]

EV Charger Constraints

According to the protocol IEC61851 [108], equation (82) states that during charging process, the lowest charging current setpoint given by the charger must be 6A, with an integer current value of step 1A.

$$(i^{e+}{}_{n,j,t} = 0)\ OR\ (i^{e+}{}_{n,j,t} \geq 6), \quad \forall\, t \in n,j,[\tilde{T}^{a}{}_{n,j}, \tilde{T}^{d}{}_{n,j}] \tag{82}$$

Import & Export Power Constraints

The import and export power must be within the distribution grid congestion limits as set by the DSO: $p^{G+}{}_{n,t}$ & $p^{G-}{}_{n,t}$, which represent the grid import and export power limit at node n at time instant t respectively, as defined by the grid. These constraints (83) & (84) are considered not to be affected by the integrated uncertainties, since it is realistic to assume that the rated power of the distribution network is many orders higher than the rated power of the station, therefore it is unlikely that the EV station will drive the distribution grid to work at its limits.

$$p^{g(imp)}{}_{n,t} \leq p^{G+}{}_{n,t}, \ \ \forall n,t \tag{83}$$

$$p^{g(ex)}{}_{n,t} \leq p^{G-}{}_{n,t}, \ \ \forall n,t \tag{84}$$

Objective function's Robust Counterpart & Requested Energy Uncertainty

Addressing again the inner max problem of the RC of the objective function in (85):

$$max\ \{\sum_{j=1}^{J}(\ B_{n,j}{}^{a} + \tilde{d}_{n,j} - \ B_{n,j,\tilde{T}^{d}{}_{n,j}})C^{p}{}_{n,j}\ \}, \ \ \forall n,j \tag{85}$$

Substituting (72) in (85), the inner max problem is transformed to (86):

$$\max_{U}\{\sum_{j=1}^{J}[\ B_{n,j}{}^{a} + \tilde{d}_{n,j} - \ (B_{n,j}{}^{a} + \Delta T \sum_{t}^{\tilde{T}^{d}{}_{n,j}}(\ p^{e+}{}_{n,j,t}\eta^{ev}{}_{n,j}))]C^{p}{}_{n,j}\ \}, \quad \forall n,j,t \leftrightarrow$$

$$\max_{U}\{\sum_{j=1}^{J}[\ \tilde{d}_{n,j} - \ \Delta T \sum_{t}^{\tilde{T}^{d}{}_{n,j}}(\ p^{e+}{}_{n,j,t}\eta^{ev}{}_{n,j})]C^{p}{}_{n,j}\ \}, \quad \forall n,j,t \tag{86}$$

As already stated, a certain requested SOC upon departure is a reasonable assumption if we consider that an EV user can never be certain about the exact SOC upon arrival at the station but the needed SOC upon departure is generally definite. Therefore, the requested energy can be replaced by the following equation (87) and the inner max problem regarding requested energy is transformed to the min problem of (88):

$$\tilde{d}_{n,j} = \ (S_{n,j,T^{d}{}_{n,j}} - \ \tilde{S}_{n,j,\tilde{T}^{a}{}_{n,j}}\ ) * B_{n,j}{}^{max}, \qquad \forall n,j \tag{87}$$

$$max\ \tilde{d}_{n,j} \rightarrow \ \min_{U}\left(\tilde{S}_{n,j,\tilde{T}^{a}{}_{n,j}}\ \ * B_{n,j}{}^{max}\right), \quad \forall n,j \tag{88}$$

Where $S_{n,j,T^{d}{}_{n,j}}$: the departure SOC of the j^{th} EV and node n

$S_{n,j,T^a{}_{n,j}}$: the arrival SOC of the j^{th} EV and node n

The inner max problem of the objective function's RC is transformed to the min problem (89), therefore duality theorem is not used for the robust counterpart of the objective function. Moreover, it is clear that, on the one hand, the minimum departure time for every EV at charger j minimizes the value of the inner min problem, hence the minimum parking time represents the worst-case scenario both for the feasibility of the constraints and for the objective value. On the other hand, regarding arrival SOC, the minimum SOC arrival represents the worst-case scenario for the requested energy and the satisfaction of the customer.

Furthermore, the smart-charging algorithm will tend to increase the charging power $p^{e+}{}_{n,j,t}$ in order to deal with the decreased parking period and satisfy the customer requested energy $d_{n,j}$. As a consequence, the minimum PV generation and maximum load demand will burden even more the power balance equation, forcing the EV station to import more or export less power from/to the grid ($p^{g(imp)}{}_{n,t}$ & $p^{g(ex)}{}_{n,t}$) respectively, increasing the charging cost. If it does not increase the charging power, the requested energy will not be met and the charging cost will be increased due to the penalty cost $C^p{}_{n,j}$, which wil be paid to the customer. Finally, the increase of the charging power due to the minimum parking time will challenge more the feasibility of the aforementioned constraints related to the charging power limits (75), (76), (77). The inner max problem (89) is formulated as follows:

$$\min_{U}\{\sum_{j=1}^{J}\tilde{S}_{n,j,\tilde{T}^a{}_{n,j}}+[\Delta T\sum_{t}^{\tilde{T}^d{}_{n,j}}(p^{e+}{}_{n,j,t}\eta^{ev}{}_{n,j})]C^p{}_{n,j}\},\ \forall t\in n,j,[\tilde{T}^a{}_{n,j},\tilde{T}^d{}_{n,j}],\ \forall n,j,t \tag{89}$$

Arrival SOC uncertainty sets & maximum deviations

Considering a zero SOC arrival as the worst-case scenario of the particular uncertainty and a maximum deviation equal to the forecasted SOC value, the following equation (90) is added for the description of the arrival SOC uncertainty:

$$\tilde{S}_{n,j,\tilde{T}^a{}_{n,j}}=S_{n,j,\tilde{T}^a{}_{n,j}}-z_{S_{n,j,\tilde{T}^a{}_{n,j}}}\hat{S}_{n,j,\tilde{T}^a{}_{n,j}},\ \forall n,j\ \leftrightarrow$$
$$\tilde{S}_{n,j,\tilde{T}^a{}_{n,j}}=S_{n,j,\tilde{T}^a{}_{n,j}}*\left(1-z_{S_{n,j,\tilde{T}^a{}_{n,j}}}\right),\ \forall n,j \tag{90}$$
$$0\leq z_{S_{n,j,\tilde{T}^a{}_{n,j}}}\leq 1,\ \forall n,j$$

Assumptions

For the aforementioned problem explanation, the following assumptions must be taken into consideration:

- $C^{e(buy)}{}_t\geq C^{e(sell)}{}_t$: As stated before, the market parties will reassure that the buying grid energy price is equal or slightly higher than the selling grid energy price. In this thesis, it is assumed that: $C^{e(sell)}{}_t=0.95*C^{e(buy)}{}_t,\ \forall t$
- $C^{e(buy)}{}_t, C^{e(sell)}{}_t\gg C^{PV},\ \forall t$: The cost of PV generation to the parties that own the PV park is very lower than the cost of buying/selling energy to the grid in order to provide incentive to the

smart-charging algorithm to use the available PV power. In this thesis, it is assumed that $C^{PV} = 0$, hence the EV station owns the PV park and it is not installed by third parties.

- ${C^p}_{n,j} > {C^{e(buy)}}_t, {C^{e(sell)}}_t, C^{PV}, \forall t$: The penalty cost to the unsatisfied customer is the highest cost of all in order to provide the incentive to the algorithm to satisfy the customer energy demand, even if PV generation is the lowest and load demand is the highest, by importing more or exporting less power from the grid.

Chapter 4: Management of Smart-Charging Uncertainties

4.1 Evolution of the Benchmark Algorithm

As already described in the previous chapter, the deterministic smart-charging algorithm is already an EMS system which utilizes the RHO concept to deal with uncertainties. When a new EV arrival is realized at any timestep of ΔT duration, the MILP optimization is triggered and a new optimization horizon is set. Moreover, the benchmark algorithm integrates more re-optimization options. The first one is monitoring the real charging data of the EV fleets and re-optimizing when the real SOC of a charging EV deviates from the obtained SOC from the optimizer (above the pre-defined threshold of 1%) in order to synchronize them. The second one is monitoring the power exchange grid limit (taking into consideration the cover of the additional load demand and the power needed for the uncontrolled-charging EVs) and re-optimizing at any time-step that the available grid limit for smart-charging deviates highly from the corresponding of the previous timestep.

Motivation Behind benchmark Smart-Charging Algorithm Improvement

In order to address the impact of the considered power system uncertainties on the energy scheduling and improve their management, an additional feature has been added to the benchmark algorithm. In addition to adjusting every new optimization process according to the data obtained from the currently connected EVs and reacting only to new arrivals, the new Prediction-Capable (P-C) algorithm is capable of predicting future EV arrivals (according to the forecasted data) at the particular node. The concept behind this insertion is that scheduling charging according only to the currently-connected EVs can potentially provoke issues, such as increased charging costs or unfinished charging (lower SOC upon departure than requested). This is due to the fact that the benchmark algorithm schedules charging without knowledge of potential future EV arrivals within the previously set optimization horizon. Therefore, it could potentially delay EV charging for later time periods, when for example charging energy price is lower. If charging is scheduled for the last timesteps before the EV departure, a simultaneous EV arrival at another charger of the node can jeopardize the charging results, forcing charging to take place in expensive time periods or leaving the customer partially "unsatisfied". The explanation of the "Prediction-Capable" algorithm is depicted in Fig. 4.1.

At the re-optimization time moment (time-triggering), a particular charger of a node can be characterized by 4 distinct charger modes:

- Charger with new EV arrival
- Charger with an already connected EV, that participates in smart-charging
- Charger with an already connected EV, that does not participate in in smart-charging
- Empty Charger

Explanation of Prediction-based Algorithm Improvement

Considering Fig. 4.1, the nominal algorithm would trigger at t_1, when a new EV arrival is realized at Charger 1 and would set the optimization horizon until "Tmax (reaction)" comparing and selecting the latest departure between the Smart-Charging (S.C) connected EVs (red colour). The No Smart-Charging (No S.C) connected EV at Charger 4 would be excluded by the optimization process and would only be considered in terms of the impact on the power exchange grid limit. On the contrary, the Prediction-Capable algorithm also triggers upon the new EV arrival at Charger 1, but it takes into account all the node chargers for the energy-scheduling.

Therefore, it firstly sets the optimization horizon until the departure of the arrived EV at Charger 1, considering only the already connected EVs at Chargers 1 & 2. Consequently, it searches for the predicted EV arrivals at all node chargers, even if the charger is empty or currently contains a No S.C

EV. After storing all the predicted arrivals at all chargers until the initial horizon end (Tmax – reaction), it sets the optimization horizon until the latest departure of the predicted arrivals (Tmax – prediction). In Fig. 4.1, the latest departure belongs to the last predicted arrival of Charger 4 (predicted EV [2]). The EVs that are predicted to arrive after the end of the initial horizon (marked with blue color) are not considered in the prediction-based optimization. The reason behind their exclusion is because prediction capability has been added to the benchmark algorithm to provide it with knowledge about the EVs that are going to arrive, while the already connected EVs are still charging. Prolonging the optimization horizon to integrate all future EVs (e.g all EVs of the total time duration) would increase exponentially the computational burden and time of the optimization and with no significant reason, since they will be integrating in the next re-optimization of the next future EV arrival.

Furthermore, an additional feature has been added to the smart-charging algorithm. The "Prediction-Capable" algorithm takes into account the preference of the future EV arrivals for smart-charging participation or not. It integrates the EV in the optimization process, if it is willing to participate or it adjusts the grid power limit accordingly, if it prefers uncontrolled charging. In addition, if a future EV arrival wants to participate in S.C, but it arrives with an SOC below the required threshold, the algorithm predicts in which timestep the EV will be charged enough to be able to be integrated in the optimization process (e.g 3rd future arrival at Charger 3). On that manner, the 1st predicted arrival at Charger 2, which is marked totally with black color, could be an EV that is not willing to participate in S.C at all or it never reaches the required threshold for S.C participation during its predicted parking time. Finally, it predicts the timestep that a currently connected No S.C EV reaches the required SOC threshold to participate and treats it as a coming S.C EV in the optimization (current EV [0] at Charger 4).

Taking everything into account, the improvements of the P-C algorithm, regarding prediction and EV users' driving patterns) can be summarized as follows:

- Prediction of the future EV arrival and adjustment of the new prediction-based optimization horizon accordingly
- Consideration of EVs that are not willing to participate in Smart-Charging
- Prediction when EVs (currently connected or future arrivals) will surpass the Smart-Charging SOC threshold of 20% and enter Smart-Charging

In the next paragraphs, the 2 Studies of the investigation (Study 1 for PV generation, Load demand, Arrival & Departure Times and Arrival SOC uncertainties & Study 2 for FCR reserves) are described. It must be noted that the mathematical formulation of Study 1 is as exactly described in Chapter 3, while Study 2 modifies some parts of the formulation for the development of the improved FCR provision model.

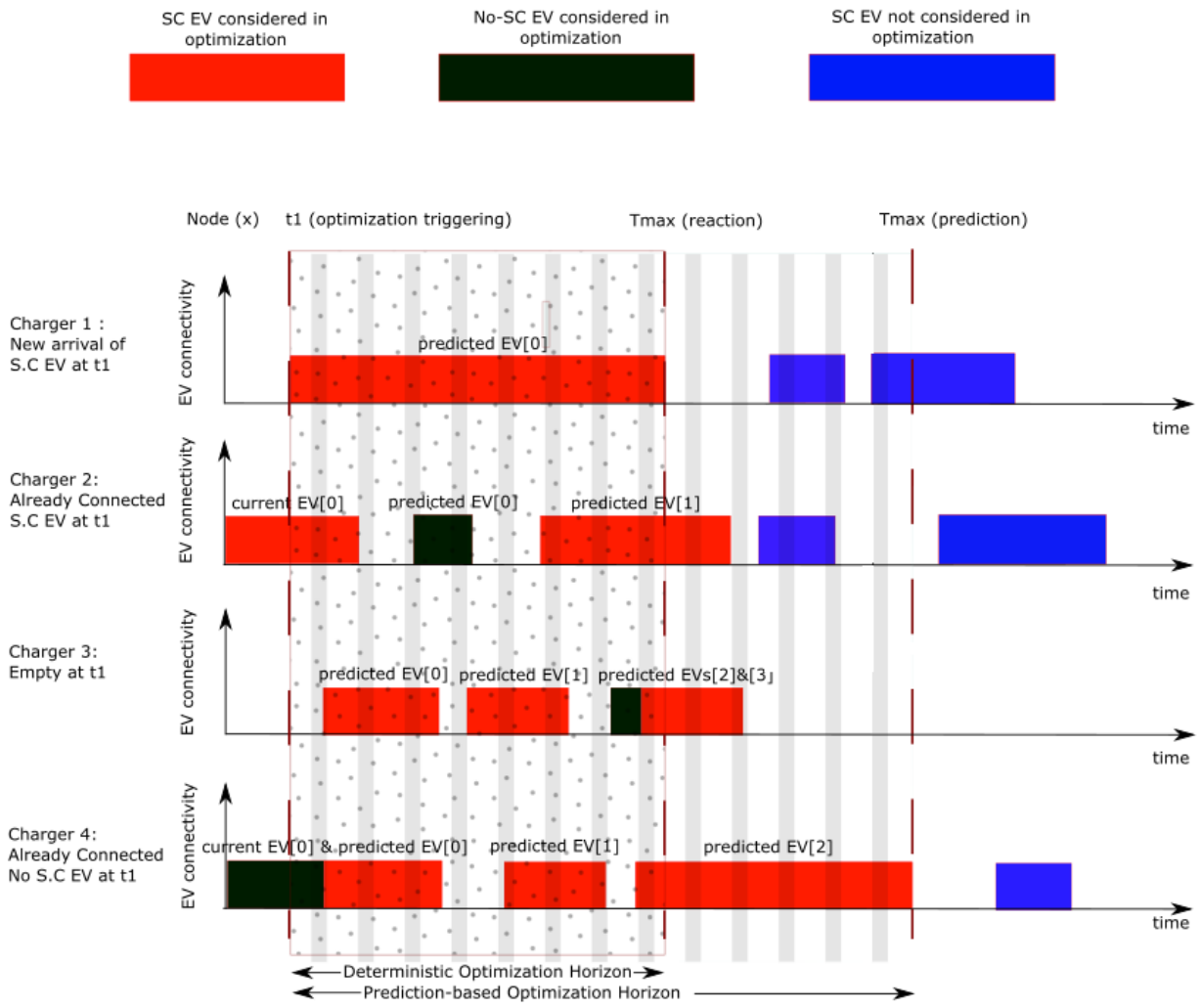

Fig. 4. 1: Concept of Smart-Charging Algorithm with prediction capabilities

4.2 Study 1: Investigation of PV generation, Load demand & EV User driving uncertainties without consideration of FCR Reserves provision

As stated in [109] & [11], uncertainty can lead up to 50% and more violation of the mean values of the uncertain variables. In order to maintain a certain level of uncertainty and extract solid results from the comparison regarding the uncertainties' impacts and management, a steady 50% deviation has been chosen for every uncertain variable considered. Moreover, the 50% deviation of every variable has been selected, because all of the uncertainties are studied individually. Therefore, management of a relatively high level of uncertainty is recommended. Potential future study of simultaneous events of uncertainties' worst-case scenarios, as recommended in Chapter 7, should integrate lower deviations in order to avoid potential problem' overconservativeness.

4.2.1 Management of PV generation & Load Demand Uncertainties with Robust Optimization

PV Generation

As already stated in the previous chapter, Robust Optimization protects the benchmark problem

against decreased PV generation, since increased PV generation represents a better case scenario for EV charging. This is justified by the fact that decreased PV generation forces constraint (59) to function at its limits. It controls the trade-off "protection-conservativeness" with the PV uncertainty index (or else maximum deviation index):

$$0 \leq z_{p_{t,n}max} \leq 1, \ \ \forall t,n \tag{91}$$

$z_{p_{t,n}max} = 1$: represents the worst-case scenario of zero PV Generation for the system while, $z_{p_{t,n}max} = 0$: represents the ideal scenario of perfect forecast of PV Generation

In order to manage all deviations of the real PV Generation from the corresponding forecasting curve and simultaneously avoid over-conservativeness of the problem (such as a continuously zero PV generation), this thesis takes advantage of the adaptability that Receding Horizon approach can provide to Robust Optimization. The explanation of the concept of algorithm's functionality below is depicted in Fig. 4.2. Every time instant of a new EV arrival or departure, a new optimization horizon is set and a re-optimization is triggered. At that time instant, the smart-charging algorithm is updated regarding the input data (PV generation, Load demand, EVs driving patterns & characteristics), that will be used during the new optimization. Therefore, the algorithm firstly is updated about the real PV generation at the time-trigger. It stores the deviation in percentage between real and forecasted PV Generation value at the time-trigger and adjusts the forecasting curve during the optimization horizon (t_1 to t_2 in Fig. 4.2) according to the initial deviation. Then it utilizes Robust Optimization, decreasing the adjusted PV Generation forecasting curve (upper bound of PV Generation constraint) by gradually increasing the uncertainty index $z_{p_{t,n}max}$. The horizon in Fig. 4.2 starts with an initial $z_{p_{t1,n}max} = 0$, which increases by 10% every hour. In order to avoid conservativeness in long parking periods, when re-optimizations occur less often, after 5 hours the uncertainty index reaches the value $z_{p_{t1,n}max} = 0.5$ and remains steady until next re-optimization.

Load Demand

The same concept is applied for management of Load Demand Uncertainty. Robust Optimization protects the benchmark problem against increase of load demand and controls "Protection-Conservativeness" by the Load uncertainty index:

$$0 \leq z_{L_{t,n}max} \leq 1, \ \ \forall t,n \tag{92}$$

$z_{L_{t,n}max} = 1$: represents the worst-case load demand scenario of double load, considered in this thesis
$z_{L_{t,n}max} = 0$: represents the ideal scenario of perfect forecast of Load Demand

Again, after adjusting the load forecasting curve according to the initial deviation of the real measurement at the optimization start, the Load uncertainty index starts from 0 at the time-trigger and increases by 20% every 1 hour. After 5 hours, it remains steady at the worst-case scenario of double load until re-optimization, in order to reduce over-conservativeness of the problem.

Finally, the benchmark algorithm saves power from the grid imported power limit in order to be able to cover the maximum forecasted load at every timestep. In order to take into account the real load demand data at every timestep, an additional feature has been added to the new Prediction-Capable version. The algorithm compares at every timestep the real load demand with the maximum forecasted

load demand and adjusts the power save for the cover of the load accordingly.

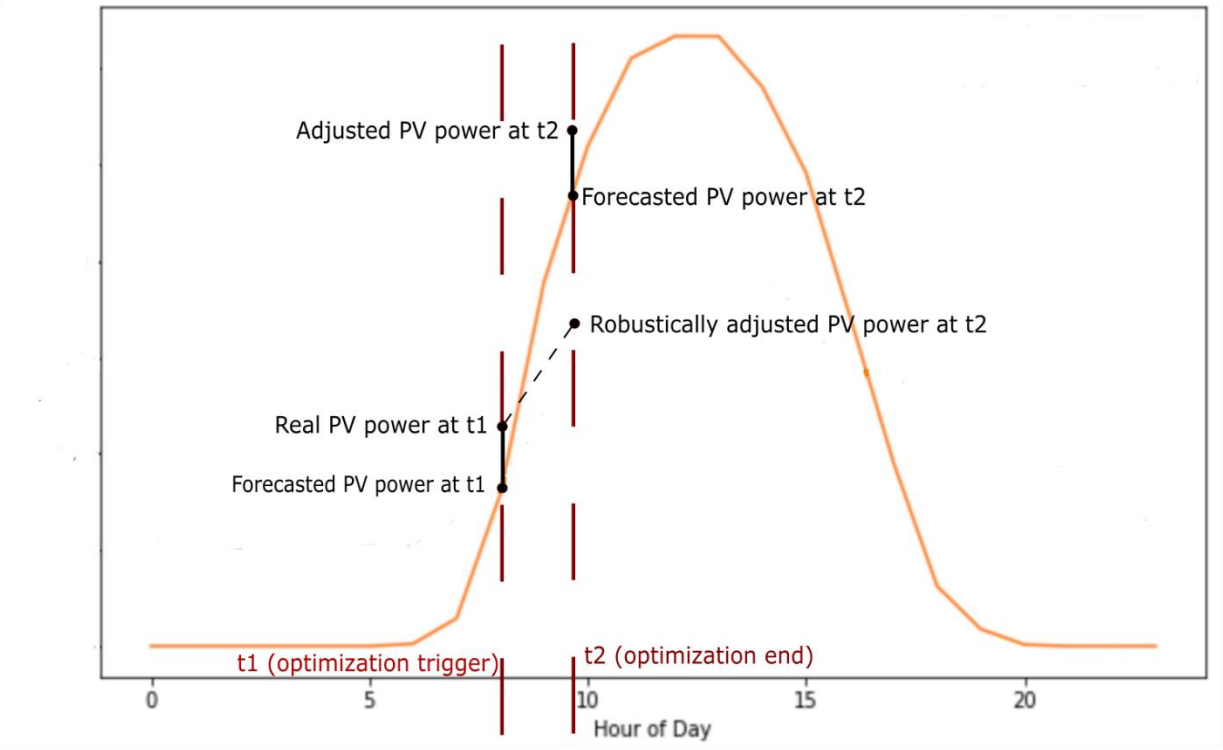

Fig. 4. 2: Concept of PV Generation Uncertainty Management using RO and RHO

4.2.2 Management of Arrival SOC and Parking Time Uncertainties with Robust Optimization

Arrival SOC

As already proven, a minimum arrival SOC represents the worst-case scenario of the particular uncertainty. The "Prediction-Capable" algorithm takes into account the predicted arrival SOC and requested energy data of the coming EVs at the node chargers. The prediction of the worst-case scenario of the minimum arrival SOC (e.g 50% SOC) should provoke a rushed charging of the currently connected cars. If the algorithm predicts an 100% accurate arrival SOC and a minimum SOC arrives, this can potentially jeopardize the optimality of results, since if it had predicted the worst-case scenario, it could have saved more space for energy charging of the coming EV. On the contrary, if the algorithm predicted the minimum arrival SOCs, but the EV arrived with the predicted SOC value, then a potential rushed-up charging, in likely "expensive" hours in terms of energy price, could have been realized without cause, showing the over-conservative aspect of Robust Optimization.

Here, the uncertainty index of arrival SOC lies in the same interval as the previous uncertainties:

$$0 \leq z_{S_{n,j,T^a{}_{n,j}\,max}} \leq 1, \quad \forall t, n \tag{93}$$

$z_{S_{n,j,T^a{}_{n,j}\,max}}$ = 1: represents the worst-case arrival SOC scenario considered

$z_{S_{n,j,T^a{}_{n,j}\,max}}$ = 0: represents the ideal scenario of perfect forecast of arrival SOC

In order to avoid over-conservativeness of solution (a zero arrival SOC of all EVs) which is unlikely to

happen, a 50% decrease has been considered as maximum deviation, hence: $z_{S_{n,j,T^a{}_{n,j}max}} = 0.5$

Parking Time

On the same manner, a minimum parking time is the worst-case scenario for the optimality of the results and the feasibility of the constraints. The uncertainty indices of departure and arrival times are $z_{T^d{}_{n,j}max}$ & $z_{T^a{}_{n,j}max}$, respectively. Considering a 50% decrease of the parking time as the worst-case scenario and maximum deviations equal to the forecasted parking time, the uncertainty indices can be derived by equations (68) as follows:

$$\hat{T}^d{}_{n,j} = \hat{T}^a{}_{n,j} = T^d{}_{n,j} - T^a{}_{n,j}, \quad \forall n,j \tag{94}$$

$$0 \leq z_{T^d{}_{n,j}max} = z_{T^a{}_{n,j}max} \leq 1, \quad \forall n,j \tag{95}$$

$$\tilde{T}^d{}_{n,j} = T^d{}_{n,j} - z_{T^d{}_{n,j}max}\hat{T}^d{}_{n,j}, \quad \forall n,j \tag{96}$$

$$\tilde{T}^a{}_{n,j} = T^a{}_{n,j} + z_{T^a{}_{n,j}max}\hat{T}^a{}_{n,j}, \quad \forall n,j \tag{97}$$

(94) – (97): $\tilde{T}^d{}_{n,j} - \tilde{T}^a{}_{n,j} = 0.5 * \left(T^d{}_{n,j} - T^a{}_{n,j}\right) \leftrightarrow$

$$T^d{}_{n,j} - z_{T^d{}_{n,j}max}\left(T^d{}_{n,j} - T^a{}_{n,j}\right) - T^a{}_{n,j} - z_{T^a{}_{n,j}max}\left(T^d{}_{n,j} - T^a{}_{n,j}\right) = 0.5 * \left(T^d{}_{n,j} - T^a{}_{n,j}\right) \leftrightarrow$$

$$z_{T^a{}_{n,j}max} + z_{T^d{}_{n,j}max} = 0.5 \tag{98}$$

Predicting that the available time for charging the future EVs is minimum (either due to delayed EV arrival or earlier EV departure) should also provoke the algorithm behave similarly with the arrival SOC uncertainty. Moreover, a biased charging beforehand by an over-conservative prediction can also provoke an acausal increase of the charging cost. However, prediction of later arrivals than the forecasted could potentially delay charging of the currently connected EVs. This can have negative impact on the satisfaction of the customers, if the algorithm wrongly predicts that there will be enough energy space to charge the currently connected EV later. Therefore, the reduction of parking time has been tested with 2 modes in this thesis:

- Reduction by delayed EV arrivals & earlier EV departures

Regarding the first mode, equal uncertainty indices are assumed (uncertainty assumed to have a similar impact to arrival and departure since it depends on human behavior) and reduction of the parking time has been performed 25% by arrival and 25% by departure, as dictated by equation (99).

$$z_{T^a{}_{n,j}max} = z_{T^d{}_{n,j}max} = 0.25, \quad \forall n,j \tag{99}$$

- Reduction only by earlier EV departures

Regarding the second mode, all uncertainty has been inserted in the EV departure time, keeping the arrival times fixed to the forecasted values, as dictated by equation (100).

$$z_{T^a{}_{n,j_{max}}} = 0 \qquad \& \qquad z_{T^d{}_{n,j_{max}}} = 0.5, \ \forall n, j \tag{100}$$

Study Cases for arrival SOC and Parking Time Uncertainties

The P-C algorithm has two parts: the Prediction part, where it utilizes the new prediction feature and the Reality part, which represents the real arrival and charging of the EVs. For the arrival SOC and Parking Time uncertainties, the investigation has been divided into two parts.

- Firstly, two study cases have been compared, where the uncertainties worst-case scenarios remained only in prediction. In other words, in the first study case the P-C algorithm predicts that the EVs will arrive with their forecasted parking time request or SOC, while in the second study case it predicts that they will arrive with the worst-case scenarios. However, the EVs actually arrive with the forecasted parking time or arrival SOC. As already explained, this comparison aims to address the level of RO over-conservativeness.

- Secondly, the same comparison has been performed, when EVs actually arrive with the worst-case scenarios of uncertainties (min arrival SOC or min Parking Time request). In other words, in the first study case, the behavior of the P-C algorithm is studied when it had predicted that it would happen, while in the second study case the behavior of the Benchmark algorithm is studied, which with no prediction capabilities, remains completely vulnerable to uncertainties. This comparison aims to address the impact of the uncertainties and their potential robust manageable by combination of RO and prediction.

4.3 Study 2: Investigation of Regulation Reserves Provision Uncertainty Impact & Management

4.3.1 Introduction to Energy Markets

In contrast with the previous decades, when the electricity sector was organized as a regulated monopoly in each country, during the last two decades, European Union has made efforts to increase competition, intending to develop an internal European Electricity Market. The 3 main means of trading electricity are the following:

- Power exchange trading platform (pool market): Generation and Demand bids are offered to the pool market by the corresponding GenCos & DemCos and during a prespecified time period a single price is defined, depending on the offered bids, which is called "market clearing price"
- Bilateral over-the-counter (OTC) trading: GenCos & DemCos interact directly and sign individual trade contracts
- Organized over-the-counter (OTC) trading: This type of energy trading constitutes a combination of the former 2 types. Generators and Consumers participate in the pool market offering their bids. However, the market is cleared and bilateral exchanges are realized continuously.

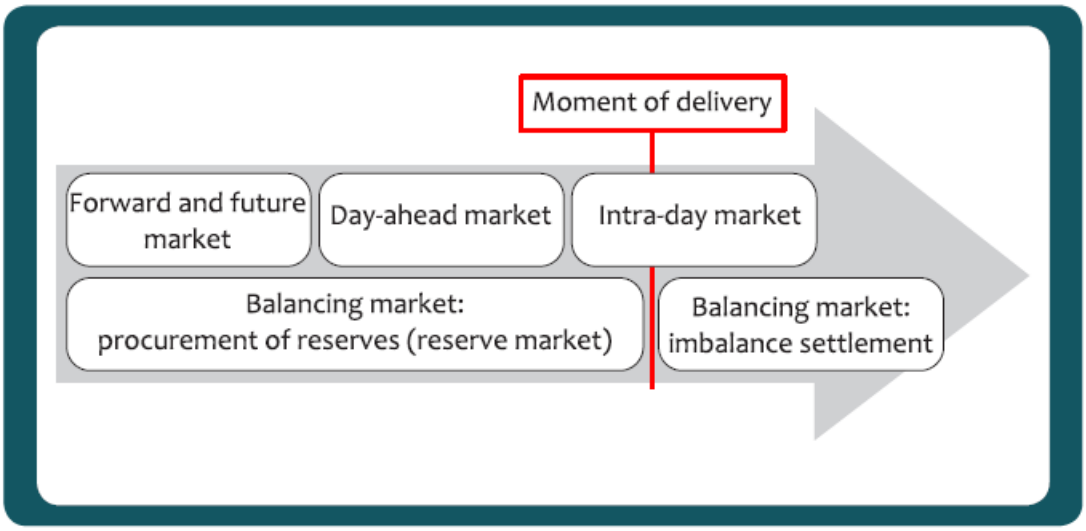

Fig. 4. 3: Overview of the different electricity market in the European Union [86]

As it can be seen in Fig. 4.3, there are various electricity markets that are being realized, a small summary of which, will be presented below. For more information, the reader is referred to [86].

- Forward and Future Market: Energy exchange contracts for delivery of a pre-arranged amount f energy up to even years in the future. While future contracts are mainly standardized, the majority of forward contracts belong to the Bilateral OTC category.
- Day-Ahead Market: In the particular market (DAM), energy trading is realized one day before the actual delivery. It constitutes one of the most significant energy markets, since the planned generation of the next day has to be in balance with the predicted consumption and the total export to other zone areas at the end of the DAM of the previous day.
- Intra-day Market: In Intra-day Markets (IDM), electricity is traded continuously during the delivery day. The main advantage of the particular market is that participants are allowed to improve and modify their arranged energy deliveries in the DAM if unexpected events, such as power outages occur. In order to enlighten the difference between the DAM & IDM markets, in 2013 the Belgian DAM (Belpex DAM) traded a total amount of 17.1 TWh in an average price of 47.45 €/MWh, whereas the Belgian IDM (Belpex CIM) traded a total of 0.6 TWh.
- Balancing Market: The TSO is responsible to deal with the system net imbalance, which is caused by the sum of the real-time imbalances of the individual Balance Responsible Parties (BRPs) and for that reason it utilizes the balancing market. The balancing market is divided into the following two categories:
    - Procurement & activation of reserves (or else reserve market): Various reserve types are contracted, such as Frequency Containment Reserves (FCR), Frequency Restoration Reserves (FRR) & Replacement Reserves (RR), which will be addressed in the following paragraphs
    - Settlement of Imbalances: This part of the balancing market constitutes actually a tariff to each imbalanced BRP and is realized after the actual delivery. It integrates the concepts of "Marginal Incremental Price (MIP)" & "Marginal Decremental Price (MDP)". MIP & MDP are defined as the highest & lowest price paid for upward & downward reserve offers, respectively [86].

4.3.2. Ancillary Services & Regulation Reserves

The integration of large number of EVs in the future electricity grid allows Smart-Charging to be involved, apart from the main purpose of sustainable EV charging with minimum charging cost and limited impact on the grid limits, with provision of ancillary services to the TSO. The utilization of the emerging V2G technology, which permits the bi-directional power flow from the grid to the EV and vice versa, grants the Charging Station with the capability of participating in both energy and ancillary services markets, providing simultaneously extra economic incentives to the customers to become EV owners [87]. Such ancillary services can be Up & Down Regulation Reserves, Spinning or non-Spinning Reserves etc. The Regulation Reserves belong to the category of ancillary services under normal conditions, which integrate also services such as Load Following or Energy Imbalance & Voltage Control. On the contrary, Spinning or non-Spinning reserves belong to the category of ancillary services under contingencies, such as Replacement or Supplemental Reserves [88]. All of the aforementioned ancillary services are highly significant for the power system reliability and can be of great use for the TSO, whose main responsibility is to ensure the stability of the power grid and a safe and qualitative power flow between production and demand.

Regulation is defined as the on-line generation, which is also characterized by Automatic Generation Control (AGC), having as main purpose firstly to track momentary frequency fluctuations production or customer load changes and secondly to aid the frequency and the interconnection frequency restoration and power flow between the balancing areas [88]. The Regulation Reserves can be divided to the following 3 categories [86]:

- Frequency Containment Reserves (FCR): These regulation reserves, also called primary reserves, are activated during large frequency deviations and are utilized for frequency stabilization within 30 sec (in EU) [89]. The primary reserves are actually a certain amount of power – capacity which is contracted via a weekly auction. Taking advantage of the so-called "droop control characteristics" of the participating generators, primary reserves are responsible of the power system stability for at least 15', when the secondary reserves are activated. Finally, they can be both up and down, therefore the TSO can ask either for drawing or releasing power in order to adjust system frequency back to the nominal levels [90]. For example, TenneT contracted a total amount of 96 MW during 2015 for the Dutch Electricity grid [89].
- Frequency Restoration Reserves (FRR): The FRR reserves, also called secondary reserves, are controlled and activated automatically and centrally within a maximum of 15 minutes and remain activated for at least 2h in order to balance energy imbalance. The main purpose of the FRR reserves is to pursue slow and low load deviations around the load demand level before the disturbance and not to correct the set points after the disturbance, which is assigned to the tertiary reserves that come next [90]. TenneT contracts approximately 300 MW of FRR reserves per year [89].
- Replacement Reserves (RR): The RR reserves, or else tertiary reserves, are activated in the range of minutes to hours and are utilized to restore balance when FRR reserves have not been able to fully accomplish it. Hence, the emergency power is essential for an extended period of time [89]. Moreover, upon their activation, they permit to the FRR units to return back to normal and be ready for the next disturbance event [91]. The set points are arranged for every contingency event maintaining bus power balance and zero Area Control Error (ACE) [90]. Finally, all provided Regulation Reserves can be both up and down, hence drawing and releasing power to the grid respectively, due to the emerging V2G technology [92]

In Fig. 4.4, the technical characteristics and purpose of all FCR, FRR & RR reserves can be observed (the red, blue & green areas respectively) along with the Inertia and spinning/non-spinning reserves,

which go beyond the scope of this project.

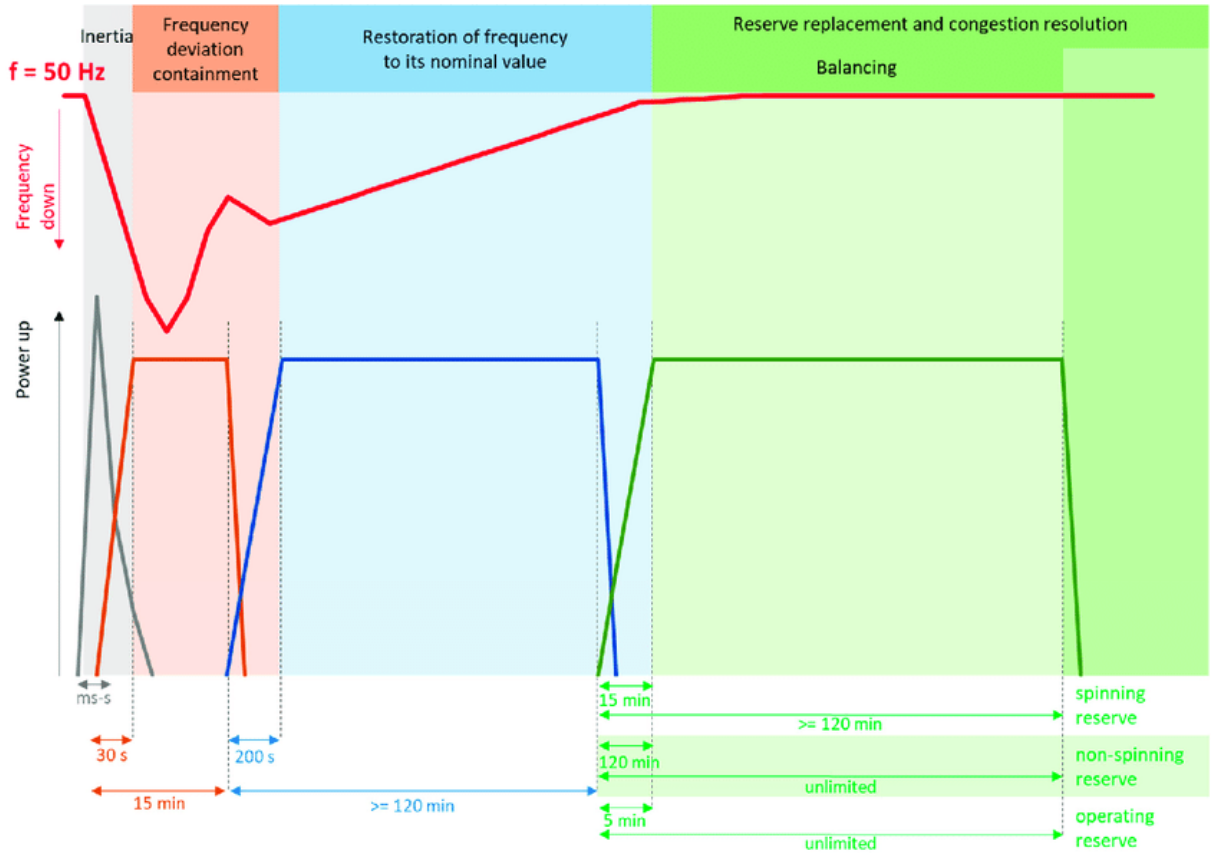

Fig. 4. 4: Technical Characteristics of Primary, Secondary & Tertiary Regulation Reserves [91]

4.3.3 EV Smart Charging & FCR Reserves

The ever-growing EV fleets are in position to offer various ancillary services, however this thesis will focus on the capability of EV fleets to provide FCR Regulation Reserves. This is justified by the fact that EVs are characterized by extremely high ramp up and down rates (even as less as 200ms according to Chademo and Combo EV charging standards) [97]. Hence, this makes EVs significantly attractive regulation providers in terms of FCR reserves, according to various researches [93], [94], [95], [96]. Other researches, however, have focused on the provision of FRR services, such as the authors in [97]. They have shown that the provision of positive aFRR reserves in Germany from 30 October 2018 to 31 July 2019, can accomplish a positive net return, which however is not yet enough to balance the investment cost of the corresponding installation.

As already can be seen and as the authors in [98] suggest, the provision of all regulation reserves is essential for the management of frequency fluctuations from the nominal levels. Their contribution is to maintain always the power-frequency balance between production and demand in the entire interconnected power grid, according to the European Union Internal Electricity Balancing Market. Moreover, the offer of regulation reserves can grant the owners of the Charging stations and the EV owners with economic revenues, therefore incentives to the former owners to utilize smart-charging and the latter to own EVs and participate in smart-charging programs. Therefore, the inclusion and consideration of regulation reserves provision in the smart-charging optimization is deemed necessary

and highly important, considering that most charging stations will participate in the regulation market in the nearest future. However, it must be noted that the installation investment for the regulation reserves is still expensive, therefore profitability by participation in the regulation market highly depends on the FCR design type, FCR price range & amount of the investment. Nevertheless, the consideration of the aforementioned aspects goes beyond the scope of this project.

As stated in [99], the regulation services are not actually provision of energy, rather provision of capacity. The FCR companies offer pre-specified regulation capacities and are obliged to be capable of actually providing the offered reserve for the entire delivery period, which can be up to 15' [89], [99]. Moreover, services will be remunerated, even if the reserves are not called by the TSO in real-time. The reserves capacity fee is determined either in a yearly or an hourly basis, depending on whether the market agreement is for a "forward and future market" or a "day-ahead" market. Finally, the FCR providers must pay a penalty fee such high as the capacity fee, if they fail to provide the capacity reserves, that they committed to provide in the bidding market [92], [99].

On that manner, there are 4 different concepts of regulation reserves that have been distinguished in this thesis for extraction of realistic results from the optimization.

- Up and down natural regulation reserves: Represent the amount of capacity reserves, that the algorithm could provide to the grid in respect of the power limits of the EVs, the EV chargers and the grid along with the decided (optimizer) EV charging power.
- Up and down offered-bid regulation reserves: Depending on the magnitude of the "natural" reserves, the algorithm finally decides the amount of this magnitude that will be offered in the bidding market. This amount of up or down regulations is always lower or equal to the corresponding "natural capacity" amount and is the amount that the algorithm will be obliged to be capable of providing for a certain period of time (e.g 15'), until the FRR reserves can be activated. Moreover, this capacity amount defines the remuneration of the algorithm even if it is not actually called by the TSO.
- Up and down called regulation reserves: In real time, there is always uncertainty in what reserve capacity will be actually called by the TSO. The TSO remunerates the algorithm for the committed capacity. However, the magnitude of the actually called capacity amount is never known beforehand and depends on the real-time power frequency balance in the interconnected grid, therefore it continuously changes. By all means, the called capacity reserves will be always lower or equal to the accepted offered reserves in the bidding market and are essential to the algorithm, because they directly affect the EVs' SOCs and power balance
- Up and down expected reserves: These reserves are integrated in the optimizer in order to schedule more efficiently the optimized EV charging. They are always lower or equal than the offered represents and they represent the reserves that the algorithm expects that the TSO will call within the optimization horizon. Hence, they are integrated in the EVs' SOC and power balance equations to represent the called reserves in the optimization.

Therefore, it can be seen that uncertainty exists in all concepts of regulation reserves. On the one hand, the bidding strategies in the day-ahead FCR market highly depend on the EV behavior uncertainty. Moreover, there is uncertainty in the percentage of the offered capacity reserves amount that will be actually accepted to participate in the regulation service. Finally, since real-time grid behavior can never be perfectly predicted, the actually called capacity reserves by the TSO remains uncertain until the time of delivery.

Fig. 4.5 aims to enlighten the aforementioned distinction of the 3 regulation reserves concepts. If the particular generator functions with an average of 90 MW output power and has offered in the bidding market 10 MW up and down capacity, the offered-bid capacity reserves will be 90-100MW & 80-90 MW,

respectively. That means that the generator is obliged to be capable of fluctuating its output between the interval 80-100MW for e.g the next hour. However, the natural capacities can be higher than the offered regulation capacities. For example, generator of Fig. 8.2 has probably 90 MW (or close to 90MW) down regulation capacity, if it zeroes its output. Finally, the TSO within the time interval (14:00, 15:00) is free to ask for any regulation reserves amount within the power interval (80 MW, 90 MW) [88].

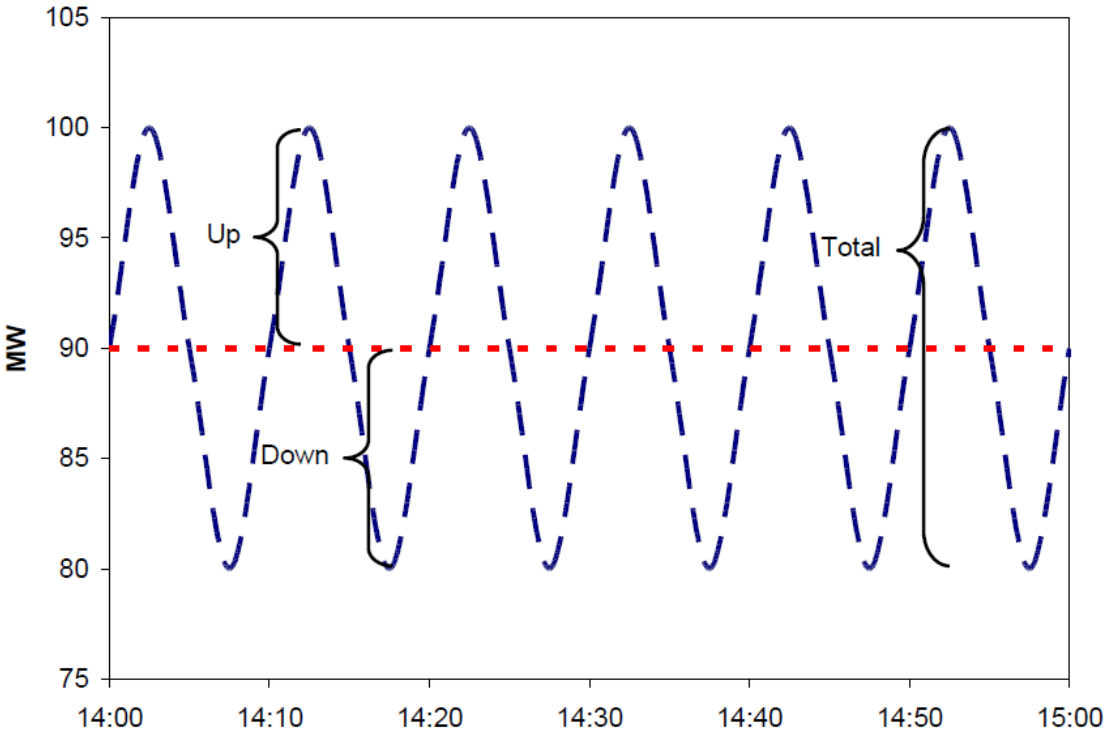

Fig. 4. 5: Concept of Up and Down FCR Regulation Reserves [82]

4.3.4 Mathematical Formulation of FCR Reserves Integration in the Optimization

"Natural" & "Offered" Regulation Reserves

Until now, the benchmark smart-charging algorithm only computed the natural reserves according to the equations that represent the aforementioned limits and simultaneously integrated them in the objective function without integrating them in the power balance or the EVs' SOCs equations ((63) & (71) respectively). Hence, it was assumed that, on the one hand the algorithm offers and on the other hand the market accepts and remunerates the algorithm for the "natural" capacity. Moreover, it is simultaneously assumed that the TSO never actually asks for them or that the net power called is zero over the time duration, therefore there is not actual impact on the SOC of the EVs.

However, it must be noted that this is an unreal situation and the solution of the problem is in reality much more complex. The offer of reserves to the regulation market and the amount of which is actually accepted is an optimization problem itself are approached by various researches with bilevel optimization. For example, authors in [100] address the DAM bidding strategy of a PEV aggregator, which offers only demand bids, with a bilevel MILP problem, whose upper problem elaborates on the charging cost minimization, while the lower problem deals with the market clearing price. Since the market clearing price depends on the behavior of the other market participants, the PEV aggregator bidding strategy utilizes historical data for the estimation of their decisions. On the same manner, the strategic bidding of a merchant energy storage operator is also addressed with a bilevel optimization

problem in [101], according to which the lower problem represents the clearance of a multi-period market and communicates with the upper problem which is responsible for the optimization decisions of the storage bids. Finally, [102] intends to compare the two different auction markets (SMP market with system marginal price or else market clearing price & PAB market with pay-as-bid auction which realizes bilateral contracts between Gencos). The authors treat the strategic bidding as a multi-agent optimization problem and instead of utilizing the classical game theory, they adopt the use of coevolutionary genetic algorithms (GA).

For the scope of this thesis, in order to avoid transition to bi-level optimization or to multi-agent optimization and game theory, efforts have been focused to integrate the natural and bid regulation capacities within the same optimizer, allowing the optimization problem to remain a single-level MILP. More specifically, the natural and bid-offered regulation capacities are represented by different series of decision variables, $p^{r(up)}$ & $p^{r(dn)}$ and $p^{r(up\_of)}$ & $p^{r(dn\_of)}$, respectively. While the first ones are integrated in all constraints, which represent the various limits that shall be respected (EVs power limits, EV chargers power limits, CC-CV regions limits and import & export grid power limits), the second ones are integrated in the objective function and are always lower than the corresponding natural reserves. This is justified by the fact that the natural capacities, therefore the regulation reserves that the algorithm is capable of providing, must be computed by the various power limits which restrict the charging capabilities of the algorithm. On the contrary, the offered regulation reserves participate in the objective function, since the algorithm is remunerated according to them and since they are always lower than the natural ones, they will respect the power limits, as well. Moreover, the natural and offered up & down regulation reserves can co-exist simultaneously, since the algorithm can offer them at the same time.

Finally, it must be noted that in reality and as stated in various investigations, such as in [100], [101], [102], the offered capacities to the TSO do not necessarily participate entirely in the bidding market, since they depend on the market clearing price. Since the bidding process and the "price-maker" capability of the algorithm have not been considered, in this thesis the participation uncertainty has been avoided. It has been assumed that the offered regulation capacities to the TSO will actually and entirely participate in the regulation market and the algorithm will be remunerated according to them.

On that manner, for Study 2, the objective function (51) is transformed to equation (101) which includes the remuneration of the algorithm by the FCR reserves provision:

$$min\ {C_n}^{opt} = \sum_{j=1}^{J} (B_{n,j}{}^{a} + d_{n,j} - B_{n,j,\tilde{T}^{d}{}_{n,j}}) C^{p}{}_{n,j}$$
$$+ \Delta T \sum_{t=1}^{T} p^{PV}{}_{n,t} C^{PV} + \Delta T \sum_{t=1}^{T} (p^{g(imp)}{}_{n,t} C^{e(buy)}{}_{t} - p^{g(ex)}{}_{n,t}\, C^{e(sell)}{}_{t})$$
$$- \Delta T \sum_{t=1}^{T} \sum_{j=1}^{J} (p^{r(up\_of)}{}_{n,j,t} C^{r(up)}{}_{n,t} + p^{r(dn\_of)}{}_{n,j,t}\, C^{r(dn)}{}_{n,t}) \quad (101)$$

Where $p^{r(up\_of)}{}_{n,j,t}$: the offered reserve power capacity for up regulation by the j^{th} EV at time t at node n (kW)

$p^{r(dn\_of)}{}_{n,j,t}$: the offered reserve power capacity for down regulation by the j^{th} EV at time t at node n (kW)

$C^{r(up)}{}_{n,t}$: the regulation income for offered reserve power capacity for up regulation by the j^{th} EV at time t at node n (€)

$C^{r(dn)}{}_{n,t}$: the regulation income for offered reserve power capacity for down regulation by the

j^{th} EV at time t at node n (€)

And the corresponding robust counterpart, as formulated in equation (102):

$$min\ C_n{}^{opt} = \min\Bigg\{ \Delta T \sum_{t=1}^{T} p^{PV}{}_{n,t} C^{PV} + \Delta T \sum_{t=1}^{T} (p^{g(imp)}{}_{n,t} C^{e(buy)}{}_t - p^{g(ex)}{}_{n,t}\, C^{e(sell)}{}_t - \Delta T \sum_{t=1}^{T} \sum_{j=1}^{J} (p^{r(up\_of)}{}_{n,j,t} C^{r(up)}{}_t + p^{r(dn\_of)}{}_{n,j,t}\, C^{r(dn)}{}_t) + \max_{U} \{ \sum_{j=1}^{J} (B_{n,j}{}^{a} + d_{n,j} - B_{n,j,\tilde{T}^d{}_{n,j}}) C^{p}{}_{n,j} \} \Bigg\} \quad (102)$$

Moreover, equations (75), (76), (77) are transformed to (103), (104) & (105) respectively:

$$p^{e+}{}_{n,j,t} + \eta^{ch}{}_{n,j} * p^{r(up)}{}_{n,j,t} \le P^{EVr}{}_{n,j}, \qquad \forall\, t \in n,j,\left[\tilde{T}^a{}_{n,j}, \tilde{T}^d{}_{n,j}\right] \quad (103)$$

$$p^{e+}{}_{n,j,t} + \eta^{ch}{}_{n,j} * p^{r(dn)}{}_{n,j,t} \le \frac{p^{max}{}_{n,j} - p^{CCO}{}_{n,j}}{S^{CV}{}_{n,j}} * S_{n,j,t} + p^{CCO}{}_{n,j}, \ \forall\, t \in n,j,\left[\tilde{T}^a{}_{n,j}, \tilde{T}^d{}_{n,j}\right] \,\&\, S_{n,j,t} \le S^{CV}{}_{n,j} \quad (104)$$

$$p^{e+}{}_{n,j,t} + \eta^{ch}{}_{n,j} * p^{r(dn)}{}_{n,j,t} \le \frac{p^{max}{}_{n,j}}{\left(1 - S^{CV}{}_{n,j}\right)} * \left(1 - S_{n,j,t}\right), \ \forall\, t \in n,j,\left[\tilde{T}^a{}_{n,j}, \tilde{T}^d{}_{n,j}\right] \,\&\, S_{n,j,t} > S^{CV}{}_{n,j} \quad (105)$$

Where $p^{r(up)}{}_{n,j,t}$: the natural reserve power capacity for up regulation by the j^{th} EV at time t at node n (kW)

$p^{r(dn)}{}_{n,j,t}$: the natural reserve power capacity for down regulation by the j^{th} EV at time t at node n (kW)

Finally, the following constraints are added in the optimization. The first one (106) limits the natural up regulation reserves to be lower than the charging power, while the following two constraints (107) & (108) bound the offered reserve capacities to the TSO to be lower than the related natural reserves.

$$p^{r(up)}{}_{n,j,t} \le \frac{p^{e+}{}_{n,j,t}}{\eta^{ch}{}_{n,j}}, \qquad \forall\, n,j,t \quad (106)$$

$$p^{r(up\_of)}{}_{n,j,t} \le p^{r(up)}{}_{n,j,t}, \qquad \forall\, n,j,t \quad (107)$$

$$p^{r(dn\_of)}{}_{n,j,t} \leq p^{r(dn)}{}_{n,j,t}, \qquad \forall\, n,j,t \tag{108}$$

"Expected Regulation Reserves"

Until now, the MILP algorithm utilizes the previously formulated constraints and objective function in order to compute the natural and offered reserve capacities to the regulation market, which define the algorithm's remuneration. These capacities are arranged before the actual call and the algorithm is obliged to provide them 30 seconds after the contingency event, while they must be able to remain active for at least 15 min [103]. However, there is always uncertainty in the actual called amount of the arranged offered capacities in real-time by the TSO, since it depends on the contingency event and the real-time power-frequency balance in the interconnected power system.

This uncertainty has been addressed combining two different parts of the algorithm. The first part represents "what the algorithm expects to be called" and is integrated in the algorithm's part of optimization/scheduling, while the second part represents "what is actually called" and is integrated in the algorithm's part that represents reality (the real charging of EVs).

The constraints and the objective function, that compute the natural and offered regulation reserve capacities respectively, have already been described. However, equations (63), (71) and (72), which dictate the battery capacity of the EVs and the power balance at every timestep, are the equations that represent "reality" in optimization and shall integrate the "expected" regulation reserves by the TSO. Therefore, the expected up and down regulation capacities are introduced, $p^{r(up\_exp)}$ & $p^{r(dn\_exp)}$ respectively, and the aforementioned equations are transformed to (109), (110) & (111) respectively, for the scope of Study 2:

$$\sum_{j=1}^{J}\left({p^{e+}}_{n,j,t}\Big/{\eta^{ch}}_{n,j} - {p^{r(up\_exp)}}_{n,j,t} + {p^{r(dn\_exp)}}_{n,j,t}\right) + {p^{local}}_{n,t} - {p^{PV}}_{n,t} = {p^{diff}}_{n,t} = {p^{g(imp)}}_{n,t} - {p^{g(ex)}}_{n,t}, \quad \forall n,j,t \tag{109}$$

$$B_{n,j,t} = {B_{n,j}}^{a} + \Delta T \sum_{\tilde{T}_{n,j}{}^{a}}^{t}\{(p^{e+}{}_{n,j,t} - \frac{{p^{r(up\_exp)}}_{n,j,t}}{{\eta^{ch}}_{n,j}} + {\eta^{ch}}_{n,j} * {p^{r(dn\_exp)}}_{n,j,t}) * {\eta^{ev}}_{n,j}\}, \qquad \forall\, t \in n,j,[{\tilde{T}^{a}}_{n,j}, {\tilde{T}^{d}}_{n,j}] \tag{110}$$

$$B_{n,j,{\tilde{T}^{d}}_{n,j}} = {B_{n,j}}^{a} + \Delta T \sum_{t}^{{\tilde{T}^{d}}_{n,j}}((p^{e+}{}_{n,j,t} - \frac{{p^{r(up\_exp)}}_{n,j,t}}{{\eta^{ch}}_{n,j}} + {\eta^{ch}}_{n,j} * {p^{r(dn\_exp)}}_{n,j,t}) * {\eta^{ev}}_{n,j}), \quad \forall\, t \in n,j,[{\tilde{T}^{a}}_{n,j}, {\tilde{T}^{d}}_{n,j}] \tag{111}$$

Where ${p^{r(up\_exp)}}_{n,j,t}$: the expected reserve power capacity for up regulation by the j^{th} EV at time t at node n (kW)

${p^{r(dn\_exp)}}_{n,j,t}$: the expected reserve power capacity for down regulation by the j^{th} EV at time t at node n (kW)

The formulation of the power balance equation and the battery capacity equations can be easily derived, observing again Fig. 3.5 of Chapter 3 [15] and considering the power flow at points [1] & [2] respectively.

While expected up and down regulation reserves $p^{r(up\_exp)}$ & $p^{r(dn\_exp)}$ remain uncertain, they must obey two main conditions.

- The expected called reserves must be always lower or equal than the corresponding offered reserves.

- While the algorithm is capable of offering both up and down FCR reserves and receive remuneration for them simultaneously, the TSO will actually call only one of them, either up or down reserves, simultaneously. Therefore, an extra decision variable $switch_{pr}$ is introduced, which is responsible to activate either $p^{r(up\_exp)}$ or $p^{r(dn\_exp)}$ at every timestep. The $switch_{pr}$ variable is decided to be an integer variable, which receives values within the interval $[-1, 0, 1]$. The first and third values represent the activation of the expected down and up regulation reserves respectively, while the middle one represents nullification.

On that manner, the following constraints are added in the optimization. While equation (112) sets the upper and lower bounds of the switch variable, equation (113) dictates that it must be set to zero when the EV is not connected, because without EV connection, no up and down regulation reserves can exist. Finally, equations (114) & (115) force the expected reserves to exist only individually and be always lower than the reserves that participate in the bidding market.

$$-1 \leq switch_{pr}{}_{n,j,t} \leq 1 \qquad \forall\, n, j, t \tag{112}$$

$$switch_{pr}{}_{n,j,t} = 0 \quad \forall\, n, j, t < \tilde{T}^{a}{}_{n,j} \;\&\; t \geq \tilde{T}^{d}{}_{n,j} \tag{113}$$

$$p^{r(up\_exp)}{}_{n,j,t} \leq p^{r(up\_of)}{}_{n,j,t} * switch_{pr}{}_{n,j,t}, \qquad \forall\, n, j, t \tag{114}$$

$$p^{r(dn\_exp)}{}_{n,j,t} \leq p^{r(dn\_of)}{}_{n,j,t} * \left(-switch_{pr}{}_{n,j,t}\right), \qquad \forall\, n, j, t \tag{115}$$

Where $switch_{pr}{}_{n,j,t}$: the decision variable that decides which regulation is expected at charger j of node n at every time instant t (up or down). It is an integer, therefore it receives only 3 values:

- 1 for up expected regulation activation
- -1 for down expected regulation activation
- 0 for no "expected regulation activation

In order to firstly reduce potential over-conservativeness (e.g expectation of a maximum of 100% called reserves) and secondly avoid total ignorance (e.g expectation of a minimum of zero "called" reserves), Robust Optimization is employed, therefore the so-called "budget of uncertainty".

Following the Bertsimas & Sim Method (Cardinality Constrained Uncertainty) for Robust Optimization, which has already been explained in Chapter 3, the decision variable Γ_i is introduced, which represents the deviation of the expected regulation reserves from the "offered" ones in the bidding market in a fragment form, therefore the "budget of uncertainty" for the whole optimization horizon. Hence, Γ_i can be formulated as expressed in equation (116)

$$\Gamma_{i_n} = \frac{\sum_{t=t_{trigger}}^{t=optim_{end}} \sum_{j=1}^{J} \left(p^{r(up\_exp)}{}_{n,j,t} + p^{r(dn\_exp)}{}_{n,j,t} \right)}{\sum_{t=t_{trigger}}^{t=optim_{end}} \sum_{j=1}^{J} \left(p^{r(up\_of)}{}_{n,j,t} + p^{r(dn\_of)}{}_{n,j,t} \right)}, \quad \forall\, n \tag{116}$$

Taking into consideration the "ENTSO-E Transparency Platform" [103] for the "offered" and "activated" FCR Reserves in the Netherlands, an uncertainty interval of $0.2 \leq \Gamma_{i_n} \leq 0.5, \ \forall n$ has been selected, for every "budget of uncertainty" index $\Gamma_{i_n}$of horizon i at node n (for this thesis the budget of uncertainty has been considered equal for all the nodes).This interval deals with extreme phenomena, such as extreme worst-case over-conservative scenarios of 100% total expected reserves or best-case unreal scenarios of zero total expected scenarios compared with the offered regulation capacities. Therefore, the following constraints (117) & (118) have been added in the optimization.

$$\sum_{t=t_{trigger}}^{t=optim_{end}} \sum_{j=1}^{J} \left({p^{r(up\_exp)}}_{n,j,t} + {p^{r(dn\_exp)}}_{n,j,t} \right) \geq 0.2 * \sum_{t=t_{trigger}}^{t=optim_{end}} \sum_{j=1}^{J} \left({p^{r(up\_of)}}_{n,j,t} + {p^{r(dn\_of)}}_{n,j,t} \right), \quad \forall n \tag{117}$$

$$\sum_{t=t_{trigger}}^{t=optim_{end}} \sum_{j=1}^{J} \left({p^{r(up\_exp)}}_{n,j,t} + {p^{r(dn\_exp)}}_{n,j,t} \right) \leq 0.5 * \sum_{t=t_{trigger}}^{t=optim_{end}} \sum_{j=1}^{J} \left({p^{r(up\_of)}}_{n,j,t} + {p^{r(dn\_of)}}_{n,j,t} \right), \quad \forall n \tag{118}$$

Called – Real Regulation Reserves by the TSO

As already explained in previous chapters, the nominal MILP algorithm utilizes Receding Horizon Approach and triggers re-optimizations at every timestep, in which certain events occur, such as EV arrivals. Apart from the optimizer, the algorithm integrates another module, which represents "reality" and mimics the real charging of the EVs. The algorithm, emulating in this module at every timestep the real charging power & current of every smart-charging EV, it synchronizes the EV SOCs that are derived by the "reality" part and by the optimizer and triggers re-optimizations, if the difference exceeds a threshold of 1%.

The algorithm's "reality" module is utilized for the representation of the actually called regulation reserves in reality by the TSO. At every timestep, the called regulation reserves are computed along with the charging power, current and real EV SOC. Fig. 4.6 depicts the functional diagram of the representation of the final FCR reserves provision by the algorithm. Observing Fig. 4.6, when the algorithm triggers a new re-optimization, the algorithm's input parameter feeder feeds the optimizer with all the data needed regarding the limits to be respected (EV, EV chargers, Grid Import and Export Power & CC-CV limits) and the characteristics of the EV fleets (arrival & departure times, SOCs, requested energy amounts). The optimizer takes into consideration all of the above in order to compute the "natural" regulation reserves that it could provide via the EV smart-charging. Moreover, utilizing Robust Optimization, the algorithm takes into consideration the reserves capacity that it expects to be called by the TSO and it calculates the regulation reserves, which can efficiently be offered to the bidding market. The algorithm's "reality" module, taking into account the offered reserves to the bidding market and informs the algorithm about the actually called reserves by the TSO at the particular timestep. The called reserves are distributed to every connected charger of the node, based on the ratio of the individual

charger's offered capacity (defined in the previous optimization) divided by the total offered capacity of the node. The algorithm updates and stores the charging data and triggers new re-optimization if needed, for example if the charging data of the optimizer module and "reality" module deviate too much (real EV SOC & optimization EV SOC differ more than 1%).

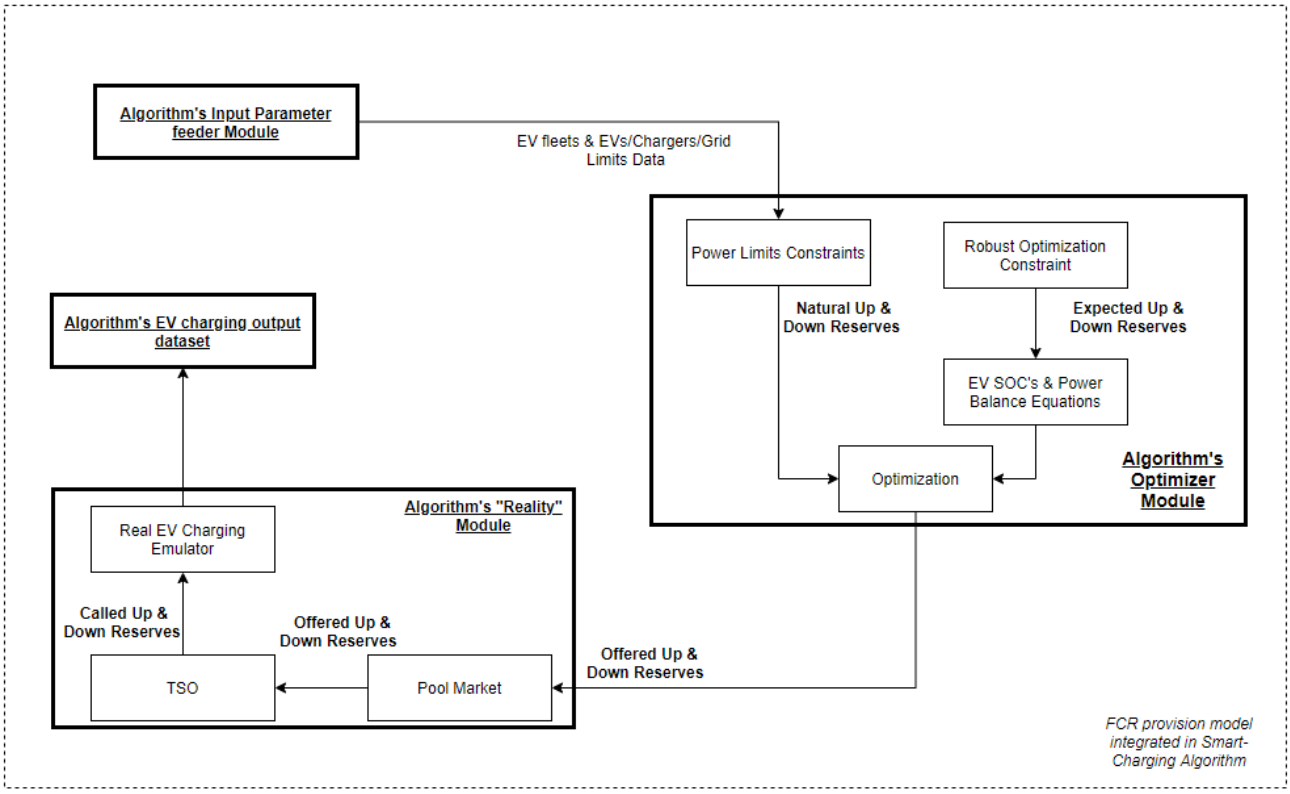

Fig. 4. 6: Functional Diagram of FCR reserves provision by Robust Smart-Charging Algorithm

Chapter 5: Study Cases & Results of the PV Generation, Load Demand & EV user patterns uncertainties' management

5.1 Introduction & Experiment Description

In Chapter 5, the study cases and results of Study 1, regarding PV Generation, Load Demand, arrival SOC and Arrival & Departure time of the EVs, are summarized. It must be noted that the constraint about the CV battery charging region has been excluded from optimization. This is due to the fact that the benchmark algorithm causes the following issue, in terms of unfinished charging energy, in the particular version that it has been investigated. As explained in Chapter 3, the minimum charging current setpoint of the optimizer is 6A. However, the algorithm's "reality" module, which emulates the real charging of the EV fleets and integrates the CV charging region, is capable of charging the EV with lower than 6A. Therefore, while optimizer organizes energy-scheduling, taking into account the CV charging region and the minimum limit of 6A to finish EV charging on time, the EV "reality" module charges the EV with lower than 6A in the last timesteps of the parking time. The above issue causes unfinished charging to multiple EVs and uncalled penalty costs, due to customer unsatisfaction. Therefore, it jeopardizes the extraction of meaningful results for the investigation of the particular thesis.

Furthermore, the 3 different types of nodes, which are integrated in the optimization, are: the "Home Node" (node 1), the "Public Node" (node 2) & the "Semi-Public Node" (node 3). For all the study cases investigated in this thesis, nodes 1, 2 & 3 integrate 3, 5 & 3 chargers respectively. The "Home Node" is consisted of home chargers, which are characterized by smaller daily EV fleets, longer parking periods and lower EV arrival SOCs, and integrates 2 PV parks with rated powers of 2.5 and 7.5 kW. The "Public" and "Semi-Public" nodes, which represent the chargers of public and semi-public areas, are characterized by greater EV fleets, shorter parking periods and higher EV arrival Socs, both integrate 2 PV parks with rated powers of 7.5kW & 5kW and 10kW & 2.5kW respectively. In Fig. 5.1 the 1kW-standardized PV Generation profile, which is used as the forecasted PV generation data, is depicted while Fig. 5.2 presents the forecasted yearly energy price cost [€/MWh] based on the 2018 Day-Ahead Market data. Finally, all forecasted loads covered by the 3 nodes are based on standardized load profiles of the NEDU 2018 database [105], while the utilized forecasted PV Generation profile data is based on the Meteonorm database [106] and the utilized DA energy price profile is based on the ENTSO-E platform database [103].

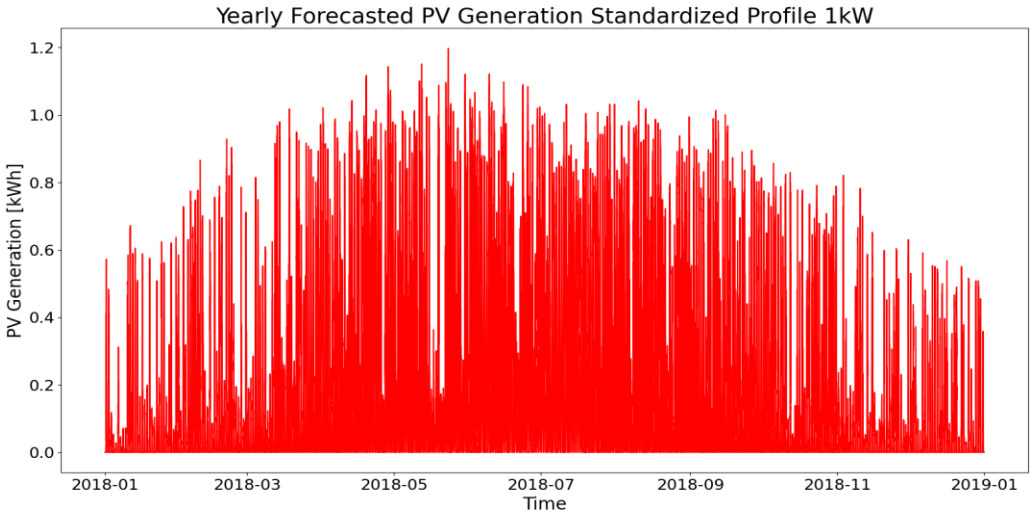

Fig. 5. 1: Forecasted yearly 1kW-standardized PV Generation Profile [106]

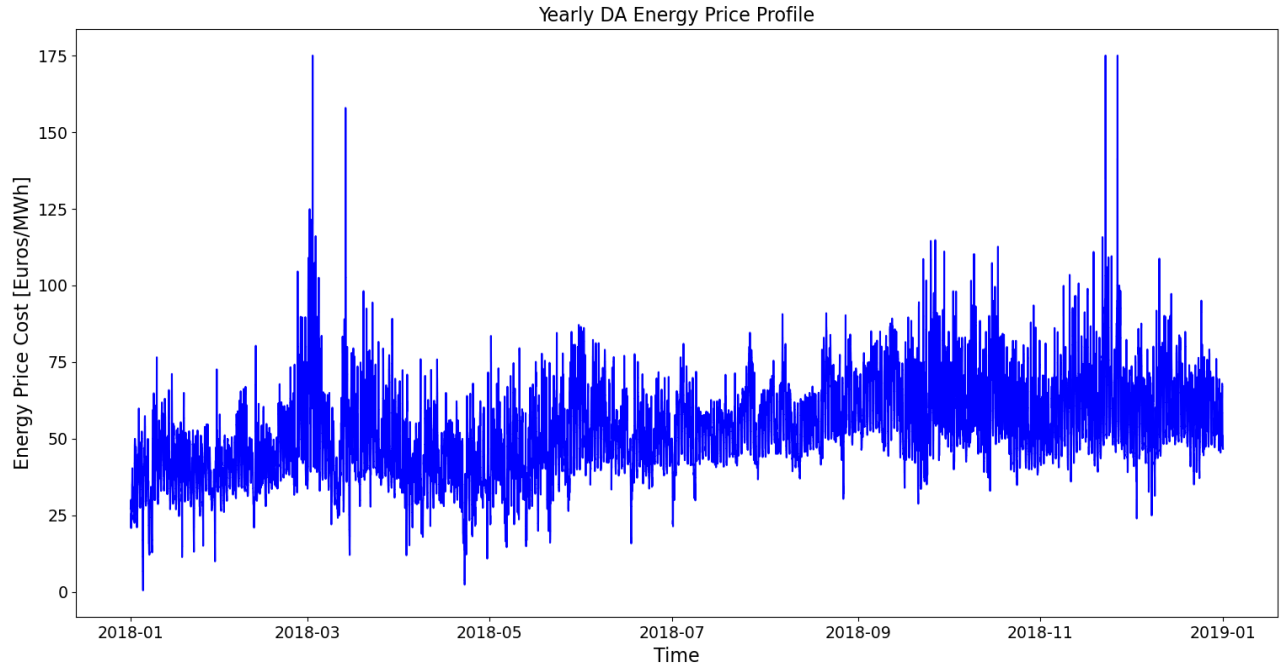

Fig. 5. 2: Yearly DA Energy Price Cost Profile [103]

Moreover, the same EV fleets have been used and the same time duration: 4 days from 7-6 00:00 until 10-6 23:55. The timestep used for the MILP optimization of the algorithm is 5 minutes.

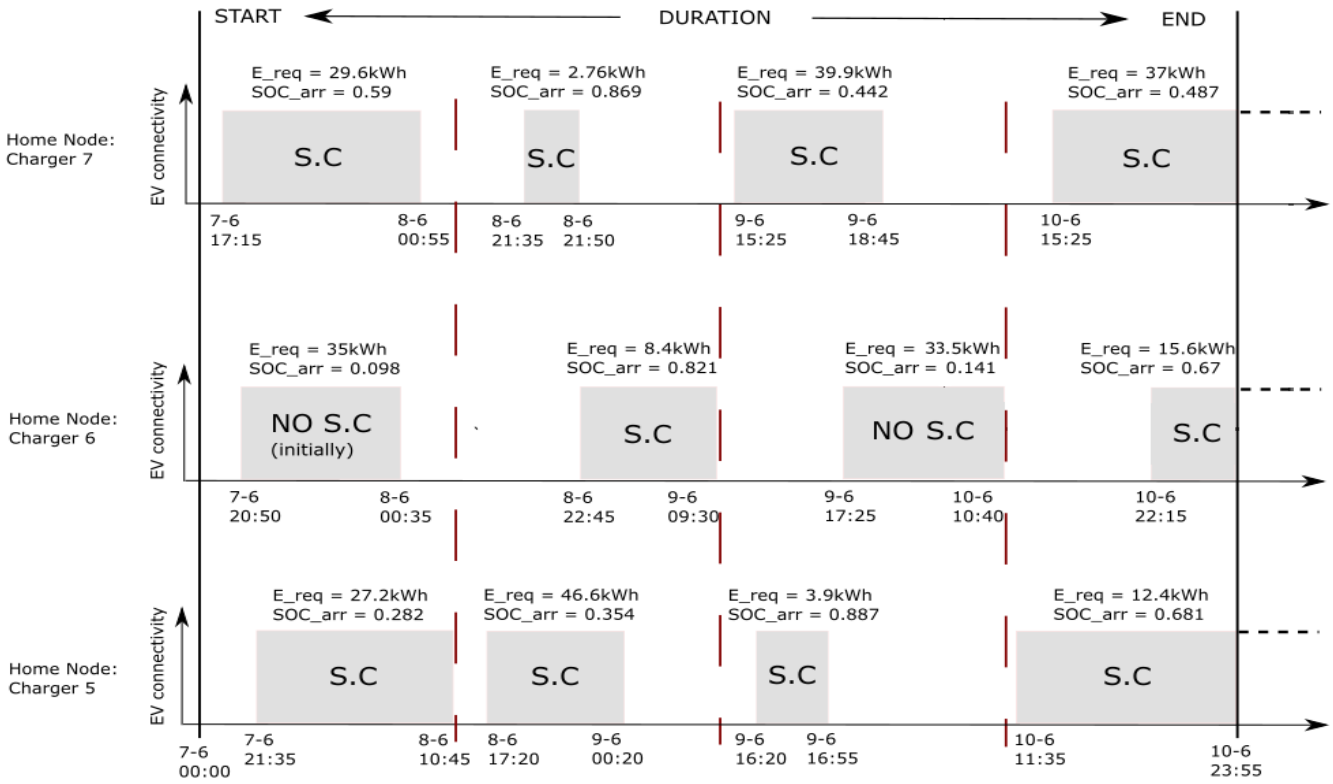

Fig. 5. 3: EV fleets at the Chargers (5, 6 & 7) of the "Home Node" during the study case duration

Without loss of generality, the plots contained in this chapter depict the results of the investigation for "Home Node". The EV fleets that pass through the Chargers 5, 6 & 7 of the "Home Node" at the studied time duration are depicted in Fig. 5.3. The requested energy (E_{req}) and arrival SOC (SOC_{arr}) are depicted for every EV for the base case (forecasted data). Moreover, the participation or not in smart-charging for every EV has been added, as well. As it can be clearly seen, the vast majority of the EVs are able and willing to participate in smart-charging. However, the first EV, that arrives at Charger 6, has an arrival SOC below the threshold of 20% and cannot immediately initiate smart-charging. Moreover, with the extra feature added to the Prediction-Capable Algorithm (P-C), the 3rd arrived EV at Charger 6 has the ability to choose not to participate in smart-charging, when its SOC reaches 20%. On the contrary, it prefers to select uncontrollable charging for the entire parking time.

Last but not least, the red dashed lines show the ends of the optimization horizons that are set during the optimization due to the prediction capability.

5.2 Benchmark & Prediction-Capable Algorithms: Base Cases

Firstly, the Benchmark and the Prediction-Capable algorithms have been compared and the cost results have been summarized at Table 5.1. Fig. 5.4 depicts the Energy Price Cost in the DAM for the time duration studied in the optimization: from 7-6 00:00 until 10-6 23:59. As it can be seen, the energy price rises highly at noon (e.g 12:00) and in the afternoon (around 18:00), when people return home from work and plug-in their vehicles. The lowest energy price is observed during the night, from 22:00 until 6:00 early in the morning. This pattern is repeated with high similarity for all 4 days of the optimization. Regarding Table 5.1 (and all Tables 5.1 – 5.6 in Chapter 5).

- Nodes 1, 2 & 3 represent the "Home", "Semi-Public" & "Public" nodes respectively
- The Grid Power Exchange Cost represents the total node cost of importing power from grid (or total income from exporting power to the grid):

$$\sum_{t=1}^{T} (p^{g(imp)}{}_{n,t} C^{e(buy)}{}_{t} - p^{g(ex)}{}_{n,t} C^{e(sell)}{}_{t}), \forall n$$

- The Unfinished Charging Gap represents the total charged energy deviation from the corresponding requested energy for every EV passed from every charger of the node:

$$\sum_{j=1}^{J} (B_{n,j}{}^{a} + \tilde{d}_{n,j} - B_{n,j,\tilde{T}^{d}{}_{n,j}}), \ \forall n, j$$

- The Penalty Cost for Charging Gap represents the total cost paid to the customers because of the previously defined unfinished charging gap for every node. However, as already explained, the penalty cost is neglected if the departure SOC is greater than 98% or its deviation from the requested departure SOC is lower or equal to 1%. This can be justified if we take into account that the total unfinished charging gap of a node is subdued to multiple uncertainties. Apart from the potential noise, which is integrated in the algorithm and can minorly deviate the real charging results from the result of the optimizer, the concept of Discrete Optimization implicates the most significant effects. Since, the algorithm functions with a predefined timestep (5 minutes in this thesis), the last timestep of a particular EV charging corresponds to a certain amount of energy, which the algorithm can choose either to undercharge or overcharge the EV before departure. The algorithm typically chooses to leave the EV slightly undercharged to avoid potential waste of energy.

$$\sum_{j=1}^{J}\{B_{n,j}{}^{a} + \tilde{d}_{n,j} - B_{n,j,\tilde{T}^{d}{}_{n,j}})C^{p}{}_{n,j}\},\ \forall n,j$$

- The Total Node Charging Cost is the sum of the Grid Power Exchange Cost and the Penalty Cost for Charging Gap for every node

Table 5. 1: Charging Costs Comparison between Benchmark and Prediction-Capable Algorithms

Benchmark Algorithm Results				
Nodes	Grid Power Exchange Cost (€)	Unfinished Charging Gap (kWh)	Penalty Cost for Charging Gap (€)	Total Node Charging Cost (€)
Node 1	1,8738	0,2721	0	1,8738
Node 2	-0,6827	0,568	0	-0,6827
Node 3	-1,7623	0,17	0	-1,7623
Prediction-Capable Algorithm Results				
Nodes	Grid Power Exchange Cost (€)	Unfinished Charging Gap (kWh)	Penalty Cost for Charging Gap (€)	Total Node Charging Cost (€)
Node 1	1,5885	0,2242	0	1,5885
Node 2	-0,6866	0,3497	0	-0,6866
Node 3	-1,8354	0,1543	0	-1,8354

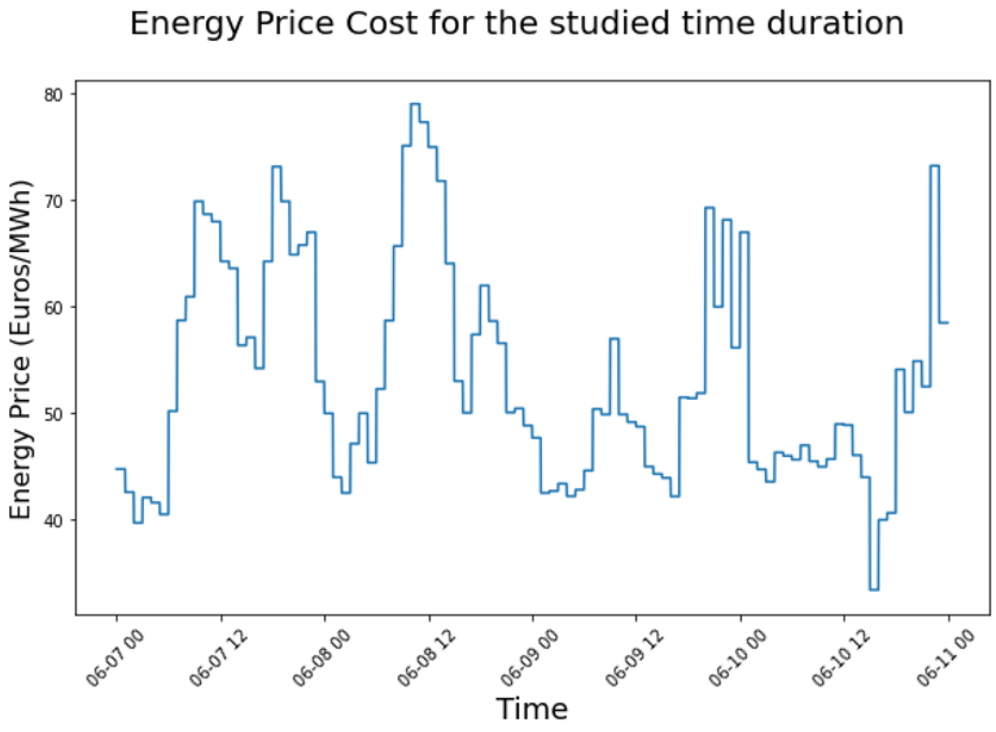

Fig. 5. 4: Energy Price Cost (€/MWh) for the time duration: 7-6 00:00 until 10-6 23:59

As it can be seen, the unfinished charging gap has been reduced in almost every node and the corresponding penalty cost has remained zero. However, due to the Discrete Optimization's inherent characteristic, there is still unfinished charging gap at the nodes in the P-C algorithm, that cannot be nullified by prediction insertion. Moreover, at all nodes, the P-C algorithm can schedule the energy management more efficiently, being able to predict the future arrivals at all the node chargers. Therefore, either the power exchange cost with the grid is reduced or the related earnings by exporting power to the grid have been increased. The negative sign at a charging cost value means that the overall earnings of the total exported power are greater than the overall cost of the total imported power from the grid.

Figs. 5.5-5.7 present the behavior, in terms of SOC and charging power of the EV fleets, at the chargers of the "Home Node" when capability of prediction is added. As it has been seen in Fig 5.5, the 1st EV arrives at Charger 7 at 7-6 17:15 and until its departure at 8-6 00:55, one EV arrival at Charger 6 at 7-6 20:50 and one EV arrival at Charger 5 at 7-6 21:35 are predicted. The Benchmark algorithm, that cannot predict the future arrivals, waits until before midnight when energy price is lower in order to charge the 1st EV at Charger 7 (see Fig. 5.7). On the contrary, the Prediction-Capable algorithm, which predicts the two future arrivals, balances the particular charging in two periods: at the time of arrival and before midnight. Moreover, charging of the 1st EV at Charger 5 does not change, because since it is the only EV connected after midnight, the algorithm chooses to charge it then in both situations.

Moreover, the same behavior is depicted at the last arrivals at the chargers. The last arrival at Charger 5 arrives at 10-6 11:35, while arrivals at 10-6 15:25 & at 10-6 22:15 at Chargers 7 & 6 respectively follow next. The Prediction-Capable Algorithm rushes to charge the EV at Charger 5 in order to save time and power to charge the EVs at Chargers 6 & 7 when they arrive.

Finally, the additional feature of "No S.C Participation Preference" can be clearly seen in Fig. 5.6. The 3rd EV arrived at Charger 6 chooses to be charged uncontrollably and its charging starts immediately, while its charging is delayed for lower price energy time periods in the nominal algorithm.

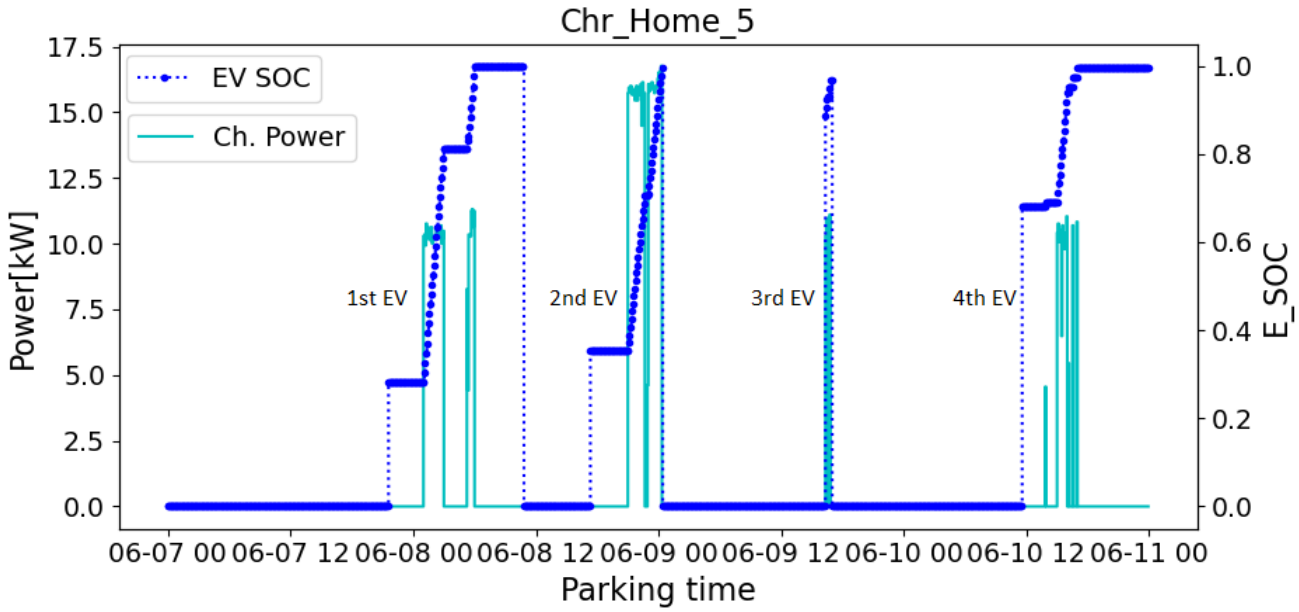

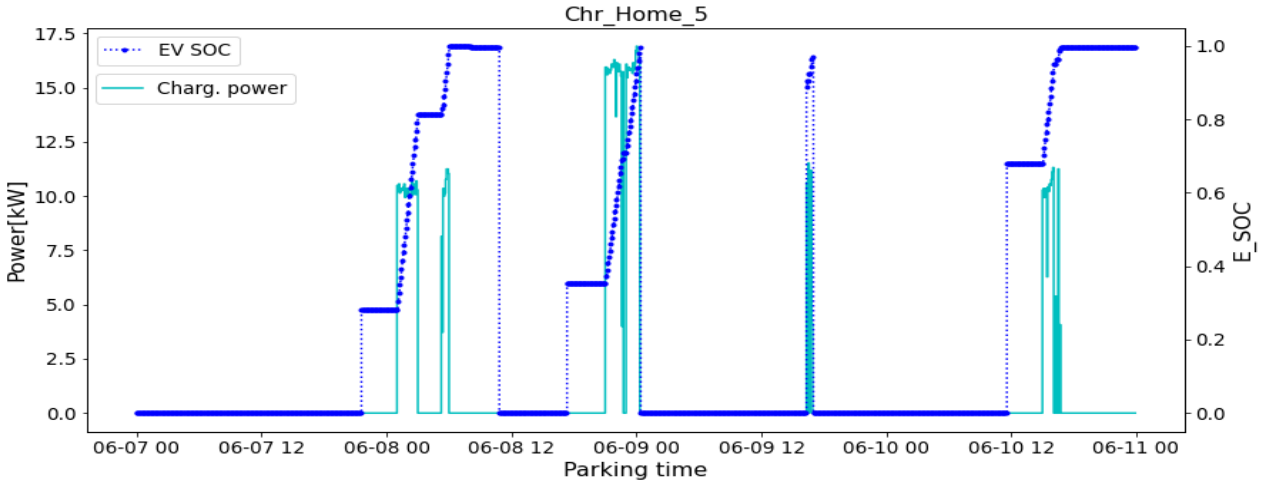

Fig. 5. 5: "Charger Home 5" Behavior in Benchmark (upper plot) & in Prediction-Capable (lower plot) Algorithms

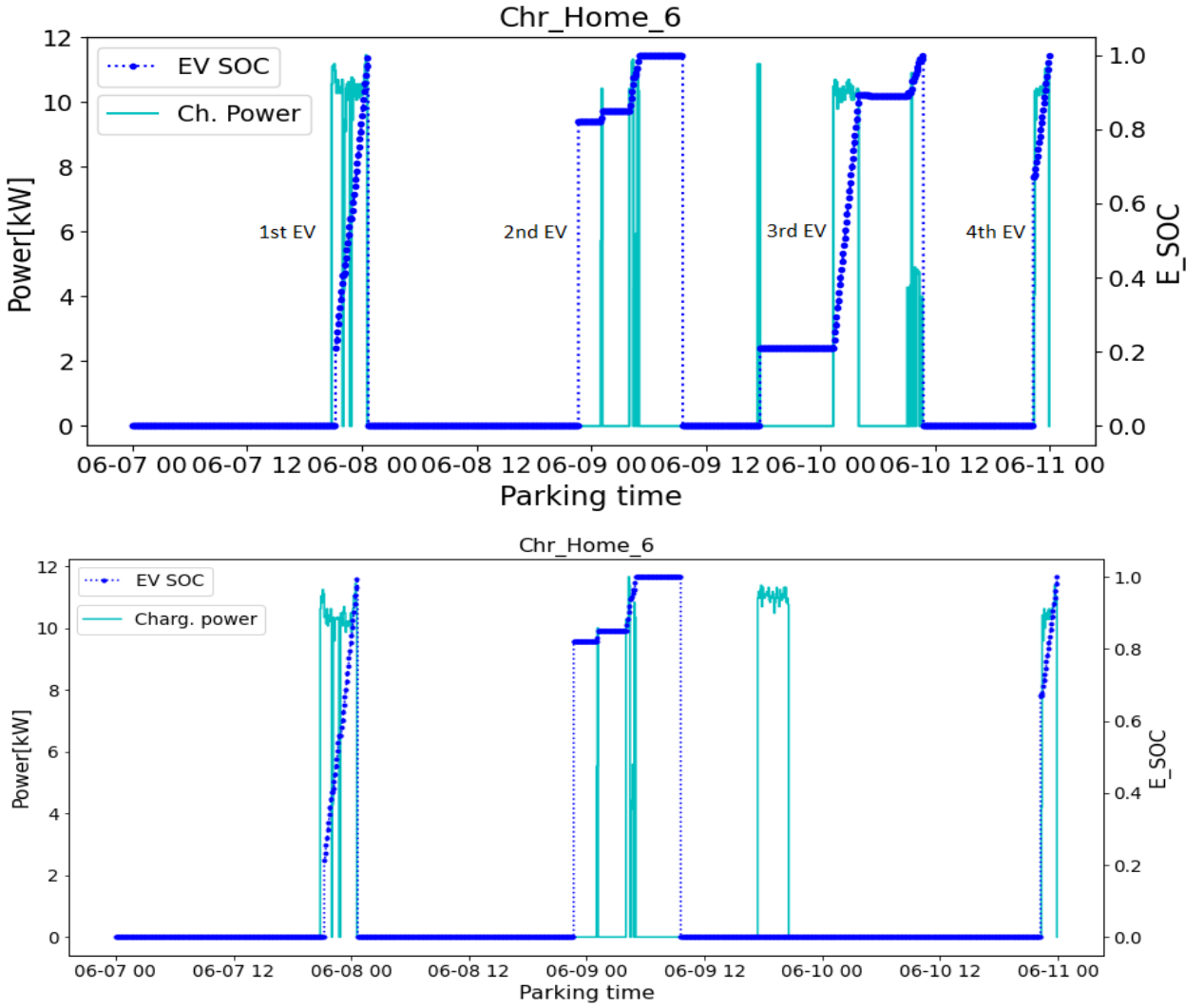

Fig. 5. 6: "Charger Home 6" Behavior in Benchmark (upper plot) & in Prediction-Capable (lower plot) Algorithms

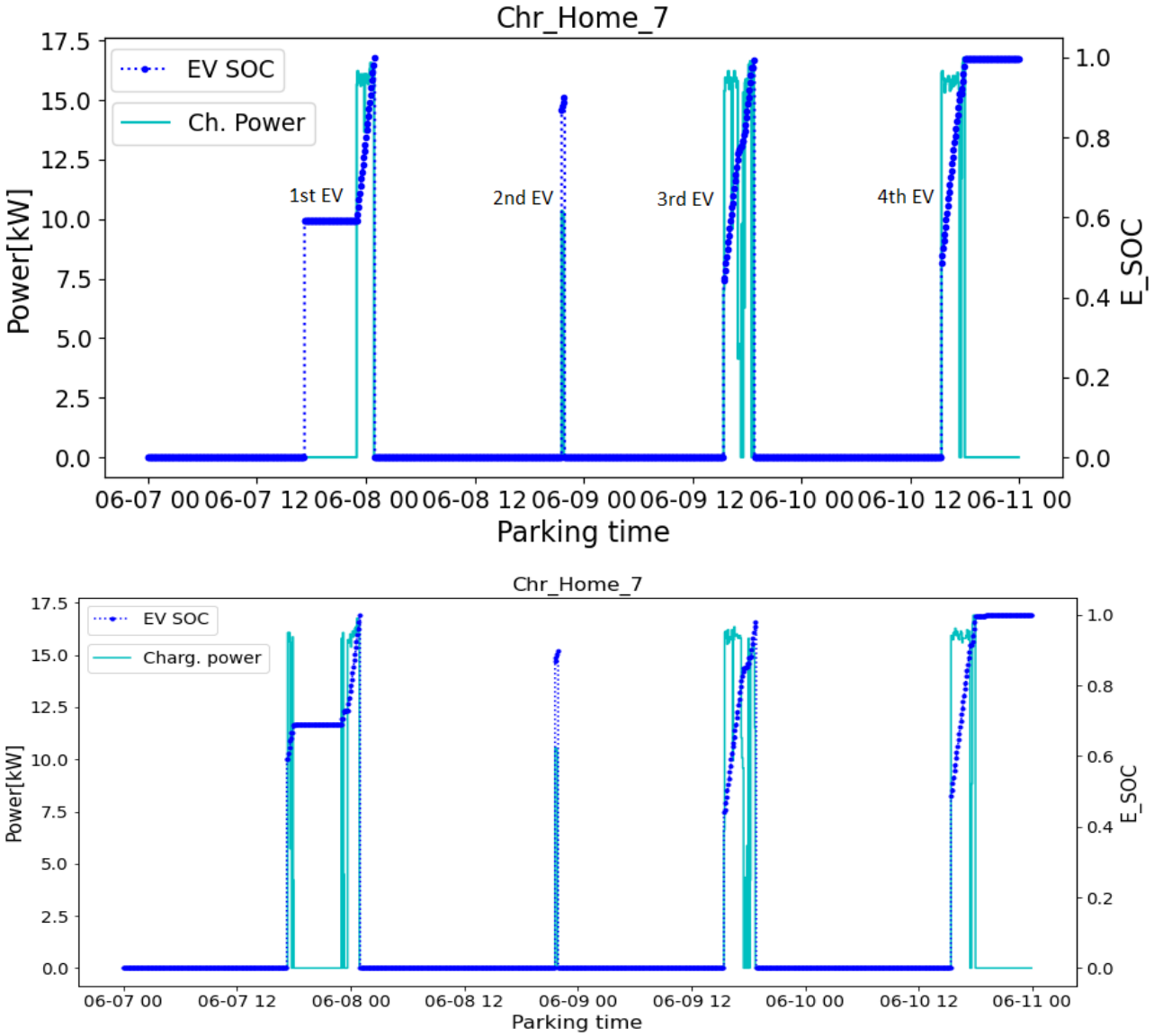

Fig. 5. 7: "Charger Home" Behavior in Benchmark (upper plot) & in Prediction-Capable (lower plot) Algorithms

5.3 SOC_{arr} Uncertainty Studies

5.3.1 SOC_{arr} Uncertainty only in Prediction

In this paragraph, the behavior of the Prediction-Capable algorithm has been evaluated, when the algorithm predicted a 100% perfect forecast (upper plots) and when it predicted the worst-case scenario of minimum SOC_{arr} (lower plots). The difference of the two study cases remains only in the prediction part, hence the EVs finally arrive with the forecasted SOC_{arr}.

As it can be clearly seen in Table 5.2, the unfinished charging gap has decreased even more in all the nodes and the penalty cost has remained zero. Moreover, a minor decrease in grid power exchange profit (and consequently in the total charging profit) is observed in Nodes 2 & 3, compared with the accurate forecast prediction. This is due to the potential overconservativeness of the protection against uncertainties by Robust Optimization. The algorithm predicts the worst-case scenario and rushes to

charge the currently connected cars, which can potentially be realized in less profitable or more costly time periods in terms of energy price. However, the penalty cost remains 0 in both situations and the difference in charging cost is of minor importance.

Table 5. 2: Charging Costs Comparison between Accurate Forecast & Minimum SOC_{arr} Prediction "P-C" study cases

Prediction-Capable "OSCD" Algorithm with Accurate Forecast Results				
Nodes	Grid Power Exchange Cost (€)	Unfinished Charging Gap (kWh)	Penalty Cost for Charging Gap (€)	Total Node Charging Cost (€)
Node 1	1,5885	0,2242	0	1,5885
Node 2	-0,6866	0,3497	0	-0,6866
Node 3	-1,8354	0,1543	0	-1,8354
Prediction-Capable Algorithm with Minimum SOC_{arr} Prediction Results				
Nodes	Grid Power Exchange Cost (€)	Unfinished Charging Gap (kWh)	Penalty Cost for Charging Gap (€)	Total Node Charging Cost (€)
Node 1	1,586	0,1463	0	1,586
Node 2	-0,677	0,29289	0	-0,677
Node 3	-1,7738	0,05185	0	-1,7738

Figs. 5.8 - 5.10 present the behavior of the 3 chargers of the "Home Node" when the P-C algorithm predicts a perfect forecasted SOC_{arr} and when it predicts the worst-case scenario of 50% decreased SOC_{arr} and consequently higher requested energy. While minor differences can be seen, the same behavior can be observed as before. Regarding the arrival of the first 3 EVs at the chargers, Charger 7 provides most of the charging energy to the 1st EV upon arrival, since it predicts a lower SOC_{arr} of the EVs at the other 2 chargers, as it can be seen in in Fig. 5.10. In Fig. 5.8, Charger 5 does not change behavior regarding the 1st EV, since it is still the only EV connected during the past midnight hours, when price energy is lower. Due to the same reason, the behavior of the 3 chargers upon arrival of the 2nd EVs does not change, too. When the 2nd EV arrives at Charger 5 at 8-6 17:20 in Fig. 5.8, it is not immediately charged, even when minimum SOC_{arr} is predicted for the other 2 coming EVs, since there is adequate time to be charged in the evening. On the contrary, in Fig. 5.9, the 2nd EV that arrives at Charger 6 at 8-6 22:45, departs at 9-6 09:30, therefore there is enough time to be charged during the night, even if it arrives with minimum SOC.

Moreover, difference of behavior can be seen at the last EV arrival at Charger 5 at 10-6 11:35. The prediction of the arrivals of the other 2 EVs at 10-6 15:25 & 10-6 22:15 at Chargers 7 & 6 respectively with minimum SOC_{arr}, forces Charger 5 to start the charging earlier (upon EV's arrival) expecting that the other 2 EVs are going to arrive with higher charging demand.

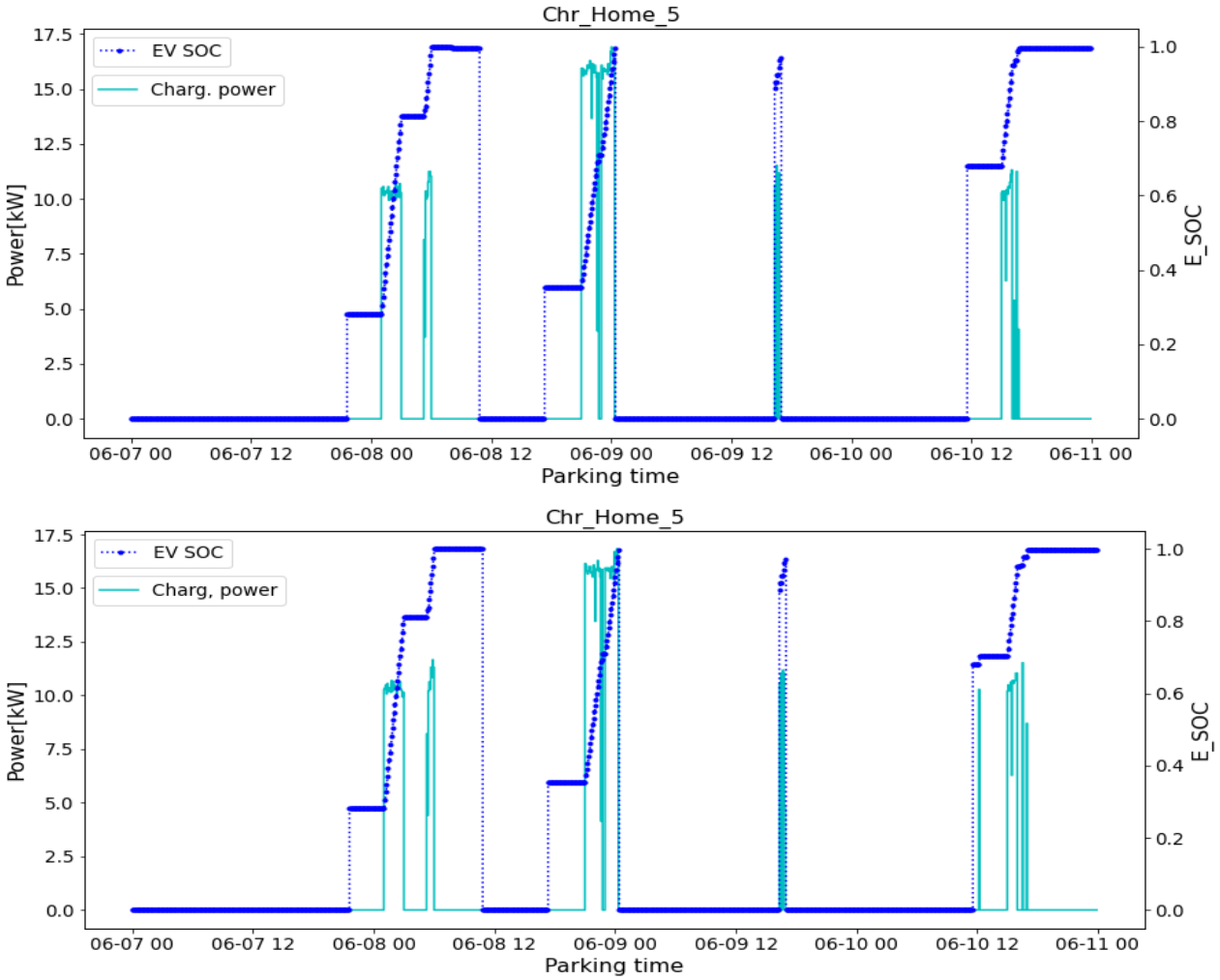

Fig. 5. 8: "Charger Home 5" Behavior in Prediction of Accurate SOC_{arr} (upper plot) & in Minimum SOC_{arr} (lower plot)

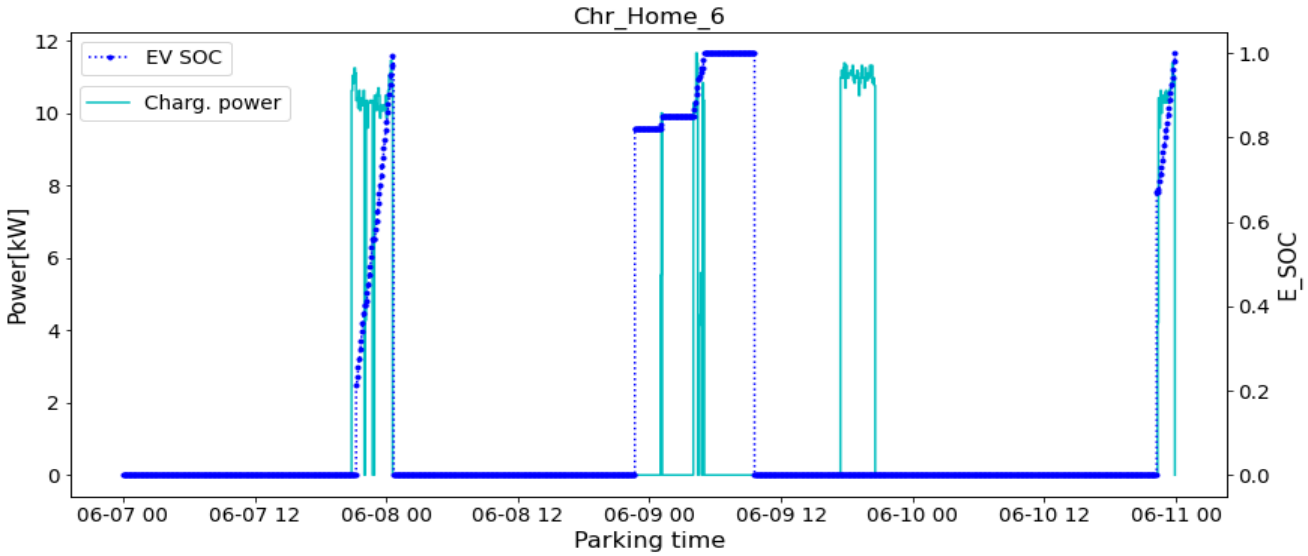

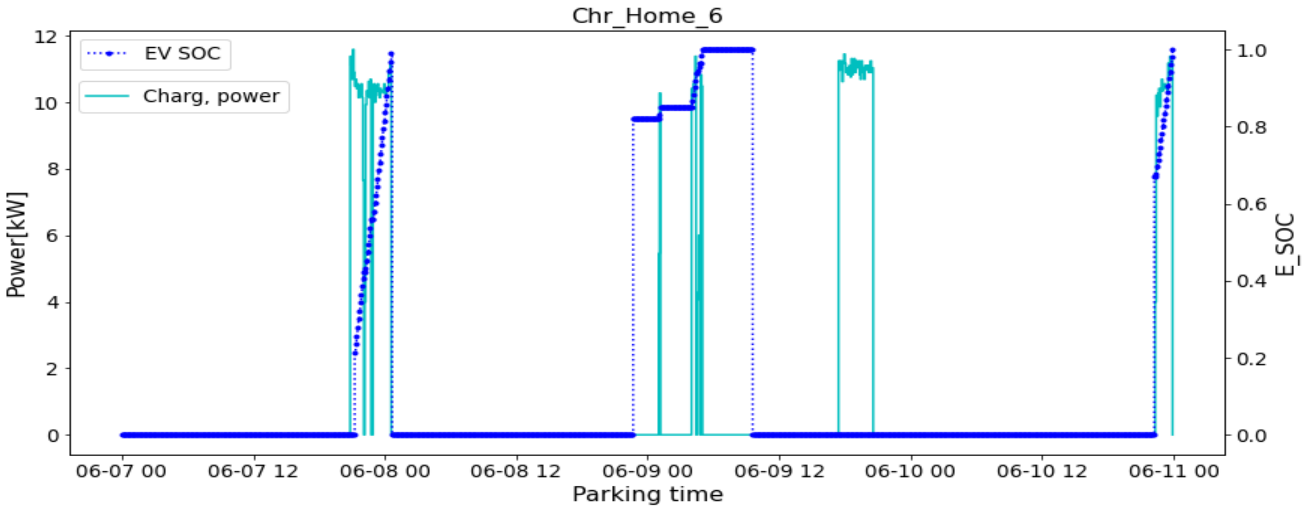

Fig. 5. 9: "Charger Home 6" Behavior in Prediction of Accurate SOC_{arr} (upper plot) & in Minimum SOC_{arr} (lower plot)

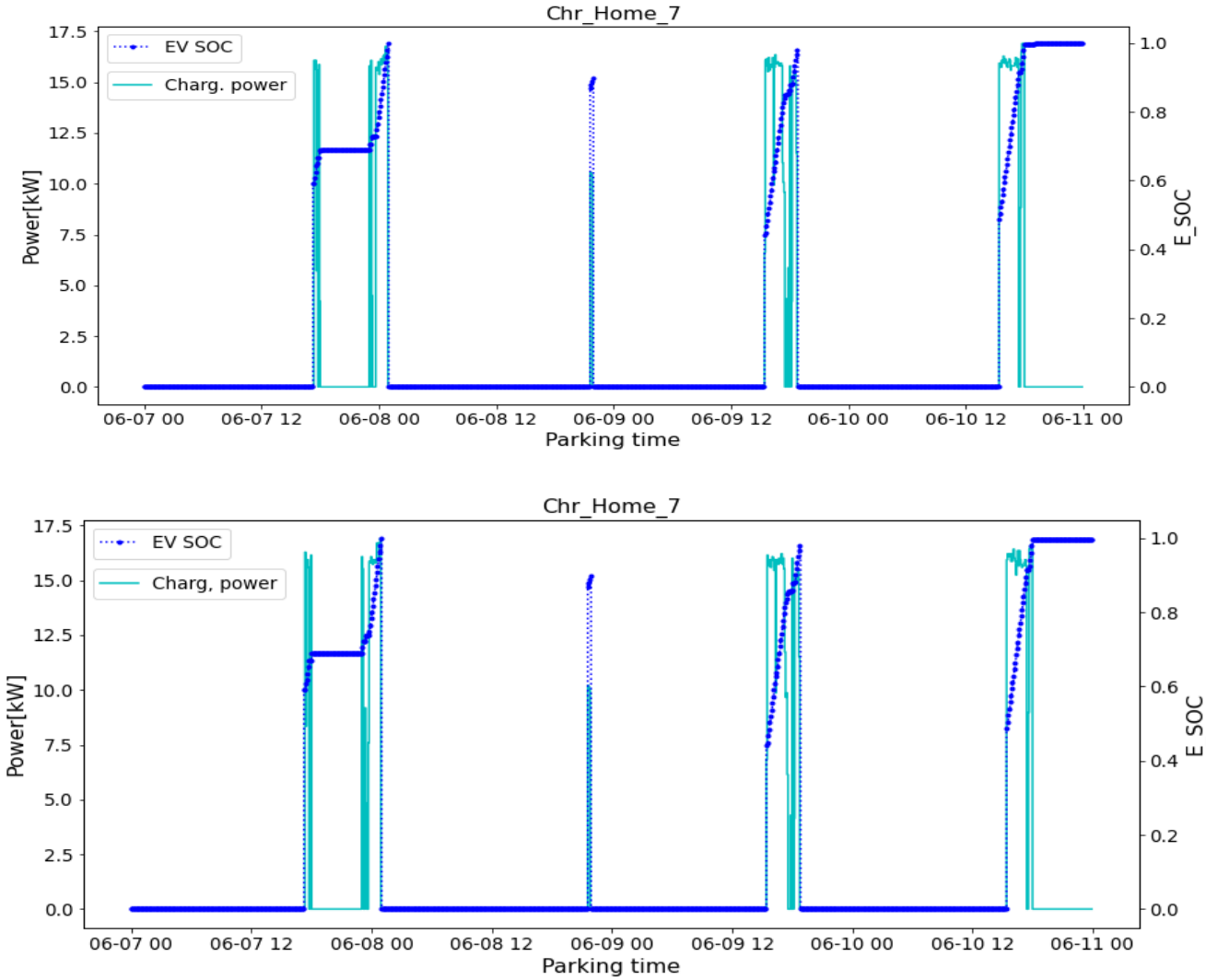

Fig. 5. 10: "Charger Home 7" Behavior in Prediction of Accurate SOC_{arr} (upper plot) & in Minimum SOC_{arr} (lower plot)

5.3.2 SOC_{arr} Uncertainty in Prediction & Reality

In this paragraph, the arrival SOC uncertainty has been studied during the case of real minimum arrival SOCs. Until now, the behavior change of the "P-C" algorithm has been shown, addressing the accurate and min arrival SOC prediction, when the EVs actually arrived with the accurate forecasted SOC. On that manner, the energy management towards the probability of uncertainty and potential Robust Optimization's over-conservativeness have been analyzed. This paragraph focuses on analyzing the impact of the arrival SOC uncertainty and its management, when the EVs actually arrived with the min SOC.

Table 5.3 summarizes the results in which the Prediction-Capable algorithm was prepared to face uncertainty in SOC_{arr} compared with the corresponding results of the Benchmark algorithm under SOC_{arr} uncertainty. The comparison of the two study cases suggests that the impact of the particular uncertainty is significant, since higher unfinished charging gap and penalty cost of 14.5€ at Node 2 can be seen, observing the results of the benchmark algorithm. Regarding P-C algorithm, the total unfinished charging gap of the EV fleets decreases, when it is prepared to face the worst-case scenario, and the corresponding penalty costs drop to zero.

Moreover, high unfinished charging gap has been observed in Node 2, in the P-C Algorithm study-case. This is again due to Discrete Optimization, however such abnormal numerical results regarding the total charging gap of the EV fleet of a node can be overlooked, if the penalty cost remains zero.

Finally, a notable decrease of energy costs & increase of energy earnings can be observed for Node 1 & Node 2 respectively, comparing the Benchmark with the P-C results, showing the ability of the P-C algorithm not only to perform successful EV charging under uncertainties (eliminating penalty costs paid to the customers), but also to perform it during efficient time periods.

Table 5. 3: Minimum Real SOC Arrival study cases: Charging Costs Comparison between Benchmark & P-C Study Cases

Benchmark "OSCD" Algorithm & Minimum Real SOC Arrival Results				
Nodes	Grid Power Exchange Cost (€)	Unfinished Charging Gap (kWh)	Penalty Cost for Charging Gap (€)	Total Node Charging Cost (€)
Node 1	2,9647	0,5077	0	2,9647
Node 2	2,8634	1,5068	14,5129	17,3763
Node 3	-0,215	0,2756	0	-0,215
Prediction-Capable Algorithm with Minimum SOC Prediction & Minimum Real SOC Arrival Results				
Nodes	Grid Power Exchange Cost (€)	Unfinished Charging Gap (kWh)	Penalty Cost for Charging Gap (€)	Total Node Charging Cost (€)
Node 1	2,6263	0,4542	0	2,62623
Node 2	2,8627	0,9143	0	2,8627
Node 3	-0,4394	0,0298	0	-0,4394

In Figs. 5.11 – 5.13, the behavior changes of Chargers 5, 6 & 7 of the "Home Node" respectively during the two study cases are depicted. Regarding Charger 5, it can be seen that the charging of the first arrived EV is not changed, because it is the only one connected during late hours, when price energy is low. On the contrary, the 2nd and 4th EVs arrived at '8-6 17:20' and '10-6 15:25' respectively are charged more overhand because of the prediction of the min arrival SOCs of the forthcoming EVs at the other two chargers. Charging changes are not observed at Charger 6 in Fig. 5.12, because EVs at Charger 6 are either not involved in smart-charging or parked alone overnight. In Fig. 5.13, the 1st EV arrived at Charger 7, which is generally susceptible to uncertainty changes because of the predicted arrivals at the other chargers, is again charged more earlier when predicted worst-case scenario has been taken in account.

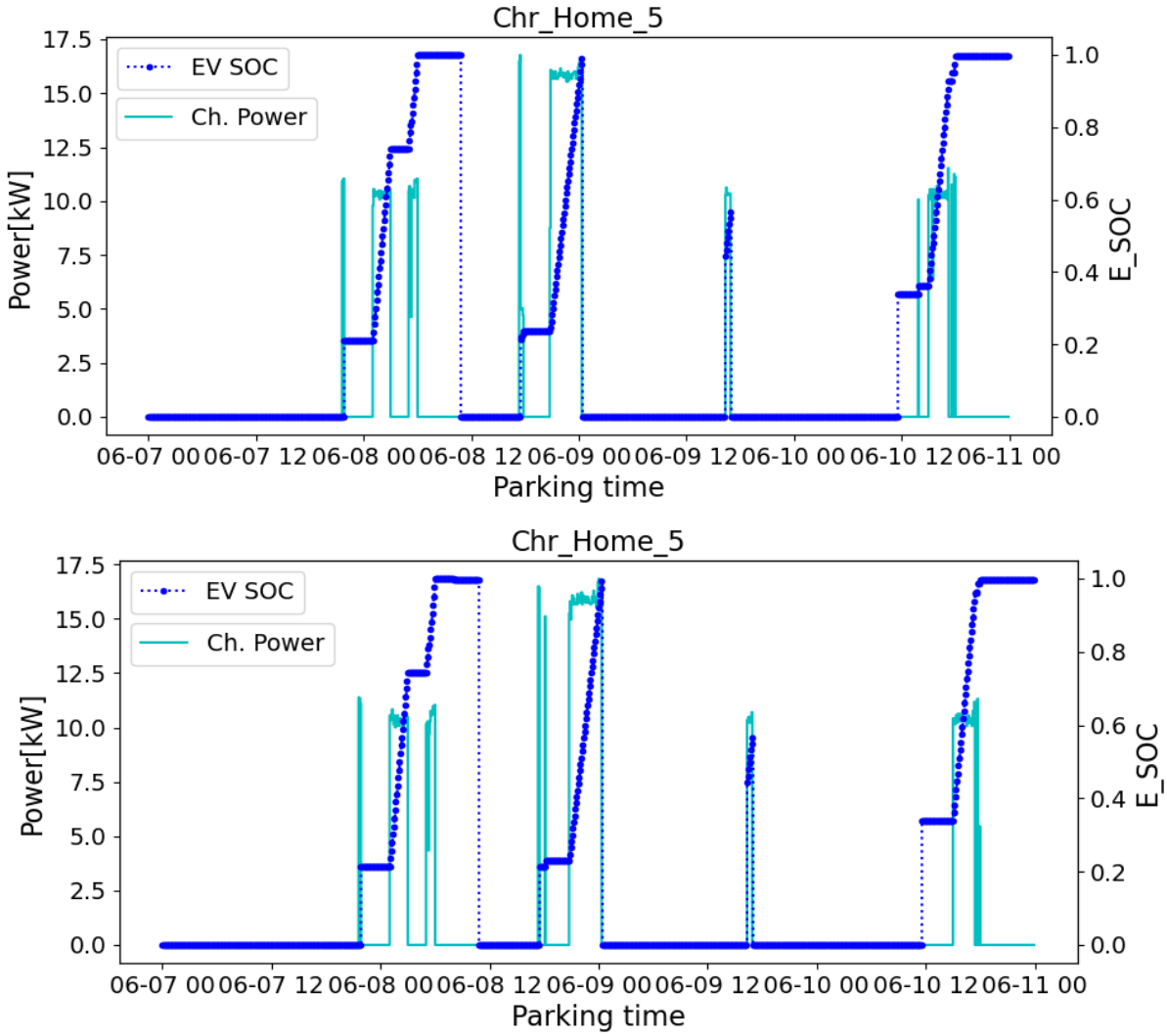

Fig. 5. 11: "Charger Home 5" Behavior in Benchmark algorithm (upper plot) & in P-C algorithm (lower plot) in Real Minimum arrival SOCs

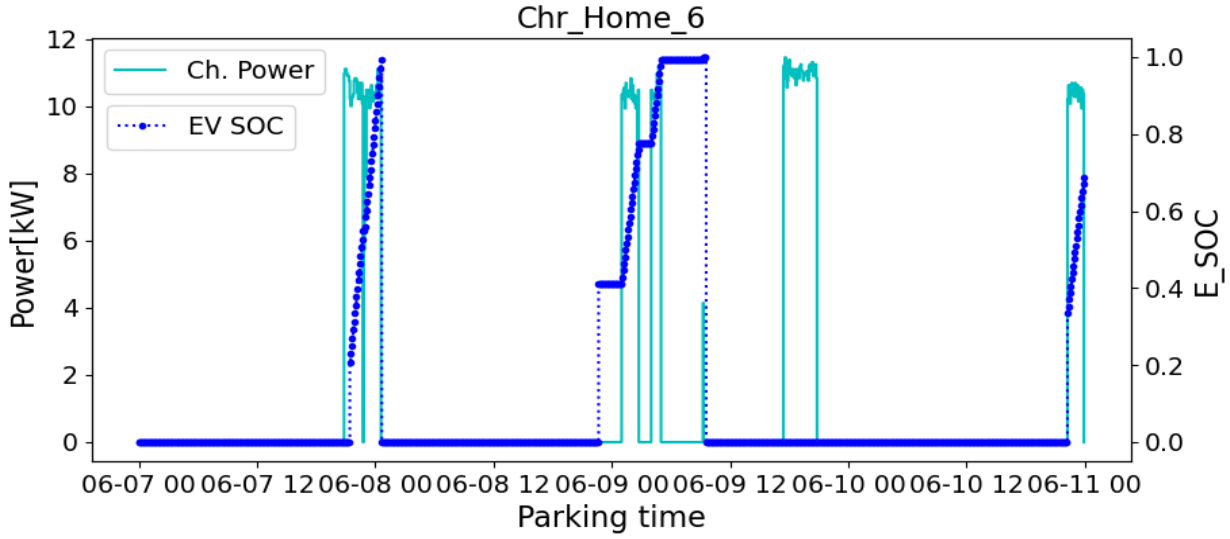

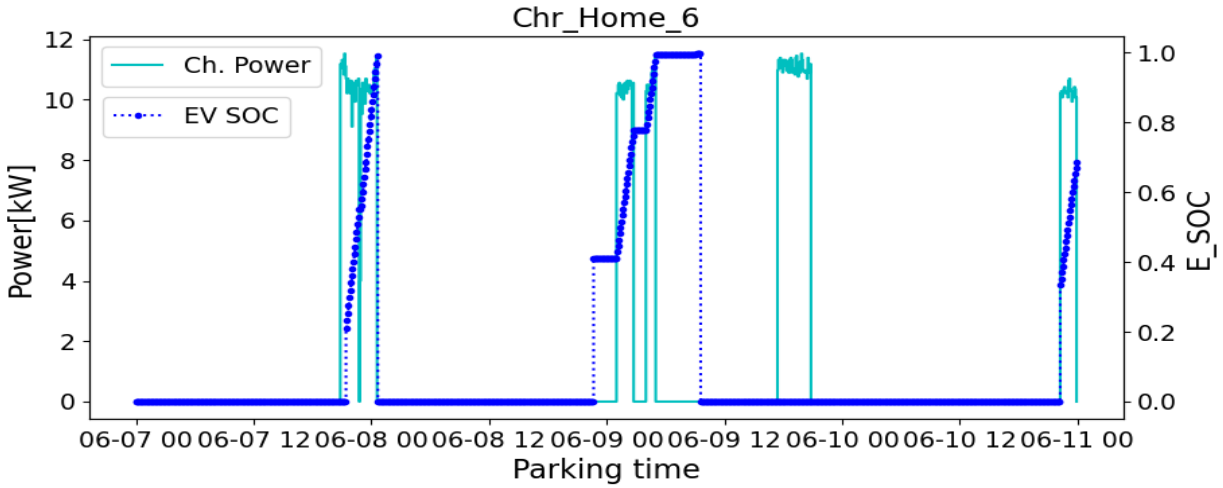

Fig. 5. 12: "Charger Home 6" Behavior in Benchmark algorithm (upper plot) & in P-C algorithm (lower plot) in Real Minimum arrival SOCs

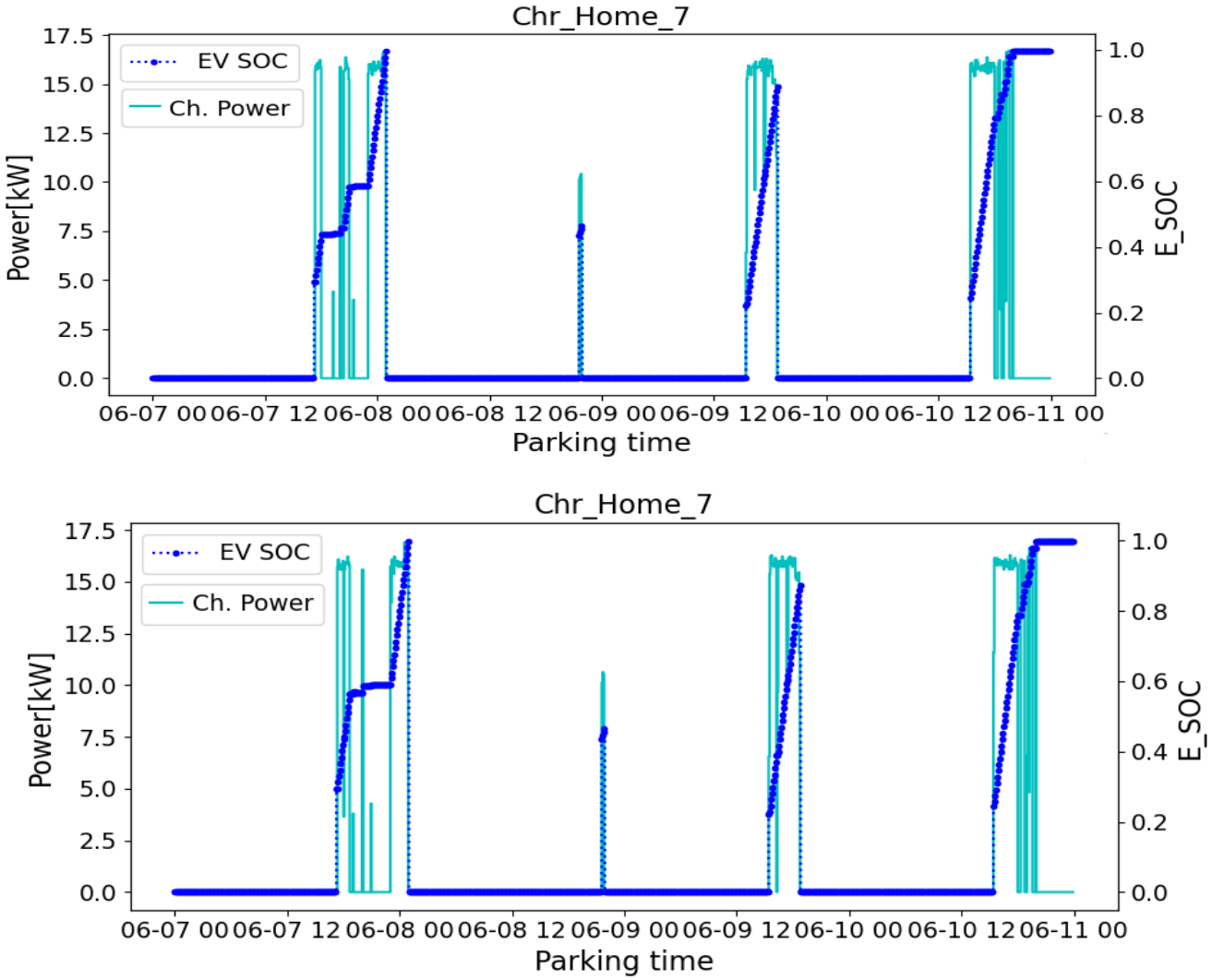

Fig. 5. 13: "Charger Home 7" Behavior in Benchmark algorithm (upper plot) & in P-C algorithm (lower plot) in Real Minimum arrival SOCs

5.4 Parking Time Uncertainty Studies

5.4.1 Parking Time Uncertainty only in Prediction

In the particular paragraph, the results of the investigation, when parking time uncertainty is integrated only in prediction (and not in reality) are summarized in Table 5.4. As explained in Chapter 4, two ways of 50% reduction of parking time have been considered, firstly by 25% arrival – 25% departure and secondly by 50% departure. Comparing the results of these two study-cases with the base-case results of the P-C algorithm aims to address the potential overconservative management of Robust Optimization regarding the parking time uncertainty.

As Table 5.4 depicts, no major differences can be detected in all study cases in terms of the grid power exchange cost, which remain practically the same. Observing the results of the first way, the prediction of minimum parking time did not improve the unfinished charging gap, such as in the study case of the minimum SOC_{arr} prediction as expected. It can be clearly seen that in Node 1, the unfinished charging gap remains almost the same, in Node 2 a small decrease is observed, while in Node 3, the charging gap has increased. Observing however the results of the second way, the total unfinished charging gap of the nodes tends to increase compared with both the first way and base-case results, apart from Node 3 ("Public Node"), where the charging gap resulted to be slightly lower than in the first case. Nevertheless, the penalty costs remained zero and the charging costs practically the same.

The answer can be found in Figs. 5.14, 5.15 & 5.16, which show the behavior difference between the base-case and the two study cases of parking time uncertainty prediction, regarding Chargers 5, 6 & 7 respectively.

Table 5. 4: Charging Costs Comparison between Accurate Forecast & Minimum Parking Time Prediction study cases of P-C Algorithm

Prediction-Capable Algorithm with Accurate Forecast Results				
Nodes	Grid Power Exchange Cost (€)	Unfinished Charging Gap (kWh)	Penalty Cost for Charging Gap (€)	Total Node Charging Cost (€)
Node 1	1,5885	0,2242	0	1,5885
Node 2	-0,6866	0,3497	0	-0,6866
Node 3	-1,8354	0,1543	0	-1,8354
Prediction-Capable Algorithm with Minimum Parking Time$_r$ Prediction Results (1st Mode: 25% arrival – 25% departure)				
Nodes	Grid Power Exchange Cost (€)	Unfinished Charging Gap (kWh)	Penalty Cost for Charging Gap (€)	Total Node Charging Cost (€)
Node 1	1,5802	0,2721	0	1,5802
Node 2	-0,6867	0,2742	0	-0,6867
Node 3	-1,8418	0,2867	0	-1,8418
Prediction-Capable Algorithm with Minimum Parking Time$_r$ Prediction Results (2nd Mode: 50% departure)				
Nodes	Grid Power Exchange Cost (€)	Unfinished Charging Gap (kWh)	Penalty Cost for Charging Gap (€)	Total Node Charging Cost (€)
Node 1	1,583	0,5231	0	1,583
Node 2	-0,6582	0,4396	0	-0,6582
Node 3	-1,83	0,1603	0	-1,83

While in the "Minimum SOC_{arr} Prediction" study case, Charger 7 rushed to charge the 1st arrived EV due to the forthcoming EVs at the other 2 chargers, the 1st way of min parking time prediction inflicts a notable delay compared with the base case (see Fig. 5.16). Moreover, the same has been observed at the last arrived EV at Charger 5 in Fig. 5.14. While it is the first arrived from the last arrivals at the Chargers, its charging is delayed instead of realized sooner as expected. This abnormal behavior can be justified by

the fact that the algorithm predicts later arrivals of the coming EVs apart from minimum parking times. Therefore, it thinks that there is enough time in order to charge the currently connected EVs later than normally. In order to avoid this undesired effect, the 2nd way inserts all uncertainty in the EVs' departures to keep the algorithm out of confusion. While this succeeds in having positive effect in Charger 5 (it can be clearly observed that the 4th arrived EV at Charger 5 is charged earlier), it has the exact opposite results in the 1st arrived EV at Charger 7 (see Fig. 5.16). The prediction that the coming EV at Charger 6 "7-6 20:50" will depart at the earliest "7-6 22:45" and not at "8-6 00:35" cause the algorithm to delay the charging of the 1st EV at Charger 5 during midnight.

Observing Fig. 5.15, no major differences can be spotted at Charger 6 in all 3 study cases. The 1st arrived EV at Charger 6 initiates charging immediately because it arrives with lower than 20% SOC and the charging of the 1st arrived EV at Charger 5 is postponed to the late hours after midnight, since it is the only one connected in both situations. The same is observed regarding the 2nd arrival at Charger 6, which remains connected alone during late hours in both situations and the 3rd arrival at Charger 6, which does not participate in smart-charging.

Finally, such as in all other study cases, EVs with very low parking time or high requested energy (e.g the 3rd arrived EV at Charger 5 or the 2nd arrived EV at Charger 7) are not affected greatly by uncertainty (in terms of earlier or delayed charging), because the algorithm charges them in all 3 study cases during the entire parking time.

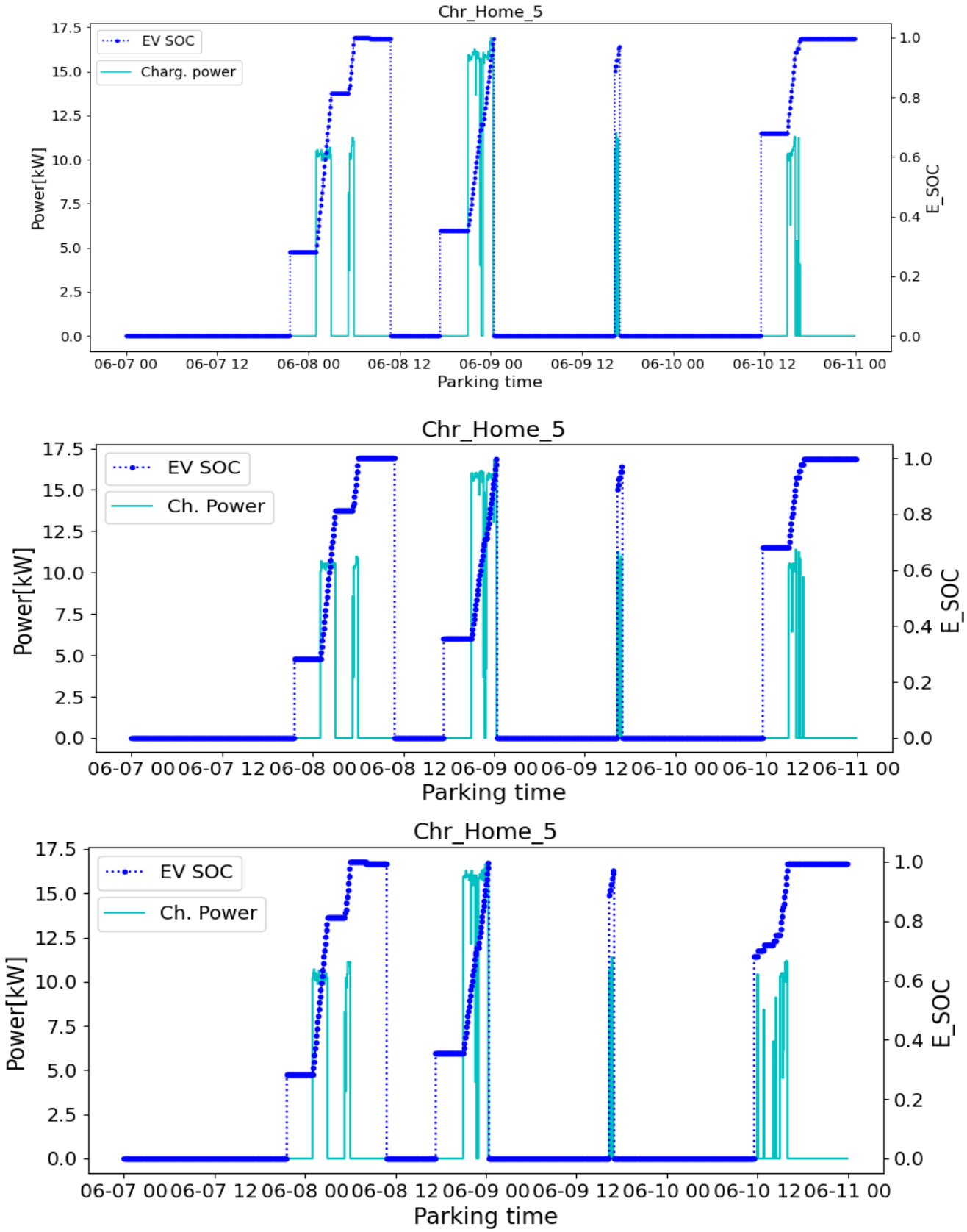

Fig. 5. 14: "Charger Home 5" Behavior in P-C base-case (upper plot), in 1st Min Parking Time Prediction (middle plot) & in 2nd Min Parking Time Prediction (lower plot)

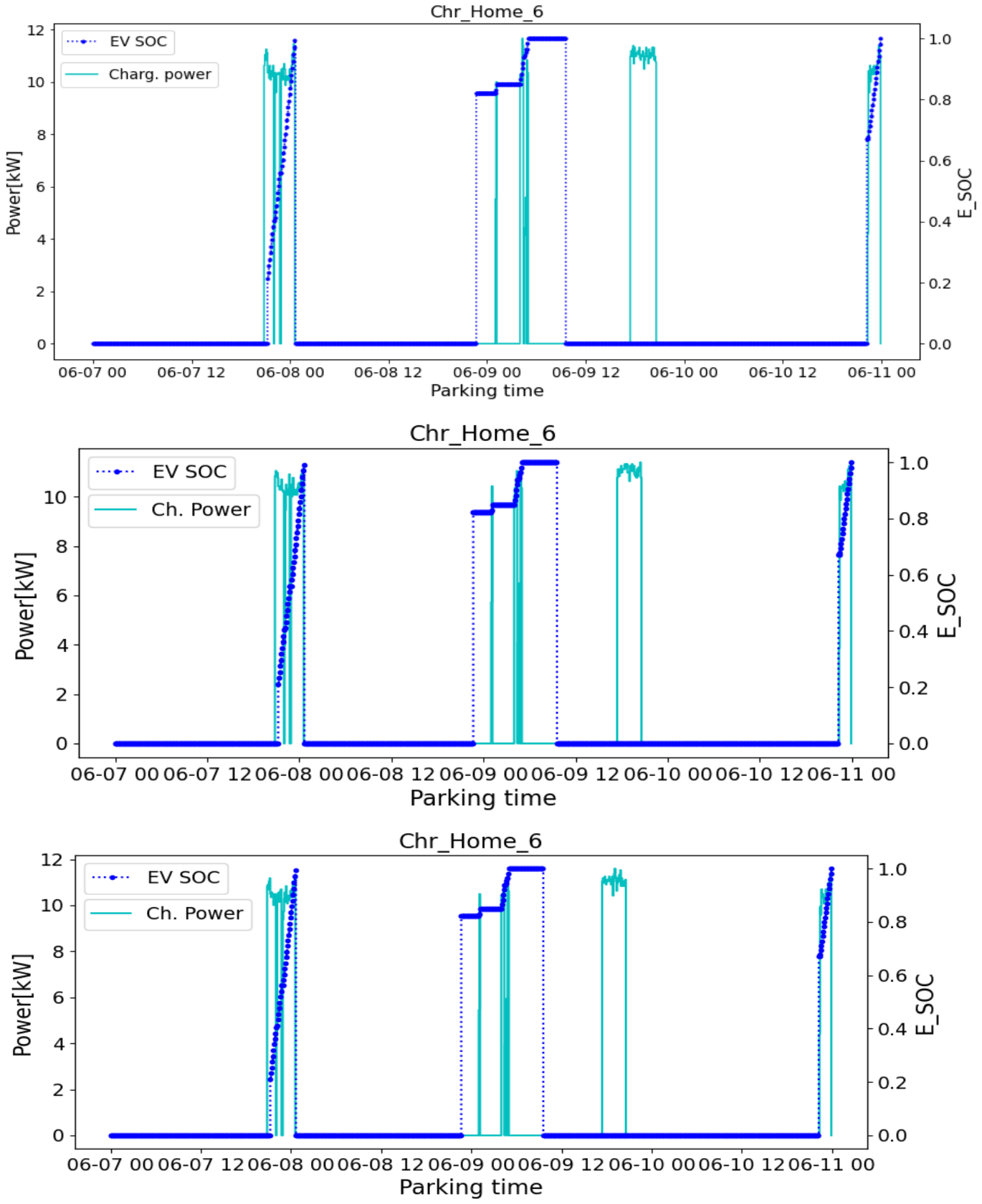

Fig. 5. 15: "Charger Home 6" Behavior in P-C base-case (upper plot), in 1st Min Parking Time Prediction (middle plot) & in 2nd Min Parking Time Prediction (lower plot)

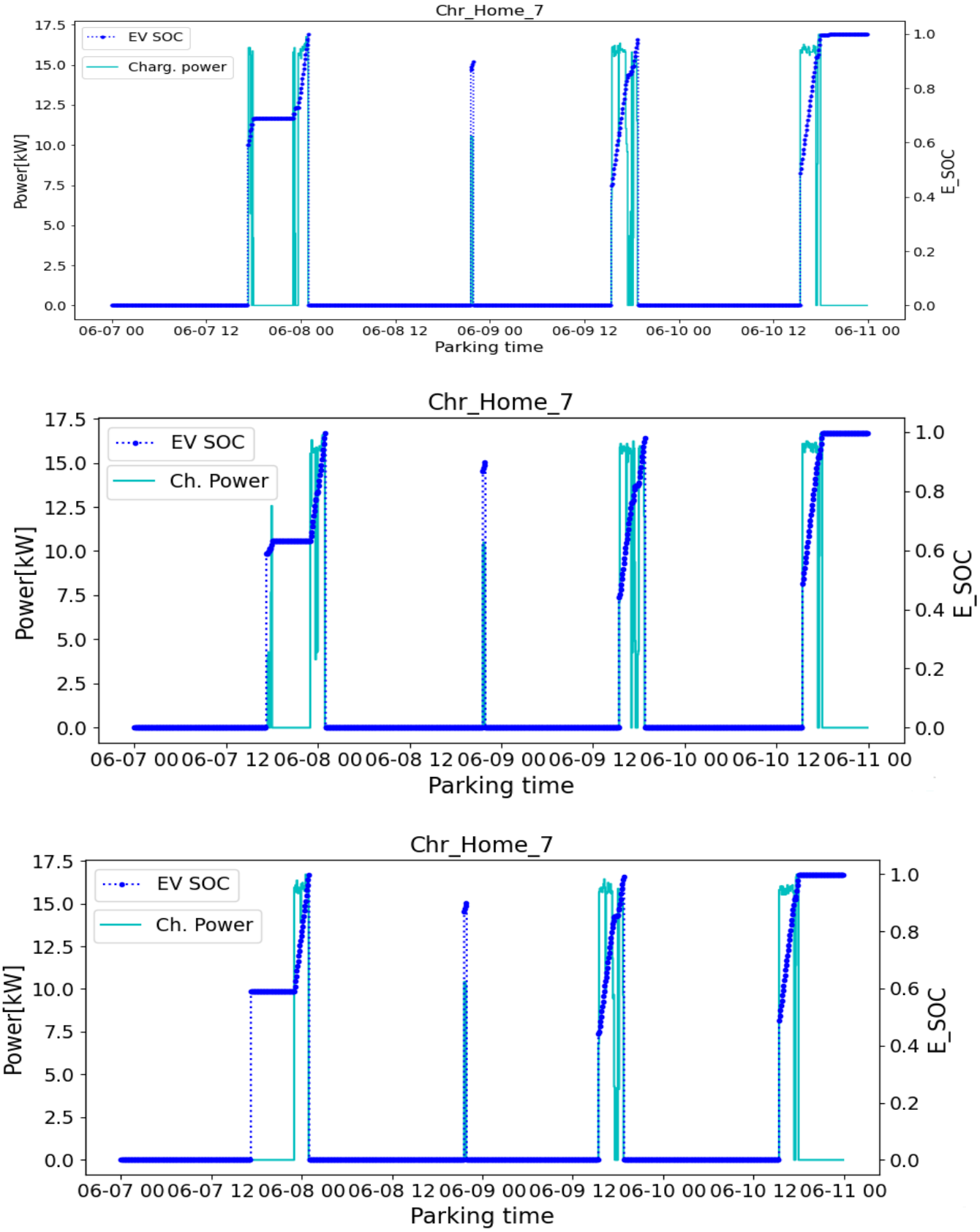

Fig. 5. 16: "Charger Home 7" Behavior in P-C base-case (upper plot), in 1st Min Parking Time Prediction (middle plot) & in 2nd Min Parking Time Prediction (lower plot)

5.4.2 Parking Time Uncertainty in Prediction & Reality

Such as in paragraph 5.3.2 & SOC_{arr} uncertainty, in this paragraph, the parking time uncertainty has been inserted in the P-C algorithm reality part in order to reveal information about the impact of the particular uncertainty and its management. Similar to 5.4.1, the reduction of the parking time has been performed with two ways: addressing arrival & departure or only departure. Table 5.5 summarizes the results of the real event of the parking time uncertainty in the P-C algorithm, when worst-case scenario is predicted, compared simultaneously with the corresponding results of the benchmark algorithm, for both ways of addressing the particular uncertainty.

Table 5. 5: Minimum Real Parking Time study cases: Charging Costs Comparison between Benchmark & P-C Study Cases

Benchmark Algorithm & Minimum Real Parking Time Results (1st way: Arrival & Departure)				
Nodes	Grid Power Exchange Cost (€)	Unfinished Charging Gap (kWh)	Penalty Cost for Charging Gap (€)	Total Node Charging Cost (€)
Node 1	1,6417	0,1606	0	1,6417
Node 2	-0,5055	0,9235	15,3666	14,8611
Node 3	-1,8606	0,8637	9,9808	8,1202
Prediction-Capable Algorithm with Minimum Parking Time Prediction & Minimum Real Parking Time Results (1st way: Arrival & Departure)				
Nodes	Grid Power Exchange Cost (€)	Unfinished Charging Gap (kWh)	Penalty Cost for Charging Gap (€)	Total Node Charging Cost (€)
Node 1	1,3131	0,4321	0	1,3131
Node 2	-0,4969	0,2825	0	-0,4969
Node 3	-1,9586	0,0394	0	-1,9586
Benchmark Algorithm & Minimum Real Parking Time Results (2nd way: Only Departure)				
Nodes	Grid Power Exchange Cost (€)	Unfinished Charging Gap (kWh)	Penalty Cost for Charging Gap (€)	Total Node Charging Cost (€)
Node 1	1,7285	1,2274	9,4824	11,2109
Node 2	-0,4584	0,3472	0	-0,4584
Node 3	-1,8904	0,6968	9,566	7,6756
Prediction-Capable Algorithm with Minimum Parking Time Prediction & Minimum Real Parking Time Results (2nd way: Only Departure)				
Nodes	Grid Power Exchange Cost (€)	Unfinished Charging Gap (kWh)	Penalty Cost for Charging Gap (€)	Total Node Charging Cost (€)
Node 1	1,408	0,3288	0	1,408
Node 2	-0,429	0,06019	0	-0,429
Node 3	-1,9911	0,1249	0	-1,9911

When uncertainty is inserted both in arrival and departure, the total unfinished charging gap for every node can result both increased or decreased, comparing the study case of P-C algorithm with the Benchmark study case. While the charging gap decreases for Nodes 2 & 3 when prediction is taken into consideration, the opposite results are observed for Node 1. As already explained, this is justified by the fact that when uncertainty affects also arrival time, parking time can inflict considerable impact even when prediction is utilized. Since arrivals constitute re-optimization triggers, arrival time uncertainty can confuse the algorithm about the right time of charging and inflict charging gaps. However, a general improvement of the grid power exchange cost can be observed for the P-C study case, while the insertion of prediction nullifies the penalty costs that appear in the Nominal study case.

On the contrary, when uncertainty is inserted only in EV departures, a clear improvement of the unfinished charging gap can be seen for the P-C study case at all nodes, since the algorithm is prepared for the worst-case scenario. Moreover, the charging costs are also improved compared with the Benchmark study case. Finally, the penalty costs that appear at Nodes 1 & 3 (9.48€ & 9.57€ respectively) are zero when prediction is utilized.

For the limited space of this thesis, Figs. 5.17 – 5.19 present the charging behavior of Chargers 5-7 in the two study cases of the P-C algorithm. The upper plot shows the results when uncertainty is inserted both in EV arrival & departure, while the lower plot shows the corresponding results when uncertainty affects only departure. As it can be seen in Fig. 5.17, Charger 5 delays the charging of the 1st EV arrived in the first case, when parking time has been reduced by 25% arrival and 25% departure compared with the 2nd case, in which the EV will depart at the earliest. On the contrary, the charging of the last arrived EV at Charger 5 is delayed in the 2nd case, because the coming EV at Charger 7 at 10-6 15:25 will depart earlier at 10-6 20:40 (instead of 10-6 23:55 in the 1st case). Hence, it is more efficient to be charged during the late hours when energy price is lower.

Similar results can be found in Fig. 5.19 for the EV fleet of Charger 7. Charger 7 decides to charge the 1st arrived EV later in the first case, because of the prediction of the earliest departures of the EVs that are going to arrive at Chargers 6 & 5 (7-6 20:50 & 7-6 21:35 respectively). On the contrary, the last arrived EV at Charger 7 (10-6 15:25) is charged earlier in the 2nd case, in which it departs at the earliest. Last but not least, in can be clearly observed in Fig. 5.18 that the 2nd arrived EV at Charger 6 is charged earlier in the 2nd case due to the earliest departure. However, EVs with very low parking time or with no Smart-Charging participation, such as the 4th and 3rd arrived EV at Charger 6 respectively, are not affected by the parking time uncertainty.

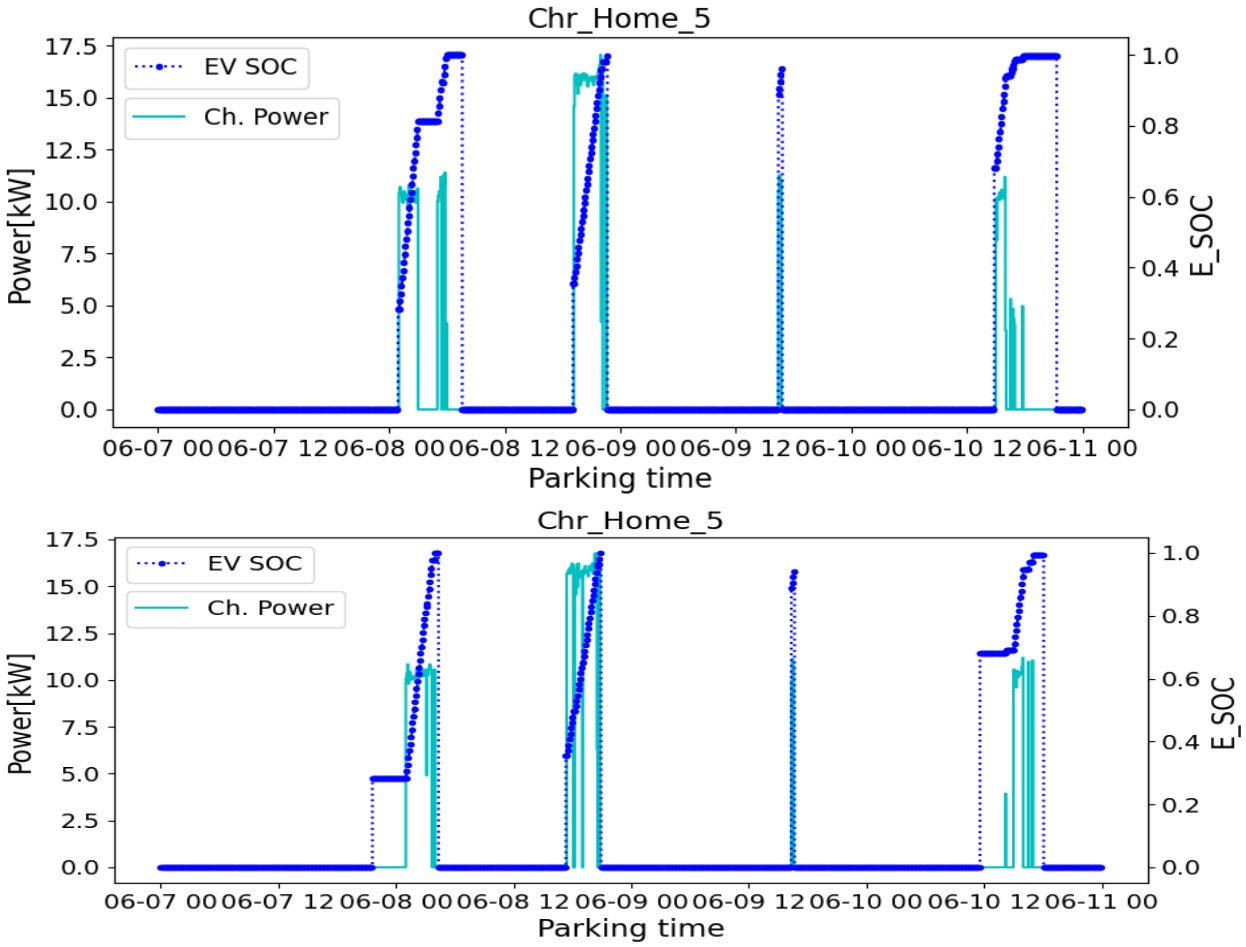

Fig. 5. 17: "Charger Home 5" Behavior in P-C Algorithm's Min Parking Time Study Case: Uncertainty affects both Arrival & Departure (upper plot) or only Departure (lower plot)

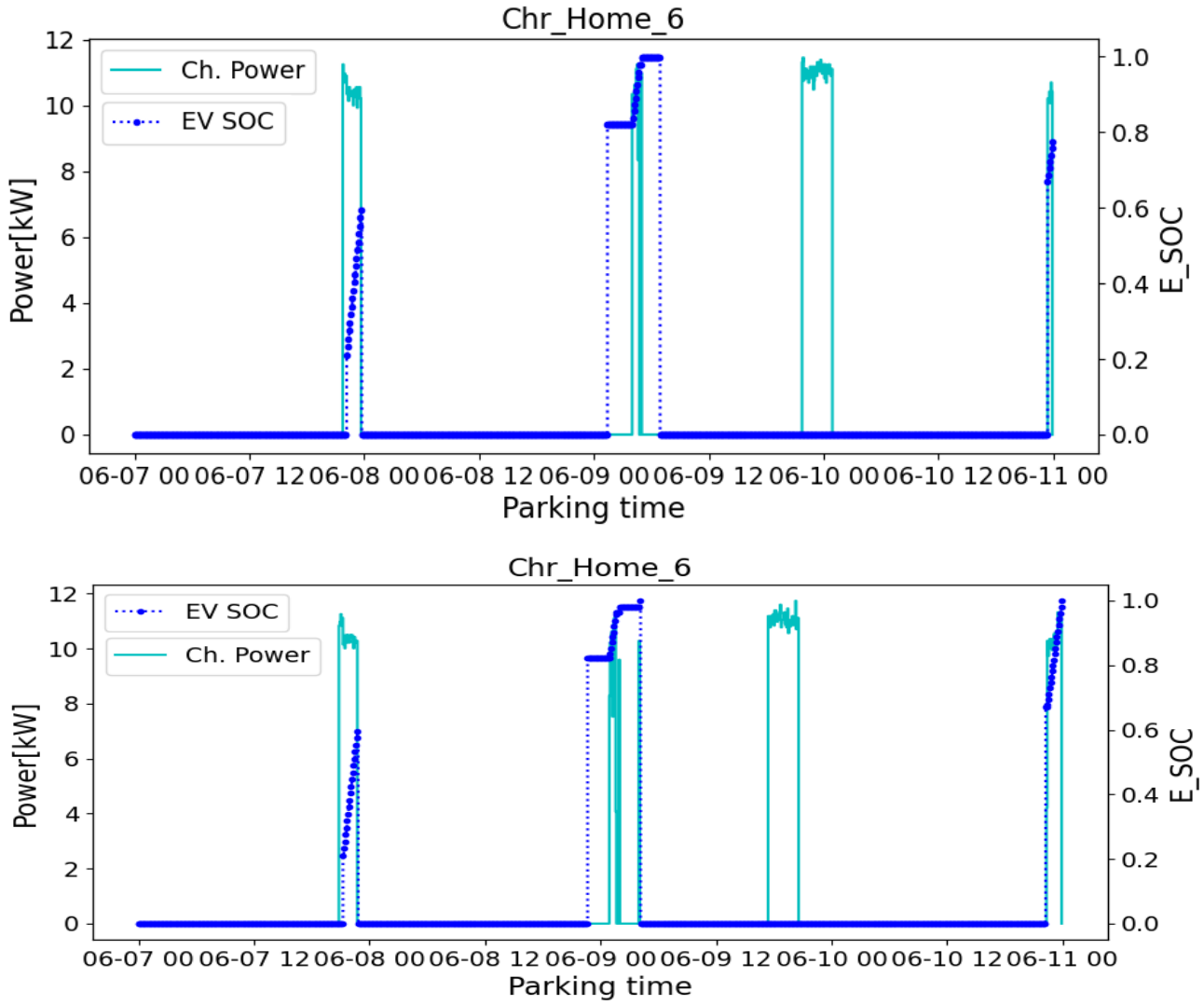

Fig. 5. 18: "Charger Home 6" Behavior in P-C Algorithm's Min Parking Time Study Case: Uncertainty affects both Arrival & Departure (upper plot) or only Departure (lower plot)

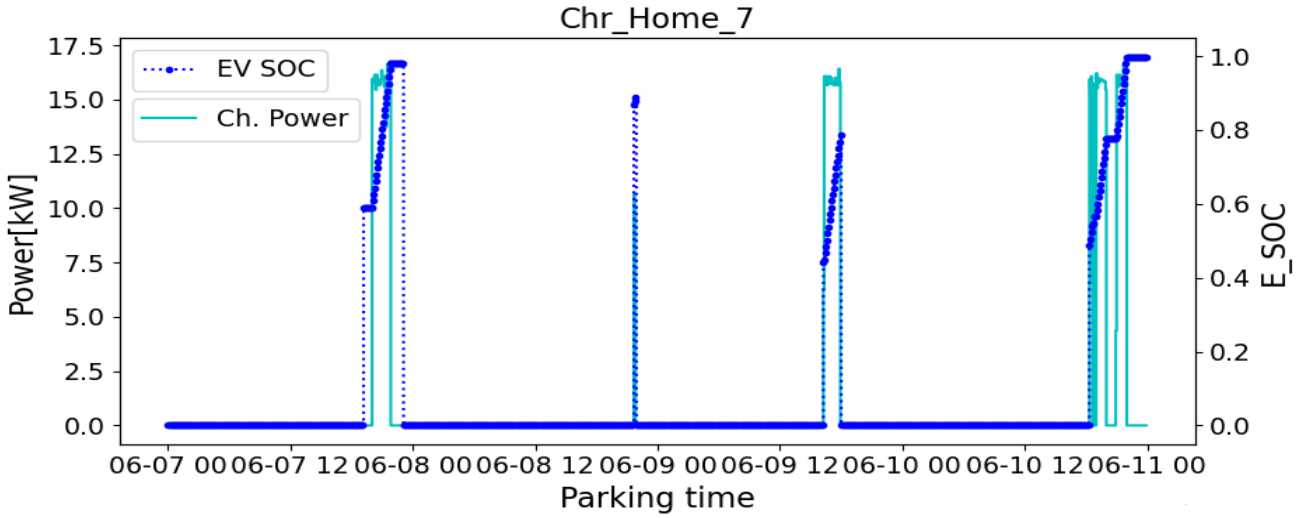

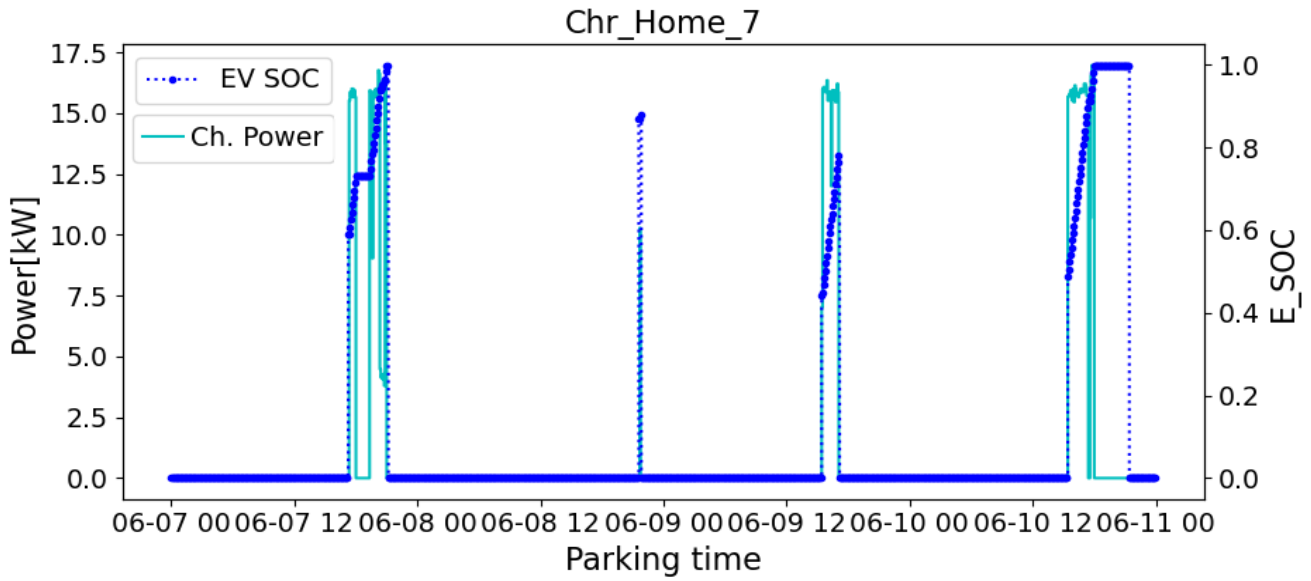

Fig. 5. 19: "Charger Home 7" Behavior in P-C Algorithm's Min Parking Time Study Case: Uncertainty affects both Arrival & Departure (upper plot) or only Departure (lower plot)

Taking everything into consideration, the 2nd case, which presents the results of the minimum parking time when uncertainty is all inserted in departure, generally causes earlier EVs charging. However, EVs that arrive first at a charger of an empty node and activate prediction may be charged earlier because of the prediction that the coming EVs are going to depart at the earliest and therefore there is time availability for charging later.

5.5 PV Generation & Load Demand Uncertainties Studies

In this paragraph chapter, the investigation has been focused on the PV Generation and Load Demand uncertainties. As it can be seen in Table 5.6, which summarizes the results between the base case – PV generation uncertainty case – Load Demand Uncertainty case in both Benchmark & P-C algorithms, integrating any of these uncertainties in the algorithm, generally improves the total unfinished charging gap of the EV fleets in both Nominal and P-C forms. This is justified by the fact that integrating these uncertainties in the optimization horizons drives the algorithm to charge EVs earlier than normally, which is also shown in Figs. 5.20-5.22. However, in both Benchmark and P-C forms, the impact on grid power exchange cost is greater than in the previous uncertainties. This can be explained if we consider the direct relation of PV Generation, Load Demand and importing/exporting energy. Decreased PV Generation and increased Load force the algorithm to import more (or export less power) from the grid increasing directly the grid power exchange cost.

Table 5. 6: Charging Costs Comparison between Benchmark & P-C OSCD Study Cases: PV Generation – Load Demand Uncertainties Consideration

Benchmark Algorithm Results				
Nodes	Grid Power Exchange Cost (€)	Unfinished Charging Gap (kWh)	Penalty Cost for Charging Gap (€)	Total Node Charging Cost (€)
Node 1	1,8738	0,2721	0	1,8738
Node 2	-0,6827	0,568	0	-0,6827
Node 3	-1,7623	0,17	0	-1,7623
Benchmark Algorithm with Minimum PV Generation Results				
Nodes	Grid Power Exchange Cost (€)	Unfinished Charging Gap (kWh)	Penalty Cost for Charging Gap (€)	Total Node Charging Cost (€)
Node 1	1,9888	0,1211	0	1,9888
Node 2	-0,3384	0,516	0	-0,3384
Node 3	-1,5413	0,2752	0	-1,5413
Benchmark Algorithm with Maximum Load Demand Results				
Nodes	Grid Power Exchange Cost (€)	Unfinished Charging Gap (kWh)	Penalty Cost for Charging Gap (€)	Total Node Charging Cost (€)
Node 1	2,1677	0,2358	0	2,1677
Node 2	-0,585	0,5172	0	-0,585
Node 3	-1,6525	0,0346	0	-1,6525
Prediction-Capable Algorithm with Accurate Forecast Results				
Nodes	Grid Power Exchange Cost (€)	Unfinished Charging Gap (kWh)	Penalty Cost for Charging Gap (€)	Total Node Charging Cost (€)
Node 1	1,5885	0,2242	0	1,5885
Node 2	-0,6866	0,3497	0	-0,6866
Node 3	-1,8354	0,1543	0	-1,8354
Prediction-Capable Algorithm with Minimum PV Generation Results				
Nodes	Grid Power Exchange Cost (€)	Unfinished Charging Gap (kWh)	Penalty Cost for Charging Gap (€)	Total Node Charging Cost (€)
Node 1	1,6908	0,0726	0	1,6908
Node 2	-0,3459	0,3833	0	-0,3459
Node 3	-1,6016	0,0237	0	-1,6016
Prediction-Capable Algorithm with Maximum Load Demand Results				
Nodes	Grid Power Exchange Cost (€)	Unfinished Charging Gap (kWh)	Penalty Cost for Charging Gap (€)	Total Node Charging Cost (€)
Node 1	1,9047	0,205	0	1,9047
Node 2	-0,5899	0,5334	0	-0,5899
Node 3	-1,7623	0,02969	0	-1,7623

Finally, comparing the related 3 study-cases of the Benchmark and P-C algorithms, it can be observed that the P-C version generally provides a more efficient and successful charging in terms of charging cost and unfinished charging gap respectively in all 3 study cases.

In Figs 5.20, 5.21 & 5.22, the behavior of the Chargers 5, 6 & 7 in the P-C OCD algorithm respectively is depicted and compared regarding the base case (accurate prediction), the PV Generation and the Load Demand uncertainties.

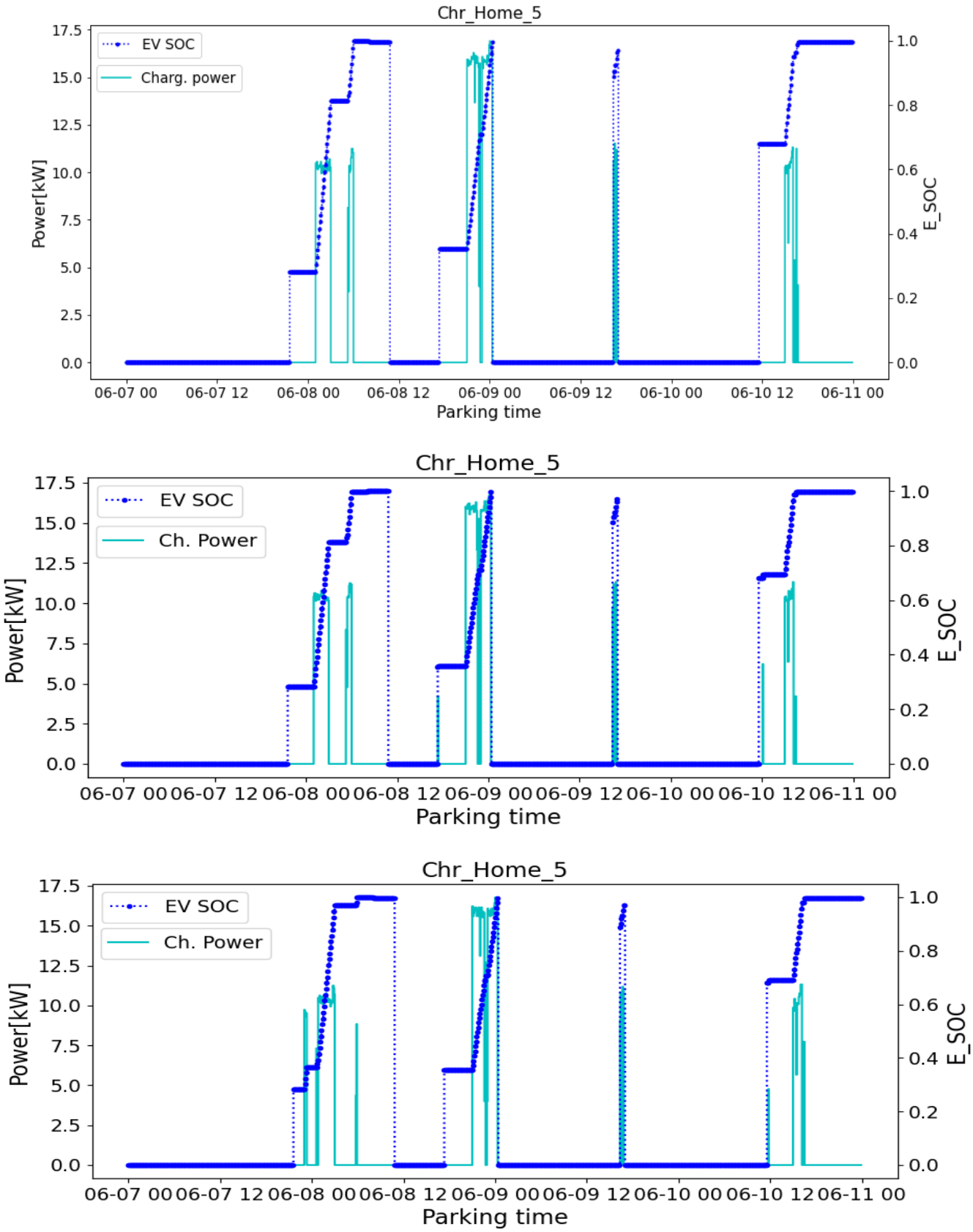

Fig. 5. 20: "Charger Home 5" Behavior in Base Case (upper plot), minimum PV Generation Prediction (middle plot) & maximum Load Demand Prediction (lower plot)

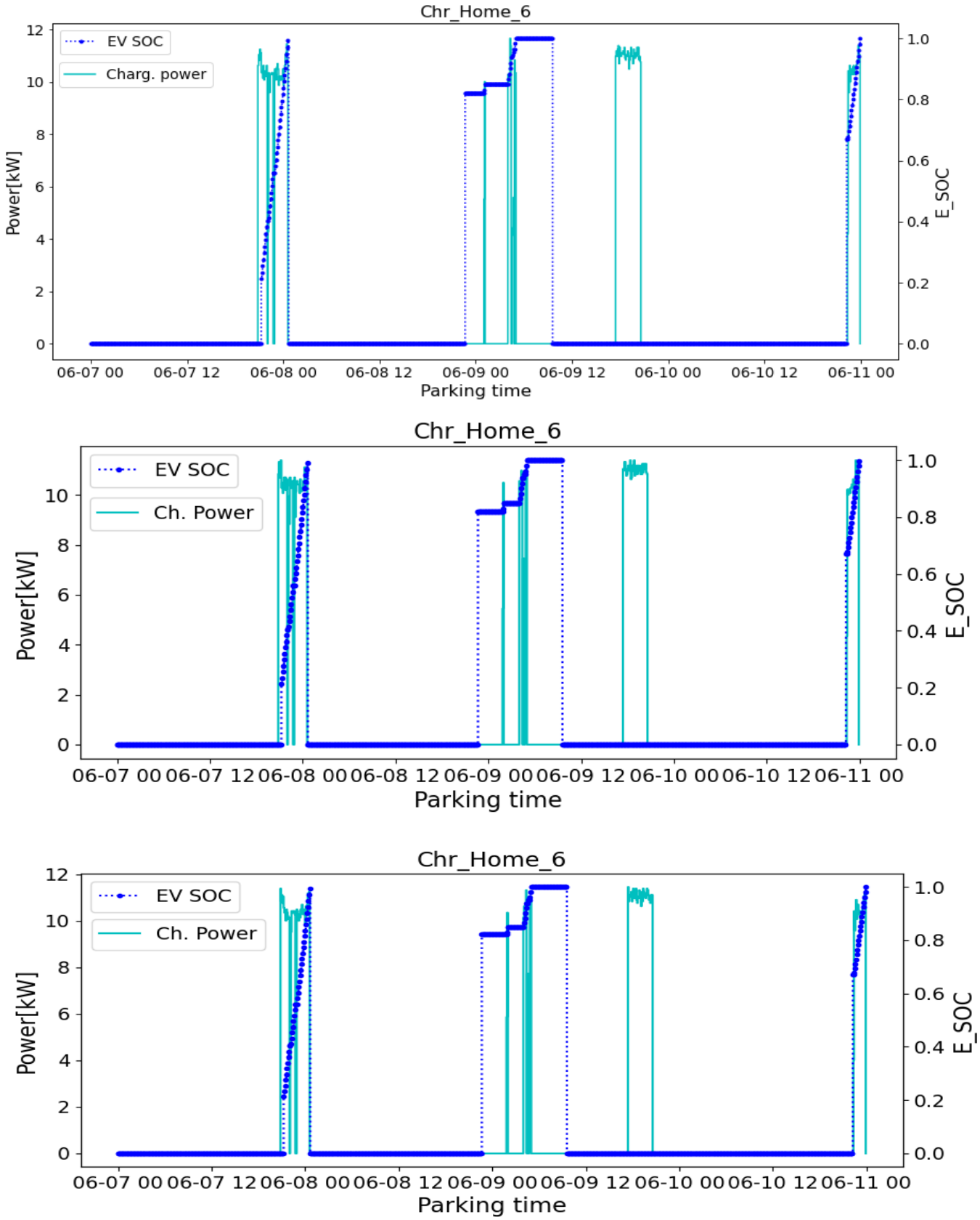

Fig. 5. 21: "Charger Home 6" Behavior in Base Case (upper plot), minimum PV Generation Prediction (middle plot) & maximum Load Demand Prediction (lower plot)

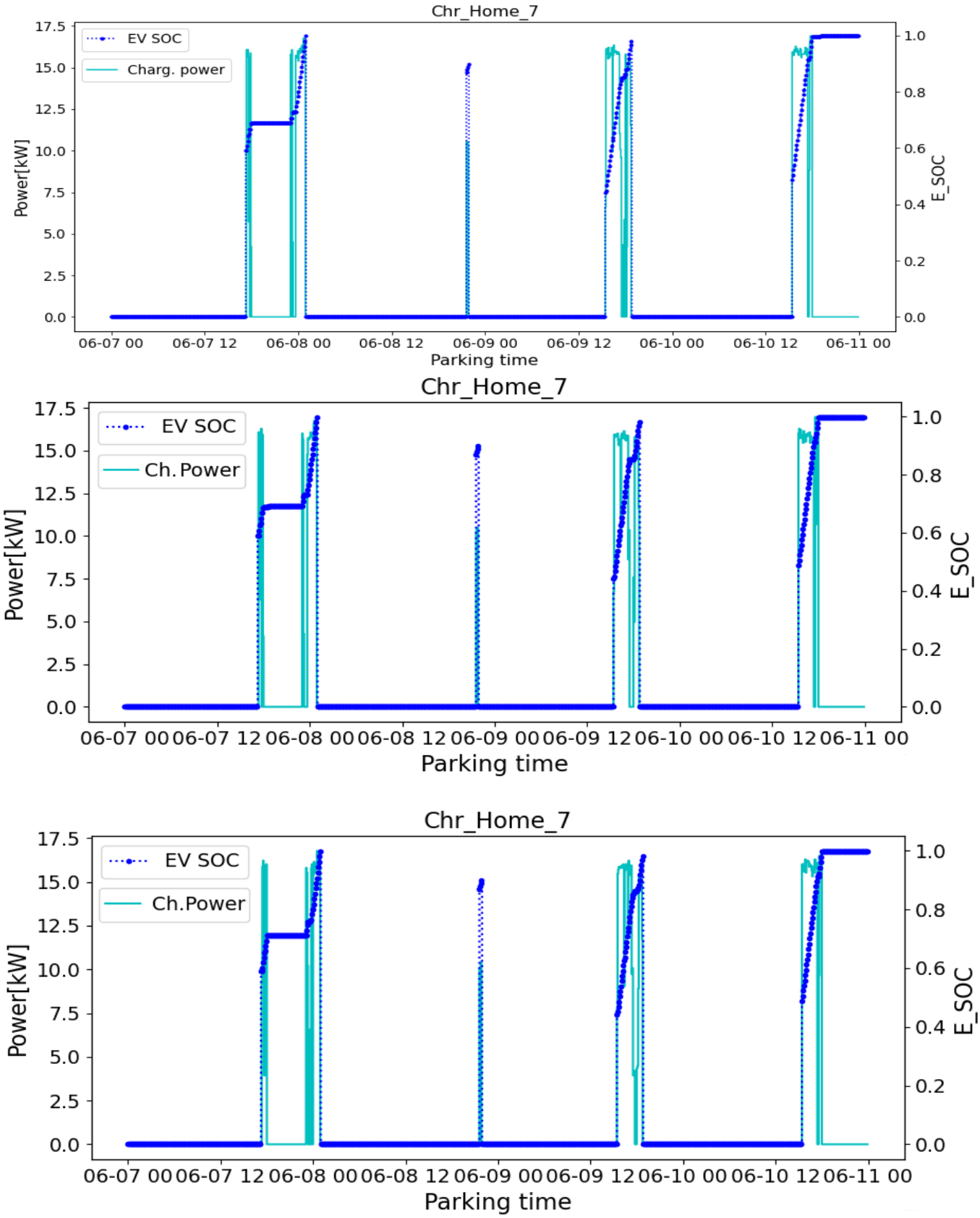

Fig. 5. 22: "Charger Home 7" Behavior in Base Case (upper plot), minimum PV Generation Prediction (middle plot) & maximum Load Demand Prediction (lower plot)

Regarding "Charger Home 5", Fig. 5.20 shows that PV generation does not affect the charging of the 3 first EV arrivals at the charger. This is due to the fact that the first 2 EVs are charged regularly (in the base case) during later hours without Sun and PV Generation, while the 3rd parks for very little parking time to be affected. On the contrary, the last EV at Charger 5, which arrives at 10-6 11:35 and departs at 23:55, initiates some charging earlier. The algorithm predicts that PV generation will reduce even more during the evening and performs a part of the charging at higher price energy period. Load Demand affects greatly the 1st EV, whose charging initiates earlier, because the prediction shows a higher load demand than usual in the future. Moreover, the 1st arrived EV at Charger 5 is the last arrived compared with the 1st arrivals at the other chargers, so few or no re-optimizations are realized until its departure time. Due to the high requested energy or minimum parking time, 2nd and 3rd EV arrivals are minorly affected. Finally, just as in PV generation uncertainty, the algorithm rushes to charge partly the 4th arrived EV, since it predicts an even higher load demand in the evening.

Regarding Chargers 6 & 7, the charging of the EV fleets has not been affected notably by any of the two uncertainties. Regarding Fig. 5.21, which shows Charger 6 behavior, this can be justified by the very high requested energy of the 1st EV arrived (35kWh), the No-SC participation of the 3rd EV arrived and the minimum parking (from 22:15 to 23:55) of the last arrived EV. Regarding the 2nd EV at Charger 6, it is the only connected EV during the after-midnight hours, which are not affected by PV generation or Load Demand, which are zero or minimum. The same reasons can be found in Fig. 5.22, considering Charger 7. For example, the 2nd EV arrived parks for a very low parking time (25'), while the 3rd EV initiates charging upon arrival in all study-cases, because of the forthcoming arrivals at the other chargers. Finally, the 2 charging periods of the 1st EV arrived at the charger (one part in the evening around 17:15) and the other before it leaves, are not changed because of the prediction of the other arrivals and because of the subsequent re-optimizations, the algorithm is updated about the real PV Generation and Load Demand data and the effect of Robust Optimization is reduced.

5.6 Summary & Conclusions

In Chapter 5, the arrival SOC, parking time, PV Generation & Load Demand have been studied individually in terms of impact on the optimality of the OSCD smart-charging algorithm results and ways of management. In subparagraph 5.6, the results of the various study cases investigated for every uncertainty are summarized and compared in order to enlighten the conclusions of the chapter.

Management of Uncertainties & Robust Optimization "Over-Conservativeness"

As already explained, the benchmark algorithm, which is normally developed to react and trigger re-optimizations upon new arrivals, has been evolved to predict future EV arrivals and utilize all (real and predicted) data in order charge efficiently the passing EV fleets. Furthermore, Robust Optimization has been used in the prediction sector of the P-C algorithm in order to manage the worst-case scenarios of the considered uncertainties. On that manner, when P-C algorithm predicts that the worst-case scenarios are going to happen regarding the future EVs, rushes the currently connected EVs charging in order to avoid potential unsatisfaction of the customers.

However, that may come at expense of deterioration of the objective (increase of the charging costs), since this rushed charging may be performed during more costly time periods in terms of energy price. Robust Optimization is characterized by the trade-off between "protection – overconservativeness" or "uncertainty tolerance – optimality", with the meaning that an over-protection against extreme case-scenarios considered can result in over-deterioration of the optimality of results. Therefore, the question is how much uncertainty we want to tolerate and how much conservative we want our solution to be.

In order to address this trade-off, the uncertainties are inserted only in the prediction part for the first set of the compared study cases. In the following Figs. 5.23 – 5.25, the charging costs (Grid Power Cost, Penalty Cost & Total Cost) of the "Home", "Semi-Public" & "Public" nodes respectively are

presented for the study cases of the "Benchmark Algorithm" and the "P-C Algorithm" when it predicts accurate forecasted data, 50% reduced future EV arrival SOCs, 50% reduced future EV parking times (25% by arrival & 25% by departure) & 50% reduced future EV parking times (50% by departure). Fig. 5.26 presents the corresponding unfinished charging gap for the 3 nodes for the aforementioned study cases. It must be noted again that, in this comparison, the uncertainties do not affect reality and they are only inserted in the prediction of the P-C version. The goal here is to enlighten firstly how much improved (efficient and successful) the EV charging is when prediction is added and secondly how much the optimality of results can be deteriorated, because of protection-preparation against potential uncertainties.

As it can be seen in all nodes, the P-C algorithm is capable of providing more efficient EV charging in terms of decreased charging costs or increased earnings, as it will be investigated more thoroughly in Chapter 7. It also provides better customer satisfaction, since the unfinished charging gap is lower in all nodes, as well (see Fig. 5.26). Therefore, it can be justified that prediction insertion in the algorithm is a useful tool for improved EV charging and it represents alone a first management mode of uncertainties. Observing the charging costs of the 3 nodes in Figs 5.23-5.25, it can be observed that the prediction of the worst-case scenario of 50% arrival SOC reduction slightly deteriorates the optimality of the charging cost in all nodes, however by simultaneously improving the unfinished charging gap as expected. This is caused by rushed EV charging that P-C algorithm performs in various EVs that are currently connected, when it predicts that the future EVs will arrive with more challenging requirements (higher requested energy). This consequently will generally improve the final unfinished charging gap, but rushed EV charging during time periods of higher energy price causes deterioration of the optimality of the charging costs.

However, regarding the related study cases of prediction of the worst-case scenario of 50% reduced parking time (either addressing arrival & departure or only departure), the results can be contradictory. For example, the 1st way of min parking time prediction (arrival & departure) does not practically provoke any changes (deterioration) of the charging costs at any of the 3 nodes. While it improves the unfinished charging gap at the Semi-Public Node, worse results can be seen at the other two nodes. The 2nd way of min parking time prediction (only departure) jeopardises the optimal charging costs only at the Semi-Public node and improves the unfinished gap only at the Public node.

As already explained, this abnormal behavior, regarding the min. parking time prediction results, is caused due to the fact that the EV arrivals & departures are directly connected with the way that receding horizon approach is implemented. The EV arrivals represent the main reason of re-optimizations triggering and the EV departures represent the endings of the set optimization horizons. A later future EV arrival prediction (or an earlier EV departure) can cause delay in the currently connected EVs charging instead of earlier charging, such as in the min. arrival SOC prediction study case. Consequently, this has a direct impact on the charging costs and the total charging gap. Nevertheless, the results mainly remain improved compared with the Benchmark study case and no penalty costs have been inflicted at any of the nodes.

Generally, it can be concluded that RO has nt resulted to be coservativeness regarding anyof the studied uncertainties. Especially for the "Home" node in Fig. 5.23, it can clearly be observed that the total cost of the node does not practically increase in any of the uncertainties' cases, in which RO is applied.

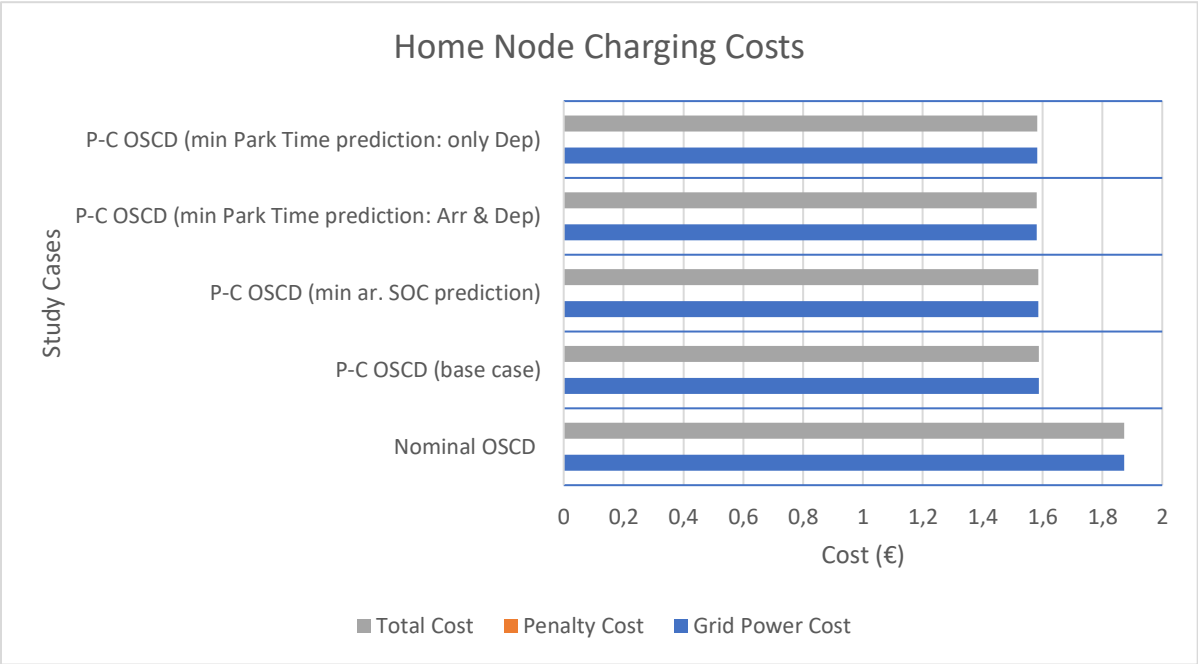

Fig. 5. 23: Home Node Charging Costs Comparison between "Benchmark-Nominal" & "P-C" (Uncertainties in Prediction) Study Cases

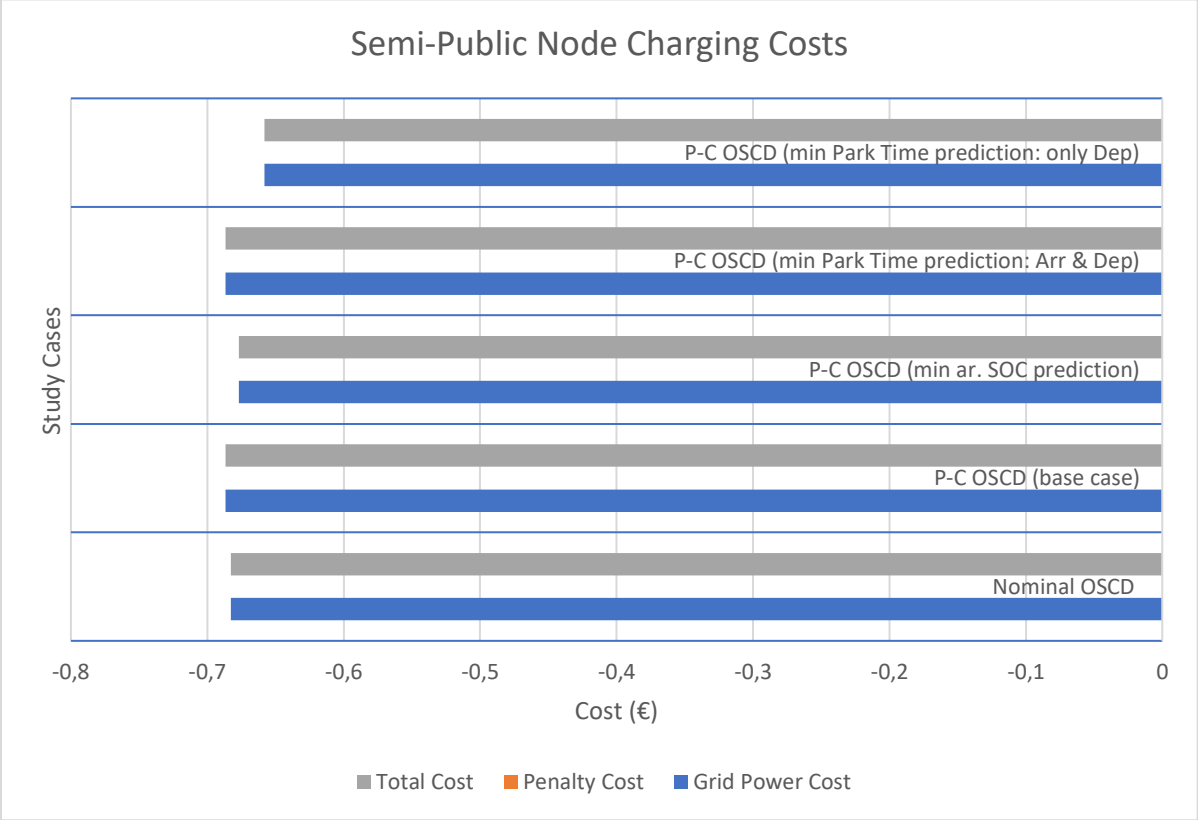

Fig. 5. 24: Semi-Public Node Charging Costs Comparison between "Benchmark-Nominal" & "P-C" (Uncertainties in Prediction) Study Cases

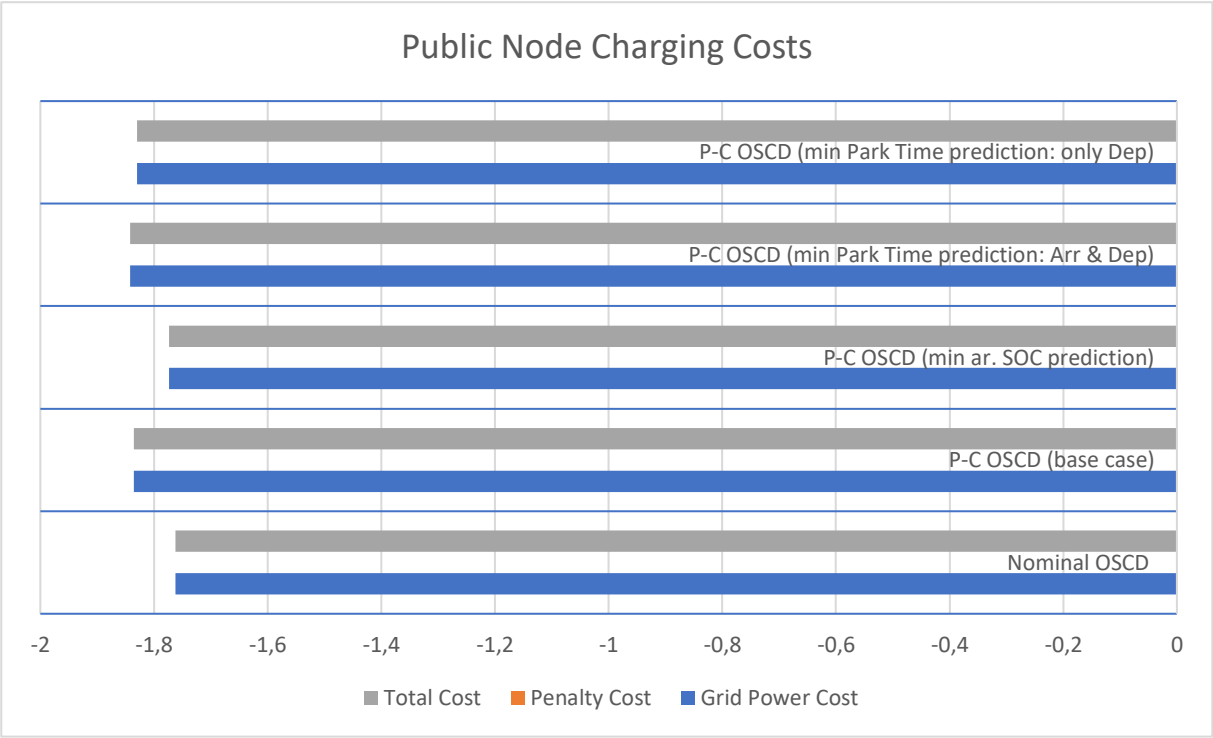

Fig. 5. 25: Public Node Charging Costs Comparison between "Benchmark-Nominal" & "P-C" (Uncertainties in Prediction) Study Cases

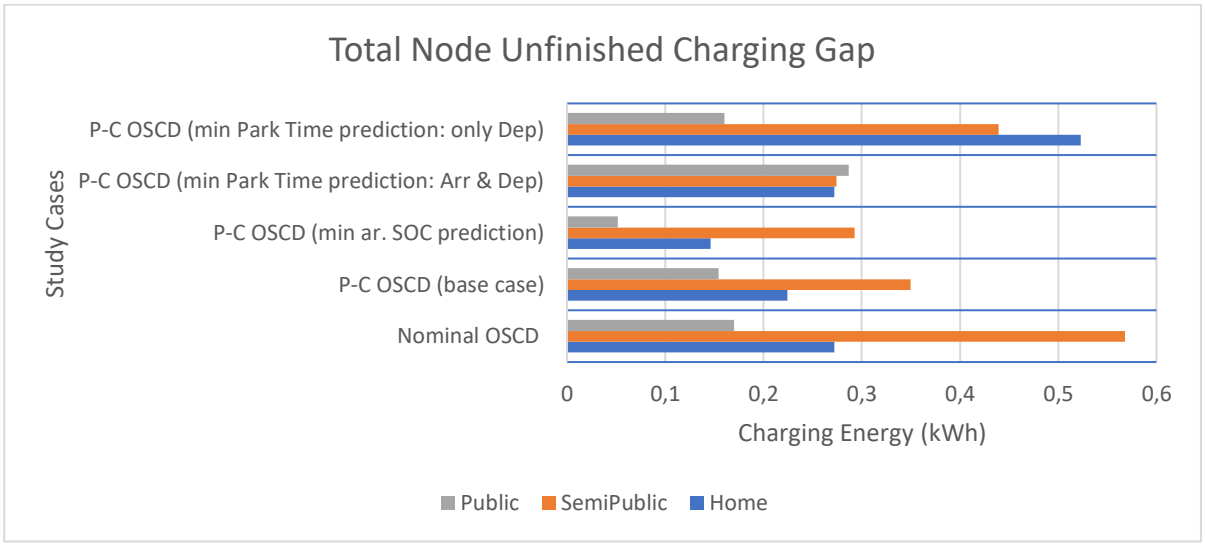

Fig. 5. 26: Total Node Unfinished Charging Gap Comparison between "Benchmark-Nominal" & "P-C" (Uncertainties in Prediction) Study Cases for Home, Semi-Public & Public Nodes

Impact of Uncertainties & Management with Robust Optimization

The second part of the paragraph summarizes the results of the study cases of every uncertainty, when uncertainty is integrated in both reality & prediction of the P-C algorithm. The main goal of this part is to address the behavior of the algorithm during real events of the uncertainties and their management by the "Prediction" feature of the P-C algorithm and the Robust Optimization. Moreover,

it aims to enlighten the impact of the uncertainties, integrating the corresponding results of the Nominal algorithm under the real worst-case scenarios events.

Arrival SOC & Parking Time Uncertainties

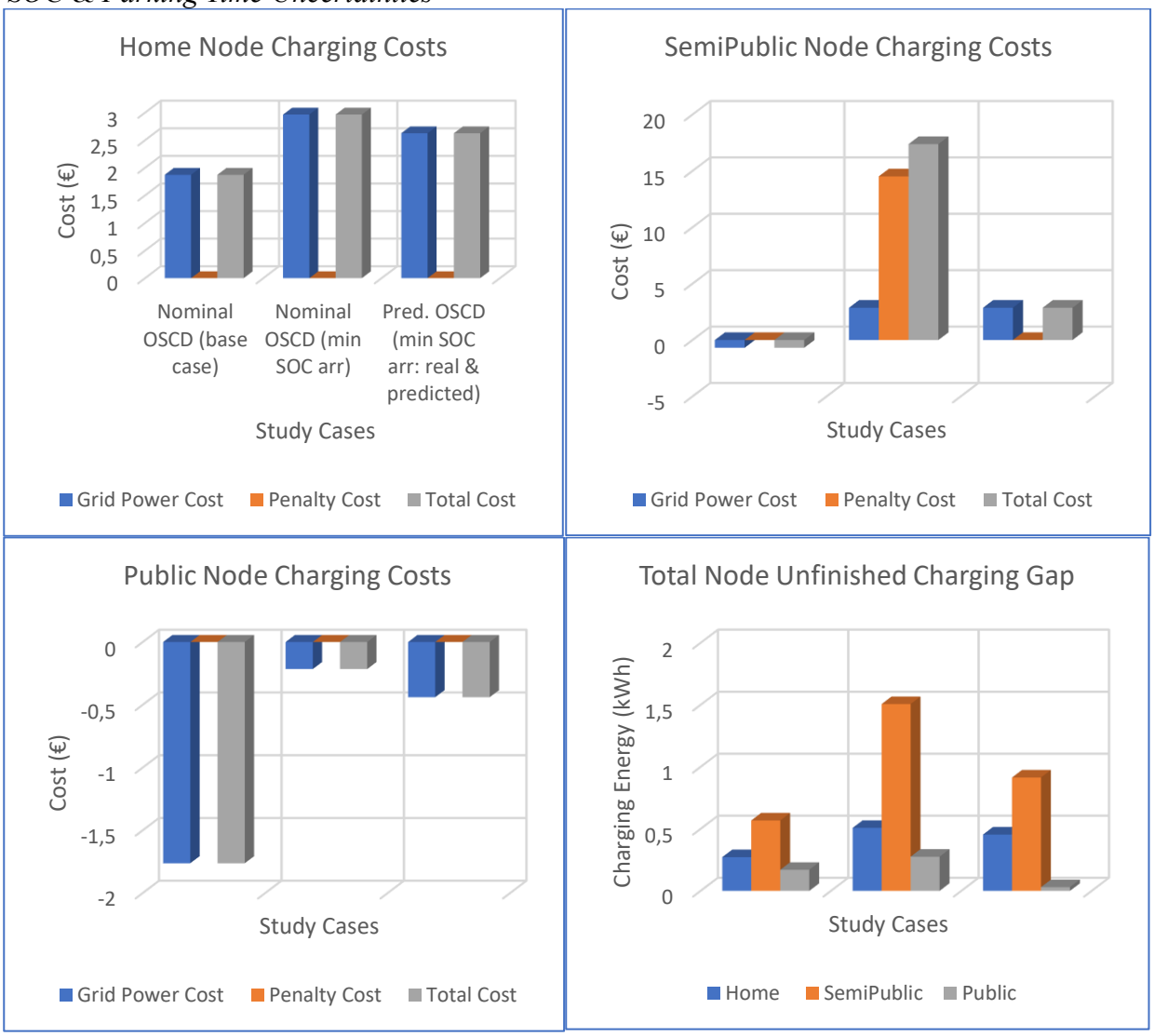

Fig. 5. 27: Summary of Charging Costs & Unfinished Charging Gap for "Nominal-Benchmark Algorithm", "Nominal-Benchmark Algorithm & min arrival SOCs" and "P-C Algorithm & min arrival SOCs" study cases

Figs 5.27 & 5.28 depict the summary of the results for the 3 Nodes for the arrival SOC & Parking Time uncertainties respectively for the following 3 study cases

- Benchmark Algorithm study case (left): no worst-case scenario of uncertainties is implemented here. It presents the charging cost and unfinished gap results in the base case of the benchmark algorithm, where all uncertainties are realized with the predicted value.
- Benchmark Algorithm study case with min arrival SOC or Parking Time (middle): This study case presents the results of the benchmark algorithm in the study case, where the considered uncertainty is realized with worst-case scenario values.
- P-C Algorithm study case with min arrival SOC or Parking time: real & predicted (right). This study case presents the results of the P-C Algorithm" in the study case, where the considered

uncertainty has been predicted and is actually realized with the worst-cases scenario values

The comparison of the first two study cases aims to reveal the impact of every uncertainty in the optimality results of the smart-charging algorithm, while the comparison of the last two uncertainties has the goal of revealing the capability of managing the uncertainty with the employment of the combination of the "Prediction feature" & "Robust Optimization". As it can be observed in Fig. 5.26, the realization of the worst-case scenario of the arrival SOC uncertainty has a serious in the charging costs in all 3 Nodes. It either increases highly the charging costs such as in Home & Semi-Public Nodes or decreases the earnings (Public Node). Moreover, penalty cost appears in the Semi-Public Node, in which the unfinished charging gap increases greatly as well (almost 1.5kWh). On the contrary, utilizing the Prediction feature of the P-C version and Robust Optimization succeeds in lowering the charging costs compared with the Benchmark case in all nodes, when uncertainty is realized. Moreover, Semi-Public does not receive a penalty cost, while a decrease in the total unfinished charging gap is observed everywhere.

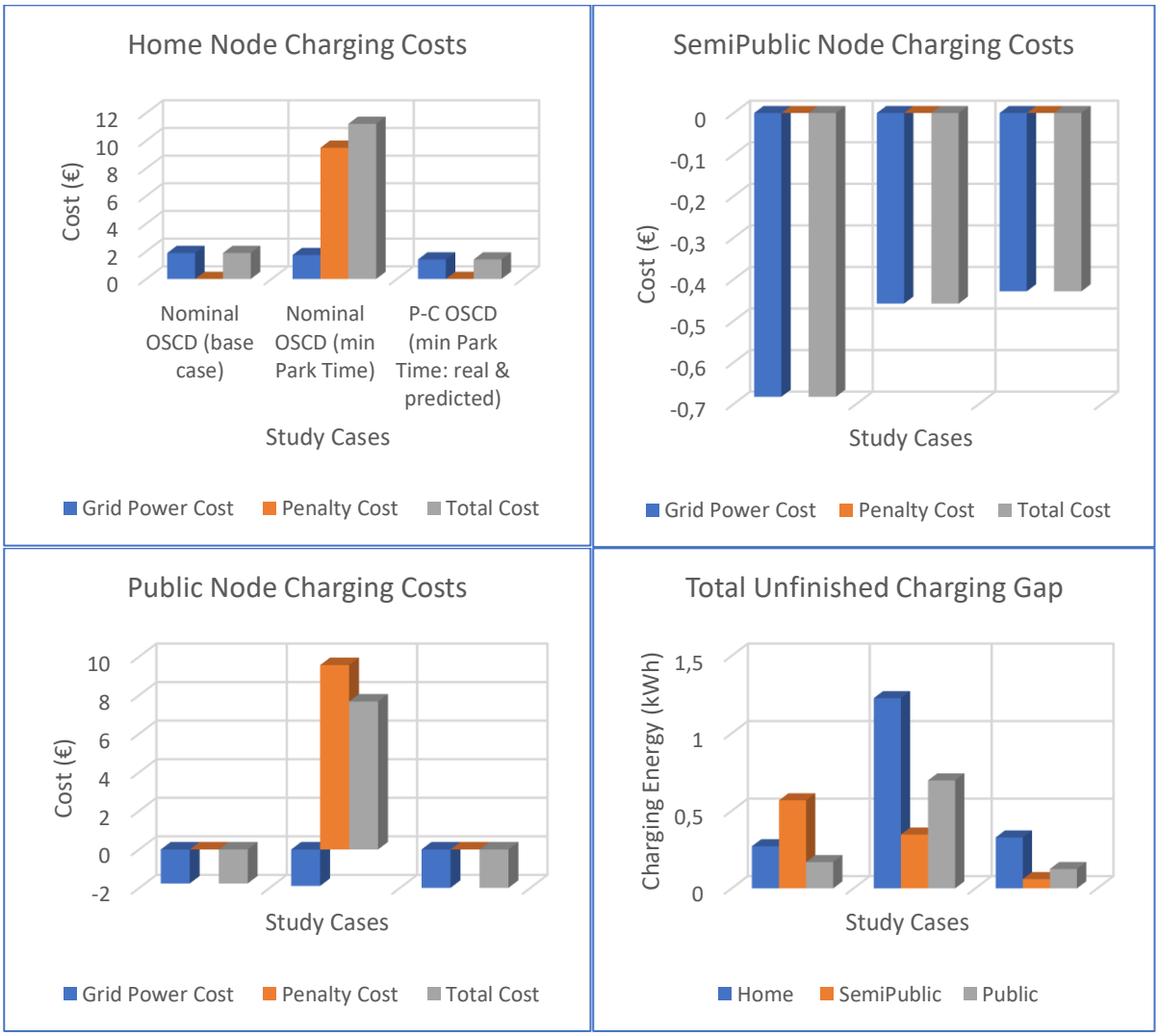

Fig. 5. 28: Summary of Charging Costs & Unfinished Charging Gap for "Nominal-Benchmark Algorithm", "Nominal-Benchmark Algorithm & min Parking Times" and "P-C Algorithm & min Parking Times" study cases

Similar results can be observed in Fig. 5.27 regarding the parking time uncertainty. The parking time uncertainty has a lower impact on the grid power cost than the arrival SOC uncertainty in all nodes, however it provokes penalty costs in both Home & Public Nodes, consequently majorly increasing the total charging cost of these 2 nodes. While the Semi-Public node shows a slight improvement of the charging gap compared with the Benchmark base-case, the parking time uncertainty generally increases the charging gap of the nodes as well. The insertion of "Prediction" and the employment of Robust Optimization does not cause an important improvement at the grid power cost, however they nullify the penalty costs, hence the total node costs highly decrease. Finally, the unfinished charging gap is improved for every node, comparing the "Benchmark" & "P-C" study cases.

PV Generation & Load Demand Uncertainties

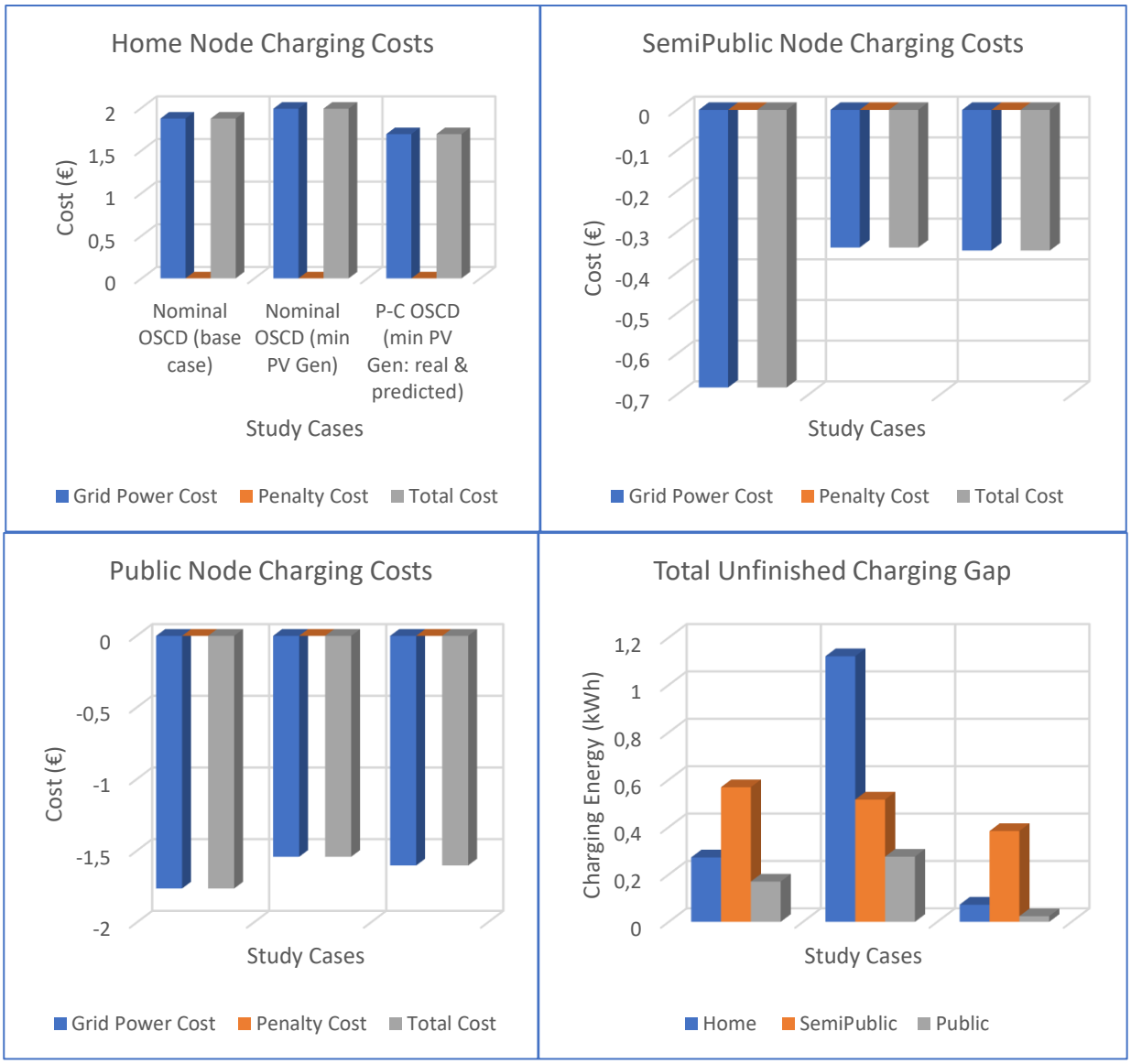

Fig. 5. 29: Summary of Charging Costs & Unfinished Charging Gap for "Nominal-Benchmark Algorithm", "Nominal-Benchmark Algorithm & min PV Generation" and "P-C Algorithm & min PV Generation" study cases

Figs. 5.29 & 5.30 depict the summary of the results for the 3 Nodes for PV generation & Load

Demand uncertainties for the same study cases such as the previous two uncertainties. The first case represents the base-case of the Benchmark Algorithm, the second one represents the realization of the uncertainty in the Benchmark Algorithm & the third one represents the corresponding realization in the P-C Algorithm, when it has been predicted. It can be clearly observed that both PV Generation & Load Demand Uncertainties deteriorate the charging costs of the Benchmark Algorithm, either increasing the costs at Home Node or decreasing the earnings at Semi-Public & Public Nodes.

However, they do not inflict penalty costs at any of the 3 Nodes. This can be justified by the fact that these two uncertainties are directly connected more with the grid power exchange cost & and less with the charging time periods and the decision about when the EVs should be charged. Therefore, they have less impact on the satisfaction of the customers and penalty costs, such as the arrival SOC and Parking Time uncertainties. Moreover, while we can see an important increase of the charging gap at the Home Node when PV Generation considered, the opposite is observed for the Semi-Public Node.

Regarding the comparison between the Benchmark & the P-C algorithms, the charging costs of the Home & Public Nodes are improved in the P-C Algorithm for both PV generation and Load Demand uncertainties. Penalty Costs remain zero in the P-C study case as well, while the unfinished charging gap is reduced for all 3 Nodes in both uncertainties

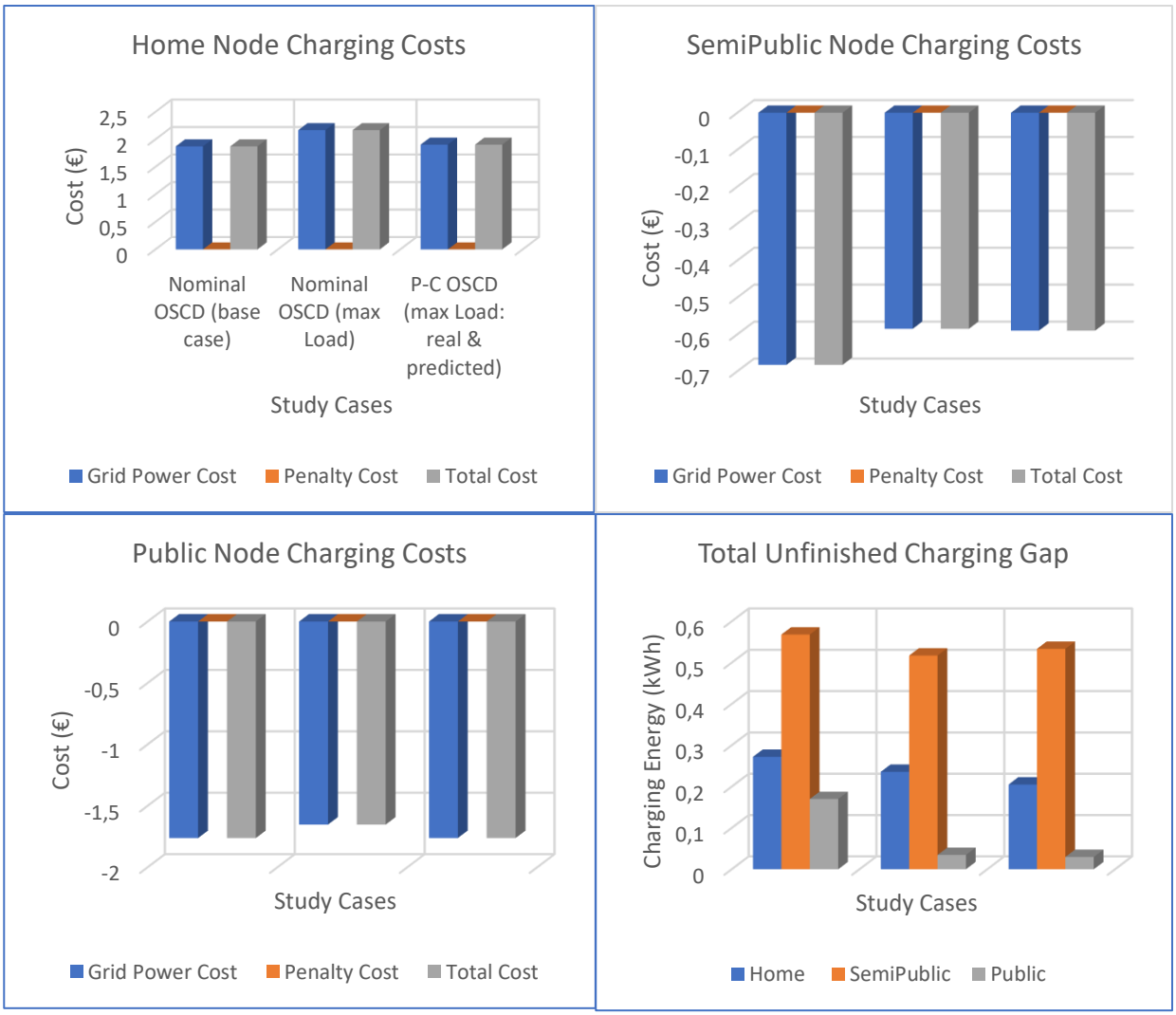

Fig. 5. 30: Summary of Charging Costs & Unfinished Charging Gap for "Nominal-Benchmark Algorithm", "Nominal-Benchmark Algorithm & max Load Demand" and "P-C Algorithm & max Load Demand" study case

Taking everything into considerations, the conclusions of this chapter can be summarized as follows:

Regarding Benchmark & P-C Algorithms

- More efficient EV charging when OSCD knows about future arrivals
- Improvement if the charging costs & the unfinished charging gap when prediction used
- Earlier EV charging of EVs, that initiate Prediction-based Horizons

Regarding use of Robust Optimization in the Prediction part of the P-C Algorithm

- Even earlier charging of EVs, that initiate Prediction-based Horizons and improvement of the unfinished charging gap for arr. SOC uncertainty
- Use of Robust Optimization with Parking Time Uncertainty in the prediction part can provide contradictory results regarding the costs and the charging gap and abnormal behavior (delayed instead of earlier charging), but penalty costs still remain zero
- Not significant increase of charging costs due to "over-conservative prediction"

Regarding Impact of Uncertainties & their Management by RO & P-C Algorithm

- Arrival SOC & Parking Time Uncertainties have a major impact on the unfinished charging gap and inflicted penalty costs at the nodes for the Benchmark Algorithm. The optimality of the charging cost results is deteriorated as well.
- PV Generation & Load Demand have a greater impact on the grid power costs of the nodes, but they do not inflict penalty costs at the Benchmark version and they do not change significantly the charging gap.
- P-C Algorithm succeeds in improving the grid power costs at most of the nodes for all uncertainties, while simultaneously nullifying potential penalty costs that appear at the Benchmark OSCD algorithm. The unfinished charging gap is generally improved as well.
- EVs involved in longer optimization horizons are charged earlier by the P-C Algorithm when PV Generation and Load Demand Uncertainties considered. While EVs normally charged during late hours are not highly affected by PV generation, they are affected by Load Demand.

Chapter 6: Study Cases & Results of the FCR Reserves uncertainty management

Regarding FCR reserves uncertainty, the investigation has been divided into two separate sub-studies. Considering the 1st part of investigation in paragraph 6.1, an ideal study case has been investigated, in which the called FCR Reserves are exactly equal to the expected FCR reserves of the optimizer. This study represents an ideal scenario with no uncertainty considered, which intends to show the functionality of the provision model. In paragraph 6.2, the FCR reserves provision model has been tested for more "realistic" study cases, addressing the "real" impact of the particular uncertainty and its potential management by RO.

6.1 Ideal Study Case: "Called" FCR Reserves equal to "Expected" FCR Reserves (Base Case)

In this paragraph, the results of a 1st "ideal" study case are summarized. This 1st investigation part integrates the 1st study case, according to which, the Called up and down FCR Reserves by the TSO, simulated by "reality" entity in the smart-charging algorithm, are equal to the expected FCR Reserves, which are utilized in the optimization in order to provide the offered Reserves. More particularly, the new robust and more "realistic" version of the smart-charging algorithm, which distinguishes the natural and offered Reserves in the bidding market and utilizes Robust Optimization to take into consideration the expected Reserves has been applied to both the Benchmark Algorithm and the Prediction-Capable Algorithm. For the 1st study case, the actually called Regulation Reserves have been set equal to the expected Reserves for both algorithms to evaluate the new reserves provision concept together with the prediction capability added to the benchmark algorithm in the previous chapters. While Figs. 6.1 – 6.3 depict the difference of the Up and Down natural, offered & expected Regulation Reserves of the "Home", "Semipublic" & "Public" nodes respectively regarding the benchmark algorithm, Figs. 6.4 – 6.6 depict the relative information regarding the P-C algorithm. Up and Down Regulation Reserves have been distinguished into two subgraphs in the figures in order to increase clarity.

As we can see in most figures, the natural and offered FCR reserves do not highly deviate, while their difference can be practically observed in Figs. 6.1 & 6.4, which represent the behavior of the "Home Node" in the benchmark and P-C Algorithm respectively. The total expected up and down regulation reserves, which in this study case have been assumed to be actually called by the TSO, constitute only a fragment of the offered reserves in the bidding market. However, at every timestep such as in reality, only a part or the whole amount of "offered" reserves can be "called".

Moreover, as it can be seen in these figures, the "Home Node" chooses to expect mostly called Down Regulation Reserves by the TSO. In comparison, the "Semi-Public Node" expects mostly called Up Regulation Reserves in both benchmark and P-C algorithms (Figs 6.2 & 6.5 respectively), whereas it offers more Down than Up Regulation Reserves in the bidding market. Finally, regarding "Public Node" in Figs. 6.3 & 6.6, offered and called Up & Down Regulation Reserves are more balanced. However, it must be noted, that both algorithms choose to expect total call of the offered Up Regulation Reserves, while only parts of the offered Down FCR reserves are expected to be called at most timesteps.

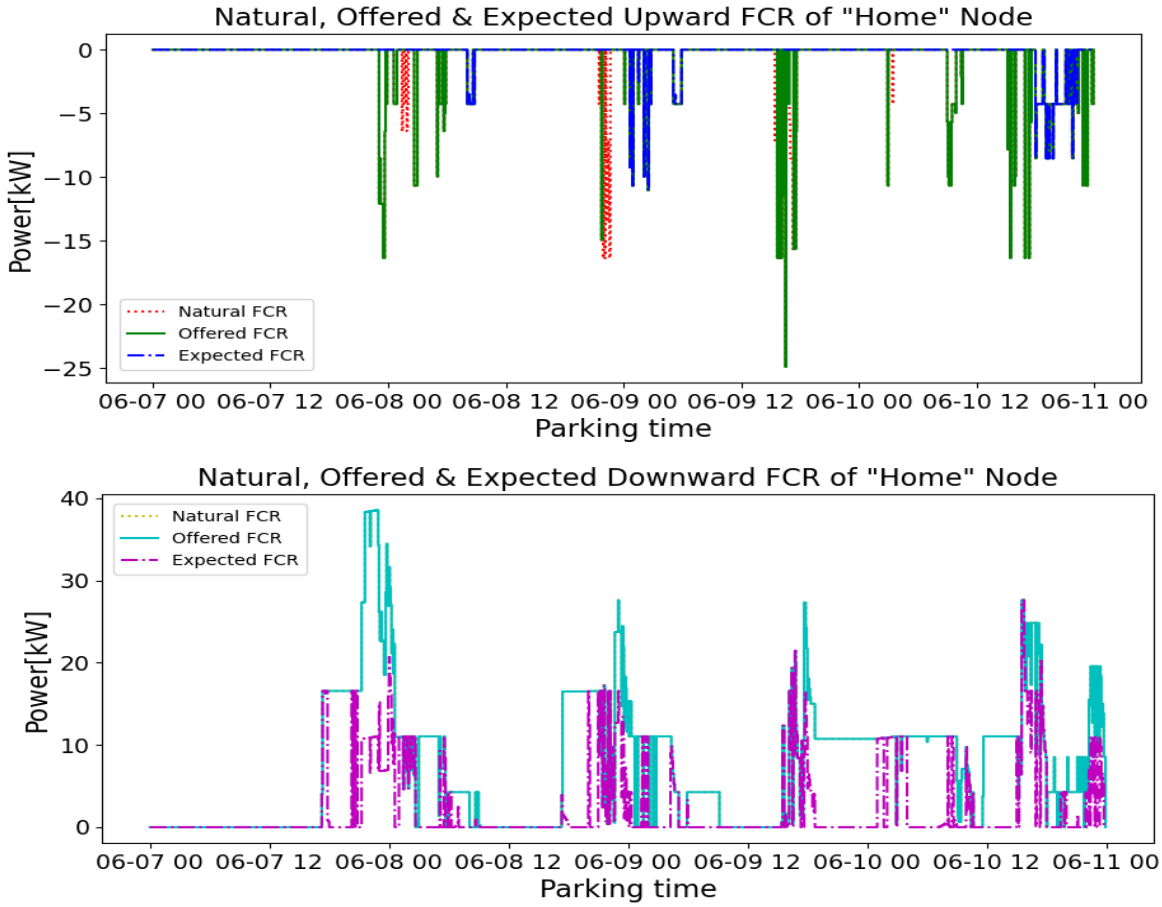

Fig. 6. 1: “Natural”, “Offered” & “Expected” Up FCR Reserves Provision of “Home Node” in Benchmark Algorithm

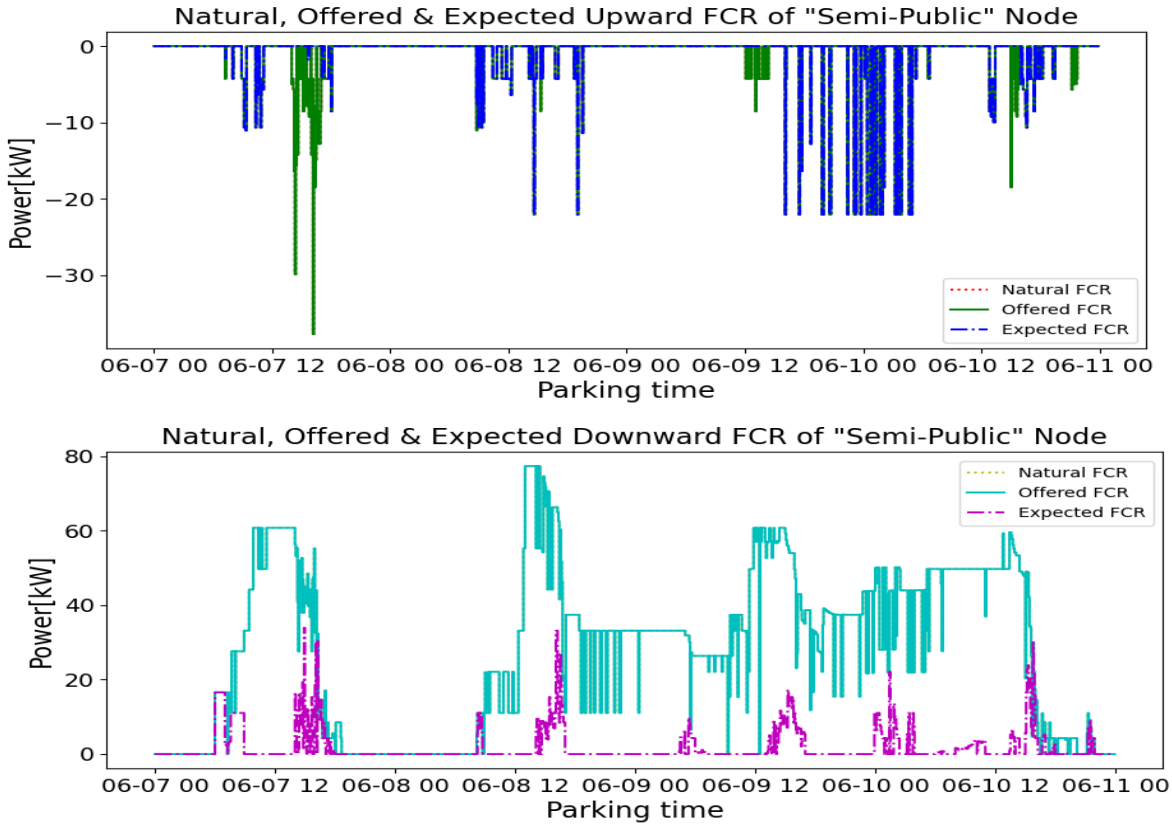

Fig. 6. 2: "Natural", "Offered" & "Expected" Up FCR Reserves Provision of "Semi-Public Node" in Benchmark Algorithm

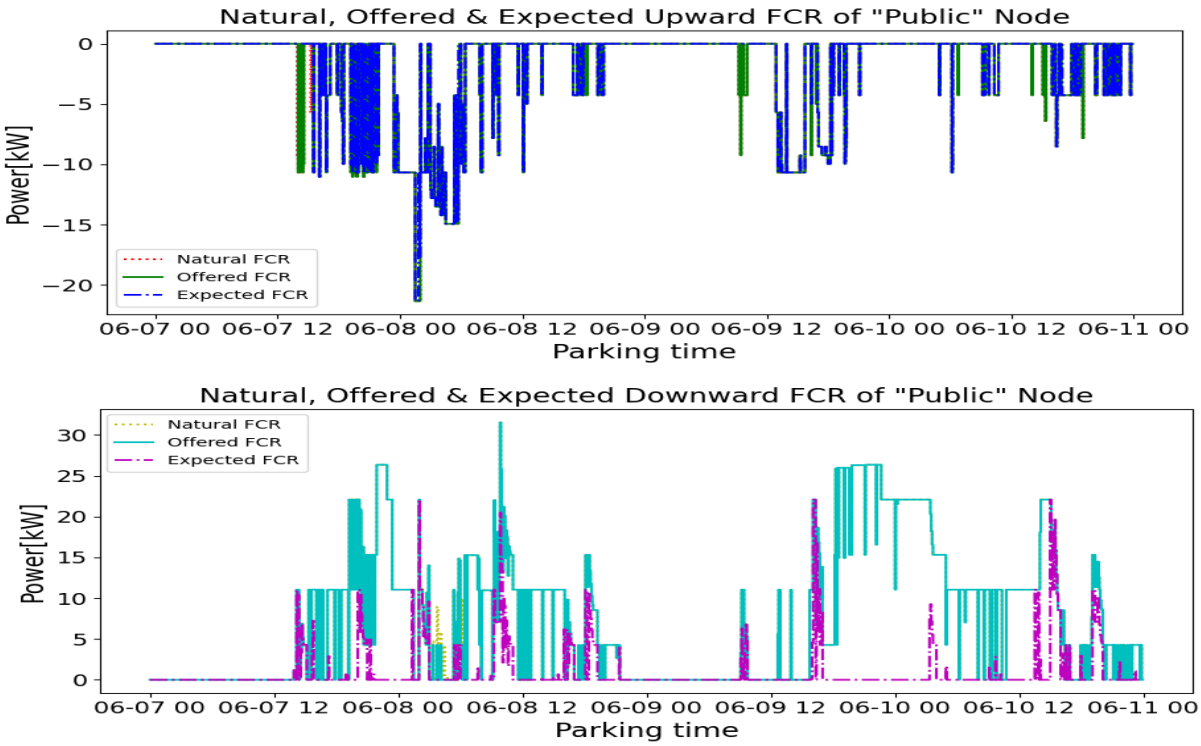

Fig. 6. 3: "Natural", "Offered" & "Expected" Up FCR Reserves Provision of "Public Node" in Benchmark Algorithm

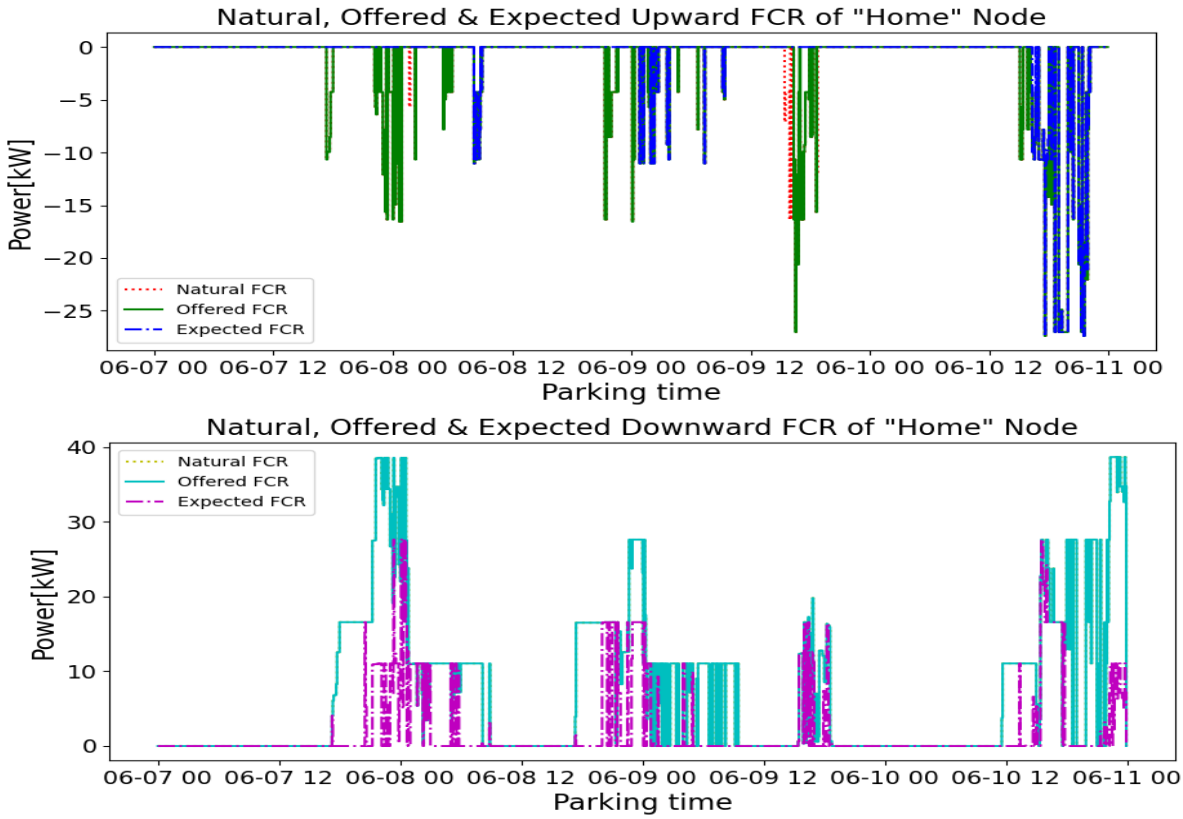

Fig. 6. 4: "Natural", "Offered" & "Expected" Up FCR Reserves Provision of "Home Node" in P-C Algorithm

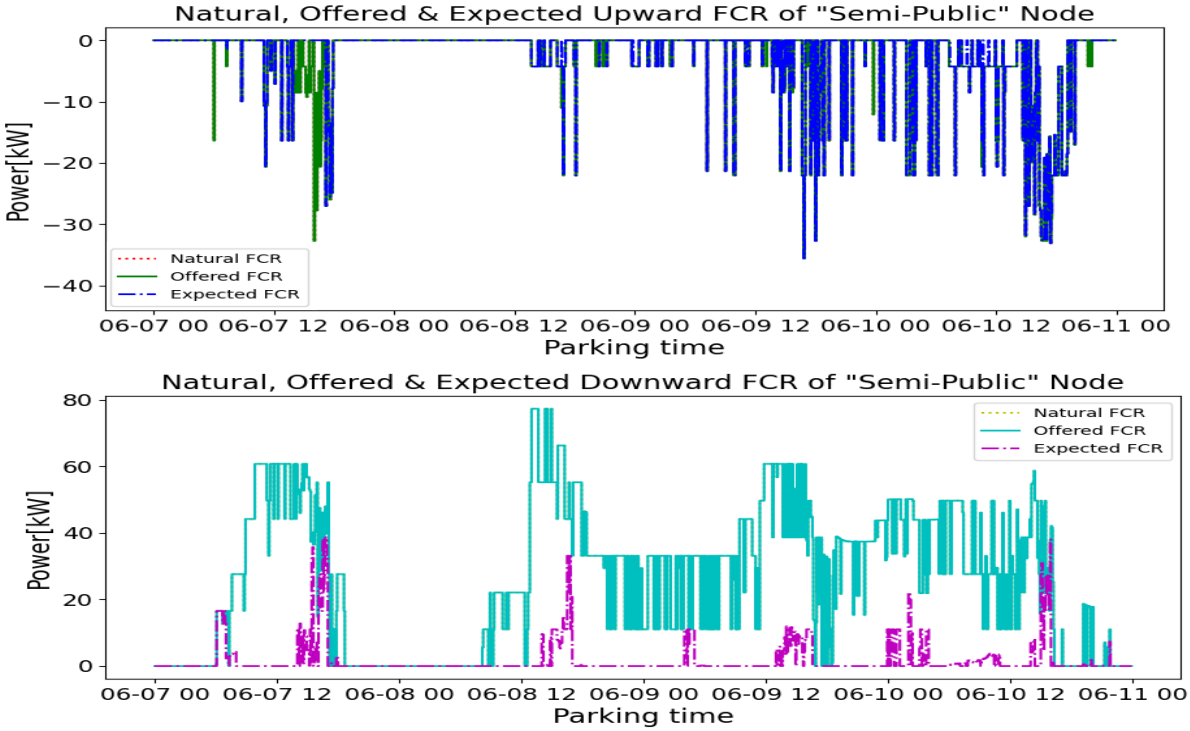

Fig. 6. 5: "Natural", "Offered" & "Expected" Up FCR Reserves Provision of "Semi-Public Node" in P-C Algorithm

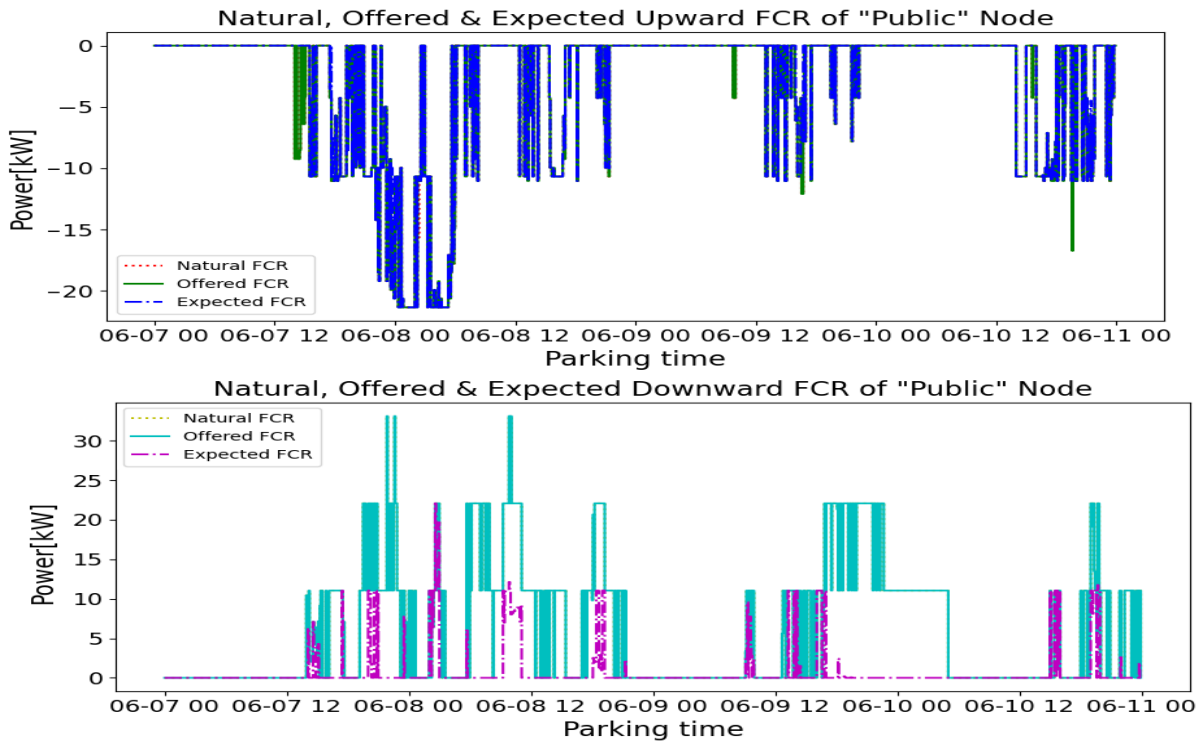

Fig. 6. 6: "Natural", "Offered" & "Expected" Up FCR Reserves Provision of "Public Node" in P-C Algorithm

Summary of Results of 1st Investigation Study of FCR Reserves Provision

For the summary of results of the "ideal" study case and the extraction of the relative conclusions, the investigation has been divided into comparisons between the improvement of the benchmark and the P-C algorithms in contrast with their basic versions and between their "improved" versions, as well.

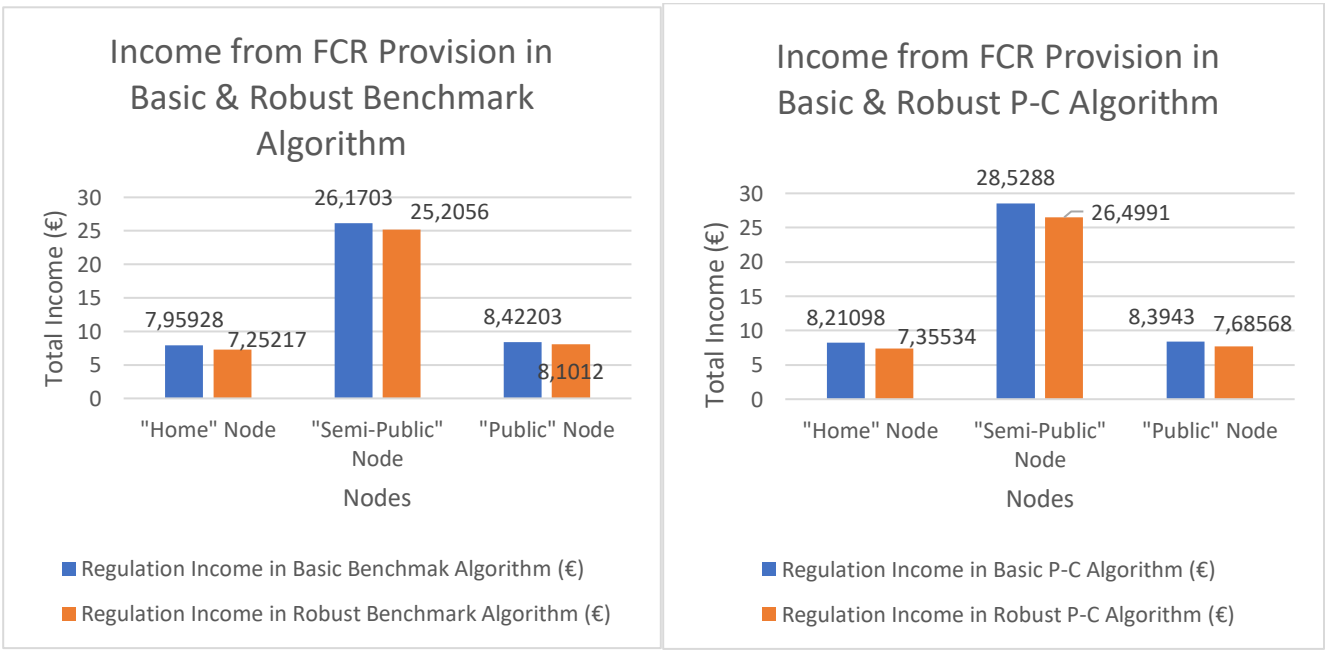

Fig. 6. 7: Comparison of Regulation Income of Basic & Robust Benchmark and P-C Algorithms at all nodes

Fig. 6.7 depicts the difference in regulation income due to the improvement in both benchmark & P-C algorithms in all 3 nodes. As expected, the distinction of offered from natural FCR reserves and the integration of Robust Optimization employment regarding expected reserves, decreases the regulation income in all 6 cases (3 nodes in benchmark and P-C algorithms). This is justified, on the one hand, by the fact that both algorithms are no longer remunerated by the ideal natural reserves, that they can ideally provide to the TSO. Moreover, expected called FCR reserves, which constitute a fragment of the participated reserves in the bidding market and are derived by applying Robust Optimization, affect the "Power Balance" & "EVs' SOCs" equations and force the algorithms to offer less FCR reserves and therefore receive less remuneration.

The aforementioned behavior can be also observed in Fig. 6.8, which depicts the reduction of the offered Regulation Reserves in both Algorithms. As it can be seen, there is a notable reduction of the offered sum of up and down reserves at all nodes, especially at "Home Node", at which reduction reaches up to 8.8% & 10.42% for benchmark and P-C algorithms respectively. It must be noted that at all nodes, there is a higher reduction of offered FCR reserves for the P-C algorithm than for the Benchmark algorithm. However, in almost all cases, the P-C algorithm receives higher remuneration than the benchmark algorithm, as it can be seen in Fig. 6.7. This can be justified by the fact that the P-C algorithm, predicting the future EV arrivals & departures, focuses more on the EV charging and focuses more on the "right" time to "offer" FCR reserves in the bidding market, therefore it receives equal or higher remuneration, even if Robust Optimization provokes it to reduce the "offered" amount.

Finally, Fig. 6.9 compares the "offered" and "not offered" natural Regulation Reserves in the latest versions of the Benchmark & P-C algorithms. Therefore, it actually provides information about the percentage of the natural reserves that has been actually offered in the bidding market for both algorithms. "Not offered" reserves are defined as the amount of natural reserves that is not offered to the bidding market, therefore "not offered" reserves are calculated by the subtraction of the offered reserves from the natural reserves in the Benchmark and P-C algorithms. As it can be seen in the left subplot, P-C algorithm is generally in position to offer more Up and Down Regulation Reserves than the benchmark algorithm. Especially at the "Semi-Public" Node, the offered sum of Up and Down FCR reserves reach 34966kW, almost 1707kW more than the corresponding FCR provision amount for the Benchmark Algorithm. However, the most notable feature can be observed in the right subgraph. The P-C algorithm, equipped with the prediction feature, is capable of offering in the bidding market most of the "natural" reserves that can ideally provide. On the contrary, while the benchmark algorithm achieves also minimum "not-offered" FCR reserves at "Public" & "Semi-Public" nodes, there is an amount of approximately 244 kW of "natural" reserves that do not participate in the bidding market. The corresponding amount of "dumped" natural reserves for the P-C algorithm at the "Home Node" is 73kW, approximately only the one third.

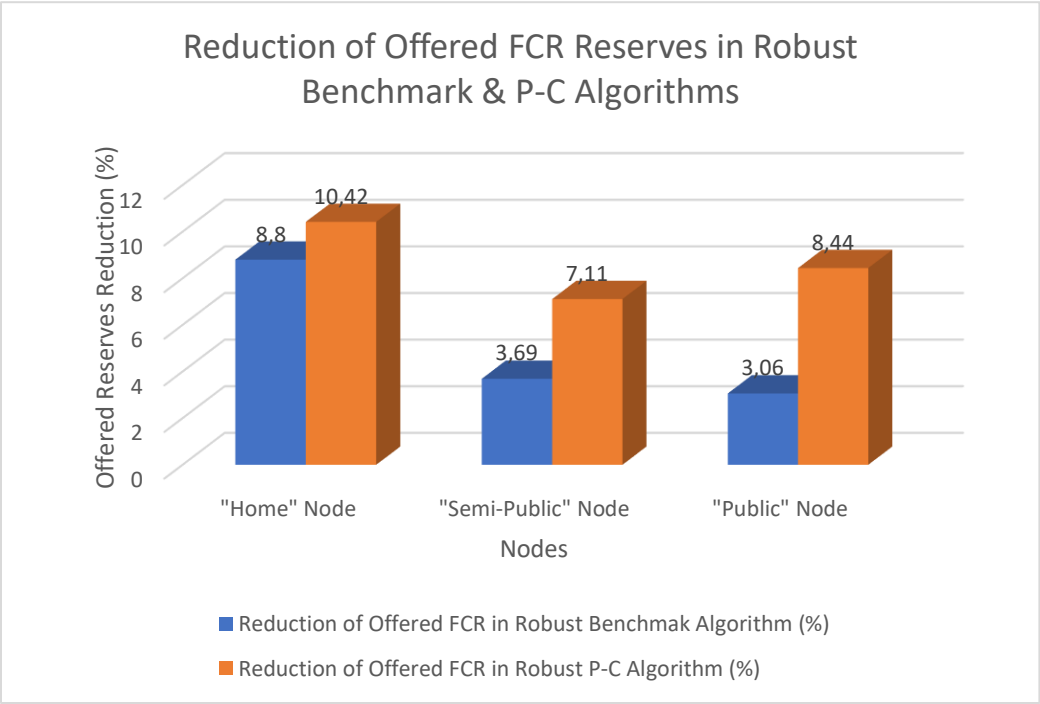

Fig. 6. 8: Comparison of Reduction of Offered Regulation Reserves of Basic & P-C Algorithms between Basic & Robust versions at all nodes

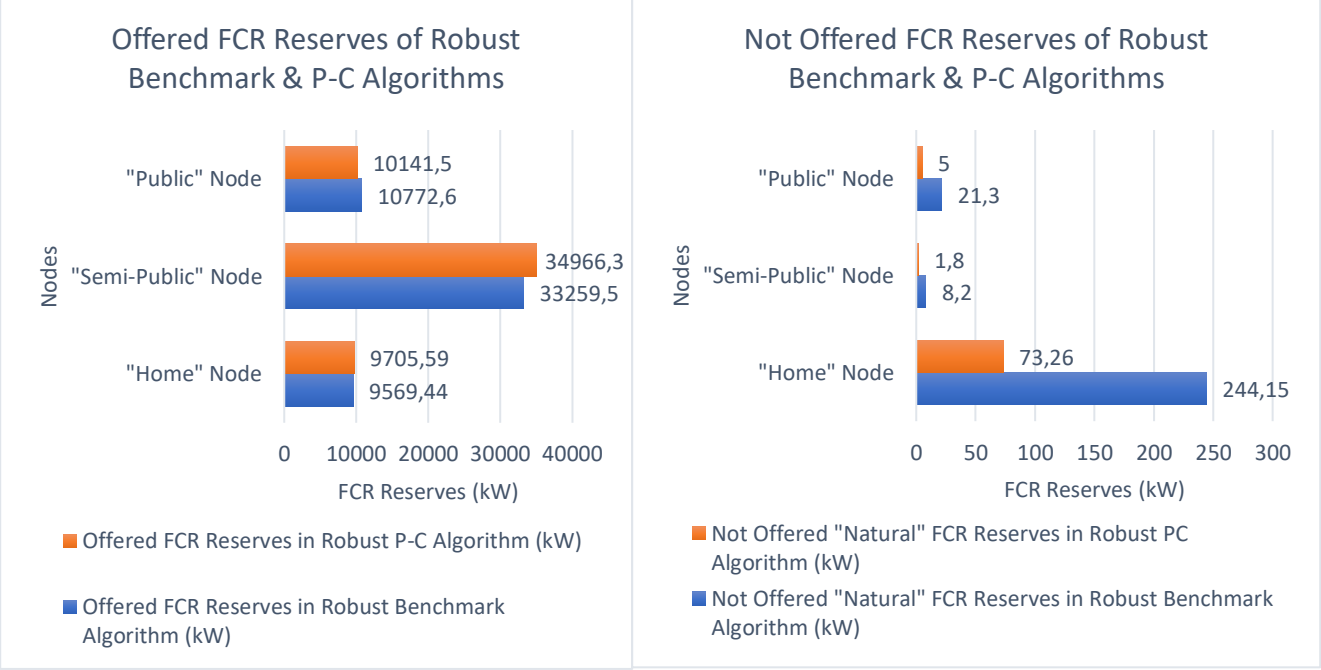

Fig. 6. 9: "Offered" & "Not-offered" Natural Regulation Reserves of Robust Benchmark & P-C Algorithms at all nodes

6.2 "Realistic" Study Cases: "Called" FCR Reserves different than "Expected" FCR Reserves (Base Case)

The 1st part of investigation serves as a base case study, representing an ideal scenario where the called FCR Reserves by the TSO are equal to the "expected" FCR Reserves of the algorithm, hence a study case with no uncertainty. However, the FCR provisions model should be investigated with a more realistic scenario for the evaluation of its functionality, because in reality the "called" reserves will never be equal to the "expected" reserves. The actually called FCR capacity by the TSO is always an uncertain parameter that must be taken into account for a robust and optimized smart-charging and FCR provision model. The expected FCR capacity, which is formulated as a Robust Optimization Constraint, serves as a "tool" of robustness and FCR uncertainty management, which helps the smart-charging algorithm to schedule robustly the EV charging, being prepared for potential "called" reserves within the optimization horizon.

Considering the "ENTSO-E Transparency Platform" database [103] in terms of accepted ("offered") and activated ("called") FCR reserves in the Netherlands for the summer time duration from 7-6-2021 to 10-6-2021, the following observations have been made and taken into account:

- The offered Up FCR reserves are called with 34% probability and by 5,35% magnitude
- The offered Down FCR reserves are called with 30,3% probability and by 1,27% magnitude
- The offered Down reserves are 3-4 times higher than the offered Up reserves while the called Down reserves are approximately half of the called Up reserves

It must be noted that in order to integrate more optimally the ENTSO-E data, the expected up FCR reserves are distinguished from the expected down FCR reserves in the optimizer, since it is obvious that up and down regulation reserves follow different patterns. Therefore, each one of the equations (117) & (118), which set the RO uncertainty set of the expected reserves, has been divided to two distinguished equations, which dictate the expected up and down reserves in terms of the offered up and down reserves, respectively.

Continuing the investigation on a same manner, such as in the previous chapters, the following 3 study cases have been formulated in order to show the impact of FCR reserves uncertainty and the possible management of it with the aid of Robust Optimization, for the "realistic" investigation part. Moreover, all 3 study cases have been investigated for both the benchmark and the Prediction-Capable Smart-Charging Algorithms in order to evaluate the contribution of the "prediction" feature to the algorithm performance.

1) Base Case – "Reality" Case: Expected Up and Down Reserves have been set in the intervals (5.35%, 10%) & (1.3%, 2.5%) respectively of the corresponding offered reserves. Probability of the "called" Up and Down Reserves has been set at 33% while an average 15.5% and 4.5% magnitude percentage has been selected for up and down FCR respectively. This low-expected – low-called FCR study case represents reality and serves as a base case, which shows the scheduling of EV charging with robust management of the FCR uncertainty
2) "Worst-Scenario" Study Case: In this study case, the "called" reserves have been increased unrealistically to 50% probability and 50% magnitude for both up and down reserves, while expected reserves remained the same as in the base case. This study case aims to reveal the impact of the FCR uncertainty and the potential deterioration of results in terms of charging gap and regulation income, in case of wrong (zero or too low) expectation.
3) "Robust" Study Case: In the third and final study case, expected up and down reserves have been both set at 25-30% while the called reserves have remained as in the base case. This study case aims to show a more "robust" smart-charging performance, in which the algorithm expects more

reserves to be called than what it actually happens. While this formulation is expected to perform a more "robust – uncertainty managed" EV charging, possible deterioration of optimal charging cost may be observed at expense of robustness.

Finally, it has been observed that expected down FCR reserves in equations (109) – (111), which represent the SOC and Power Balance equations, provoke huge unfinished charging gaps and cost penalties. This is justified by the fact that the utilization of expected down FCR reserves for EV charging represents a very good scenario, since it helps the algorithm to charge the EV fleets without paying for imported power. In contrast, the algorithm chooses to schedule EV charging utilizing all down reserves allowed in order to charge and simultaneously receive remuneration. However, since the actually "called" down FCR reserves by the TSO in the algorithm's "reality" module are highly lower, the EVs are left uncharged and the optimized smart-charging fails. Therefore, the expected down reserves are excluded from the aforementioned equations.

Summary of Results of 2nd Investigation Part of FCR Reserves Provision

In Figs. 6.10 – 6.12, the results of the 2nd part of investigation of the FCR reserves provision are summarized. Fig. 6.10 depicts the performance of the Benchmark Algorithm (blue color) and Prediction-Capable Algorithm (orange color) during the 3 study cases in terms of total unfinished charging gap of the 3 nodes ("Home", "Semi-Public", "Public"). As it can be observed, the Prediction-Capable Algorithm performs EV charging with lower charging gap than the "Benchmark" Algorithm at all study cases. Moreover, the charging gap decreases in the "Robust" study case due to higher expectations of the Algorithm by the RO constraint, which forces, on the one hand, a rushed – more robust charging and on the other hand, lower FCR offer to the bidding market and more focus on the satisfaction of the customer. Finally, high charging gaps appear in the "worst scenario" study case especially for the Benchmark algorithm that reach a total 10,21 kWh uncharged energy, but for the Prediction-Capable as well.

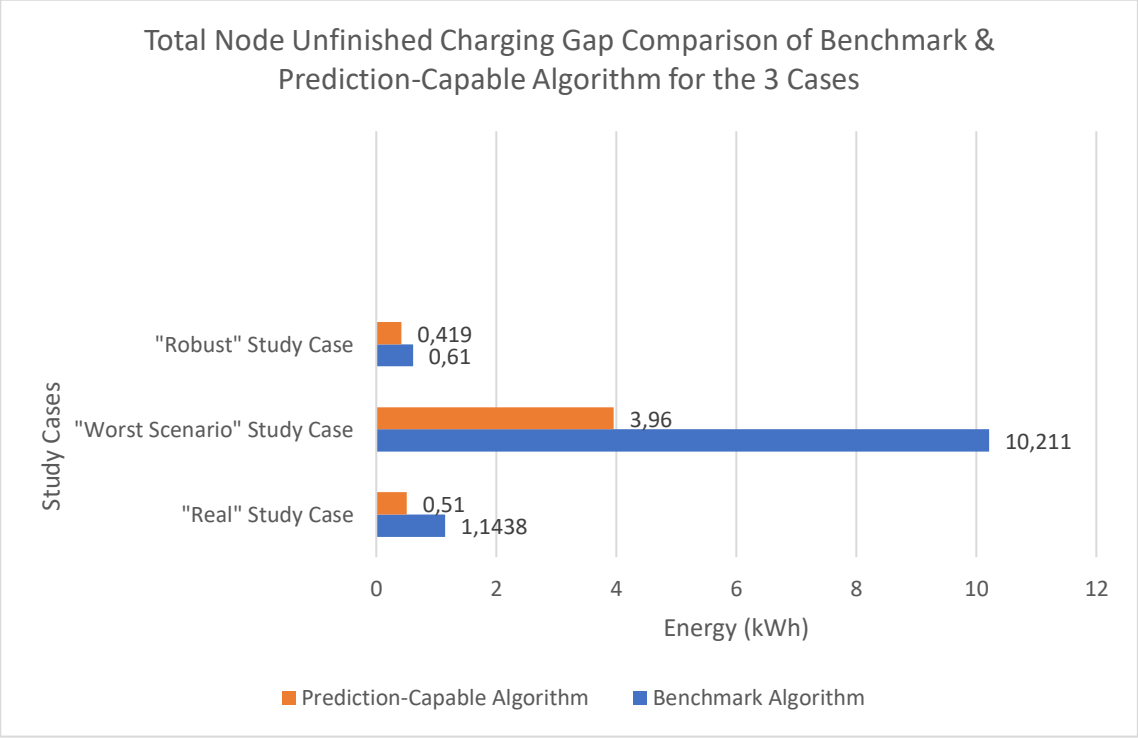

Fig. 6. 10: Total Unfinished Charging Gap of Benchmark and Prediction-Capable Algorithms at "Real", "Worst-Scenario" & "Robust" Study Cases

Fig. 6.11 shows the corresponding comparison of the two algorithms in terms of penalty cost and regulation income. Regarding penalty cost, it can be observed that no penalty cost appears in both algorithms in "Real" and "Robust" study cases. However, in the "Worst-scenario" study case, due to the high charging gaps that have appeared, high penalty costs are inflicted to the Benchmark and Prediction-Capable Algorithms that reach 64,83 & 155,57 € respectively.

Regarding regulation income, "Worst Scenario" study case does not affect it in both algorithms, while "Robust" case slightly decreases it. This is due to the fact, that the regulation income is directly connected with the remunerated offered FCR reserves. In "Real" & "Worst" cases, the expected reserves are the same (low) so the offered reserves remain at the same level. In "Robust" Case, in which expected reserves are increased, the algorithm decreases the offered reserves in order to suppress indirectly the expected reserves as well and focus more on the sufficient charging of the EV fleets. In other words, the algorithm offers less FCR when it expects high levels of FCR in order to be more flexible and capable of robustly and sufficiently charging the EV fleets, therefore it is remunerated less. Finally, one interesting observation that can be made in Fig. 6.11 is that the Benchmark Algorithm has always a slightly higher regulation income than the Prediction-Capable Algorithm, which is due to the fact that it offers higher level of up and down FCR, such as it can be seen in Fig. 6.12. This is probably justified by the fact that the "Prediction-Capable" Algorithm uses longer optimization horizons due to the predicted EV arrivals. Predicting that EVs are going to arrive, focuses more on charging the currently connected EVs sufficiently (with lower charging gap) than on offering FCR reserves. Moreover, the use of longer optimization horizons may cause delay of FCR offer afterwards within the horizon, which delay is constantly transferred to the next horizon due to the constant re-optimizations. Furthermore, as already explained, "Robust" case decreases the offered FCR reserves, however this can be seen only for the up FCR, because the up expected reserves jeopardize highly the successful EV charging (the algorithm needs to save energy to provide to the grid for ancillary services, which could have been used to charge the EVs).

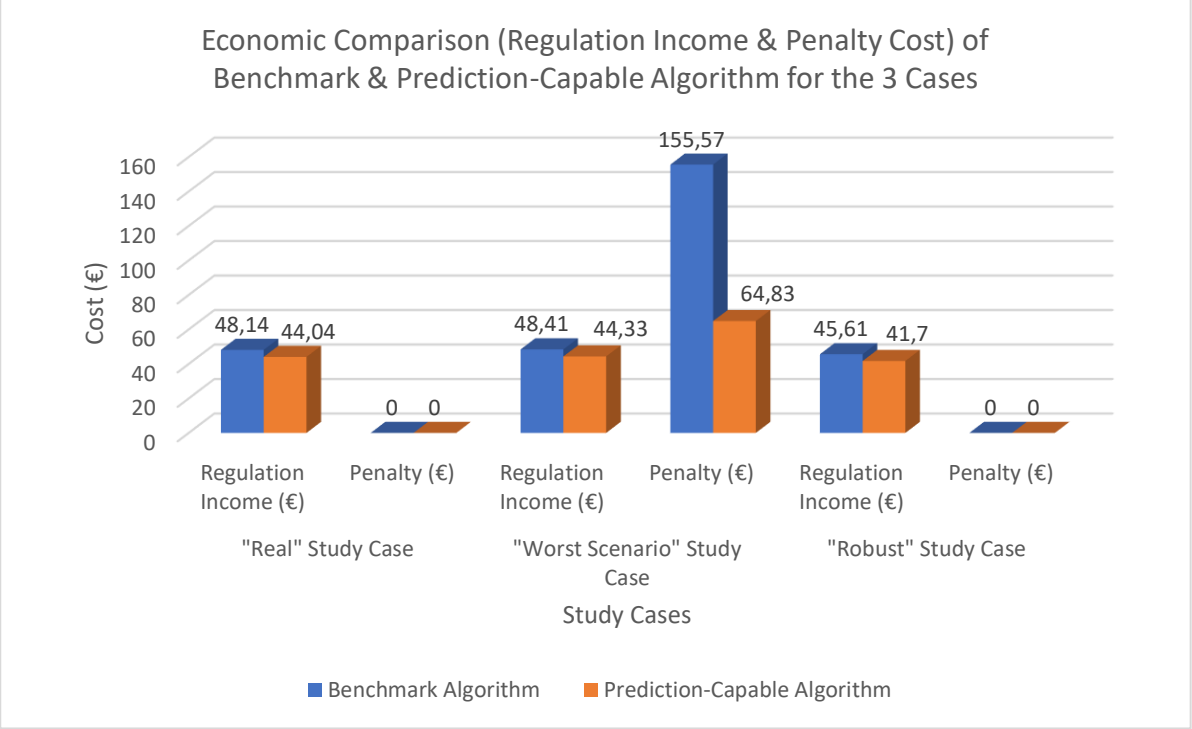

Fig. 6. 11: Regulation Income & Penalty Cost of Benchmark and Prediction-Capable Algorithms at "Real", "Worst-Scenario" & "Robust" Study Cases

Finally, it can be seen that the offered down FCR are extremely higher than the offered up reserves in every case for both algorithms. This can be justified by the following reasons:

- Firstly, as it can be seen in the ENTSO-E database [98], the offered down reserves are approximately 4 times higher than the corresponding up reserves.

- Secondly, as already stated, the offered up reserves affect negatively the EV charging in contrast with the offered down reserves. The algorithm prefers to offer more down reserves, with which it can charge the EVs without paying for imported power and simultaneously receive remuneration for offering ancillary services. Because this can be deemed unreal, due to the assumption that all the amount of offered reserves will be accepted in the biding market, one more testing has been made with the integration of a constraint that forces the algorithm to offer up reserves that are least the $^1/_4$ of the down reserves. Despite consequences, such that the charging gaps are generally increased and the total offered reserves are generally decreased, the rest of the findings in terms of comparison of the two algorithms remained the same. That is why these results are not integrated in the thesis.

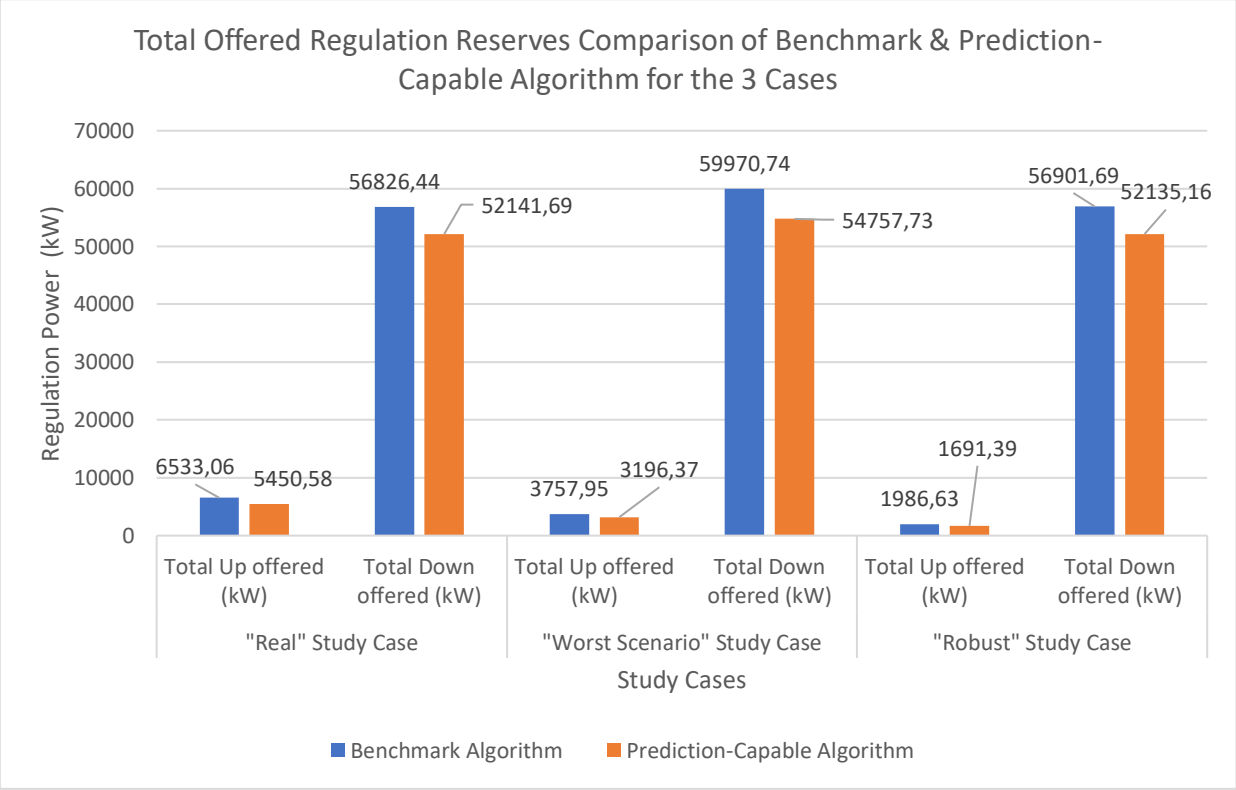

Fig. 6. 12: Total offered Up & Down FCR Reserves of Benchmark and Prediction-Capable Algorithms at "Real", "Worst-Scenario" & "Robust" Study Cases

Chapter 7: Summary & Discussion of Results from Smart-Charging Uncertainties Management

Taking into account all the findings and information of Studies 1 & 2, Chapter 7 presents a summary of the results of this thesis investigations for the extraction of clear and solid conclusions. Such as in the previous chapters, Chapter 7 is divided into two paragraphs.

The first paragraph summarizes the results regarding integration of RO in "prediction – expectation" of the algorithm, intending to enlighten the so-called "Price of Robustness" and answer the research question about:

"How much can the optimality of results be deteriorated at expense of robustness, regarding each uncertainty?"

The second paragraph summarizes the results regarding integration of RO in "prediction – expectation" and reality part of the algorithm, intending to enlighten the so-called "Impact of Uncertainty" (and "Value of Robustness") and answer the research question about:

"Which system uncertainty is more crucial in terms of impact on the optimality of the smart-charging results and which system uncertainty is more robustly manageable in a Smart-Charging Algorithm, that utilizes Robust Optimization Approach?"

7.1 Summary of Results about RO over-conservativeness & "Price of Robustness"

Fig. 7.1 depicts the behavior of the "Home", "Semi-public" and "Public" Nodes with the use of box – scatter plots, regarding the unfinished charging gaps of every EV charging session of the EV fleets that have been charged by the algorithm of the time duration considered: 7-6 00:00 until 10-6 23:55.

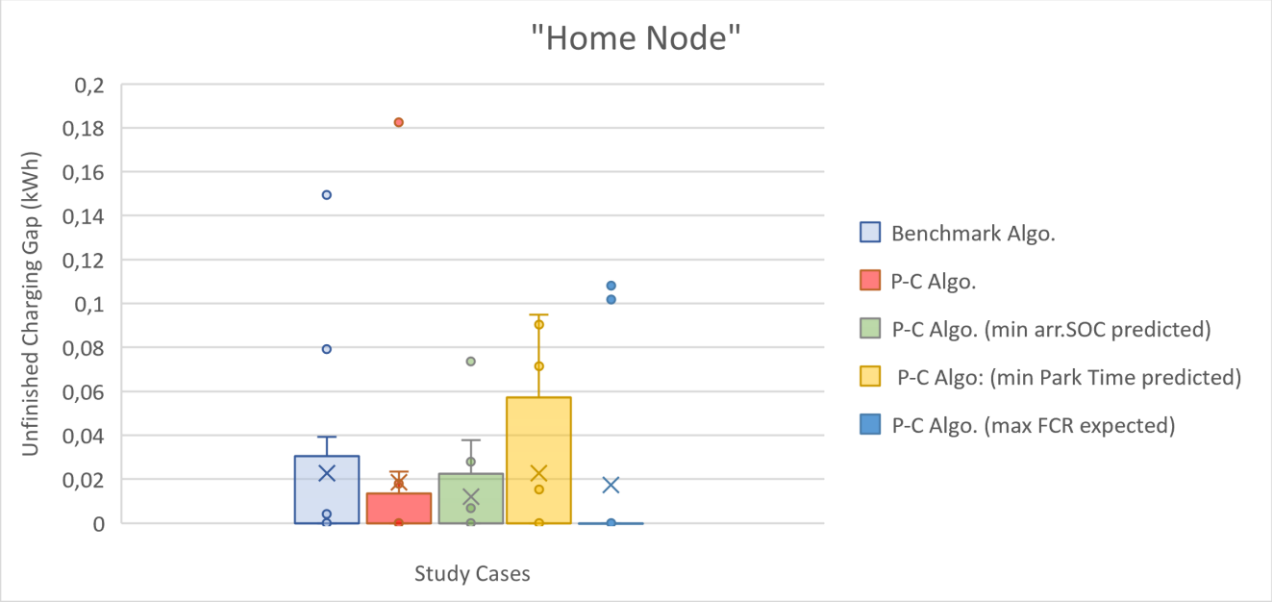

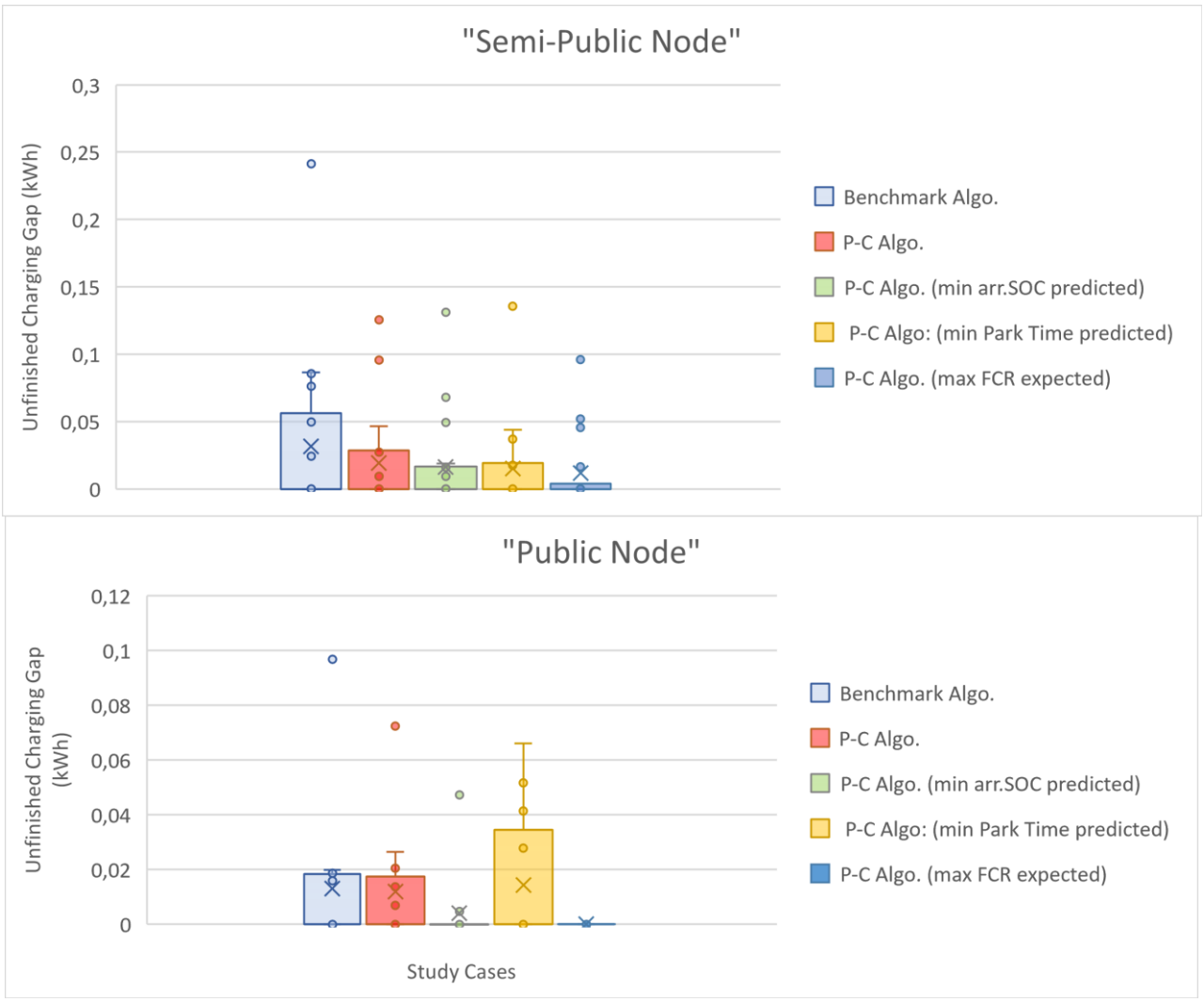

Fig. 7. 1: Unfinished Charging Gaps of every EV charging Session in "Home", "Semi-Public" & "Public" Nodes for the study Cases with no uncertainty worst-case scenario realization

Moreover, Fig. 7.2 depicts the comparison of the charging cost increase (or charging income decrease) for all uncertainties considered, when the P-C Algorithm utilizes RO in the "prediction – expectation" part, in order to prepare for the worst-case scenario and charge the connected EVs more robustly. This comparison is performed for every uncertainty with the base-case of P-C Algorithm (prediction of accurate forecast) and the cost deviation revealed is called "Price of Robustness". For every uncertainty charging cost increase, the corresponding contribution of every node is depicted, for the extraction of significant information about every node robustness.

Observing Fig. 7.1, the utilization of the prediction feature without Robust Optimization (red colored box plot) is an efficient tool of robustness for the "Home" and "Semi-public" nodes, since both the mean value and max value of EV charging gaps (x mark) decrease. Moreover, the box plot IQR size (inter-quantile range), which is the range between the 1st and 3rd quantiles therefore between the 25% and 75% values of charging gap values and is presented by the box itself, decreases in the P-C case for the particular nodes. Hence, when prediction feature is utilized in "Home" and "Semi-Public" Nodes, not only the total EV charging gap decreases, but the EV charging gaps are generally less spread out and the values are more concentrated around the mean value, because the mean deviation and variance are highly

decreased. However, not the same conclusions are derived for "Public" Node, since while the mean value slightly decreases, the values variance is practically the same and the maximum EV charging gap even increases (the upper straight line), if outliers are excluded.

Moreover, it can obviously be seen that integration of the FCR reserves provision in prediction with RO manages the most robust EV charging in all nodes, since when the algorithm "expects" the worst-case scenario, it can almost nullify the EV charging gap in terms of mean, variance and maximum values, apart from some outliers at the "Semi-Public" Node. In addition, it can be seen the arrival SOC uncertainty provides highly robust EV charging, as well, for the same reasons, even though at "Home" Node the maximum EV charging gap is increased while the IQR is increased (less concentrated values around the mean value).

On the contrary, regarding Parking Time uncertainty, it can be concluded that it manages the less robust EV charging, since it produces contradictory results at the three nodes. While "Semi-Public" Node succeeds in utilizing effectively Prediction and RO to charge more satisfyingly the EV drivers, "Home" and "Public" Nodes produce same total and mean EV charging gaps, while the maximum values and the sparsity in the IQR zone highly increase. This can be justified by the fact, that has already been explained earlier in Chapter 5. Prediction of Parking Time uncertainty worst-case scenarios may confuse the algorithm. Later EV arrivals prediction may cause delayed EVs charging, since the algorithm expects that the future EVs to arrive, will arrive later than it actually happens in reality. Therefore, the algorithm thinks that there is time to charge the currently-connected EVs later. Even in the 2nd study case of Parking Time Uncertainty prediction (with all uncertainty inserted in the departure for the predicted EVs), similar confusions have been observed, as already explained. The algorithm may predict that it is more efficient to charge the currently connected EVs after the departure of an EV, that will arrive in the future. For that reason, only the 1st case is depicted in this paragraph.

Furthermore, observing Fig. 7.2, arrival SOC and FCR provision uncertainties management by RO and "Prediction" are equally costly, constituting the 5% of the total charging cost, with Parking Time's "Price of Robustness" remaining low only at 2%. However, none of these "Prices of Robustness" can be considered high, therefore it can be concluded that RO employment is not costly and over-conservative, since it does not deteriorate the optimality of the charging cost.

Last but not least, comparing the behavior of the 3 Nodes in Figs. 7.1 & 7.2, the "Semi-Public" Node can be defined as the least affected by RO overconservativeness, since it contributes with the least robustness cost, always less than 2% and even close to 0% for Parking Time Uncertainty study case, regarding all uncertainties. Moreover, the "Semi-Public" Node succeeds in charging the EV fleets more robustly than the other two nodes, when uncertainties worst-case scenarios are integrated in the prediction part of the algorithm. This is possibly due to the fact that, compared with the "Home" Node, the "Semi-Public" node is characterized by lower requested energies and higher arrival SOCs. Therefore, the "Prediction" of the worst-case scenarios of uncertainties has a higher impact on earlier EV charging by the algorithm causing the charging gap of the EVs decrease in most of the EV charging sessions. The reason why the results of the "Semi-public" Node are more optimal than of the "Public" Node are justified by a factor, that is explained more thoroughly in the next paragraph. The EV fleet of the "Semi-Public" Node is greater than the one of the "Public" node and therefore more re-optimizations are triggered. A higher amount of re-optimizations aids the algorithm to perform more efficient EV charging, decrease the over-conservative effect of Robust Optimization.

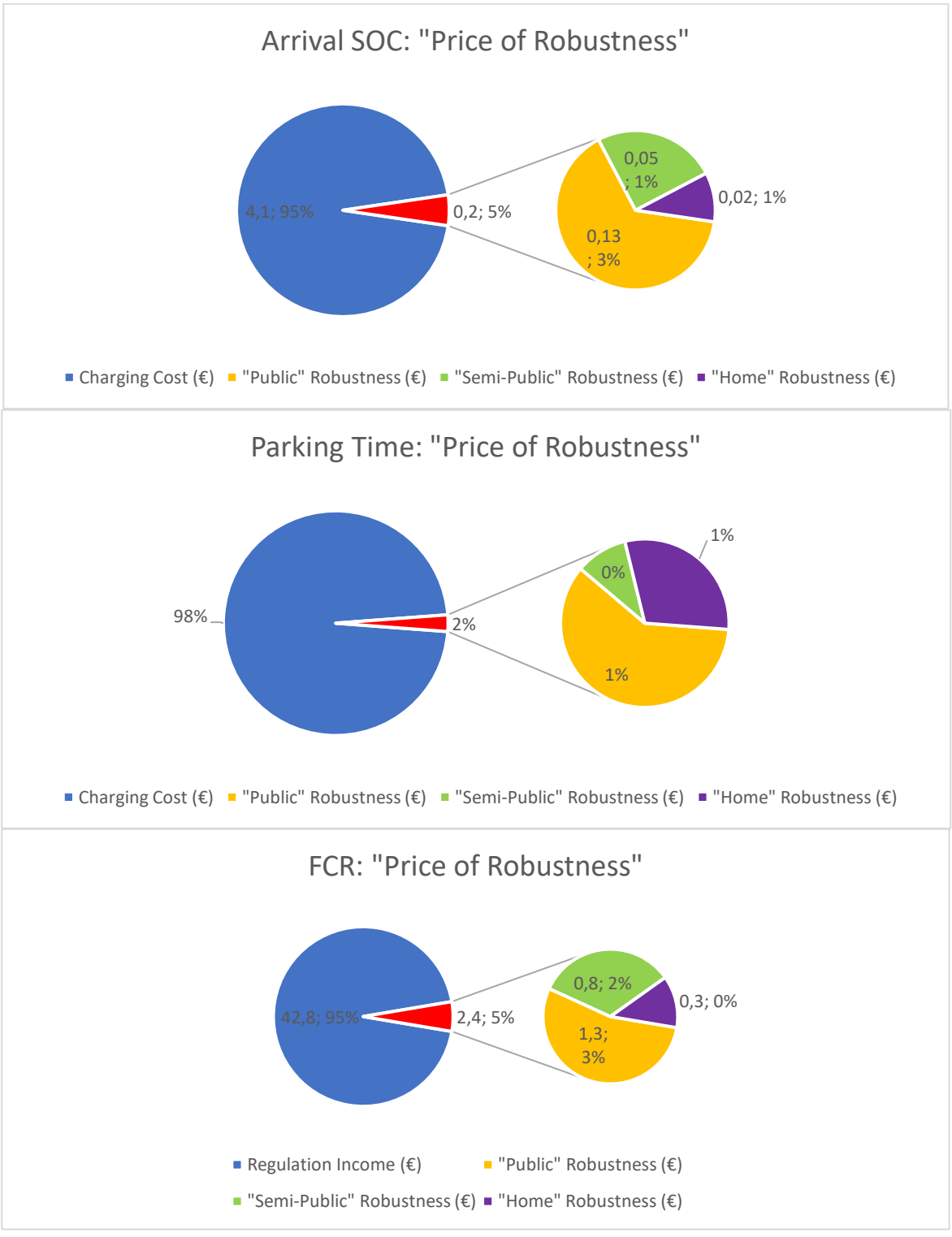

Fig. 7. 2: “Price of Robustness” for Arrival SOC, Parking Time & FCR provision uncertainties

Regarding unfinished charging gap, no solid conclusions can be derived by comparing the "Home" & "Public" Nodes, since for example the prediction of arrival SOC uncertainty provides more robust EV charging at the "Public" Node, but "Prediction" tool works more successfully at "Home" Node. However, the "Public" Node can be characterized as the most expensively manageable node, since it is responsible for more than 50% of the "Price of Robustness" for all uncertainties study cases. This can be justified by the fact that "Public" Node is characterized by lower parking times and energy demands and simultaneously by higher EV arrivals' frequency, than e.g the "Home" Node. Hence, when the algorithm predicts the worst-case scenarios and decides that it has to rush the charging of the currently connected EVs, it has less options for charging efficiently the EVs, than the "Home Node". The "Home" Node with the long parking times of the EV fleets, is less affected by charging cost increase at expense of robustness, since the algorithm is left with still many options for sustainable and economic EV charging.

7.2 Summary of Results about "Impact of Uncertainty" & "Value of Robustness"

Figs. 7.3 – 7.5 depicts the behavior of the three known nodes respectively with the use of box – scatter plots, regarding the unfinished charging gaps of every EV charging session in the Benchmark & P-C Algorithms study cases, of which the worst-case scenarios actually occur in reality. All uncertainties worst-case scenarios of Benchmark and P-C Algorithms are compared with the corresponding base case.

As it can be seen in Fig 7.3, the highest impact on EV charging gap is inflicted to the "Home" Node by the FCR uncertainty worst-case scenario. The total unfinished charging gap is more than 5 times higher than in the base case for the Benchmark Algorithm, leaving one EV with almost 3 kWhs gap while one EV leaves with 4 kWhs charging gap! However, observing the subfigure of the P-C Algorithm, the FCR uncertainty's impact is totally managed when the Algorithm has the capability of predicting the worst-case scenario employing Robust Optimization. Parking Times uncertainty has a notable impact as well at the Benchmark algorithm, slightly increasing both the mean and maximum EV charging gap values as well as the variance around the mean value, which is again managed in the P-C algorithm. This is justified by the fact that the EVs that arrive at the "Home" node usually stay for very high parking times. Therefore, a 50% reduction of the Parking Time of the EVs provokes a considerable impact on the available time for charging. On the other hand, arrival SOC uncertainty inflicts a less significant impact, since the EVs arrive normally with already very low SOC. Finally, the PV Generation and Load demand have the least impact on the charging gaps of the EV charging sessions in both algorithms, since firstly the algorithm can always re-compensate the lost produced energy by importing power from the grid and secondly the EV charging at the particular node des not depend generally so much on these uncertainties, since it is performed during the night.

Fig. 7.4 depicts the behavior of the "Semi-Public" Node for all uncertainties study cases for the Benchmark and P-C algorithms. At this node, it can be seen that arrival SOC uncertainty has a greater impact than FCR uncertainty on unfinished charging gap of the node, increasing both the max and mean values and the sparsity in the IQR range. This is logical, if we consider the fact that "Semi-Public" Node is typically characterized by higher arrival SOCs than the "Home" Node. Therefore, a 50% reduction of the arrival SOCs provokes a higher impact on the smart-charging at the particular node, compared with the "Home" Node, where the EV fleets arrive with very low SOC already. Moreover, Load Demand uncertainty has significant impact as well while PV Generation uncertainty provokes higher maximum value. On the contrary, Parking Time and FCR uncertainties' impacts remain very low. On the one hand, these observations are due to the fact that the "Semi-Public" Node typically charges the EV fleets during the day. Therefore, PV Generation and Load Demand uncertainties can be considered more important, since EV smart-charging depends generally more on these uncertainties at the "Semi-Public" Node.

It must be noted that a very interesting observation is that while the arrival SOC and Parking time uncertainties impacts are highly managed at the "Semi-Public" by the P-C Algorithm utilizing prediction and RO, PV Generation and Load Demand impacts are slightly managed even with the use of prediction.

This can be explained if we consider the way that they are formulated in Chapter 4. The gradual decrease and increase of the PV Generation and Load Demand respectively within the optimization horizon is actually the same for the P-C and Benchmark algorithms, until the next re-optimization by the next future arrived EV. Therefore, they are slightly managed by prediction feature. However, their impacts remain low at this node, as well.

On the other hand, the EV fleets usually park for lower parking times at the "Semi-Public" Node. Hence, a furtherly decreased parking time has lower impact on smart-charging customer satisfaction regarding the final charging gap. Finally, the impact of FCR uncertainty remain low in the P-C Algorithm, as well.

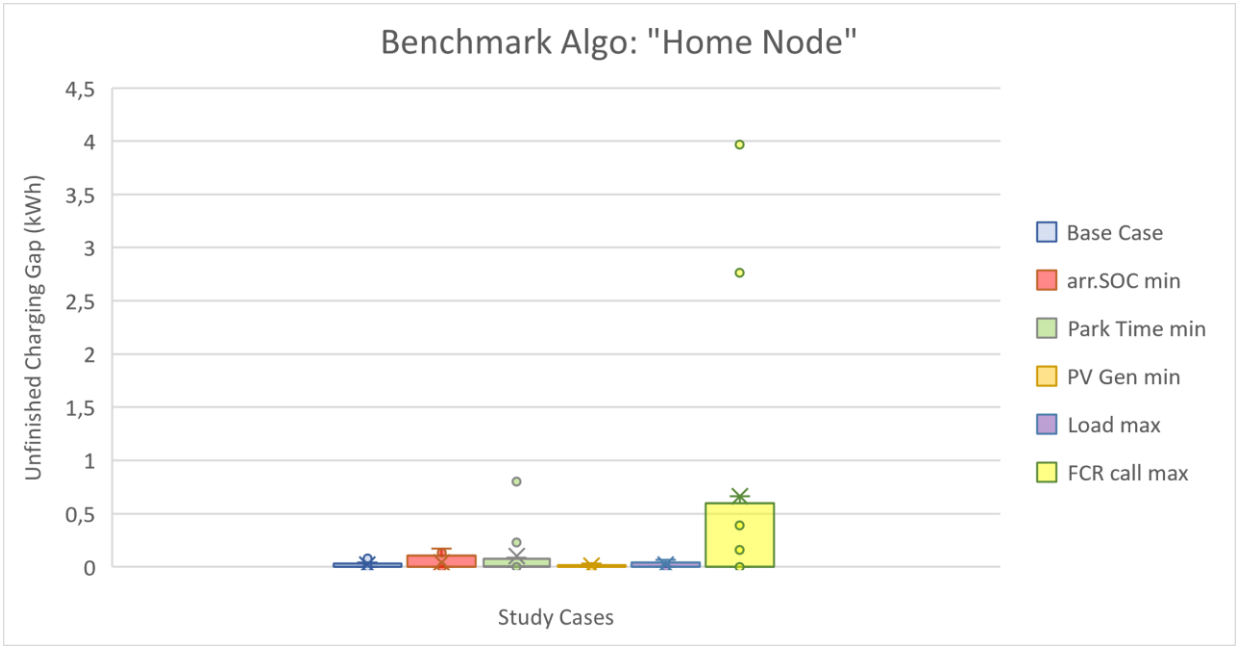

.

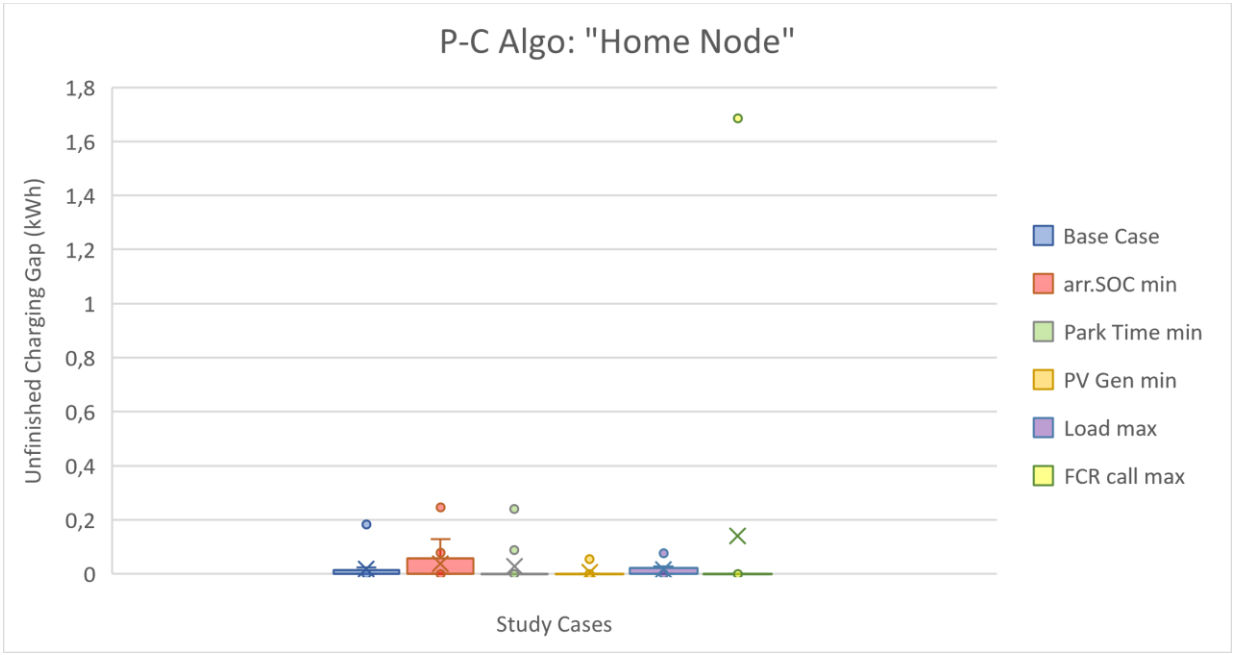

Fig. 7. 3: Unfinished Charging Gaps of every EV charging Session in "Home" Node for Benchmark & P-C algorithms' Study Cases with uncertainty worst-case scenarios occurrence in reality

As it can be observed in Fig. 7.5, the FCR uncertainty inflicts the greatest impact with a mean value of 0,17 kWhs, nearly 3 times greater than the mean value of the base case, while producing charging gaps in EV charging sessions that can reach up to 0,35 and 0,4 kWhs or even up to 0,61 kWhs (outlier). Arrival SOC's impact remains low to moderate at the "Public" Node, while Parking Time uncertainty induces higher impact to the "Public" Node, in contrast with the corresponding results in the "Semi-Public" node. Moreover, the impact of the Load Demand and PV Generation uncertainties remain low, as in the other two nodes.

There is a general observation that the results regarding the "Semi-Public" and "Public" nodes differ greatly, while they are both characterized by similar characteristics (high arrival SOCs, low Parking Times, EV charging typically during the day, etc) [104]. This is justified by another factor, integrated in the optimization: the number of the Chargers. The "Semi-Public" node integrates 5 chargers, while the "Public" node only 3. Moreover, the EV fleet that passes through the "Semi-Public" node is consisted of 18 EVs, while the corresponding fleet of the "Public" node integrates only 12 EVs during the time of 4 days studied. For that reason, the arrival SOC affects significantly more the "Semi-Public" node than the "Public" node. The high difference of arrival SOCs, when worst-case scenarios are realized, combined with the large EV fleets, inflict high charging gaps and penalty costs to the "Semi-Public" node, while the less challenging EV fleet of the "Public" node has a lower impact. On the contrary, the large EV fleets of the "Semi-Public" node provokes more re-optimizations and shorter optimization horizons. More re-optimizations contribute to more successful and efficient EV charging and less effect by uncertainties, in contrast with the "Public" node, which results to be more vulnerable.

Finally, this node can be defined as the most robustly managed by P-C algorithm, since all uncertainties' impacts are nullified when Prediction and Robust Optimization are utilized for their management.

Despite the several differences of the 3 nodes, some general observations can be made for the uncertainties. Generally, arrival SOC, Parking Time and FCR reserves uncertainties have the highest impact regarding unfinished charging gap. The first one affects highly the "Semi-Public Node" (almost double mean value of 0,1 kWh and max value of 0.9 kWh as well as the gaps variance increases as well), while the second one affects mostly the "Public" Node. It can be decided that the FCR reserves uncertainty has the highest impact on charging gap, since it deteriorates optimality the most at both the "Home" and "Public" Nodes. However, the FCR uncertainty can be defined as the most robustly manageable as well, since P-C algorithm succeeds in almost nullifying the total charging gap at both nodes. Despite the contradictory results of the Parking Time Uncertainty in the previous subparagraph, the Parking Time uncertainty is also highly manageable such as the FCR uncertainty. This is justified now by the fact that the algorithm does not get confused, since the future EVs arrive and request the same parking time as the algorithm has predicted, because prediction and reality parts are both in accordance with the worst-case scenario. Finally, Load Demand and PV Generation have generally low impact on the EV charging gap, even though results show that they are not so well-manageable, as already explained.

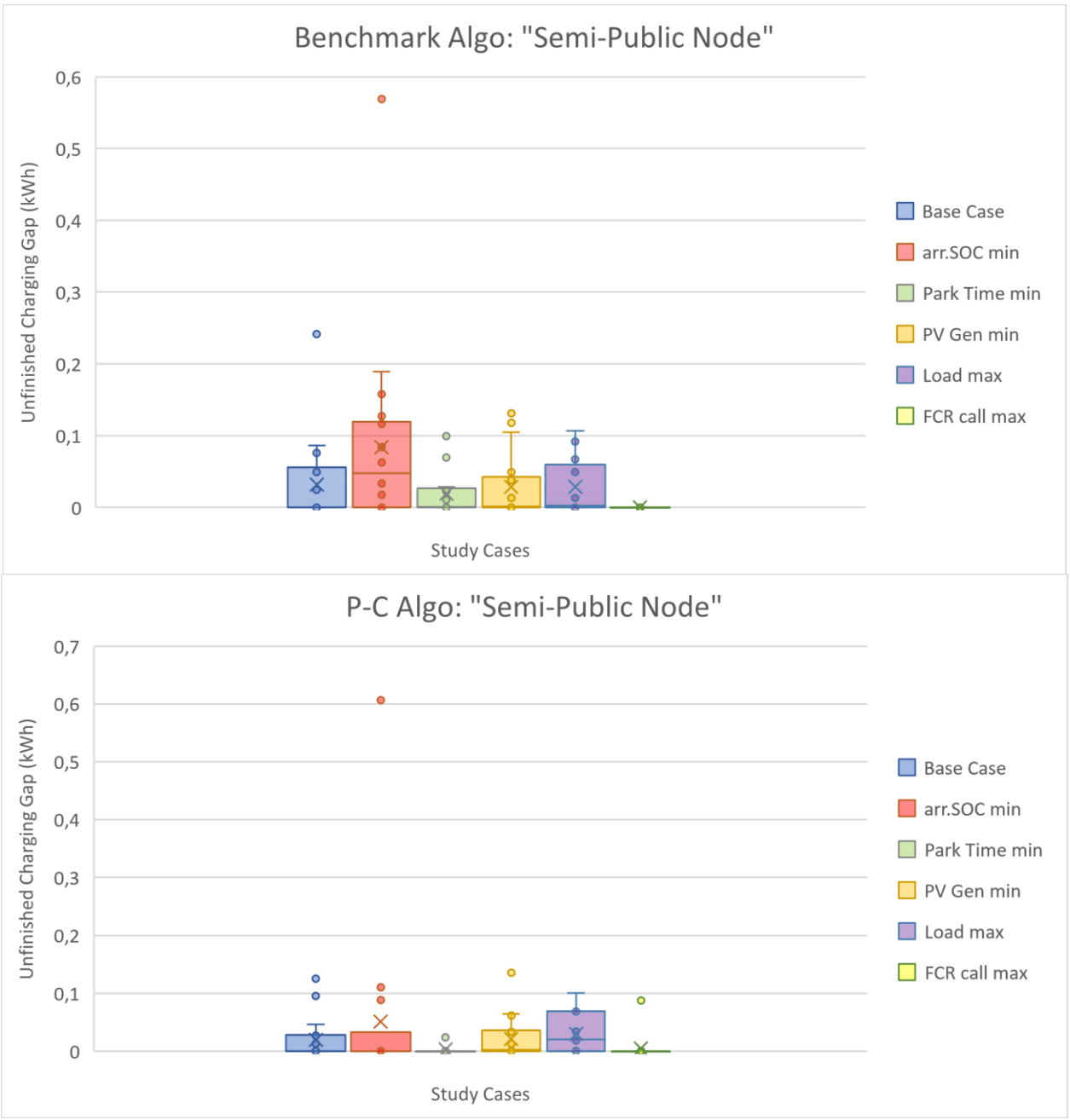

Fig. 7. 4: Unfinished Charging Gaps of every EV charging Session in "Semi-Public" Node for Benchmark & P-C algorithms' Study Cases with uncertainty worst-case scenarios occurrence in reality

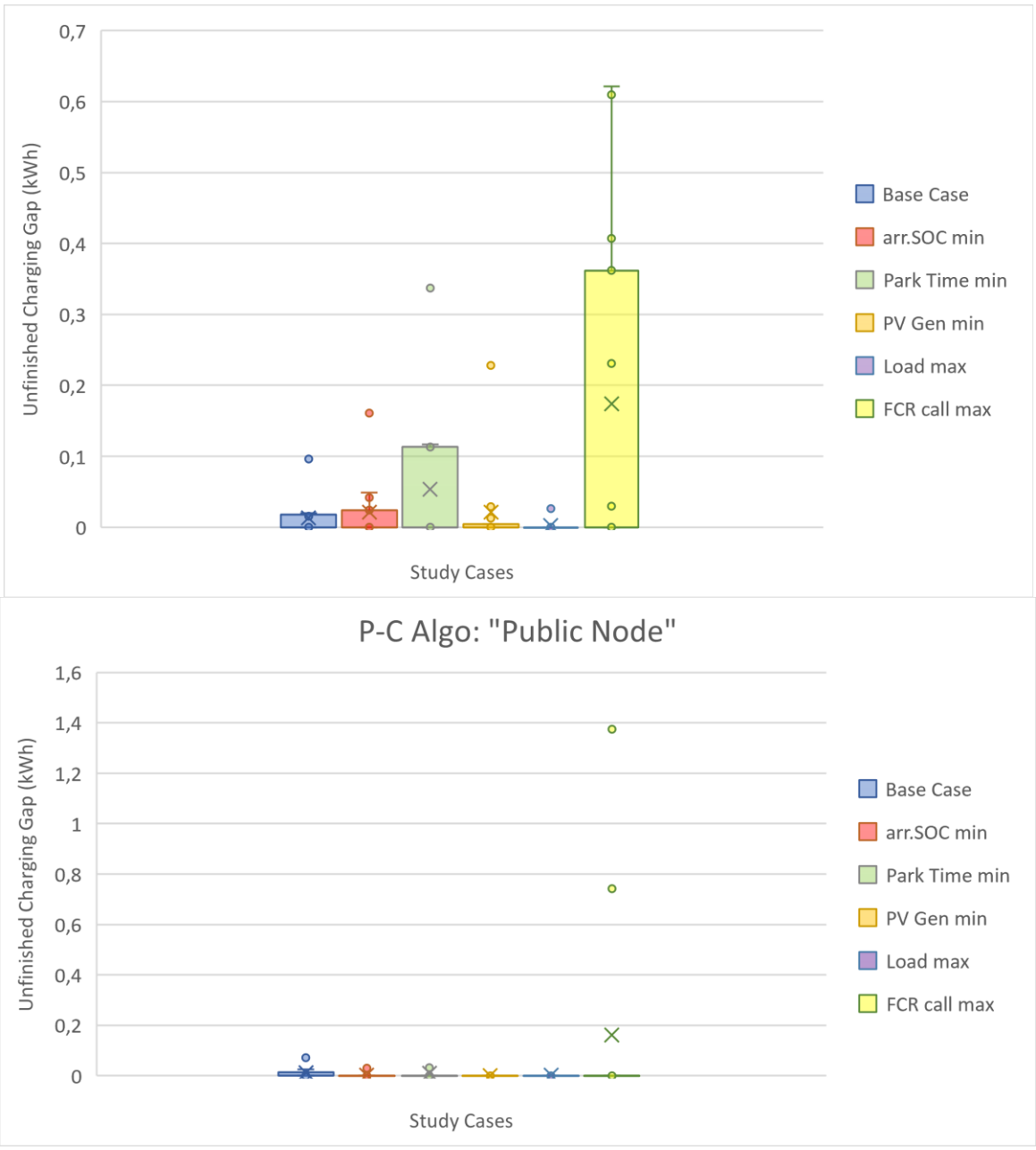

Fig. 7. 5: Unfinished Charging Gaps of every EV charging Session in "Public" Node for Benchmark & P-C algorithms' Study Cases with uncertainty worst-case scenarios occurrence in reality

Until now, the impact of every uncertainty has been addressed only in terms of customer satisfaction, hence in terms of unfinished charging gap in the EV charging sessions. Fig. 7.6 intends to enlighten the total "Impact of Uncertainty" and "Value of Robustness" for every uncertainty considered in this thesis. The "Value of Robustness" is defined as the difference in charging cost comparing the performance of the Benchmark Algorithm and P-C Algorithm, when uncertainties actually occur in reality. In every uncertainty sub-figure, the corresponding contribution of robustness in cost savings (or income increases) at each of the 3 nodes is depicted. The "Impact of Uncertainty" is defined firstly the rise of charging cost (or decrease of charging income) and secondly the rise of unfinished charging gap, when the Base Case of benchmark algorithm (everything happens as predicted) and the Cases, when

uncertainties worst-case scenarios actually occur in reality, are compared. It must be noted that no "Value of Robustness" is defined for PV Generation and Load Demand uncertainties, because no study cases, with uncertainty worst-case scenario integration only in "prediction - expectation" part of the P-C Algorithm, have been formulated in the thesis.

As already explained, the FCR reserves uncertainty has the highest impact producing a total of approximately 55 kWh charging gap to the Benchmark algorithm compared with the 0,51 kWh of the base case, which is nearly 100 times greater! This can be seen in the left part of the 3rd subfigure, that shows the "Value of Robustness", which is the sum of the total costs decrease of 31,43 € and 41,12 € for the "Home" and Public" nodes respectively in the P-C Algorithm. Moreover, as we can see, the Benchmark Algorithm instead of earning a total 45,2 € amount by the EV smart-charging, it is charged a total amount of 27,62 €, when FCR worst-case scenario occurs. Furthermore, Parking time and arrival SOC uncertainties provokes a more than double total unfinished charging gap to the algorithm. However, the economic impact of Parking Time Uncertainty can be defined as greater than of the arrival SOC, since the total cost is 32,3 times greater compared with the 8,5 greater of the arrival SOC uncertainty. Moreover, Parking time uncertainty inflict penalty costs of 9,5 € and 9,8 € at the "Home" and "Public" nodes respectively, while arrival SOC uncertainty affects most the "Semi-Public" Node, inflict a penalty cost of 14,5 € (in reality these are the total costs that integrate both the penalty costs and the charging costs, however when penalty costs appear, they are greatly higher than the charging costs). Combination of RO and prediction in the P-C Algorithm succeeds in nullifying these penalty costs, therefore these cost savings can be defined as the value of robust management of FCR.

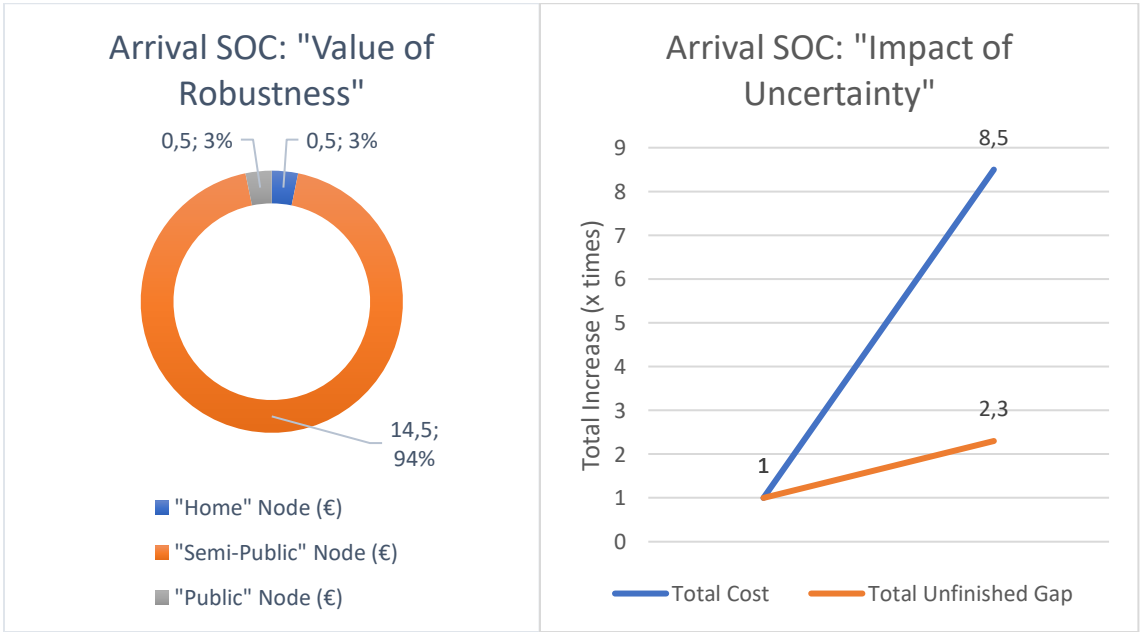

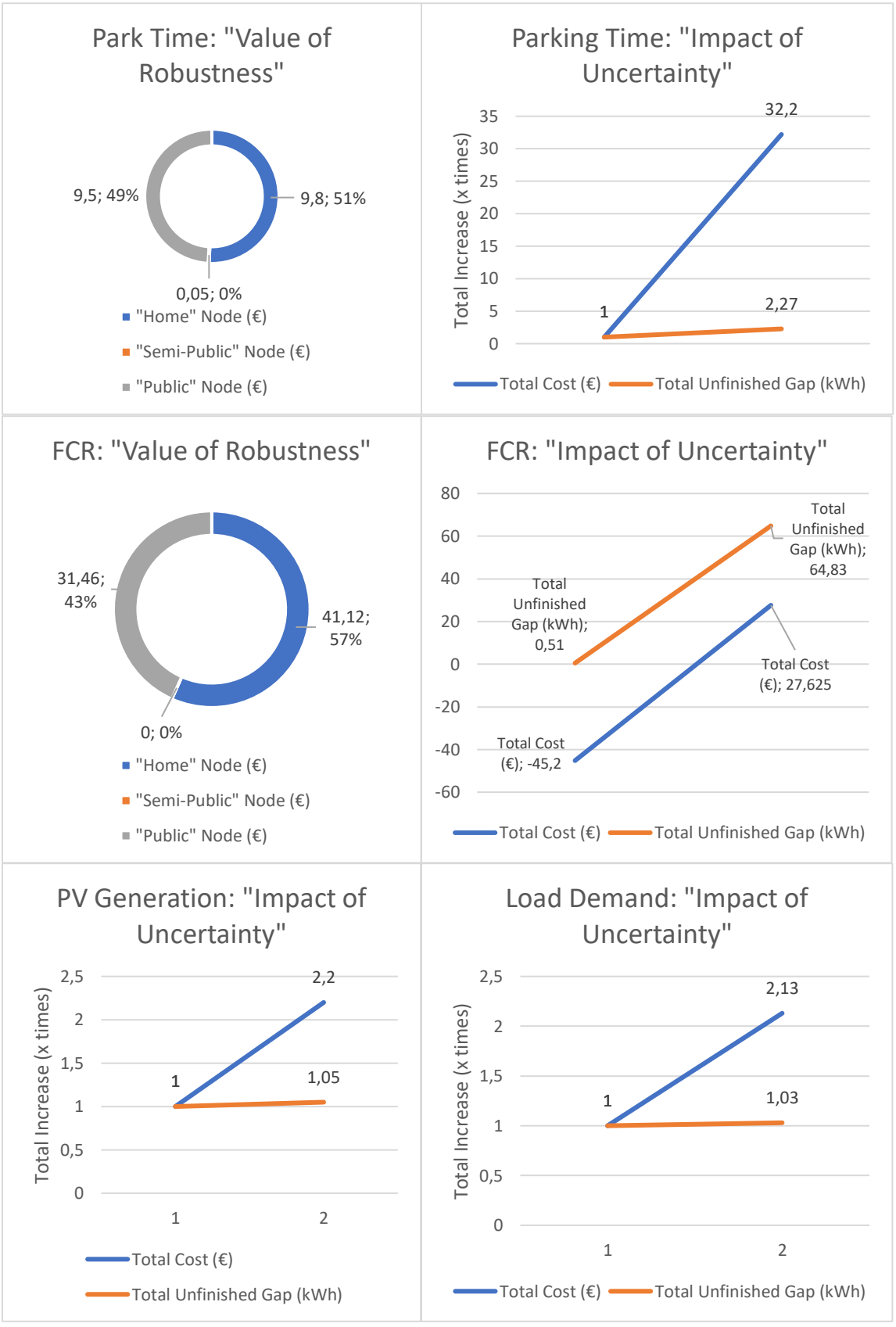

Fig. 7. 6: "Value of Robustness" and "Impact of Uncertainty" for Arrival SOC, Parking Time, FCR provision, PV Generation and Load Demand uncertainties

PV Generation and Load demand, as already observed in Figs. 7.3 – 7.5 that represent the behavior of the 3 nodes individually, do not have a notable impact on the total unfinished charging gap, which practically remains the same. On the contrary, their economic impact on smart-charging optimality is worthy to be mentioned, since it is increased by approximately 2,2 times for both uncertainties. Nevertheless, this increase remains significantly lower than the other uncertainties, especially than the FCR uncertainty's impact, hence PV Generation and Load Demand can be defined as the uncertainties with the least economic and charging gap impacts. This can be easily explained if we consider that the Load Demand and PV generation uncertainties are directly connected with the imported/exported power from the grid and less with the EV users. Since the grid limits are generally higher than the rated capacity of the algorithm, when worst-case scenarios of these uncertainties appear, the algorithm usually has the capability of importing more or exporting less power to the grid in order to satisfy the customers. Therefore, the impact on the EV charging gap is practically zero. In addition, the cost of the imported power (or the savings of the exported power) is typically significantly less than the penalty costs from the customers' unsatisfaction, therefore the economic impact of the uncertainties remain considerably lower as well.

Chapter 8: Conclusions & Future Work Motivation

8.1 Thesis Contributions

Taking everything into consideration, the emerging and continuously growing EV fleets are capable of acting as "smart loads" and providing ancillary services to the power grid. However, if their charging is not performed on a smart and controlled manner, several drawbacks may be inflicted to the grid, such as voltage instability, harmonics distortion etc. Moreover, apart from low charging cost and protection of the power grid balance, smart-charging can provide several other benefits, such as reduction of potential need of grid reinforcements and increase of energy cost savings.

Since many parameters that are related with Smart-Charging are uncertain with high volatility, this thesis purpose has been to address the impact of every uncertainty and their potential management with the use of "Robust Optimization" uncertainty handling technique. According to this thesis findings, uncertainty handling is necessary to be investigated, since the optimality of deterministic smart-charging algorithm results can be seriously deteriorated when only a low prediction error is inserted in optimization.

Taking advantage of the already implemented "Receding Horizon Approach" of the Benchmark algorithm, the combination of RHO and RO for uncertainty handling has been evaluated for uncertainty management. According to the author's knowledge, little research has been realized on the combined "RHO – RO" uncertainty handling technique on energy scheduling and more specifically on EV smart-charging optimization.

Moreover, the completely "reactive" Benchmark algorithm has been improved to be able to predict and take into account the future prediction patterns in order to perform more sustainable EV charging.

- Firstly, the P-C Algorithm takes into account possible "No Smart-Charging Participation" option" in case the customer is not willing to participate in smart-charging and wishes to charge his/her EV with uncontrolled charging, a feature that was not integrated in the Benchmark Algorithm.

- Secondly, applying Robust Optimization on the newly integrated prediction feature, worst-case scenarios of future EV charging uncertainties can be taken into consideration for more "robust" charging.

Furthermore, the investigation of 6 different essential uncertain parameters (PV Generation, Load Demand, EV arrival and departure times, arrival SOC, FCR reserves provision) is another major contribution of this thesis, compared with the state-of-the-art investigations.

Finally, this thesis has contributed to a development of a more realistic and robust FCR reserves provision model, distinguishing the only considered natural FCR reserves in the Benchmark Algorithm from the offered FCR reserves in the bidding market and the actually called FCR reserves by the TSO, providing also the capability of "expecting" FCR reserves with Robust Optimization employment.

Last but not least, this thesis developed a more "real" model for PV generation and Load Demand forecasting curves utilization in optimization. Apart from employing Robust Optimization, gradually decreasing and increasing PV generation and Load Demand in the optimization horizon respectively, the algorithm utilizes the "real" timely PV and Load data at every re-optimization time instant. In that way, the algorithm is able to modify the forecasted curves according the forecasted error of the first instant. Hence, more "real" and robust PV generation and Load demand curves are utilized during the entire optimization problem, using the advantage of RHO, according to which, the optimization algorithm can

re-update at every re-optimization instant and take into account new updated real data for more accurate optimization.

Overall, this thesis contributions can be summarized as follows:

- Investigation of combined Receding Horizon Approach and Robust Optimization (RHO – RO) for uncertainty handling
- Insertion of Prediction capability in the Benchmark Algorithm
- Insertion of "No Smart-Charging" option in the Benchmark Algorithm
- Investigation of 6 major important smart-charging uncertainties
    - PV Generation, Load Demand, Arrival & Departure Times, arrival SOC, FCR reserves provision
- Development of a more "realistic" and robust FCR reserves provision model for Offered and Called FCR Regulation Reserves
- Development of a more "realistic" and robust PV Generation and Load demand forecasting curves utilization with the use of "real" data and the RHO advantage of considering new updated real data at every re-optimization

8.2 Thesis Conclusions

Taking everything into account, this thesis purpose is the study and analysis of the impact of several uncertainties, related with EV smart-charging as well as their potential management with the utilization of Robust Optimization Approach. This thesis conclusions can be categorized as follows:

1) Regarding prediction feature insertion in the Benchmark Algorithm

Prediction feature can be defined as a useful "tool" of robustness itself. Having the capability of predicting future EV arrivals, the algorithm can charge more robustly the EV fleets, decreasing the total unfinished charging gap, even without utilizing RO. However, a certain amount of charging gap could not be totally nullified due to Discrete Optimization's inherent drawback. Moreover, the P-C Algorithm is able to perform generally more efficient EV charging with the utilization of prediction, slightly decreasing the charging costs (or increasing the charging income).

2) Regarding use of RO in the Prediction part of the Algorithm for Robust EV Charging and RO Overconservativeness Analysis

As already explained, while RO has the advantage of uncertainty management under consideration of the worst-case scenario occurrence, avoiding the high computational expense of stochastic approaches, a significant drawback is the potential over-deterioration of the deterministic optimality at expense of robustness. In other words, the problem may result over-conservative. In order to address this potential drawback of the particular uncertainty handling approach, a major part of the research has been devoted to inserting RO only in the Prediction Part of the algorithm, whereas uncertainties occur with their forecasted values. Forcing the algorithm to predict worst-case scenarios without applying them in reality, the potential RO over-conservativeness drawback is addressed for every uncertainty and their "price of robustness" is calculated.

On that manner, the FCR reserves uncertainty manages the most robust EV charging, almost nullifying the charging gap, when it is inserted in the "prediction – expectation" part, while arrival SOC follows with significantly improved robust charging results as well. Moreover, both of these uncertainties produce a relatively low "Price of Robustness", which represents approximately the 5% of the total charging cost. Parking time uncertainty manages the least robust EV charging, both in the cases that

uncertainty is inserted in arrival and departure times or only in departure time, because it can potentially provoke "confusion" to the algorithm about when it should charge the connected EVs. Confusion results greater when uncertainty affects arrival (1st case), because EV arrival times constitute re-optimization time triggers and are more essential for the optimization. Parking time's "Price of robustness" is the lowest of all, since it represents only the 2% of the total charging cost, but since the robust charging results are contradictory, it is not taken into account. However, the 5% "price of robustness" compared with the total charging cost, is still a very low percentage, therefore it can be concluded that RO does not result 'over-conservative" for none of the considered uncertainties.

3) Regarding "Impact of Uncertainties" and their potential management by RO, "Prediction" capability & RHO

The "impact" of an uncertainty is directly connected with the "value" of robustness for its management. Comparing the Benchmark algorithm results with the P-C algorithm results, when it predicts the worst-case scenarios that actually happen in reality, it has been concluded that the RHO as an individual uncertainty handling technique is not enough and penalty costs appear at the nodes. FCR reserves uncertainty has the greatest impact on total charging gap (100 times greater than in the base case) in terms of mean, max charging gap values and sparsity, increasing the IQR range (distance between 25% and 75% of the total gap values' range) at most of the nodes. FCR uncertainty has also the greatest impact on the charging costs, since it is responsible for forcing the algorithm to pay the grid for EV charging in a study case, in which the algorithm should normally result remunerated and receive income from the grid for the smart-charging. However, FCR uncertainty is also the most robustly manageable, since P-C algorithm succeeds in nullifying the penalty costs that appear in the Benchmark algorithm and highly reducing the total charging gap. Moreover, parking time and arrival SOC uncertainties have the same charging gap impact with a total of 230% increase, while, economically, parking time uncertainty can be considered as more important, since it increases the total charging costs more than 32 times. Both of these uncertainties' impacts can be defined as robustly manageable, especially parking time's impact, since the P-C Algorithm manages to avoid the penalty costs and highly decrease the charging gaps. On the contrary, PV Generation and Load demand uncertainties have practically no impact on the unfinished charging gaps, rather only on the charging costs, which are increased approximately by 220%. This is justified by the fact that these uncertainties have less relation with the EV user driving patterns and can be directly compensated with energy exchange from the grid. Therefore, a lower PV Generation or a higher Load Demand can be covered by importing more power from the grid (or exporting less power) and, on that way, the unfinished charging gaps are not practically affected. However, their economic impact remains significantly lower than the corresponding impacts of the other uncertainties, since the cost of imported power is significantly lower than penalty costs paid to the customers. Hence, they can be defined as the uncertainties with the least total impact.

4) Regarding Benchmark and P-C Algorithms

As it has already been explained, under events of the uncertainties' worst-case scenarios, RHO utilized by the Benchmark Algorithm is not enough. Robust Optimization, combined with prediction is generally capable of performing efficient EV charging under uncertainties, avoiding potential penalty costs at the nodes, while simultaneously satisfying greatly the customers by reducing the total charging gaps. The only drawback of the P-C Algorithm, compared with the Benchmark Algorithm, has been found in the study cases of FCR reserves provision under uncertainty. In almost all the study cases considered: "Real", "Worst-Scenario" & "Robust (reader is referred to Chapter 5), the Benchmark Algorithm is remunerated hi gher for the FCR provision, compared with the P-C Algorithm, because it

offers a higher amount of reserves to the bidding market. This drawback has been justified by the utilization of the longer optimization horizons by the P-C Algorithm, due to the future EV arrivals predicted and integrated in optimization. The P-C Algorithm, utilizing longer optimization horizons, decides to focus on charging more robustly the EVs and leaving FCR reserves provision for later. This constantly happens in continuous re-optimizations, resulting in total less FCR reserves offer to the bidding market. Nevertheless, it should be noted, that when the FCR reserves provision model was tested for an "ideal" case, in which the "expected" called FCR reserves were exactly the same as the actually "called" FCR reserves in reality, the opposite results were observed and the P-C Algorithm was remunerated higher at all nodes. Hence, it can be concluded that when no uncertainty is considered, the P-C Algorithm produces more optimal charging costs and receives higher regulation income than the Benchmark Algorithm, while when uncertainty is inserted, the P-C Algorithm focuses more on charging robustly the EV fleets.

5) Regarding Comparison of "Home", "Semi-Public" & "Public" Nodes

Concerning, firstly, the study cases in which Robust Optimization is inserted only in prediction, the "Semi-Public" Node can be defined as the node, which is the least affected by RO overconservativeness, since it is responsible for the least robustness cost (always less than 2% for all uncertainties), while it simultaneously manages to charge the EV fleets more robustly. The reason behind this observation is that since EVs that arrive at the "Semi-Public" Node, typically arrive with higher SOCs, compared with the "Home" Node, the prediction of the worst-case scenario has a greater impact on earlier EV charging, causing the total final unfinished gap to decrease more. However, the "Price of Robustness" remains very low at "Home" & "Public" nodes as well, while they both manage to decrease their unfinished charging gap more. Hence, we can conclude that the management of uncertainties by Robust Optimization does not result to be over-conservative in this thesis.

Concerning, secondly, the study cases in which uncertainties' worst-case scenarios actually happen in reality, the "Home" and "Public" nodes are mostly affected by FCR provisions uncertainty in terms of charging gap, which is increased 5 and 3 times respectively (certain EVs depart with 3 kWhs and 4k Whs charging gap at the "Home" Node because of FCR worst-case scenario!). However, the utilization of "Prediction" and RO in the P-C Algorithm reduces greatly the FCR impact and eliminates the penalty costs. The "Semi-Public" Node is highly affected by the arrival SOC uncertainty, which is depicted by the corresponding percentage of the "Semi-Public" Node at the total "Value of Robustness", which reaches up to 95% compared to the other two nodes. Since the "Semi-Public" node is characterized by typically high arrival SOCs and low parking times, the arrivals of the EVs with minimum SOC deteriorates highly the optimal and successful EV charging. On the contrary, the "Home Node" is more affected by Parking Time uncertainty, since the EVs at the particular node typically request high Parking Times and a 50% reduction of the worst-case scenario inflicts a significant impact. Furthermore, while "Semi-Public" and "Public" nodes are typically characterized by the same features (high arrival SOCs, low Parking Times and typically EV charging during the daylight), the "Public" Node behaves differently.

On the one hand, it is less affected by arrival SOCs. This is justified by the fact that "Public" node has only 3 integrated chargers and an EV fleet of only 12 EVs during the studied duration (the corresponding value of the "Semi-Public" node are 5 chargers and 18 EVs). Therefore, the less challenging EV fleet, passing through the "Public" node, is the reason that it is less affected by arrival SOC uncertainty. On the other hand, the fewer EVs of the "Public" node triggers fewer re-optimizations and set longer optimization horizons and as a consequence the "Public" node is considerably affected by the rest of uncertainties.

Last but not least, the "Public" node can be defined as the most robustly manageable, since customer satisfaction in terms of preferred departure SOC is totally managed under all uncertainties' events.

"Public" and "Home" nodes are affected the most by uncertainties such economically (there are penalty costs inflicted in most uncertainties' worst-case scenarios) as operationally as well (higher unfinished charging gaps). Hence, the "Semi-Public" Node represents the node that is the least affected by uncertainties regarding charging costs and customer satisfaction. Finally, the conclusions of this thesis can be summarized in Tables 8.1 – 8.2 in the form of "heatmaps".

Table 8. 1: "Heatmap" of Uncertainties' Evaluation

	Evaluation indices			
Uncertainties	Price of Robustness	Economic Impact	Charging Gap Impact	Hardly Manageable by RO & Prediction
Arrival SOC	1	2	2	1
Parking Time	1	3	2	1
PV Generation		1	1	1
Load Demand		1	1	1
FCR Reserves	1	3	3	1

Table 8. 2: "Heatmap" of Nodes' Evaluation

	Nodes		
Evaluation indices	"Home"	"Semi-Public"	"Public"
Robustly Expensive	1	1	1
Prone to arrival SOC	2	3	2
Prone to Parking Time	3	1	3
Prone to PV Generation	1	1	1
Prone to Load Demand	1	1	1
Prone to FCR Reserves	3	1	3
Economically Vulnerable	3	2	3
Operationally Vulnerable	2	1	2
Hardly Manageable by RO & Prediction	2	2	1

Table 8.1 depicts the evaluation of the uncertainties regarding their price of robustness, economic & charging gap impacts and the difficulty of their management by "Prediction" and RO. Table 8.2 depicts the corresponding evaluation of the 3 Nodes ("Home", "Semi-Public" & "Public") regarding their economic and operational vulnerability by the different uncertainties (and generally) as well as their expense and difficulty of managing their robustness.

The "Colors" and "Values" of the Tables – Heatmaps explanation is as follows:

- Green Color (1): Low
- Yellow Color (2): Moderate
- Red Color (3): High
- Grey Color: Not applicable

8.3 Recommendations for Future Research

The EVs are normally charged in two regions, the "Constant-Current" (CC) region & the "Constant-Voltage" (CV) region. According to the CC-CV EV charging, an EV is charged with typically high (potentially maximum) constant current until its SOC reaches a predefined threshold, e.g 80%, and then it is slowly charged with continuously decreasing charging current in the CV region between 80% and 100% SOC. However, this inflicts a significant drawback on successful EV charging. While the optimizer cannot give command for EV charging under 6A, the EV is charged with lower than 6A current due to the CV region in reality. This drawback potentially increases the unfinished charging gap of the EV fleets, because the optimizer schedules EV charging without taking into consideration this lower than 6A charging region of the EVs. Efforts have been performed in this thesis to decrease the CV region importance by increasing the EVs requested energy while being in the CV region, however while the charging gaps have been improved by a factor of 30%, the problem still remains. Therefore, for the scope of this thesis and because this is a challenge that is not yet properly addressed in the Benchmark algorithm, the CV charging region of the EVs has been ignored in this investigation. This has been chosen for extraction of clear and solid conclusions from results of uncertainty management by Robust Optimization and Prediction Capability and the comparisons regarding the impact of the various different uncertainties. However, since the CV charging constitutes an important aspect of real charging, the results of this investigation in terms of uncertainties impact and management would be interesting to be re-addressed with the insertion of the CV region.

Moreover, this thesis has addressed various significant EV smart-charging uncertainties but only individually. Each uncertainty impact and management have been investigated alone, with the other uncertainties steady at their forecasted values. However, most of these uncertainties are completely independent in reality, therefore the assumption of individual uncertainty events can be deemed "unreal" and the probability of simultaneous uncertainty events should be investigated as well. Tests in this thesis have already been performed, combining PV Generation and Load Demand uncertainties, and have shown significant charging cost increase and cost penalty appearances even in the "Prediction-Capable" Algorithm, which can be seen in Appendix, which integrates the numerical results comparison about charging costs and unfinished charging gaps of the 3 nodes between the P-C Algorithm base case and the P-C case, where both PV Generation and Load Demand uncertainties are considered. Moreover, the behavior of the chargers of the "Home" Node in the 2 cases is also integrated.

Finally, the market-bidding process has not been considered in the scope of this thesis, since possible "price-making" capabilities of the algorithm have not been taken into account (no uncertainty in energy price). Therefore, a single-level optimization for the "offered" FCR reserves to the power grid has been considered enough. A final recommendation for future research could be the treat of the developed FCR provision model as a bi-level optimization problem. On that manner, in the first

optimization layer, the algorithm takes into account the behavior and the "offers" of the other agents, that participate in the pool bidding market in order to decide the amount of "offered" up and down regulation reserves. After the decision of the "market clearing price", the algorithm re-runs the optimization for the optimal charging of the EV fleets. The assumption that all the "offered" FCR reserves actually participate in the bidding market can be addressed as well with an interactive optimization layer from the power grid size, depending on the load demand and the contingency events, predicted in the DA bidding market.

References

[1] J. K. Pradhan, P. P. Verma, V. Khemka, V. E. Anoop, S. T. P. Srinivas, and K. S. Swarup, "Uncertainty handling for Electric Vehicle aggregator using IGDT," *2018 20th Natl. Power Syst. Conf. NPSC 2018*, pp. 0–5, 2018, doi: 10.1109/NPSC.2018.8771745.

[2] N. Mehboob, "Smart Charging of Plug-in Electric Vehicles in Distribution Systems Considering Uncertainties," 2016.

[3] M. S. Javadi, A. Anvari-Moghaddam, and J. M. Guerrero, "Robust energy hub management using information gap decision theory," *Proc. IECON 2017 - 43rd Annu. Conf. IEEE Ind. Electron. Soc.*, vol. 2017-January, pp. 410–415, 2017, doi: 10.1109/IECON.2017.8216073.

[4] M. Nour, J. P. Chaves-Ávila, G. Magdy, and Á. Sánchez-Miralles, "Review of positive and negative impacts of electric vehicles charging on electric power systems," *Energies*, vol. 13, no. 18, 2020, doi: 10.3390/en13184675.

[5] Á. Lorca, X. A. Sun, E. Litvinov, and T. Zheng, "Multistage adaptive robust optimization for the unit commitment problem," *Oper. Res.*, vol. 64, no. 1, pp. 32–51, 2016, doi: 10.1287/opre.2015.1456.

[6] M. Shamshirband, J. Salehi, and F. Samadi Gazijahani, "Look-ahead risk-averse power scheduling of heterogeneous electric vehicles aggregations enabling V2G and G2V systems based on information gap decision theory," *Electr. Power Syst. Res.*, vol. 173, no. March, pp. 56–70, 2019, doi: 10.1016/j.epsr.2019.04.018.

[7] J. A. P. Lopes, F. J. Soares, and P. M. R. Almeida, "Integration of electric vehicles in the electric power system," *Proc. IEEE*, vol. 99, no. 1, pp. 168–183, 2011, doi: 10.1109/JPROC.2010.2066250.

[8] D. Dreucci, "EV Penetration Impact on a Distribution Grid", TU Delft, Delft, 2020

[9] L. D. Herdt, "Hardware-in-the-Loop Simulation of Controlled and Uncontrolled EV Charging in a Distribution Grid", TU Delft, Delft, 2020

[10] M. S. Sumitro, "Optimal Power Management System of EVs Charging from PV System in a Low Voltage Distribution Network", TU Delft, Delft, 2018

[11] Y. Zhou, D. K. Y. Yau, P. You, and P. Cheng, "Optimal-cost scheduling of electrical vehicle charging under uncertainty," *IEEE Trans. Smart Grid*, vol. 9, no. 5, pp. 4547–4554, 2018, doi: 10.1109/TSG.2017.2662801.

[12] M. G. Vaya, G. Andersson, and S. Boyd, "Decentralized control of plug-in electric vehicles under driving uncertainty," *IEEE PES Innov. Smart Grid Technol. Conf. Eur.*, vol. 2015-January, no. January, pp. 1–6, 2015, doi: 10.1109/ISGTEurope.2014.7028989.

[13] X. Gong, T. Lin, and B. Su, "Optimal bidding strategy of a electric vehicle aggregator in electricity market," *Dianwang Jishu/Power Syst. Technol.*, vol. 40, no. 9, pp. 2596–2602, 2016, doi: 10.13335/j.1000-3673.pst.2016.09.003.

[14] Y. He, B. Venkatesh, and L. Guan, "Optimal scheduling for charging and discharging of electric vehicles," *IEEE Trans. Smart Grid*, vol. 3, no. 3, pp. 1095–1105, 2012, doi: 10.1109/TSG.2011.2173507.

[15] "Deliverables," *OSCD*. [Online]. Available: https://www.oscd.eu/deliverables/. [Accessed: 03-Aug-2021].

[16] S. A. Alavi, A. Ahmadian, and M. Aliakbar-Golkar, "Optimal probabilistic energy management in a typical micro grid based-on robust optimization and point estimate method," *Energy Convers. Manag.*, vol. 95, pp. 314–325, 2015, doi: 10.1016/j.enconman.2015.02.042.

[17] A. Soroudi and T. Amraee, "Decision making under uncertainty in energy systems: State of the art," *Renew. Sustain. Energy Rev.*, vol. 28, pp. 376–384, 2013, doi: 10.1016/j.rser.2013.08.039.

[18] A. R. Jordehi, "How to deal with uncertainties in electric power systems? A review," *Renew. Sustain. Energy Rev.*, vol. 96, no. August, pp. 145–155, 2018, doi: 10.1016/j.rser.2018.07.056.

[19] S. A. Alavi, A. Ahmadian, and M. Aliakbar-Golkar, "Optimal probabilistic energy management in a typical micro-grid based-on robust optimization and point estimate method," *Energy Convers. Manag.*, vol. 95, pp. 314–325, 2015, doi: 10.1016/j.enconman.2015.02.042.

[20] R. L. Harrison, "Introduction to Monte Carlo simulation," *AIP Conf. Proc.*, vol. 1204, pp. 17–21, 2009, doi: 10.1063/1.3295638.

[21] R. Y. Rubinstein and D. P. Kroese, *"Simulation and the Monte Carlo Method"*. 3rd ed. Wiley. Hoboken, NJ, 2017.

[22] R. C. Leou, C. L. Su, and C. N. Lu, “Impact analysis of electric vehicles on distribution systems considering uncertainties,” *IECON Proc. (Industrial Electron. Conf.*, pp. 2063–2068, 2013, doi: 10.1109/IECON.2013.6699449.

[23] B. Yang, L. F. Wang, C. L. Liao, and L. Ji, “Coordinated charging method of electric vehicles to deal with uncertainty factors,” *IEEE Transp. Electrif. Conf. Expo, ITEC Asia-Pacific 2014 - Conf. Proc.*, pp. 1–6, 2014, doi: 10.1109/ITEC-AP.2014.6940696.

[24] O. Cappe, S. J. Godsill, and E. Moulines, “An overview of existing methods and recent advances in sequential Monte Carlo,” *Proc. IEEE*, vol. 95, no. 5, pp. 899–924, 2007, doi: 10.1109/JPROC.2007.893250.

[25] O. M. Tachinina, I. V. Alekseeva, O. I. Lysenko, and S. M. Chumachenko, “Scenario-based approach for control of multi-object dynamic system motion,” *2015 IEEE 3rd Int. Conf. Actual Probl. Unmanned Aer. Veh. Dev. APUAVD 2015 - Proc.*, no. 1, pp. 305–308, 2015, doi: 10.1109/APUAVD.2015.7346627.

[26] K. Cai, W. Li, F. Ju, and X. Zhu, “A scenario-based optimization approach to robust estimation of airport apron capacity,” *ICNS 2018 - Integr. Commun. Navig. Surveill. Conf.*, pp. 3A11-3A18, 2018, doi: 10.1109/ICNSURV.2018.8384852.

[27] C. Zhang, Z. Z. Lin, F. S. Wen, and J. S. Huang, “A scenario-based network reconfiguration framework under uncertainties,” *IET Conf. Publ.*, vol. 2012, no. 611 CP, 2012, doi: 10.1049/cp.2012.1836.

[28] J. M. Morales and J. Pérez-Ruiz, “Point estimate schemes to solve the probabilistic power flow,” *IEEE Trans. Power Syst.*, vol. 22, no. 4, pp. 1594–1601, 2007, doi: 10.1109/TPWRS.2007.907515.

[29] F. S. Gazijahani, H. Hosseinzadeh, N. Tagizadeghan, and J. Salehi, “A new point estimate method for stochastic optimal operation of smart distribution systems considering demand response programs,” *2017 Electr. Power Distrib. Networks Conf. EPDC 2017*, pp. 39–44, 2017, doi: 10.1109/EPDC.2017.8012738.

[30] S. Sannigrahi, S. R. Ghatak, and P. Acharjee, “Point Estimate Method based Distribution System Planning using MOPSO Technique,” *2020 IEEE Int. Conf. Power Electron. Smart Grid Renew. Energy, PESGRE 2020*, pp. 1–6, 2020, doi: 10.1109/PESGRE45664.2020.9070380.

[31] S. A. Alavi, A. Ahmadian, and M. Aliakbar-Golkar, “Optimal probabilistic energy management in a typical micro-grid based-on robust optimization and point estimate method,” *Energy Convers. Manag.*, vol. 95, pp. 314–325, 2015, doi: 10.1016/j.enconman.2015.02.042.

[32] Y. Yang, X. R. Li, and D. Han, “An improved α-cut approach to transforming fuzzy membership function into basic belief assignment,” *Chinese J. Aeronaut.*, vol. 29, no. 4, pp. 1042–1051, 2016, doi: 10.1016/j.cja.2016.03.007.

[33] BELLMAN RE and ZADEH LA, “Decision-Making in a Fuzzy Environment,” *Manage. Sci.*, vol. 17, no. 4, 1970, doi: 10.1142/9789812819789_0004.

[34] A. V. Yazenin, “On the problem of possibilistic optimization,” *Fuzzy Sets Syst.*, vol. 81, no. 1, pp. 133–140, 1996, doi: 10.1016/0165-0114(95)00245-6.

[35] J. F. Tang, D. W. Wang, R. Y. K. Fung, and K.-L. Yung, “Understanding of fuzzy optimization: theories and methods,” *J. Syst. Sci. Complex.*, vol. 17, no. 1, pp. 117–136, 2004.

[36] H. J. Zimmermann, *“Fuzzy Set Theory – and Its Applications”.* 4th ed. Kluwer Academic Publishers, New York, 2001.

[37] M. K. Luhandjula, “Fuzzy optimization: Milestones and perspectives,” *Fuzzy Sets Syst.*, vol. 274, pp. 4–11, 2015, doi: 10.1016/j.fss.2014.01.004.

[38] M. K. Luhandjula, “Fuzzy optimization: An appraisal,” *Fuzzy Sets Syst.*, vol. 30, no. 3, pp. 257–282, 1989, doi: 10.1016/0165-0114(89)90019-5.

[39] H. Zhang and D. liu, *“Fuzzy Modeling and Fuzzy Control”.* 1st ed. Birkhauser, Boston. 2006

[40] A. Soroudi, “Possibilistic-scenario model for DG impact assessment on distribution networks in an uncertain environment,” *IEEE Trans. Power Syst.*, vol. 27, no. 3, pp. 1283–1293, 2012, doi: 10.1109/TPWRS.2011.2180933.

[41] S. Pirouzi, J. Aghaei, M. A. Latify, G. R. Yousefi, and G. Mokryani, “A robust optimization approach for active and reactive power management in smart distribution networks using electric vehicles,” *IEEE Syst. J.*, vol. 12, no. 3, pp. 2699–2710, 2018, doi: 10.1109/JSYST.2017.2716980.

[42] H. G. Beyer and B. Sendhoff, “Robust optimization - A comprehensive survey,” *Comput. Methods Appl. Mech. Eng.*, vol. 196, no. 33–34, pp. 3190–3218, 2007, doi: 10.1016/j.cma.2007.03.003.

[43] M. Pourahmadi-Nakhli, A. R. Seifi, and R. Taghavi, “A nonlinear-hybrid fuzzy/probabilistic load flow for radial distribution systems,” *Int. J. Electr. Power Energy Syst.*, vol. 47, no. 1, pp. 69–77, 2013, doi: 10.1016/j.ijepes.2012.10.020.

[44] W. Li and J. Zhou, "Power system risk assessment using a hybrid method of fuzzy set and Monte Carlo simulation," *2009 IEEE Power & Energy Society General Meeting*, 2009, pp. 1-1, doi: 10.1109/PES.2009.5275942.

[45] Z. Zhou, C. Sun, R. Shi, Z. Chang, S. Zhou, and Y. Li, “Robust Energy Scheduling in Vehicle-To-Grid Networks,” *IEEE Netw.*, vol. 31, no. 2, pp. 30–37, 2017, doi: 10.1109/MNET.2017.1600220NM.

[46] G. Taguchi, “Quality Engineering through Design Optimization”, *Kraus International Publications*, New York, 1984.
[47] N. Korolko and Z. Sahinoglu, “Robust optimization of EV charging schedules in unregulated electricity markets,” *IEEE Trans. Smart Grid*, vol. 8, no. 1, pp. 149–157, 2017, doi: 10.1109/TSG.2015.2472597.

[48] A. Ben-Tal and A. Nemirovski, “Robust optimization - Methodology and applications,” *Math. Program. Ser. B*, vol. 92, no. 3, pp. 453–480, 2002, doi: 10.1007/s101070100286.

[49] A. Soroudi and A. Keane, “Robust optimization based EV charging,” *2014 IEEE Int. Electr. Veh. Conf. IEVC 2014*, no. 1, pp. 2–7, 2015, doi: 10.1109/IEVC.2014.7056223.

[50] M. Shamshirband, J. Salehi, and F. Samadi Gazijahani, “Look-ahead risk-averse power scheduling of heterogeneous electric vehicles aggregations enabling V2G and G2V systems based on information gap decision theory,” *Electr. Power Syst. Res.*, vol. 173, no. March, pp. 56–70, 2019, doi: 10.1016/j.epsr.2019.04.018.

[51] J. K. Pradhan, P. P. Verma, V. Khemka, V. E. Anoop, S. T. P. Srinivas, and K. S. Swarup, “Uncertainty handling for Electric Vehicle aggregator using IGDT,” *2018 20th Natl. Power Syst. Conf. NPSC 2018*, pp. 0–5, 2018, doi: 10.1109/NPSC.2018.8771745.

[52] S. Bahramara, R. Mafakheri, P. Sheikhahmadi, M. Lotfi, and J. P. S. Catalao, “Information Gap Decision Theory-Based Approach for Modeling Operation Problem of a Grid-Connected Micro-Grid with Uncertainties,” *SEST 2019 - 2nd Int. Conf. Smart Energy Syst. Technol.*, 2019, doi: 10.1109/SEST.2019.8849076.

[53] S. I. Vagropoulos and A. G. Bakirtzis, "Optimal Bidding Strategy for Electric Vehicle Aggregators in Electricity Markets," in IEEE Transactions on Power Systems, vol. 28, no. 4, pp. 4031-4041, Nov. 2013, doi: 10.1109/TPWRS.2013.2274673.

[54] M. G. Vaya and G. Andersson, “Smart Charging of Plug-in Electric Vehicles Under Driving Behavior Uncertainty”, *Springer India*, 2014, doi: 10.1007/978-81-322-1798-5_6.

[55] E. Valsera-Naranjo, D. Martinez-Vicente, A. Sumper, R. Villafafila-Robles and A. Sudria-Andreu, “Deterministic and probabilistic assessment of the impact of the electric vehicles on the power grid”, *2011 IEEE Power and Energy Society General Meeting,* 2011, pp. 1=8, doi: 10.1109/PES.2011.6039546.

[56] J. Fluhr, K. Ahlert and C. Weinhardt, “A Stochastic Model for Simulating the Availability of Electric Vehicles for Services to the Power Grid”, *2010 43rd Hawaii International Conference on System Sciences*, 2010, pp. 1-10, doi: 10.1109/HICSS.2010.33

[57] X. Bai and W. Qiao, "Robust Optimization for Bidirectional Dispatch Coordination of Large-Scale V2G," in *IEEE Transactions on Smart Grid*, vol. 6, no. 4, pp. 1944-1954, July 2015, doi: 10.1109/TSG.2015.2396065.

[58] A. M. Shalamzari, “Robust Multi-Class Multi-Period Scheduling of MRI Services with Wait Time Targets,” 2018.

[59] D. Bertsimas and M. Sim, “The price of robustness,” *Oper. Res.*, vol. 52, no. 1, pp. 35–53, 2004, doi: 10.1287/opre.1030.0065.

[60] M. Sim, “Robust Optimization”, Ph. D. dissertation, MIT Univ., Massachusetts, USA, 2004.

[61] D. Bertsimas, D. B. Brown, and C. Caramanis, “Theory and applications of robust optimization,” *SIAM Rev.*, vol. 53, no. 3, pp. 464–501, 2011, doi: 10.1137/080734510.

[62] A. Ahmadi, “Robust Optimization”, presented to G. Hall, Princeton Univ., Princeton, NJ, USA, Apr. 25, 2016.
[63] D. Bertsimas and M. Sim, “Robust discrete optimization and network flows,” *Math. Program.*, vol. 98, no. 1–3, pp. 49–71, 2003, doi: 10.1007/s10107-003-0396-4.

[64] F. Ruiter, “Primal and dual approaches to adjustable robust optimization”, Ph. D. dissertation, CentER, Tilburg Univ., Tilburg, Netherlands, 2018.

[65] D. Bertsimas and A. Thiele, “Robust and Data-Driven Optimization: Modern Decision Making Under Uncertainty,” *Model. Methods, Appl. Innov. Decis. Mak.*, no. January 2021, pp. 95–122, 2006, doi: 10.1287/educ.1063.0022.

[66] G.-C. Rota, *Robust statistics*, vol. 60, no. 1. 1986.

[67] J. Wang, B. Chen, P. Li, and Y. Che, “Distributionally robust optimization of home energy management system based on receding horizon optimization,” *Front. Energy*, vol. 14, no. 2, pp. 254–266, 2020, doi: 10.1007/s11708-020-0665-4.

[68] P. Artzner, F. Delbaen, J. M. Eber, and D. Heath, “Coherent measures of risk,” *Math. Financ.*, vol. 9, no. 3, pp. 203–228, 1999, doi: 10.1111/1467-9965.00068

[69] S. Pirouzi, J. Aghaei, T. Niknam, M. Shafie-khah, V. Vahidinasab, and J. P. S. Catalão, “Two alternative robust optimization models for flexible power management of electric vehicles in distribution networks,” *Energy*, vol. 141, pp. 635–651, 2017, doi: 10.1016/j.energy.2017.09.109.

[70] S. L. Janak, X. Lin, and C. A. Floudas, “A new robust optimization approach for scheduling under uncertainty. II. Uncertainty with known probability distribution,” *Comput. Chem. Eng.*, vol. 31, no. 3, pp. 171–195, 2007, doi: 10.1016/j.compchemeng.2006.05.035.

[71] A. Ben-Tal, “Recent Advances in Robust Optimization,” Oper. Res. Proc. 2006, pp. 69–69, 2007, doi: 10.1007/978-3-540-69995-8_10.

[72] S. H. Choi, A. Hussain, and H. M. Kim, “Adaptive robust optimization-based optimal operation of microgrids considering uncertainties in arrival and departure times of electric vehicles,” *Energies*, vol. 11, no. 10, 2018, doi: 10.3390/en11102646.

[73] A. Moreira, A. Street and J. M. Arroyo, "Energy and reserve scheduling under correlated nodal demand uncertainty: An adjustable robust optimization approach," *2014 Power Systems Computation Conference*, 2014, pp. 1-8, doi: 10.1109/PSCC.2014.7038415.

[74] B. C. Dean, M. X. Goemans and J. Vondrdk, "Approximating the stochastic knapsack problem: the benefit of adaptivity," *45th Annual IEEE Symposium on Foundations of Computer Science*, 2004, pp. 208-217, doi: 10.1109/FOCS.2004.15.

[75] D. Bertsimas and C. Caramanis, "Finite Adaptability in Multistage Linear Optimization," in *IEEE Transactions on Automatic Control*, vol. 55, no. 12, pp. 2751-2766, Dec. 2010, doi: 10.1109/TAC.2010.2049764.

[76] A. Marandi and D. den Hertog, “When are static and adjustable robust optimization problems with constraint-wise uncertainty equivalent?,” *Math. Program.*, vol. 170, no. 2, pp. 555–568, 2018, doi: 10.1007/s10107-017-1166-z.

[77] Á. Lorca, X. A. Sun, E. Litvinov, and T. Zheng, “Multistage adaptive robust optimization for the unit commitment problem,” *Oper. Res.*, vol. 64, no. 1, pp. 32–51, 2016, doi: 10.1287/opre.2015.1456.

[78] B. Zeng, H. Dong, R. Sioshansi, F. Xu, and M. Zeng, “Bilevel Robust Optimization of Electric Vehicle Charging Stations with Distributed Energy Resources,” *IEEE Trans. Ind. Appl.*, vol. 56, no. 5, pp. 5836–5847, 2020, doi: 10.1109/TIA.2020.2984741.

[79] A. Ben-Tal, A. Goryashko, E. Guslitzer and A. Nemirovski, “Adjustable robust solutions of uncertain linear programs”, *Math. Program.,* no. 99, pp. 351-376, 2003. doi: 10.1007/s10107-003-0454-y

[80] H. Michalska and D. Q. Mayne, “Robust receding horizon control of constrained nonlinear systems,” *IEEE Trans. Automat. Contr.*, vol. 38, no. 11, pp. 1623–1633, 1993, doi: 10.1109/9.262032.

[81] Y. Kuwata, A. Richards, T. Schouwenaars and J. P. How, “Distributed Robust Receding Horizon Control for Multivehicle Guidance”, in IEEE Transactions on Control Systems Technology, vol. 15, no. 4, pp. 627-641, July 2007, doi: 10.1109/TCST.2007.899152.

[82] Y. Park, J. S. Shamma, and T. C. Harmon, “A Receding Horizon Control algorithm for adaptive management of soil moisture and chemical levels during irrigation,” *Environ. Model. Softw.*, vol. 24, no. 9, pp. 1112–1121, 2009, doi: 10.1016/j.envsoft.2009.02.008.

[83] J. Silvente, G. M. Kopanos, E. N. Pistikopoulos, and A. Espuña, “A rolling horizon optimization framework for the simultaneous energy supply and demand planning in microgrids,” *Appl. Energy*, vol. 155, pp. 485–501, 2015, doi: 10.1016/j.apenergy.2015.05.090.

[84] S. Neyshabouri and B. P. Berg, “Two-stage robust optimization approach to elective surgery and downstream capacity planning,” *Eur. J. Oper. Res.*, vol. 260, no. 1, pp. 21–40, 2017, doi: 10.1016/j.ejor.2016.11.043.

[85] X. Lin, S. L. Janak, and C. A. Floudas, “A new robust optimization approach for scheduling under uncertainty: I. Bounded uncertainty,” *Comput. Chem. Eng.*, vol. 28, no. 6–7, pp. 1069–1085, 2004, doi: 10.1016/j.compchemeng.2003.09.020.

[86] KU Leuven Energy Institute, “The current electricity market design in Europe,” *EI-FACT SHEET 2015-01 The*, p. 4, 2015.

[87] E. Sortomme and M. A. El-Sharkawi, “Optimal scheduling of vehicle-to-grid energy and ancillary services,” *IEEE Trans. Smart Grid*, vol. 3, no. 1, pp. 351–359, 2012, doi: 10.1109/TSG.2011.2164099.

[88] J. M. Bert, “Ancillary services : Technical and Commercial Insights,” *Orthop. Clin. North Am.*, vol. 39, no. 1, pp. 1–4, v, 2008, [Online]. Available: http://www.ncbi.nlm.nih.gov/pubmed/20228656.

[89] B. Kirby, “The Value of Flexible Generation,” *Power-Gen*, pp. 1–16, 2013, [Online]. Available: http://www.consultkirby.com/files/PowerGen-2013_The_Value_of_Flexible_Generation_Nov_2013.pdf.

[90] F. D. Galiana, F. Bouffard, J. M. Arroyo, and J. F. Restrepo, “Scheduling and pricing of coupled energy and primary, secondary, and tertiary reserves,” *Proc. IEEE*, vol. 93, no. 11, pp. 1970–1982, 2005, doi: 10.1109/JPROC.2005.857492.

[91] F. Bovera, G. Rancilio, D. Falabretti, and M. Merlo, “Data-driven evaluation of secondary-and tertiary-reserve needs with high renewables penetration: The Italian case,” *Energies*, vol. 14, no. 8, 2021, doi: 10.3390/en14082157.

[92] G. R. C. Mouli, M. Kefayati, R. Baldick, and P. Bauer, “Integrated PV charging of EV fleet based on energy prices, V2G, and offer of reserves,” *IEEE Trans. Smart Grid*, vol. 10, no. 2, pp. 1313–1325, 2019, doi: 10.1109/TSG.2017.2763683.

[93] W. Kempton and J. Tomi´c, “Vehicle-to-grid power implementation: From stabilizing the grid to supporting large-scale renewable energy”, *J. Power Sources*, vol. 144, no. 1, pp. 280–294, 2005, doi: 10.1016/j.jpowourc.2004.12.022

[94] H. Lund and W. Kempton, “Integration of renewable energy into the transport and electricity sectors through V2G,” Energy Policy, vol. 36, no. 9, pp. 3578–3587, 2008, doi: 10.1016/j.enpol.200806.007

[95] M. Caramanis and J. M. Foster, "Management of electric vehicle charging to mitigate renewable generation intermittency and distribution network congestion," *Proceedings of the 48h IEEE Conference on Decision and Control (CDC) held jointly with 2009 28th Chinese Control Conference*, 2009, pp. 4717-4722, doi: 10.1109/CDC.2009.5399955.

[96] M. Kefayati and C. Caramanis, “Efficient energy delivery management for PHEVs”, *2010 1st IEEE Int. Conf. Smart Grid Commun. SmartGridComm 2010,* no. i, pp. 525-530, 2010, doi: 10.1109/SMARTGRID.2010.5621990.

[97] F. Rücker, M. Merten, J. Gong, R. Villafáfila-Robles, I. Schoeneberger, and D. U. Sauer, “Evaluation of the effects of smart charging strategies and frequency restoration reserves market participation of an electric vehicle,” *Energies*, vol. 13, no. 12, pp. 1–31, 2020, doi: 10.3390/en13123112.

[98] I. Pavic, H. Pandzic, and T. Capuder, “Electric vehicles as frequency containment reserve providers,” *6th IEEE Int. Energy Conf. ENERGYCon 2020*, pp. 911–917, 2020, doi: 10.1109/ENERGYCon48941.2020.923658.

[99] P. Hasanpor Divshali and C. Evens, “Optimum day-ahead bidding profiles of electrical vehicle charging stations in FCR markets,” *Electr. Power Syst. Res.*, vol. 190, no. September 2019, p. 106667, 2021, doi: 10.1016/j.epsr.2020.106667.

[100] X. Gong, T. Lin, and B. Su, “Optimal bidding strategy of a electric vehicle aggregator in electricity market,” *Dianwang Jishu/Power Syst. Technol.*, vol. 40, no. 9, pp. 2596–2602, 2016, doi: 10.13335/j.1000-3673.pst.2016.09.003.

[101] Y. Wang, Y. Dvorkin, R. Fernández-Blanco, B. Xu, T. Qiu, and D. S. Kirschen, “Look-Ahead Bidding Strategy for Energy Storage,” *IEEE Trans. Sustain. Energy*, vol. 8, no. 3, pp. 1106–1127, 2017, doi: 10.1109/TSTE.2017.2656800.

[102] F. Careri, C. Genesi, P. Marannino, M. Montagna, S. Rossi, and I. Siviero, “Bidding strategies in day-ahead energy markets: System marginal price vs. pay as bid,” *2010 7th Int. Conf. Eur. Energy Mark. EEM 2010*, no. March, pp. 1–7, 2010, doi: 10.1109/EEM.2010.5558675.

[103] “Central collection and publication of electricity Generation, transportation and consumption data and information for the Pan-european market.,” *Data view*. [Online]. Available: https://transparency.entsoe.eu. [Accessed: 08-Aug-2021].

[104] Y. Yu, A. Shekhar, D. Reihs, S. Wagh, D. Stahleder, G.R.C. Mouli, F. Lehfuss and P. Bauer, “Data-Driven Analysis of Electric Vehicle Charging Behavior and Its Potential for Demand Side Management”, *IOP Conference Series: Earth and Environmental Science*, 2019, doi: 223. 012034. 10.1088/1755-1315/223/1/012034.

[105] NEDU. 2018. *NEDU - NEDU*. [online] Available at: <https://www.nedu.nl/> [Accessed 11 August 2021].

[106] Meteonorm (de). 2018. *Intro - Meteonorm (de)*. [online] Available at: <https://meteonorm.com/> [Accessed 11 August 2021].

[107] “Home: Dover Fueling Solutions, fueling global innovation.,” *Dover Fueling Solutions*. [Online]. Available: https://www.doverfuelingsolutions.com/. [Accessed: 16-Aug-2021].

[108] EC 61851 Electric Vehicle conductive charging system,” International Electrotechnical Commission, Standard, 2019

[109] H. J. Greenberg and T. Morrison, “Robust Optimization”, Colorado Univ., Denver, USA, 2013.

[110] A. Nemirovski, “Lectures on Robust Convex Optimization”, Georgia Univ., Atlanta Georgia, USA, 2012.

Appendix A: Studies on Combination of Uncertainties (PV Generation & Load Demand)

Table A. 1: Charging Costs Comparison between Accurate Forecast & PV Generation – Load Demand Uncertainties Consideration

Prediction-Capable Algorithm with Accurate Forecast Results				
Nodes	Grid Power Exchange Cost (€)	Unfinished Charging Gap (kWh)	Penalty Cost for Charging Gap (€)	Total Node Charging Cost (€)
Node 1	1,5885	0,2242	0	1,5885
Node 2	-0,6866	0,3497	0	-0,6866
Node 3	-1,8354	0,1543	0	-1,8354
Prediction-Capable Algorithm with Minimum PV Generation & Maximum Load Demand Prediction				
Nodes	Grid Power Exchange Cost (€)	Unfinished Charging Gap (kWh)	Penalty Cost for Charging Gap (€)	Total Node Charging Cost (€)
Node 1	2,0116	1,1194	11,9815	13,993
Node 2	-0,2612	0,3102	0	-0,2612
Node 3	-1,5225	0,0158	0	-1,5225

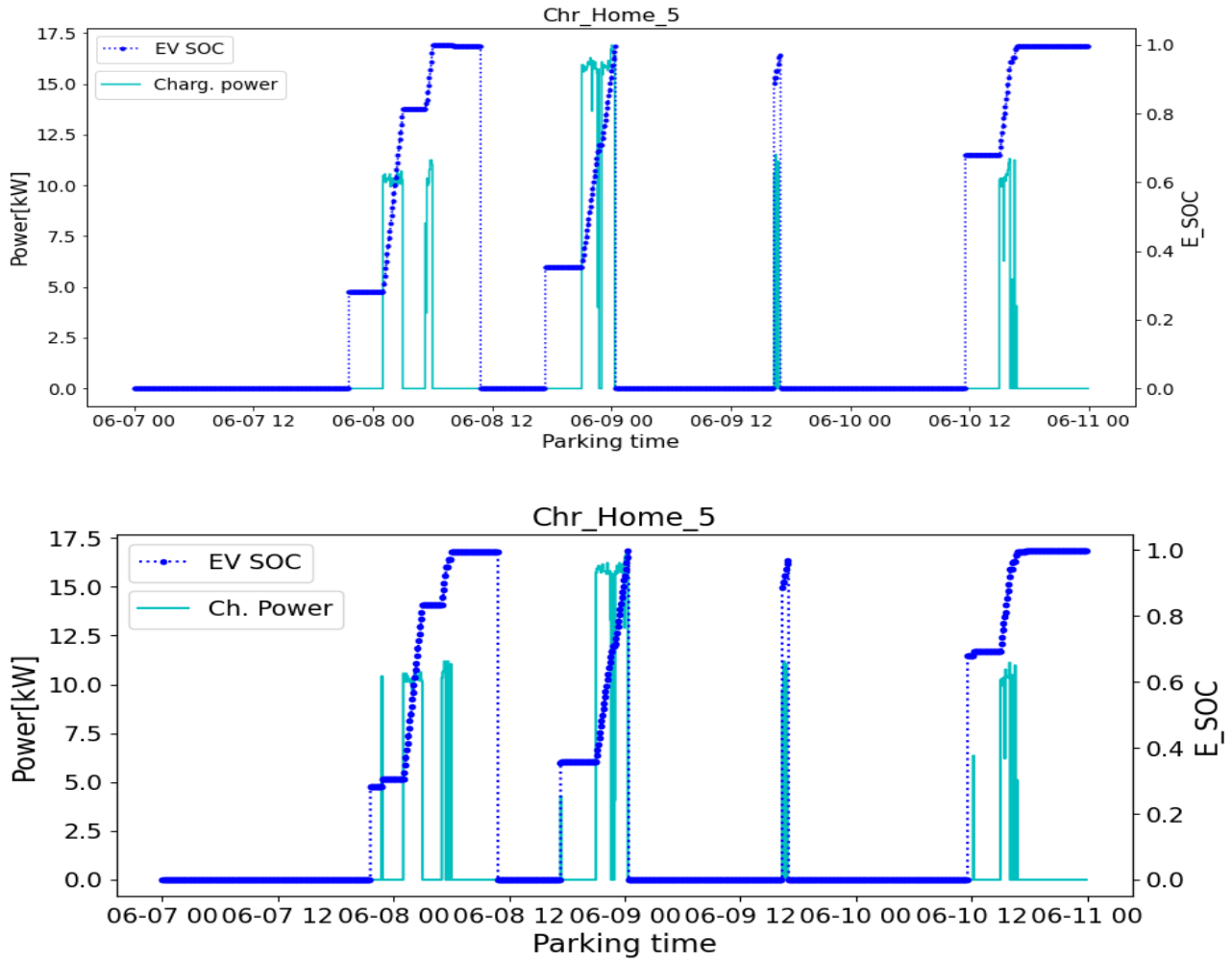

Fig. A. 1: "Charger Home 5" Behavior in Base Case (upper plot) & in Minimum PV Generation - Maximum Load Demand Prediction (lower plot) of P-C Algorithm

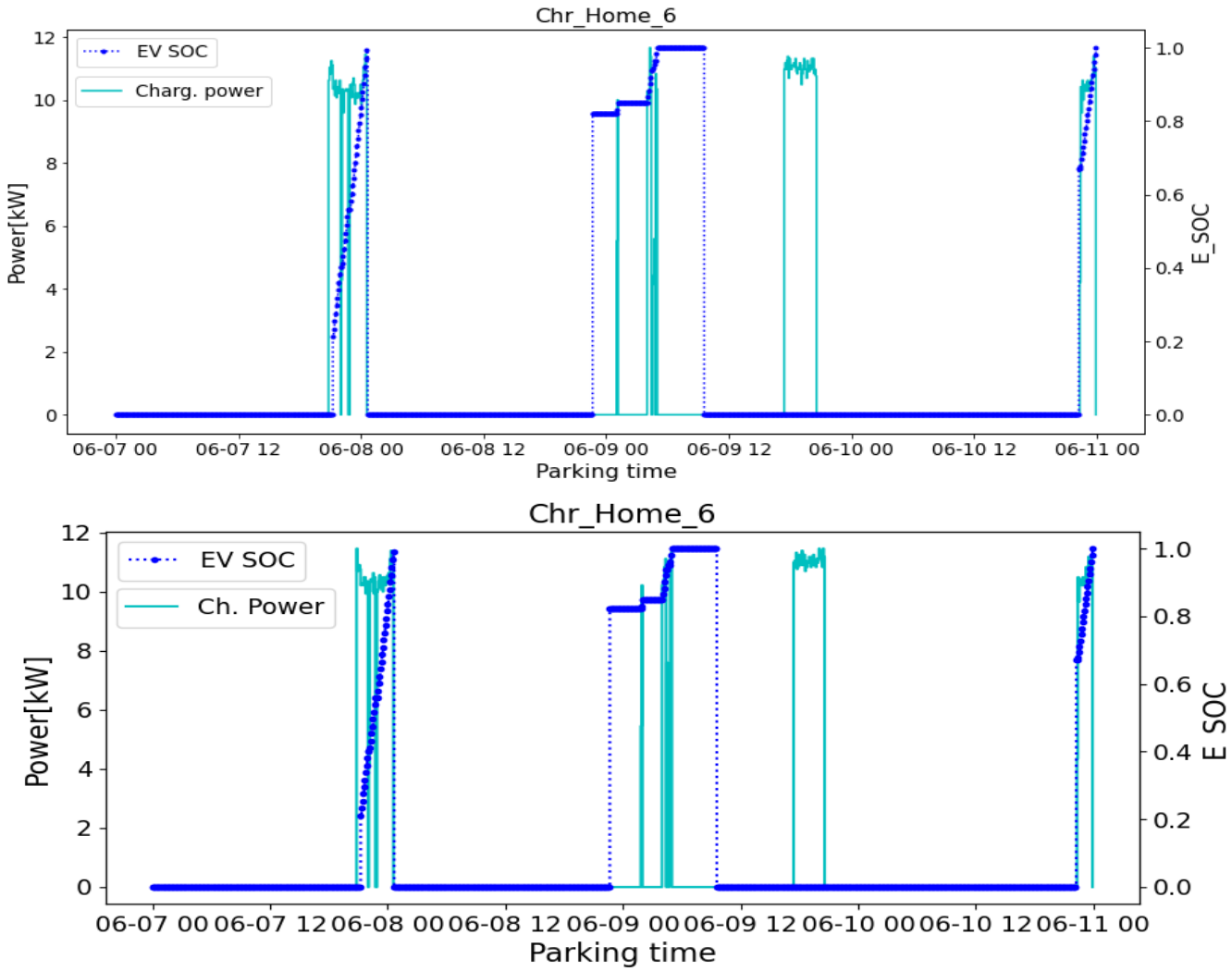

Fig. A. 2: "Charger Home 6" Behavior in Base Case (upper plot) & in Minimum PV Generation - Maximum Load Demand Prediction (lower plot) of P-C Algorithm

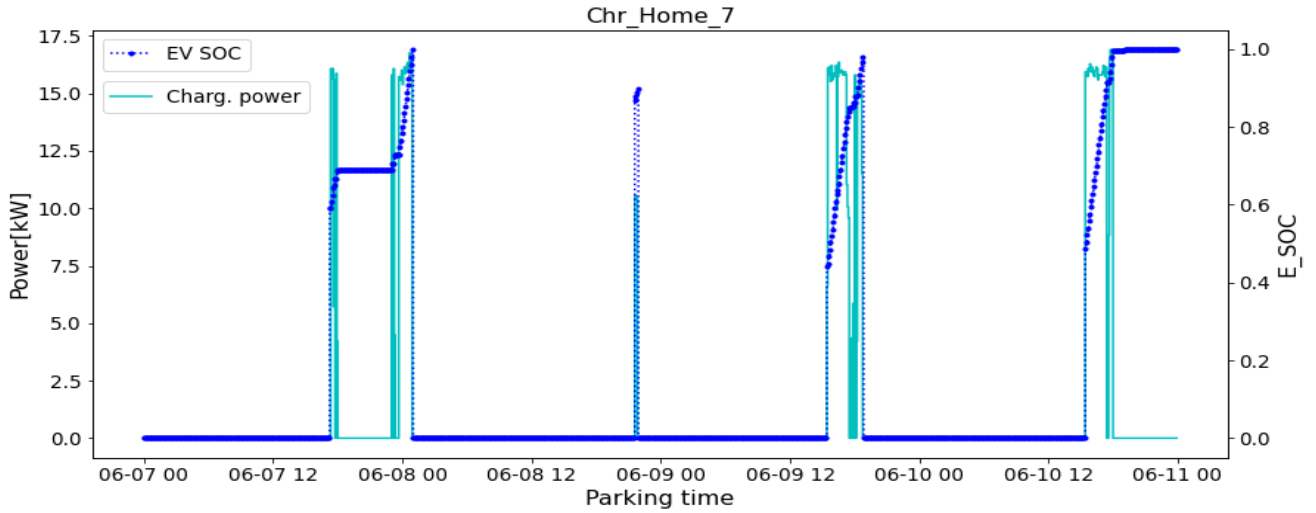

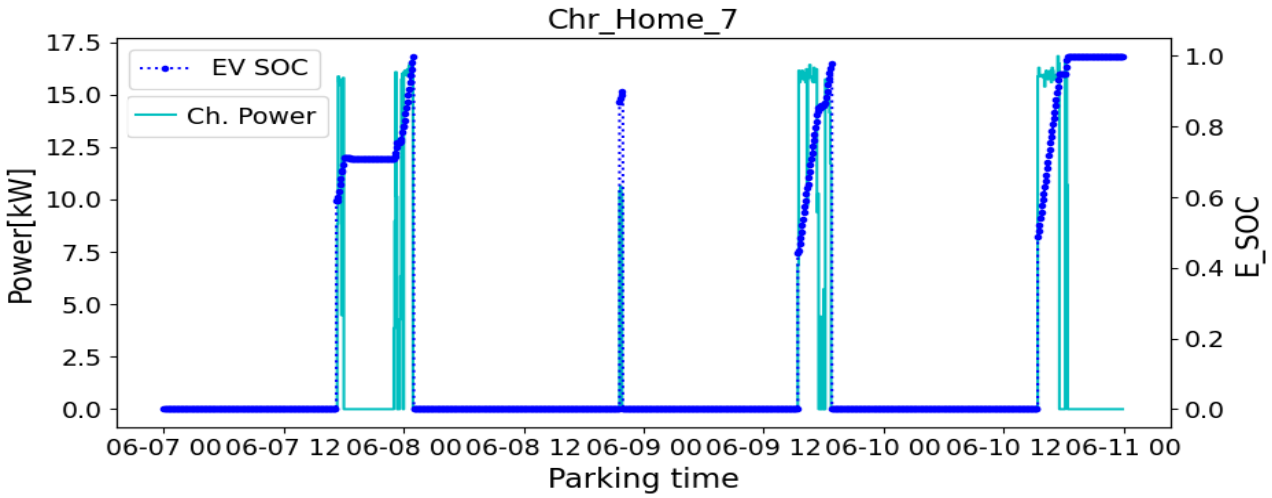

Fig. A. 3: "Charger Home 6" Behavior in Base Case (upper plot) & in Minimum PV Generation - Maximum Load Demand Prediction (lower plot) of P-C Algorithm